



Universiteit
Leiden
The Netherlands

Liposome-based vaccines for immune modulation: from antigen selection to nanoparticle design

Lozano Vigario, F.

Citation

Lozano Vigario, F. (2024, September 10). *Liposome-based vaccines for immune modulation: from antigen selection to nanoparticle design*. Retrieved from <https://hdl.handle.net/1887/4082551>

Version: Publisher's Version

License: [Licence agreement concerning inclusion of doctoral thesis in the Institutional Repository of the University of Leiden](#)

Downloaded from: <https://hdl.handle.net/1887/4082551>

Note: To cite this publication please use the final published version (if applicable).

Liposome-based vaccines for immune modulation

From antigen selection to nanoparticle design

Fernando Lozano Vigario

Cover design: Ridderprint | www.ridderprint.nl

Thesis lay-out: Ridderprint | www.ridderprint.nl

Printing: Ridderprint | www.ridderprint.nl

© Copyright, Fernando Lozano Vigario, 2024

All rights reserved. No part of this book may be reproduced in any form or by any means without permission of the author.

Liposome-based vaccines for immune modulation

From antigen selection to nanoparticle design

Proefschrift

ter verkrijging van

de graad van doctor aan de Universiteit Leiden,

op gezag van rector magnificus prof.dr.ir. H. Bijl,

volgens besluit van het college voor promoties

te verdedigen op dinsdag 10 september 2024

klokke 16:00 uur

door

Fernando Lozano Vigario

geboren te Guareña, Spain

in 1992

Promotores

Prof. dr. J.A. Bouwstra

Prof. dr. A. Kros

Dr. B.A. Slütter

Promotiecommissie

Prof. dr. H. Irth

Prof. dr. E.C.M. de Lange

Prof. dr. Koen Raemdonck (Universiteit Gent)

Prof. dr. E. Mastrobattista (Universiteit Utrecht)

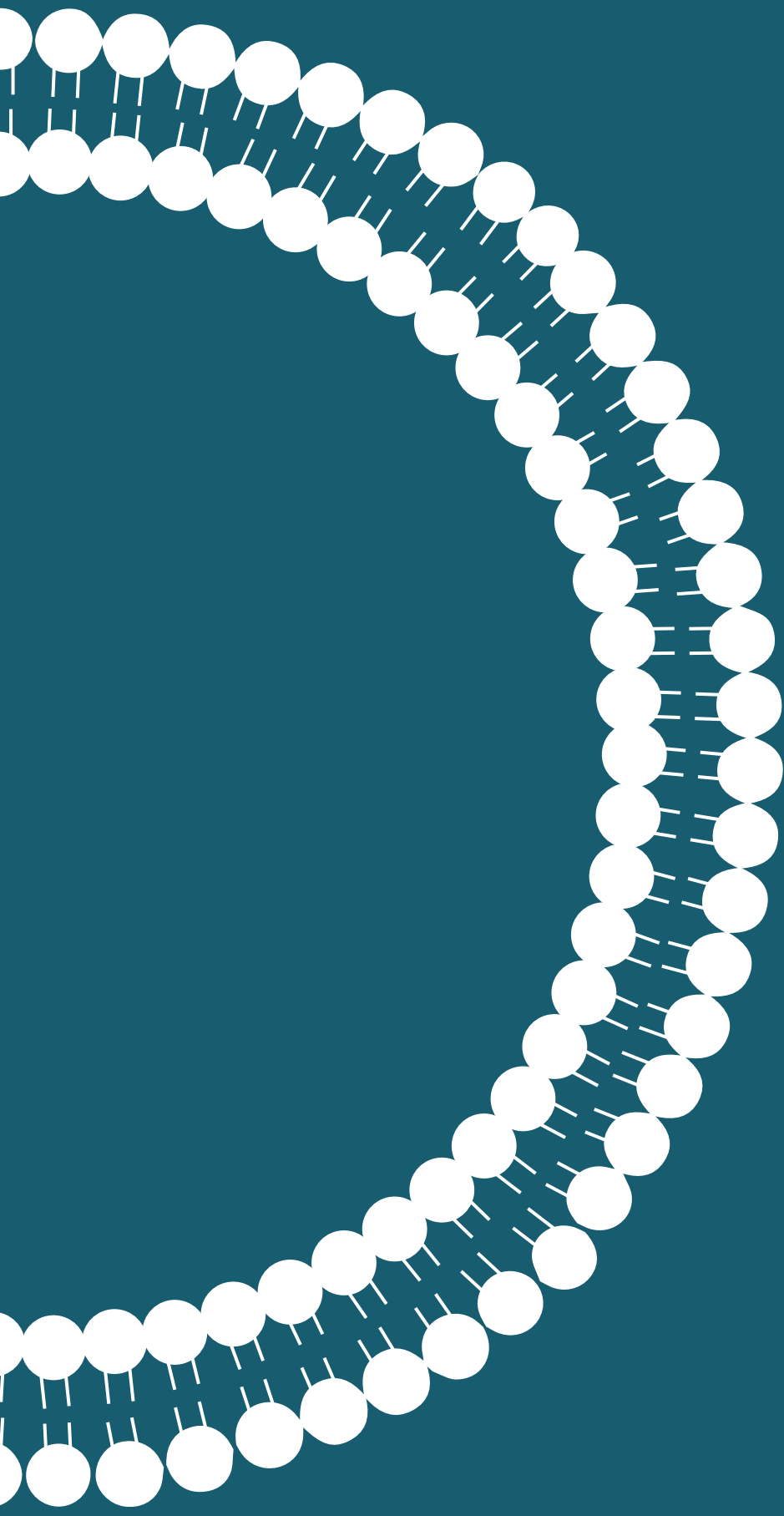
Dr. Anton Gisterå (Karolinska Institutet)

The research described in this thesis was performed at the division of BioTherapeutics of the Leiden Academic Centre for Drug Research (LACDR), Leiden University (Leiden, The Netherlands). The research was financially supported by Health Holland and Samen Werkende Gezondheidsfondsen (SGF), grant no. LSHM18056-SGF.

To my family

TABLE OF CONTENTS

Chapter 1	Introduction and Thesis Outline	9
Chapter 2	Tolerogenic vaccines for the treatment of cardiovascular diseases	21
Chapter 3	Immunopeptidomics analysis of human atherosclerosis plaques identifies antigenic drivers of atherosclerosis	43
Chapter 4	Liposomal Formulations loaded with Vitamin D3 Induce Regulatory Circuits in Human Dendritic Cells	69
Chapter 5	The Use of a Staggered Herringbone Micromixer for the Preparation of Rigid Liposomal Formulations Allows Efficient Encapsulation of Antigen and Adjuvant	105
Chapter 6	Surface composition of nanoparticles rather than its rigidity, affects tolerogenic behaviour <i>in vivo</i>	125
Chapter 7	Nasal subunit vaccination with cationic liposomes induces Influenza-specific resident CD8 ⁺ T cells in the airways and reduces viral burden upon infection	153
Chapter 8	General summary and future perspectives	179
Appendices		
	Nederlandse Samenvattig	196
	Curriculum Vitae	202
	List of Publications	203



Chapter 1

Introduction and Thesis Outline

INNATE AND ADAPTIVE IMMUNITY

The immune system consists of cells and organs in charge of protecting the organism against external and internal threats. The immune system can be broadly divided into two arms, the innate and adaptive immunity. The innate immunity responds quickly but it is not specific, while the adaptive immune response takes more time to be mounted but it acts in a specific manner. The main link between innate and adaptive immune responses are antigen-presenting cells (APCs) such as dendritic cells (DCs). APCs can take up antigens, process them and present them on the cell surface bound to Major Histocompatibility Complex (MHC) molecules, called Human Leukocyte Antigen (HLA) in human. There are two major types of MHC molecules, MHC class I mostly presents antigens derived from proteins expressed within the cell, while MHC class II presents antigens that have been taken up from the extracellular environment. Antigens presented via MHC molecules can be recognized by cells from the adaptive immune system, such as T cells. T cells can recognize MHC-presented antigens via their T cell receptor (TCR). The vast diversity of TCRs allows the recognition of virtually any antigen that the immune system can encounter. When a T cell with a specific TCR recognizes their cognate antigen, it can undergo clonal expansion, giving rise to an antigen-specific T cell population that can react to that antigen throughout the body. When an antigen-specific T cell recognizes its target antigen it can, for example, directly kill the cell presenting that antigen or secrete molecules to potentiate the immune response. T cells can be broadly divided by the expression of two markers, cluster of differentiation 4 (CD4⁺) and cluster of differentiation 8 (CD8⁺), and therefore are called CD4⁺ T cells and CD8⁺ T cells. CD4⁺ T cells, also known as helper T cells, recognize antigens presented by MHC class II molecules, while CD8⁺ T cells, also known as cytotoxic T cells, can recognize antigens presented by MHC class I. An overactivation of the immune system in response to endogenous antigens is the root cause of autoimmune diseases such as multiple sclerosis or rheumatoid arthritis, and it also contributes to other diseases with high societal impact such as atherosclerosis, the main underlying cause of cardiovascular diseases (CVD).

ATHEROSCLEROSIS AS AN AUTOIMMUNE-LIKE DISEASE

Atherosclerosis is a chronic inflammatory disease of the arteries characterized by the accumulation of lipid-rich low-density lipoprotein (LDL) particles in the intima layer of the arteries. This deposition of LDL triggers an immune response that leads to the infiltration and accumulation of immune cells in the lesion site. The growth of the atherosclerotic lesions can narrow the arterial lumen, restricting blood flow towards certain parts of the body. Furthermore, the lesion can eventually rupture

generating a thrombus that can lead to myocardial infarction or stroke. The role of the immune system in the development of atherosclerosis has traditionally been underappreciated compared to the role of lipid metabolism, however several lines of evidence highlight the importance of immunity in both the initiation and progression of atherosclerosis¹⁻⁴. One of the key players are T cells, with both CD4⁺ and CD8⁺ T cells found in atherosclerosis plaques of CVD patients^{5, 6}.

The role played by the different T cell subsets in atherosclerosis is, to this day, subject of intensive research. In the case of CD8⁺ T cells some evidence points towards pro-atherogenic role⁷ while other studies suggest an atheroprotective role^{8, 9}. The different subpopulations of CD4⁺ T cells are also known to have different functions in the development of atherosclerosis lesions. T helper 1 (Th1) CD4⁺ T cells are pro-inflammatory T cells that exert their function by releasing pro-inflammatory cytokines such as IFN γ that contributes to the activation of macrophages and further increases the inflammatory response^{10, 11}. The pro-atherogenic or anti-atherogenic role of T helper 2 (Th2) cells is still controversial. The main cytokine produced by Th2 cells is IL-4 which can counteract the effect of atherogenic Th1 responses¹² however other experiments in mice have shown that the depletion of IL-4 reduced atherosclerosis plaque formation¹³. On the other hand, Th2 cells also produce IL-10, IL-5 or IL-13 and these cytokines have shown to be anti-atherogenic¹⁴⁻¹⁶. The other major subset of CD4⁺ T cells is T helper 17 (Th17) cells, seems to have different roles in human and mouse atherosclerosis. These cells mainly produce IL-17, and while studies in mouse models of atherosclerosis have shown evidence of both pro-atherogenic and anti-atherogenic functions of Th17 cells, clinical evidence from patients shows that increased levels this T cell subset and IL-17 in circulation are linked to unstable angina and acute myocardial infarction¹⁷. Finally, another key population of CD4⁺ T cells are T regulatory cells (Tregs). Tregs mostly secrete the anti-inflammatory cytokines IL-10 and TGF β and increased levels of Tregs are atheroprotective in both mice and human^{18, 19}. Tregs can be identified in mice by the expression of the transcription factor foxhead box protein P3 (FoxP3), although in human FoxP3 alone is not a reliable marker of Tregs since it is also expressed by other T cells subsets upon activation²⁰. Recent evidence suggests that Tregs can evolve from an anti-inflammatory phenotype towards a Th1/Th17 phenotype as atherosclerosis develops²¹.

Most studies that try to identify the role of different T cell subsets in atherosclerosis do not take into account the antigen-specificity of the response and that might lead to apparently contradictory functions of the same T cell population. T cells specific for an atherosclerosis-relevant antigen could potentially have different effect on atherosclerosis compared to T cells targeting other antigens. T cells exert their function upon recognition of their target antigen, therefore the antigen-specificity of

T cell responses is key to unveil the role of each T cell population in atherosclerosis. Despite intensive research, the driving antigens of the immune responses in atherosclerosis are not fully elucidated. Recent single-cell TCR sequencing data showed presence of clonally expanded CD4⁺ T cells in the plaque, suggesting antigen-specific T cell activation. Furthermore, these expanded CD4⁺ T cells also expressed markers of recent T cell activation such as CD69, indicating that T cell activation occurs in the plaque. These data also showed an important overlap in the gene expression of T cells in plaques and T cells isolated from the synovial fluid of patients with psoriatic arthritis, a known autoimmune disease²². These results provide evidence of the long suspected autoimmune component of atherosclerosis. The potential target antigens for autoimmunity in atherosclerosis include heat-shock proteins (HSP)^{23, 24} and β 2-Glycoprotein I (β 2GPI)²⁵, however the main suspect is ApolipoproteinB-100 (ApoB100), the main protein in LDL particles. The presence of antibodies and T cells against ApoB100 has been shown in both mouse models of atherosclerosis and in patients samples^{26, 27}. These new insights into the role of autoimmunity in atherosclerosis could inform the development of new therapeutic approaches for the treatment of CVDs.

NEW THERAPEUTIC APPROACHES IN ATHEROSCLEROSIS

Since atherosclerosis has been traditionally considered a disease related to lipid metabolism, and more specifically to dysregulated LDL levels, the main therapeutic approach has targeted the high levels of LDL in patients. Lipid-lowering drugs, such as statins or proprotein convertase subtilisin/kexin type 9 (PCSK9) inhibitors, are very effective at reducing LDL levels and the risk of cardiovascular disease^{28, 29}, however they do not target the important inflammatory component of atherosclerosis. In fact, patients undergoing intensive lipid-lowering therapy still present significant risk of suffering a cardiovascular event³⁰. New therapeutic interventions that target the immune response in atherosclerosis could be the next frontier to significantly reduce the incidence of cardiovascular diseases. The Canakinumab Anti-Inflammatory Thrombosis Outcome Study (CANTOS) clinical trial showed that targeting inflammation is effective at reducing the risk of cardiovascular events in patients using standard lipid-lowering therapies but with elevated inflammatory markers³¹. This trial, however, also showed that the chronic use of therapies that dampen the overall immune response of patients leads to higher risk of fatal infections that can overshadow the benefits. The induction of antigen-specific immune tolerance mediated by Tregs could harness the advantages of anti-inflammatory therapies while avoiding the unwanted side effects of systemic immune suppression.

Several approaches are in development for the induction of antigen-specific immune tolerance for the treatment of autoimmune diseases, such as the administration of glycosylated autoantigens or the delivery of the target antigens using tolerogenic nanoparticles^{32, 33}. Nanoparticles can be used to deliver antigens to antigen-presenting cells and therefore induce an antigen-specific immune response (Figure 1). In the case of vaccines to treat inflammatory and/or autoimmune diseases, nanoparticles can be used to co-deliver a target auto-antigen and a tolerogenic adjuvant. Furthermore, certain nanoparticles such as liposomes are versatile systems that can drive the immune response towards a proinflammatory or an anti-inflammatory response depending on their physicochemical characteristics³⁴. Liposomes are nanometric delivery systems consisting of a phospholipid bilayer enclosing an aqueous core. The phospholipid composition determines physicochemical properties of the nanoparticle such as surface charge and rigidity but also the set of proteins that will interact with the nanoparticle in a biological fluid, also known as protein corona³⁵. In turn, the physicochemical properties and the protein corona will determine the immune response elicited by the nanoparticles. For example, cationic liposomes are known to induce potent pro-inflammatory responses that can target and eliminate tumour cells³⁶. On the other hand, highly rigid anionic liposomes are known to have anti-inflammatory properties and are able to induce antigen-specific immune tolerance mediated by Tregs³⁷.

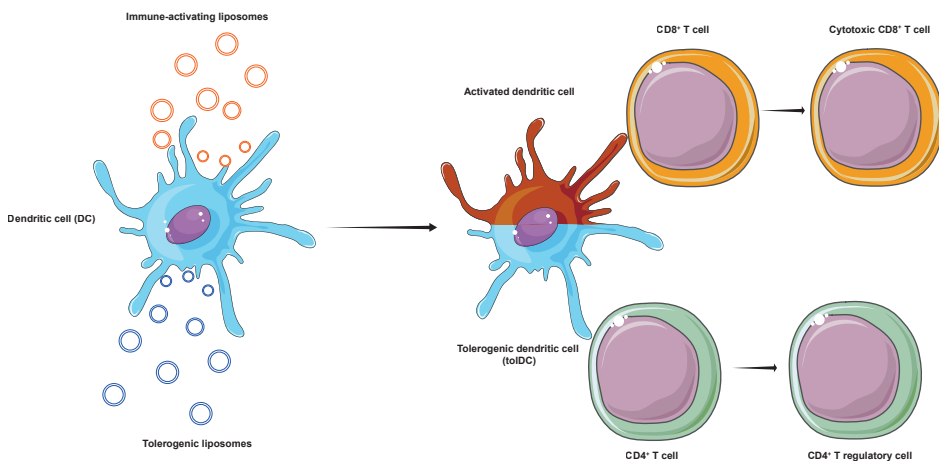


Figure 1. Overview of induction of pro-inflammatory or tolerogenic responses by dendritic cells (DCs) primed by different type of liposomes. The delivery of antigens to the DCs using immune-activating liposomes, such as cationic liposomes, leads to the generation of an antigen-specific cytotoxic CD8+ T cell response, useful to fight viral infections. The delivery of antigens to DCs using tolerogenic anionic liposomes leads to the generation of CD4+ T regulatory cell responses, useful to temper down immunity in the context of autoimmune diseases.

The preparation of highly rigid liposomes requires the use of phospholipids with high transition temperature, such as 1,2-distearoyl-sn-glycero-3-phosphocholine (DSPC) and 1,2-distearoyl-sn-glycero-3-phospho-(1'-rac-glycerol) (DSPG). These two phospholipids have a transition temperature of 55°C therefore the preparation of liposomes containing these lipids requires working at temperatures above 55°C. At a lab-scale, the most common methods to prepare these formulations is the lipid film hydration method followed by extrusion³⁸. This method consists of the generation of a suspension of multilamellar vesicles by hydration of a dry lipid film. This suspension is subsequently forced through filters with increasingly smaller pore sizes to obtain a monodisperse formulation with the desired particle size, usually in the range of 100-200 nm. This preparation method presents several disadvantages such batch-to-batch variability and poor scalability due to the need of extrusion at high pressure and temperature, therefore new preparation methods are needed to further develop these formulations beyond pre-clinical testing. Microfluidic systems for the preparation of nanoparticles have been extensively studied in the last few years and this has led to the development of commercial microfluidic-based platforms for nanoparticle production³⁹. Microfluidic systems allow the production of nanoparticle formulations in a continuous manner therefore one of the advantages of these systems is the scale-up potential⁴⁰.

Besides the production of tolerogenic liposomal formulations in large-scale, the translation of results from *in vitro* efficacy studies to *in vivo* and from animal models to human remain a challenge. The translation from *in vitro* to *in vivo* can be hindered by the very different biological environment in cell culture medium versus the mouse biological fluids. The difference in protein composition in these different environments can lead to the formation of significantly different protein coronas, that can in turn lead to different biological effects⁴¹. On the other hand, the translation of tolerogenic formulations from animal models, such as mice, to human is particularly challenging due to key differences in dendritic cells and Tregs in both organisms, therefore the use of human *in vitro* and *ex vivo* systems during pre-clinical testing of tolerogenic nanoparticle formulations is key.

LIPOSOMES AS IMMUNE POTENTIATORS IN PROPHYLACTIC VACCINES

In contrast to anionic liposomes, cationic liposomes are known for their immune activating properties, therefore these lipid nanoparticles can be used as prophylactic vaccines against infectious diseases. The induction of local anti-viral immune responses in the airways through vaccination is key for protection against respiratory viruses, such as SARS-CoV2 or influenza, however this has proven to

be difficult to achieve using subunit vaccines, the safest and easiest to manufacture type of vaccines available nowadays⁴². The use of cationic liposomes to co-deliver antigens and adjuvants such as cyclic-dimeric guanosine monophosphate (c-di-GMP) has been studied before as a therapeutic anti-cancer vaccine, and it has shown to induce potent antigen-specific CD8⁺ T cell responses⁴³. Furthermore, the cationic surface charge of these liposomes makes them suitable for intranasal delivery due to the favourable electrostatic interaction with the airways mucosa⁴⁴. The combination of immune activating properties and the mucosal delivery of these formulations would make them an ideal subunit vaccine to induce local immune responses in the airways.

This thesis aims to advance the field of nanoparticle-based tolerogenic vaccines for the treatment of atherosclerosis. We examined three key aspects of these formulations including the elucidation of target antigens for these vaccines and the study of liposome-based and polymer-lipid hybrids for antigen delivery. Additionally, we developed a microfluidic method for the preparation of tolerogenic liposomal formulations, which allows for efficient encapsulation of peptide antigens and vitaminD3. Furthermore, we explore the use of liposomes to modulate the immune response towards activation and induction of protective anti-viral immunity.

THESIS OUTLINE

In **chapter 2**, we review the state of development of tolerogenic vaccines to treat cardiovascular disease. We summarized the lessons learned on the development of tolerogenic therapies for other inflammatory and autoimmune diseases such as rheumatoid arthritis, type 1 diabetes, or multiple sclerosis, and analysed the pre-clinical data available on the use of peptide-based vaccines to halt the development of atherosclerosis. Furthermore, we highlight the main challenges in the clinical translation of this therapeutic approach, such as the selection of the appropriate antigens, formulations, and target patient population for clinical trials. In **chapter 3**, we identify possible candidates for tolerogenic vaccines against atherosclerosis. To that end we used immunopeptidomics to identify antigens presented by HLA molecules in human atherosclerosis plaques from patients. We selected 20 peptides derived from ApoB100 that presented a high binding affinity for a wide range of HLA types. We observed that at least 25% of atherosclerosis patients present significant CD4⁺ T cell responses against these ApoB100 peptides and that the level of T cell responses against these antigens correlated to the vulnerability of atherosclerosis plaques. These findings make the identified ApoB100 peptides potential targets for tolerogenic vaccines against atherosclerosis. In **chapter 4**, we explore the tolerogenic capacity of previously reported DSPG liposomes in human

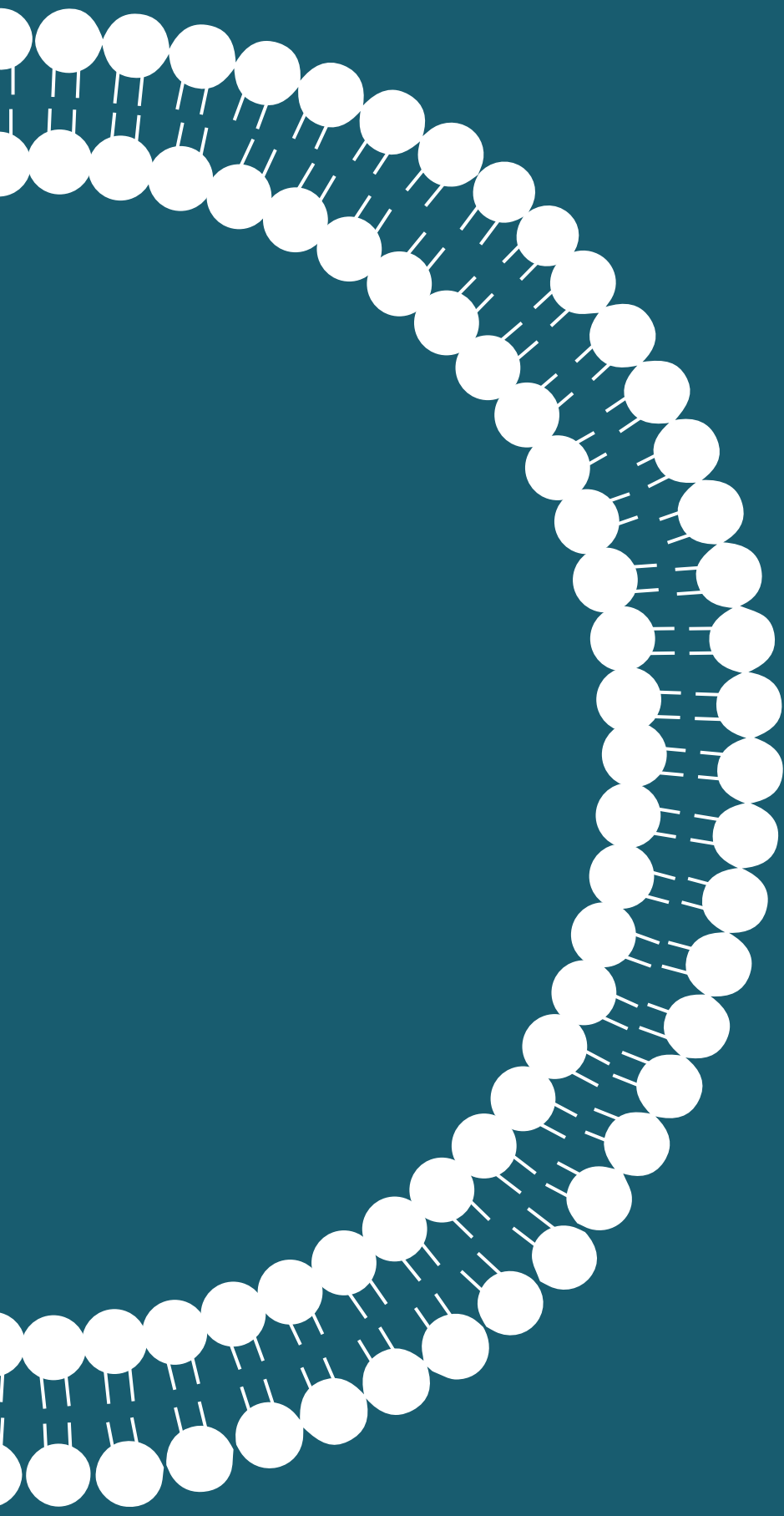
in vitro and *ex vivo* skin model and we showed that the inclusion of vitaminD3 in the anionic liposomal formulation is required to induce T regulatory cells in human experimental models. In **chapter 5**, we develop a microfluidic method to produce tolerogenic liposomes containing DSPG in a continuous and scalable manner. Furthermore, we show that this microfluidics system can be used to encapsulate the tolerogenic adjuvant vitaminD3 and ApoB100-derived immunogenic peptides with high efficiency. In **chapter 6**, we explore the role of nanoparticle rigidity in the tolerogenic capacity of formulations by comparing DSPG-containing liposomes to solid PLGA nanoparticles covered with an anionic lipid bilayer. In **chapter 7**, we use cationic liposomes loaded with peptides derived from SARS-CoV2 or influenza and the adjuvant c-di-GMP, inducing strong antigen-specific T cell responses systemically but also locally in the lungs. The T cell responses induced by vaccination with the liposome formulation correlated with lower viral load in the lungs of vaccinated mice upon viral challenge. In **chapter 8**, we summarize and discuss the main findings of this thesis.

REFERENCES

1. Libby P. Inflammation in atherosclerosis. *Nature*. 2002;420(6917):868-74.
2. Tsiantoulas D, Diehl CJ, Witztum JL, Binder CJ. B cells and humoral immunity in atherosclerosis. *Circ Res*. 2014;114(11):1743-56.
3. Ley K, Miller YI, Hedrick CC. Monocyte and macrophage dynamics during atherogenesis. *Arterioscler Thromb Vasc Biol*. 2011;31(7):1506-16.
4. Paulsson G, Zhou X, Tornquist E, Hansson GK. Oligoclonal T cell expansions in atherosclerotic lesions of apolipoprotein E-deficient mice. *Arterioscler Thromb Vasc Biol*. 2000;20(1):10-7.
5. Jonasson L, Holm J, Skalli O, Bondjers G, Hansson GK. Regional accumulations of T cells, macrophages, and smooth muscle cells in the human atherosclerotic plaque. *Arteriosclerosis*. 1986;6(2):131-8.
6. Hansson GK, Holm J, Jonasson L. Detection of activated T lymphocytes in the human atherosclerotic plaque. *Am J Pathol*. 1989;135(1):169-75.
7. Kyaw T, Winship A, Tay C, Kanellakis P, Hosseini H, Cao A, et al. Cytotoxic and proinflammatory CD8+ T lymphocytes promote development of vulnerable atherosclerotic plaques in apoE-deficient mice. *Circulation*. 2013;127(9):1028-39.
8. Chyu KY, Zhao X, Dimayuga PC, Zhou J, Li X, Yano J, et al. CD8+ T cells mediate the athero-protective effect of immunization with an ApoB-100 peptide. *PLoS One*. 2012;7(2):e30780.
9. van Duijn J, Kritikou E, Benne N, van der Heijden T, van Puijvelde GH, Kroner MJ, et al. CD8+ T-cells contribute to lesion stabilization in advanced atherosclerosis by limiting macrophage content and CD4+ T-cell responses. *Cardiovasc Res*. 2019;115(4):729-38.
10. Chen J, Xiang X, Nie L, Guo X, Zhang F, Wen C, et al. The emerging role of Th1 cells in atherosclerosis and its implications for therapy. *Front Immunol*. 2022;13:1079668.
11. Voloshyna I, Littlefield MJ, Reiss AB. Atherosclerosis and interferon-gamma: new insights and therapeutic targets. *Trends Cardiovasc Med*. 2014;24(1):45-51.
12. Davenport P, Tipping PG. The role of interleukin-4 and interleukin-12 in the progression of atherosclerosis in apolipoprotein E-deficient mice. *Am J Pathol*. 2003;163(3):1117-25.
13. King VL, Szilvassy SJ, Daugherty A. Interleukin-4 deficiency decreases atherosclerotic lesion formation in a site-specific manner in female LDL receptor-/- mice. *Arterioscler Thromb Vasc Biol*. 2002;22(3):456-61.
14. Pinderski Oslund LJ, Hedrick CC, Olvera T, Hagenbaugh A, Territo M, Berliner JA, Fyfe AI. Interleukin-10 blocks atherosclerotic events in vitro and in vivo. *Arterioscler Thromb Vasc Biol*. 1999;19(12):2847-53.
15. Binder CJ, Hartvigsen K, Chang MK, Miller M, Broide D, Palinski W, et al. IL-5 links adaptive and natural immunity specific for epitopes of oxidized LDL and protects from atherosclerosis. *J Clin Invest*. 2004;114(3):427-37.
16. Cardilo-Reis L, Gruber S, Schreier SM, Drechsler M, Papac-Milicevic N, Weber C, et al. Interleukin-13 protects from atherosclerosis and modulates plaque composition by skewing the macrophage phenotype. *EMBO Mol Med*. 2012;4(10):1072-86.
17. Cheng X, Yu X, Ding YJ, Fu QQ, Xie JJ, Tang TT, et al. The Th17/Treg imbalance in patients with acute coronary syndrome. *Clin Immunol*. 2008;127(1):89-97.

18. Ait-Oufella H, Salomon BL, Potteaux S, Robertson AK, Gourdy P, Zoll J, et al. Natural regulatory T cells control the development of atherosclerosis in mice. *Nat Med*. 2006;12(2):178-80.
19. George J, Schwartzberg S, Medvedovsky D, Jonas M, Charach G, Afek A, Shamiss A. Regulatory T cells and IL-10 levels are reduced in patients with vulnerable coronary plaques. *Atherosclerosis*. 2012;222(2):519-23.
20. Roncarolo MG, Gregori S. Is FOXP3 a bona fide marker for human regulatory T cells? *Eur J Immunol*. 2008;38(4):925-7.
21. Wolf D, Gerhardt T, Winkels H, Michel NA, Pramod AB, Ghosheh Y, et al. Pathogenic Autoimmunity in Atherosclerosis Evolves From Initially Protective Apolipoprotein B(100)-Reactive CD4(+) T-Regulatory Cells. *Circulation*. 2020;142(13):1279-93.
22. Depuydt MAC, Schaftenaar FH, Prange KHM, Boltjes A, Hemme E, Delfos L, et al. Single-cell T cell receptor sequencing of paired human atherosclerotic plaques and blood reveals autoimmune-like features of expanded effector T cells. *Nature Cardiovascular Research*. 2023.
23. Wick G, Jakic B, Buszko M, Wick MC, Grundtman C. The role of heat shock proteins in atherosclerosis. *Nat Rev Cardiol*. 2014;11(9):516-29.
24. Almanzar G, Ollinger R, Leuenberger J, Onestingel E, Rantner B, Zehm S, et al. Autoreactive HSP60 epitope-specific T-cells in early human atherosclerotic lesions. *J Autoimmun*. 2012;39(4):441-50.
25. George J, Harats D, Gilburd B, Afek A, Levy Y, Schneiderman J, et al. Immunolocalization of beta2-glycoprotein I (apolipoprotein H) to human atherosclerotic plaques: potential implications for lesion progression. *Circulation*. 1999;99(17):2227-30.
26. Bjorkbacka H, Alm R, Persson M, Hedblad B, Nilsson J, Fredrikson GN. Low Levels of Apolipoprotein B-100 Autoantibodies Are Associated With Increased Risk of Coronary Events. *Arterioscler Thromb Vasc Biol*. 2016;36(4):765-71.
27. Marchini T, Hansen S, Wolf D. ApoB-Specific CD4(+) T Cells in Mouse and Human Atherosclerosis. *Cells*. 2021;10(2).
28. Cheung BM, Lauder IJ, Lau CP, Kumana CR. Meta-analysis of large randomized controlled trials to evaluate the impact of statins on cardiovascular outcomes. *Br J Clin Pharmacol*. 2004;57(5):640-51.
29. Sabatine MS, Giugliano RP, Keech AC, Honarpour N, Wiviott SD, Murphy SA, et al. Evolocumab and Clinical Outcomes in Patients with Cardiovascular Disease. *N Engl J Med*. 2017;376(18):1713-22.
30. Murphy SA, Cannon CP, Wiviott SD, McCabe CH, Braunwald E. Reduction in recurrent cardiovascular events with intensive lipid-lowering statin therapy compared with moderate lipid-lowering statin therapy after acute coronary syndromes from the PROVE IT-TIMI 22 (Pravastatin or Atorvastatin Evaluation and Infection Therapy-Thrombolysis In Myocardial Infarction 22) trial. *J Am Coll Cardiol*. 2009;54(25):2358-62.
31. Ridker PM, Everett BM, Thuren T, MacFadyen JG, Chang WH, Ballantyne C, et al. Antiinflammatory Therapy with Canakinumab for Atherosclerotic Disease. *N Engl J Med*. 2017;377(12):1119-31.
32. Tremain AC, Wallace RP, Lorentz KM, Thornley TB, Antane JT, Raczy MR, et al. Synthetically glycosylated antigens for the antigen-specific suppression of established immune responses. *Nat Biomed Eng*. 2023.

33. Krienke C, Kolb L, Diken E, Streuber M, Kirchhoff S, Bukur T, et al. A noninflammatory mRNA vaccine for treatment of experimental autoimmune encephalomyelitis. *Science*. 2021;371(6525):145-53.
34. Benne N, van Duijn J, Kuiper J, Jiskoot W, Slutter B. Orchestrating immune responses: How size, shape and rigidity affect the immunogenicity of particulate vaccines. *J Control Release*. 2016;234:124-34.
35. Pattipeiluhu R, Crielgaard S, Klein-Schiphorst I, Florea BI, Kros A, Campbell F. Unbiased Identification of the Liposome Protein Corona using Photoaffinity-based Chemoproteomics. *ACS Cent Sci*. 2020;6(4):535-45.
36. Varypataki EM, Benne N, Bouwstra J, Jiskoot W, Ossendorp F. Efficient Eradication of Established Tumors in Mice with Cationic Liposome-Based Synthetic Long-Peptide Vaccines. *Cancer Immunol Res*. 2017;5(3):222-33.
37. Benne N, van Duijn J, Lozano Vigario F, Leboux RJT, van Veelen P, Kuiper J, et al. Anionic 1,2-distearoyl-sn-glycero-3-phosphoglycerol (DSPG) liposomes induce antigen-specific regulatory T cells and prevent atherosclerosis in mice. *J Control Release*. 2018;291:135-46.
38. Zhang H. Thin-Film Hydration Followed by Extrusion Method for Liposome Preparation. *Methods Mol Biol*. 2017;1522:17-22.
39. Zhang H, Yang J, Sun R, Han S, Yang Z, Teng L. Microfluidics for nano-drug delivery systems: From fundamentals to industrialization. *Acta Pharm Sin B*. 2023;13(8):3277-99.
40. Jahn A, Stavis SM, Hong JS, Vreeland WN, DeVoe DL, Gaitan M. Microfluidic mixing and the formation of nanoscale lipid vesicles. *ACS Nano*. 2010;4(4):2077-87.
41. Lee SY, Son JG, Moon JH, Joh S, Lee TG. Comparative study on formation of protein coronas under three different serum origins. *Biointerphases*. 2020;15(6):061002.
42. Burchill MA, Tamburini BA, Pennock ND, White JT, Kurche JS, Kedl RM. T cell vaccinology: exploring the known unknowns. *Vaccine*. 2013;31(2):297-305.
43. Benne N. Vaccination and targeted therapy using liposomes: opportunities for treatment of atherosclerosis and cancer. The Netherlands: Leiden University; 2020.
44. Leal J, Smyth HDC, Ghosh D. Physicochemical properties of mucus and their impact on transmucosal drug delivery. *Int J Pharm*. 2017;532(1):555-72.



Chapter 2

Tolerogenic vaccines for the treatment of cardiovascular diseases

Fernando Lozano Vigario¹, Johan Kuiper¹, Bram Slütter¹

¹Division of BioTherapeutics, Leiden Academic Centre for Drug Research,
Leiden University, Leiden, The Netherlands

Adapted from EBioMedicine, Volume 57, July 2020, 10.1016/j.ebiom.2020.102827

ABSTRACT

Atherosclerosis is the main pathology behind most cardiovascular diseases. It is a chronic inflammatory disease characterized by the formation of lipid-rich plaques in arteries. Atherosclerotic plaques are initiated by the deposition of cholesterol-rich LDL particles in the arterial walls leading to the activation of innate and adaptive immune responses. Current treatments focus on the reduction of LDL blood levels using statins; however, the critical components of inflammation and autoimmunity have been mostly ignored as therapeutic targets. The restoration of immune tolerance towards atherosclerosis-relevant antigens can arrest lesion development as shown in pre-clinical models. In this review, we evaluate the clinical development of similar strategies for the treatment of inflammatory and autoimmune diseases like rheumatoid arthritis, type 1 diabetes or multiple sclerosis and analyse the potential of tolerogenic vaccines for atherosclerosis and the challenges that need to be overcome to bring this therapy to patients.

Keywords

Atherosclerosis, Inflammation, Tolerance, Vaccination

INFLAMMATION AND AUTOIMMUNITY IN ATHEROSCLEROSIS

Atherosclerosis is the main underlying cause of acute cardiovascular events such as myocardial infarction or stroke¹. Traditionally, atherosclerosis has been primarily considered a pathology related to dyslipidaemia, therefore lipid-lowering therapies such as statins have been the mainstream option for prevention of cardiovascular events. However, in recent years several lines of evidence have highlighted the importance of the immune component of atherosclerosis². The development of an atherosclerotic lesion initiates with the infiltration of lipoproteins, mainly low-density lipoproteins (LDL), from the blood into the intima of the arteries. The infiltration and accumulation of LDL particles into the arterial intima leads to the chemical modification of some components of the lipoprotein and the formation of modified LDL, mainly oxidized LDL (oxLDL). The presence of oxLDL in the sub-endothelial space of the artery triggers an inflammatory response that involves both the innate and the adaptive arms of the immune system³.

The initial accumulation of oxLDL leads to the over-expression of adhesion molecules in endothelial cells, promoting the infiltration of monocytes from the blood. These monocytes will differentiate into macrophages, which phagocytose LDL particles and eventually become foam cells, characterized by the presence of large cholesteryl esters deposits in the cytoplasm and the secretion of pro-inflammatory cytokines like IL-1 β ⁴.

Other innate immune cells such as dendritic cells (DCs) play an important role in the development of the plaque. DCs, a subset of antigen-presenting cells, are the link between the innate and the adaptive immune responses. DCs in the atherosclerotic plaque phagocytose antigens such as LDL from the environment, process them and present small ApoB100-derived peptides bound to Major Histocompatibility Complex (MHC) molecules in their surface. These cells mostly migrate to draining lymph nodes, present ApoB100 peptides to naïve T cells and stimulate their differentiation and expansion into antigen-specific effector T cells. In the plaque, these effector T cells will recognize the antigens presented by antigen-presenting cells, releasing pro-inflammatory cytokines such as IFN- γ that contribute to the development of the lesion^{5, 6}.

There are several subsets of effector T cells with a role in atherosclerosis. T helper (Th) CD4⁺ cells form a major population in the plaque next to CD8⁺ T cells⁷. The different subsets of Th cells might have completely different roles in the development of atherosclerosis. For instance, Th1 cells have a pro-atherogenic effect due to the secretion of pro-inflammatory cytokines, mainly IFN- γ ⁸. On the other hand, T regulatory cells (Tregs) are a subset of Th cells that are thought to have anti-atherogenic functions as lower frequency and functional impairment of

Tregs have been observed in patients with coronary artery disease^{9, 10}. Tregs can suppress effector T cells, such as Th1 cells, and therefore control inflammatory responses.

The important role of LDL in the initiation of atherosclerotic lesions, the presence of both auto-reactive T and B cells as well as anti-oxLDL antibodies has led to the notion of the autoimmune component of atherosclerosis^{11, 12}. Interestingly, there is a well-defined correlation between autoimmune disorders and the development of atherosclerosis¹³. For instance, rheumatoid arthritis patients have a higher risk of cardiovascular disease and have a 1.5 to 2-times higher rate of cardiovascular events than the general population¹⁴.

The importance of the immune component of atherosclerosis is evidenced by the presence of residual cardiovascular risk in a significant percentage of patients undergoing lipid-lowering therapies, highlighting the need of novel approaches in the treatment of cardiovascular diseases (CVD)¹⁵.

ANTI-INFLAMMATORY THERAPIES IN CLINICAL TRIALS

Despite the widespread use of statins, cardiovascular diseases are still the number 1 cause of death globally. This can be partially explained by the presence of the significant residual cardiovascular risk observed in patients even under intensive statin treatment and low levels of LDL¹⁶. Randomized clinical trials have shown that the frequency of cardiovascular events is lower in patients with low levels of high-sensitivity C-reactive protein (hsCRP), a biomarker of inflammation¹⁷. These observations suggest that targeting inflammation in atherosclerosis might contribute further to the reduction in cardiovascular risk¹⁸.

Targeting pro-inflammatory cytokines to reduce the residual inflammatory risk of cardiovascular events is a strategy that has been studied in clinical trials. The CANTOS (Canakinumab Antiinflammatory Thrombosis Outcome Study) trial assessed the efficacy of the anti-IL1 β human monoclonal antibody canakinumab to prevent vascular events in patients with previous history of myocardial infarction and presenting high levels of hsCRP marker. IL-1 β , a pro-inflammatory cytokine, triggers the upregulation of inflammatory markers and adhesion molecules in endothelial cells, promotes the recruitment of immune cells to the atherosclerotic plaque and induces smooth muscle cell proliferation^{19, 20}. Altogether, this contributes to the initiation and development of atherosclerosis plaques²¹. Patients included in the CANTOS trial had undergone aggressive secondary prevention therapies including high dose of statins. The results showed that the treatment with 150 mg of Canakinumab once every 3 months leads to a 15% reduction in the incidence of

non-fatal myocardial infarction, non-fatal stroke or cardiovascular death compared to placebo. The results also showed a significant reduction in the inflammatory biomarkers hsCRP and IL-6 but no effects on LDL or HDL levels, therefore the clinical benefit could be attributed to the attenuated inflammation²². The results from this study point out to the importance of targeting the cardiovascular risk associated to inflammation in addition to the reduction of LDL cholesterol levels.

Similarly, results from COLCOT (Colchicine Cardiovascular Outcomes Trial) have shown that low doses of colchicine (0.5 mg/day), a potent anti-inflammatory drug, led to a significant reduction in the risk of death from cardiovascular causes, resuscitated cardiac arrest, myocardial infarction, stroke and angina compared to the placebo group²³.

Another approach to target inflammation in atherothrombosis is the use of low doses of methotrexate. Low-dose methotrexate is already used in the treatment of certain inflammatory conditions and observational studies have associated this treatment with lower frequency of cardiovascular events²⁴. However, in the Cardiovascular Inflammation Reduction Trial (CIRT), low-dose methotrexate did not reduce the levels of inflammatory biomarkers IL-1 β , IL-6 or CRP in patients with previous history of myocardial infarction or coronary disease and did not reduce the frequency of nonfatal myocardial infarction, nonfatal stroke, cardiovascular death or unstable angina²⁵.

The apparent contradictory results from CANTOS, COLCOT and CIRT studies highlight the complexity of the inflammatory pathways involved and the importance of taking this into consideration when designing anti-inflammatory interventions for cardiovascular diseases.

ANTIGEN-SPECIFIC TOLERANCE IN INFLAMMATORY AND AUTOIMMUNE DISEASES

The presented therapeutic strategies induce a systemic anti-inflammatory state that can have important side effects in the long term, such as higher risk of infections, as shown in both the CANTOS and the COLCOT trials^{22, 23, 26}. An alternative approach to the use of systemic anti-inflammatory molecules could be the induction of antigen-specific tolerance towards disease-specific autoantigens. This approach has been translated into clinical trials for diseases such as rheumatoid arthritis (RA), type 1 diabetes (T1D) and multiple sclerosis (MS) but has not been clinically applied for treatment of CVD. Lessons learned from these clinical trials can help to advance the application of this strategy in CVD.

Two main approaches for the induction of antigen-specific immune tolerance have been studied so far in clinical trials. One is the administration of tolerogenic dendritic cells (tolDCs) or Tregs with capacity to induce immune tolerance. Another approach is the administration of autoantigens at low doses, together with tolerogenic adjuvants or using tolerogenic administration routes.

An example of the former is a phase I clinical trial that studied the safety of the administration of tolDCs loaded with autoantigens from synovial fluid for treatment of RA²⁷. For this trial, tolDCs were differentiated from peripheral blood mononuclear cells (PBMCs) from patients in the presence of dexamethasone and vitamin D3²⁸. Safety assessment was made based on the proportion of patients experiencing flares in the target knee within 5 days after administration of tolDCs. None of the patients reported aggravated symptoms indicating that the therapy is safe. Furthermore, an exploratory efficacy assessment showed symptoms resolution in 2 out of 3 patients receiving the highest cell dose.

In another phase I clinical trial, the safety and biological activity of autologous tolDCs loaded with the citrullinated peptides relevant for RA were administered intradermally to RA patients²⁹. The safety of the treatment was confirmed as only mild adverse effects were detected. Furthermore, the results showed a decrease in the levels of CRP and pro-inflammatory cytokines and a reduction in the population of effector T cells. Unfortunately, clinical efficacy was not evaluated in this trial, mainly due to the low number of patients included in the trial. This limitation was related to the high costs associated to the manufacture of autologous tolDCs, one of the main drawbacks of cell-based therapies.

The administration of autologous tolDC also appeared to be safe and well-tolerated in a phase I clinical trial in T1D³⁰. Safety was evaluated not only based on the presence of adverse reactions, but also by measuring the presence in serum of autoantibodies and cytokines different to those usually present in T1D and following changes in immune cell populations with flow cytometry. Patients received intradermal injection of 1×10^7 cells either not manipulated or differentiated into tolDCs. The results from the trial did not show any noticeable adverse effect on patients, neither significant change in immune cell populations.

Another cell-based strategy to induce tolerance is the administration of Tregs. In a phase I clinical trial for T1D, the administration of autologous polyclonal Tregs showed that the therapy was well tolerated, and no major adverse reactions were observed³¹. Clinical parameters like c-peptide levels, insulin use and haemoglobin A1c levels were included as secondary outcomes in the study. However, due to the reduced number of patients enrolled in the study (16 patients in 4 dose cohorts), no assessment of the clinical efficacy of the treatment could be done. Previous reports

have highlighted potential problems with Treg cell therapies regarding phenotypic changes in the Tregs, switching from an anti-inflammatory to a pro-inflammatory phenotype or the contamination with effector T cells that could aggravate the disease^{32, 33}. Therefore, in this study, the stability of the Treg phenotype after *in vitro* expansion and the suppressive activity of the Tregs before the administration had to be closely monitored.

The other approach for the induction of antigen-specific tolerance is the use of peptides. A clinical trial in RA have studied the efficacy of tolerance induction towards heat-shock proteins (HSP). HSP are naturally produced by cells under certain stress situations such as inflammation. The release of HSP by stressed cells induces an anti-inflammatory response mediated by HSP-specific Tregs in order to control the inflammatory process³⁴. In a phase II trial, RA patients received an oral dose of the HSP40-derived peptide dnaJP1 to induce mucosal tolerance. The peptide dnaJP1 has been previously identified as an important T cell epitope in RA³⁵. The results showed a significant improvement in clinical response, defined by a reduction in swollen joints, pain, disability and/or acute phase reactant levels, in the group treated with dnaJP1 compared to placebo. Furthermore, this improvement was accompanied by a reduced production of pro-inflammatory TNF α in *ex vivo* re-stimulated PBMCs³⁶.

Results of clinical trials for peptide-based treatments in T1D are also promising. In a phase Ib trial, the intradermal administration of a proinsulin peptide to T1D patients showed to be safe and well tolerated³⁷. The results showed a less pronounced loss of insulin production capacity in the treatment groups compared to the placebo group. Consequently, no significant increase in average insulin doses was observed in the treatment groups while a progressive increase was seen in the placebo group. Furthermore, treated patients showed higher levels of anti-inflammatory IL-10 production when CD4⁺ T cells were *ex vivo* stimulated with proinsulin.

In the context of MS, the application of tolerogenic vaccines has provided mixed results regarding their efficacy and tolerability. A phase II clinical trial in 2005 showed that the intravenous administration of the synthetic peptide MBP8298, derived from myelin basic protein (MBP), had a beneficial effect only in a subgroup of MS patients presenting HLA haplotypes DR2 and/or DR4. Patients receiving MBP8298 also showed a reduction in the level of anti-MBP autoantibodies, indicating tolerization towards the antigen³⁸. However, in a phase III trial, the same peptide and dosage failed to show a significant reduction in disease progression in HLA-DR2⁺ and/or HLA-DR4⁺ patients³⁹.

Cocktails of different peptides derived from MBP have performed better in clinical trials. In phase Ib and IIa clinical trials, the administration of a cocktail composed

of 4 peptides derived from MBP led to a reduced number of brain lesions compared to baseline. The trial design included a dose escalation period of 8 weeks, with peptide doses increasing from 25 μg to 800 μg followed by a full-dose (800 μg peptide cocktail) period in order to avoid unwanted T cell activation and systemic pro-inflammatory cytokine release, a common concern in these peptide-based therapies⁴⁰.

Other clinical trials have highlighted the importance of the administration route for the induction of tolerance. Oral, sublingual, nasal and dermal administration routes are the most commonly used due to the natural role of mucosal and skin immunity in tolerance induction⁴¹. For instance, the transdermal administration route has shown to be optimal to induce tolerance towards myelin peptides in MS patients. A clinical trial studied the administration of a mixture of three peptides derived from MBP, proteolipid protein (PLP) and myelin oligodendrocyte glycoprotein (MOG), to MS patients using a transdermal skin patch. Skin biopsies showed an increase in activated Langerhans cells, a type of antigen-presenting cells found in the skin, and an increase in DCs in draining lymph nodes in patients receiving the peptides mixture compared to the placebo group. The treatment also attenuated the proliferative response of CD4⁺ T cells, an increased production of IL-10 and a decrease in IFN- γ production upon *ex vivo* re-stimulation with the peptides. The study however did not include any clinical endpoints to assess the effect of the treatment in the progression of the disease⁴².

Overall, the clinical trials have shown that tolerance induction is a feasible approach that can attenuate some of the pro-inflammatory responses present in diseases such as RA, T1D or MS but they have also shown the limitations of both peptide-based and cell-based therapies (Table 1). Peptide-based approaches present advantages such as relatively straight-forward development of stable formulations of peptides thanks to the extensive work carried out in the formulation of subunit vaccines for infectious disease as well as the lower cost of manufacture compared to cell-based therapies and often admit more convenient administration routes such as oral or intradermal. But this strategy also presents some disadvantages, for instance the dose should be carefully selected as too high doses can induce unwanted pro-inflammatory responses while too low doses will not have the desired tolerogenic effect. Furthermore, the proteolytic degradation of the peptide in biological fluids should also be taken into account when choosing the peptide dose. Lastly, appropriate HLA-peptide interaction is a prerequisite for the effectivity of peptide-based immunotherapies therefore HLA typing of patients is often required in this type of therapies, as described in the clinical trial with MBP8298 peptide³⁸. The main advantage of cell-based therapies is that the administration of tIDCs or Tregs can directly induce immune tolerance through expansion of antigen-

specific Tregs or induction of anergy in effector T cells, respectively. However, these therapies often involve the isolation of autologous cells from patients, the induction of a tolerogenic phenotype *ex vivo* and the subsequent reinfusion to the patient, which is costly and time-consuming⁴³. Furthermore, there are concerns over the variability and stability of the tolerogenic phenotype induced *ex vivo*.

Table 1. Main advantages and disadvantages of peptide-based and cell-based strategies for the induction of tolerance.

Peptide-based therapies		Cell-based therapies	
Advantages	Disadvantages	Advantages	Disadvantages
Lower cost of manufacture	HLA genotyping often required	Direct tolerance induction	Expensive and time-consuming manufacture
Stable peptide formulations are relatively straight-forward	Peptides subject to proteolytic degradation		Variability of tolerogenic phenotype
Easier administration	Doses need to be carefully selected		

The formulation of peptide-based vaccines is crucial not only for stability of the peptide but also for the induction of tolerance. The use nanoparticles as delivery systems for immune modulation is currently under investigation and has the potential to overcome some of the problems associated with peptide and cell-based therapies. For instance, the delivery of peptides using nanoparticles can prevent degradation by proteases in biological fluids, allow the specific delivery to target cells such as DCs, include tolerogenic adjuvants to induce the desired tolerogenic phenotype *in vivo* and these nanoparticle formulations can be manufacture in high volumes at lower cost than cell-based therapeutics.

TOLEROGENIC VACCINES IN ATHEROSCLEROSIS

Despite the strong evidence supporting the role of inflammation and autoimmunity in the development of atherosclerosis, to the best of our knowledge no clinical trials have been carried out to study the safety, tolerability, feasibility, or efficacy of antigen-specific tolerance induction to halt the development of atherosclerosis.

One of the obstacles in the development of vaccines for atherosclerosis is the lack of well-defined epitopes responsible for the initiation and maintenance of the inflammatory responses in atherosclerosis. However, several reports have shown that the induction of tolerance towards oxLDL and HSP attenuate atherosclerosis

in pre-clinical models⁴⁴⁻⁴⁶. Therefore, peptides derived from ApoB100 or HSP have been the main focus of attention in the search of relevant epitopes in atherosclerosis.

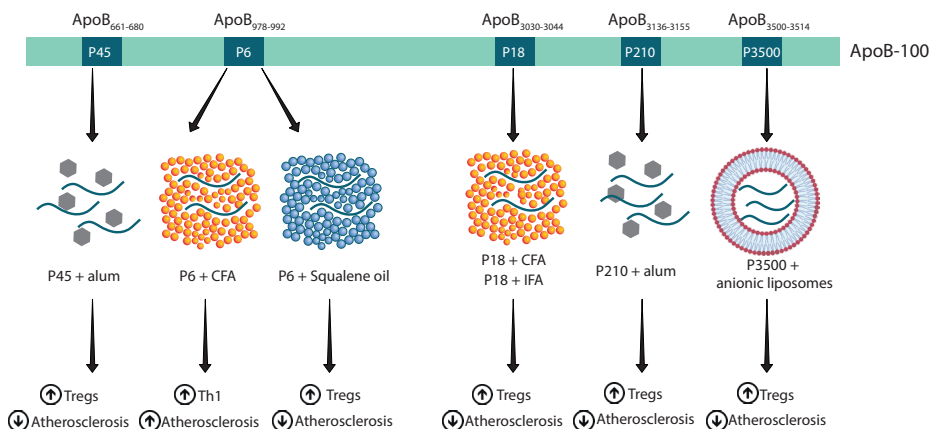


Figure 1. Summary of the effect of immunization with ApoB100-derived peptides and different adjuvants reported in literature. Alum, aluminium salt; CFA, complete Freund's adjuvant; IFA, incomplete Freund's adjuvant; Tregs, T regulatory cells; Th1, T helper cell 1.

Oral administration of oxLDL or malondialdehyde-treated LDL induced Treg-mediated tolerance in LDLR^{-/-} mice, accompanied by a significant reduction in atherosclerotic lesions initiation and progression⁴⁵. This report indicates the potential of ApoB100-derived antigens as candidates for peptide-based vaccination strategies in atherosclerosis. Figure 1 summarizes the effect on atherosclerosis of immunization with different ApoB100-derived peptides and adjuvants. Immunization of LDLR^{-/-} (LDLR^{tm1Her}) mice expressing human ApoB100 with P210 (human ApoB100₃₁₃₆₋₃₁₅₅) has shown to reduce atherosclerosis in pre-clinical studies and the mechanism of action of this therapeutic strategy has been related to the induction of Tregs. The administration of peptide P45 (human ApoB100₆₆₁₋₆₈₀) or P210 together with alum salts adjuvant has shown to reduce the area of atherosclerotic plaques by 66 and 55% respectively compared to control. The authors also speculate with the activation of Tregs as the mechanism of action mediating this anti-atherogenic effect^{47,48}. In another study, the administration of P210 without any adjuvant led to a 30% reduction in plaque size compared to control group and abrogated the growth of advanced atherosclerotic lesions. Furthermore, this effect was associated with a 30% increase in the Treg frequency in lymph nodes and Treg depletion abolished the atheroprotective effect of the immunization⁴⁹.

The immunization with peptide P6 (ApoB100₉₇₈₋₉₉₂) together with Complete Freund's adjuvant (CFA) has shown to promote atherosclerosis in murine models while the same peptide can have atheroprotective effects when administered with a different immunization regime consisting in a prime immunization with P6 in CFA followed by 4 booster immunization with Incomplete Freund's Adjuvant (IFA), known to induce suppressive immune responses⁵⁰⁻⁵². The same P6 peptide in combination with the squalene oil-based adjuvant Addavax also induced a 52% reduction in aortic lesion area in ApoE^{-/-} mice compared to peptide alone⁵³. These results highlight the importance of the careful selection of adjuvants to achieve atheroprotection.

The selection of atheroprotective peptides to be used in a tolerogenic vaccine should also consider the binding affinity to different HLA haplotypes. Peptides that can bind to a wide range of HLA haplotypes, such as peptides P265 and P295 from human ApoB100 described by Gisterå et al. would cover most of the world population⁵⁴. Similarly, peptide P18 (human ApoB100₃₀₃₀₋₃₀₄₄) was identified *in silico* and *in vitro* as a strong binder to the most common HLA-DR haplotypes. Immunization of ApoE^{-/-} mice with P18 showed an induction of Tregs and a 35% reduction in atherosclerosis lesion size⁵⁵. These studies underline the importance of taking into account the wide variability of HLA haplotypes from early phases of pre-clinical research.

The use of nanoparticles with intrinsic tolerogenic capacity, such as specific liposomal formulations, to deliver ApoB100 peptides has also shown promising results in murine models of atherosclerosis. The use of a liposomal formulation containing 1,2-distearoyl-sn-glycero-3-phosphoglycerol (DSPG) to deliver the peptide P3500 (ApoB100₃₅₀₀₋₃₅₁₄), similar to P3 peptide (ApoB100₃₅₀₁₋₃₅₁₅) previously reported to induce atheroprotection by Ley's group, showed to reduce lesion size by 50% compared to control^{51, 56}.

Other antigen candidates for immunomodulatory vaccines for atherosclerosis are HSP-derived peptides. These proteins are over-expressed under cellular stress, and they are involved in several inflammatory and autoimmune diseases including atherosclerosis^{57, 58}. HSP-specific Tregs could halt inflammation in atherosclerosis in a by-stander manner due to the constitutive over-expression of HSP in inflamed tissue. Therefore, the induction of HSP-specific Tregs could circumvent the problem of the lack of well-defined primary antigenic trigger in atherosclerosis³⁴. Vaccination studies with HSP have provided mixed results, with some showing an increase in atherosclerosis upon immunization while others showed an anti-atherogenic effect⁵⁹⁻⁶³. A key difference between these studies might be the adjuvant used. In the studies showing a pro-atherogenic effect of HSP immunization, the protein was administered together with CFA or IFA. Contrarily, the studies showing an

anti-atherogenic effect of the immunization with HSP proteins or peptides either use tolerogenic adjuvants, such as the combination of alum salts and anti-CD45RB antibodies, or are administered without adjuvants, and the effects have been linked to the induction of Tregs. Therefore, the election of the appropriate adjuvants and administration route to promote tolerance seems to be critical.

Overall, pre-clinical data supports effectiveness of tolerance induction towards atherosclerosis-relevant peptides to halt the development of atherosclerosis. The delivery of these antigens in the absence of TLR stimulation or in the presence of molecules that promote tolerance, can induce the expansion of Tregs and reduce the pro-inflammatory responses in atherosclerosis^{49, 53}.

Most of the studies have focused on arresting the development of growing atherosclerotic plaques, however the majority of clinical manifestations of atherosclerosis occur at advanced stages of the disease. Therefore, the induction of atherosclerosis lesion regression and/or plaque stabilization is clinically most relevant. The potential of Tregs to induce plaque regression and stabilization has been shown in pre-clinical animal models. It has been reported that the administration of CD3 antibodies combined with a reduction in non-HDL cholesterol levels can increase the Treg to effector T cells ratio and induce 25% regression in plaque size in a mouse model of atherosclerosis. Furthermore, this effect was abolished upon Treg depletion, indicating a critical role of Tregs in the atherosclerosis regression⁶⁴. In another study, Tregs were induced in a LDLr^{-/-} mouse model by administration of an IL-2 and anti-IL-2 antibody complex, achieving a 10-fold increase in Tregs. This Treg expansion led to stabilization of advanced atherosclerotic lesions established before starting the treatment⁶⁵. These results show the potential of tolerogenic vaccines inducing Tregs expansion to stabilize and prompt regression of atherosclerotic lesions.

CLINICAL TRANSLATION

Despite considerable pre-clinical research carried out in the field of tolerogenic vaccination for atherosclerosis, the promise of an atherosclerosis vaccine remains unfulfilled. There are several challenges in the translation from pre-clinical models to clinical trials. First of all, the animal models to study atherosclerosis exhibit important difference with the human situation. For instance, ApoB100 expressed in mice undergoes different post-translational modifications and has a different structural conformation than human expressed ApoB100, and therefore can trigger different immune responses⁶⁶. Furthermore, the immune system of mice presents considerable differences with human, such as several cytokines and immune receptors⁶⁷. The use of humanized mice that resemble more closely the human

situation, for instance expressing human ApoB100 or with humanized immune system, can overcome some of these challenges^{47, 68}.

A prerequisite for the clinical translation of this therapeutic strategy is the selection of antigen or antigens for vaccination. It is not clear whether there is a common driving antigen for all HLA haplotypes in atherosclerotic patients. Furthermore, specific subtypes of HLA, such as HLA-DRB1*01, have been associated with increased risk of coronary artery disease and myocardial infarction⁶⁹. This can be important in the selection of antigens for potential vaccine as it might be interesting to select peptides with strong binding affinity for those HLA haplotypes more prevalent in atherosclerosis patients. Therefore, it is yet to be determined if a broadly applicable vaccine can be developed or a personalized strategy should be followed instead.

The selection of the vaccine formulation is another important point to carefully consider. Initially, the most obvious formulations would include the peptide or peptides and the appropriate adjuvants, resembling formulations of subunit vaccines that have been widely investigated. Further developments should include nanoparticle formulations such as delivery systems with intrinsic tolerogenic capacity⁵⁶.

The next step is the design of clinical trials for a tolerogenic vaccine against atherosclerosis, and this will require a careful selection of the target population. Should only patients with high inflammatory risk be admitted or should any patient with clinically confirmed atherosclerosis be eligible? For this decision we should consider what design will better show the potential for this therapeutic approach. For instance, patients presenting high inflammatory risk would potentially benefit the most from the therapy and perhaps should be the focus of the first trials.

Finally, another parameter that can be challenging is the selection of the endpoints of the clinical trials. This requires the definition of biomarkers for atherosclerotic progression, regression, and cardiovascular risk. The assessment of the atherosclerotic plaque morphology, size or parameters related to plaque stability could be done using imaging techniques such as tomography, however this would represent a significant technical challenge in large clinical studies. Due to the immune-modulating nature of the therapeutic approach, the monitoring of both humoral and cellular adaptive immune responses, as well as the antigen-specificity of those responses would be necessary. Furthermore, the levels of inflammatory biomarkers like CRP or pro-inflammatory cytokines like IL-6 or IL-1 β , have shown to be good predictors of cardiovascular risk and should be used to monitor the efficacy of an atherosclerosis vaccine⁷⁰.

CONCLUSIONS

Cardiovascular diseases and their main underlying pathology, atherosclerosis, remain amongst the top causes of mortality globally. High levels of LDL cholesterol were once considered the only driving force underlying the formation and progression of atherosclerotic plaques. However, despite the broad use of lipid-lowering therapies, a significant proportion of patients remains at risk for cardiovascular complications. Recent evidence shows the importance of inflammation and a possible autoimmune component in the aetiology of atherosclerosis, but no therapies have been developed yet to target this key component of the disease. The induction of immune tolerance towards the self-antigens driving the deleterious immune responses in atherosclerosis is a promising new strategy. This can be achieved by inducing antigen-specific Tregs, which have the capacity to arrest pro-inflammatory responses and restore immune balance. In certain aspects, atherosclerosis resembles other inflammatory and autoimmune diseases like rheumatoid arthritis, multiple sclerosis, or type 1 diabetes therefore the lessons learnt in clinical trials of immune modulating vaccines for these diseases can be used to advance in the development of similar strategies for atherosclerosis. Although there are still challenges to overcome in the clinical translation of pre-clinical results, immune-modulating vaccines for atherosclerosis can represent a leap forward in the treatment of CVD.

OUTSTANDING QUESTIONS

There are several questions that still need to be addressed in order to advance in the clinical development of tolerogenic vaccines for cardiovascular disease. To start, it is still not clear what aspects and how should we improve pre-clinical models to test the efficacy of this therapeutic approach and facilitate clinical translation.

Regarding the design of vaccine formulations for tolerance induction, the most optimal tolerogenic adjuvant for human use still needs to be defined.

On the other hand, there are still aspects of immune responses in atherosclerosis that need to be elucidated, for example, is there a single antigenic determinant driving immune response? The answer to this question will determine if we can develop a widely applicable tolerogenic vaccine or if we should follow a personalised strategy instead.

Related to the design of clinical trials, the preferred target population for a tolerogenic vaccine against atherosclerosis needs to be determined as well as the endpoints of these studies. Should this strategy be aimed only to patients with high-inflammatory risk or to the general population of atherosclerosis patients? Can we

design large-scale clinical trials with endpoints that rely not only on general markers of cardiovascular disease but also on plaque morphology and immunophenotyping?

SEARCH STRATEGY AND SELECTION CRITERIA

References for this review were identified using PubMed database. Only references related to clinical trials were included for the search terms “rheumatoid arthritis”, “multiple sclerosis”, “type 1 diabetes” in combination with “vaccine”, “tolerogenic vaccine”, “T regulatory cells”, “tolerogenic dendritic cells”. Other search terms used were “atherosclerosis”, “cardiovascular disease” in combination with “vaccination”, “tolerance”, “immune response”, “antigens”, “T regulatory cells”, “tolerogenic dendritic cells” “nanoparticles”, “adjuvants”. For this second part the search was not limited to clinical trials. Only articles published in English were included with preference for articles published in the past 10 years.

AUTHORS CONTRIBUTION

FLV, JK and BS designed the concept and outline of original draft. FLV wrote the original manuscript, JK and BS reviewed and supported the editing of the original manuscript. FLV, BS and JK edited final manuscript.

DECLARATION OF COMPETING INTEREST

The authors have nothing to disclose.

FUNDING

FLV is supported by Health Holland and Samen Werkende Gezondheidsfondsen (SGF), grant no. LSHM18056-SGF. The funding source had no role in the preparation of this manuscript.

REFERENCES

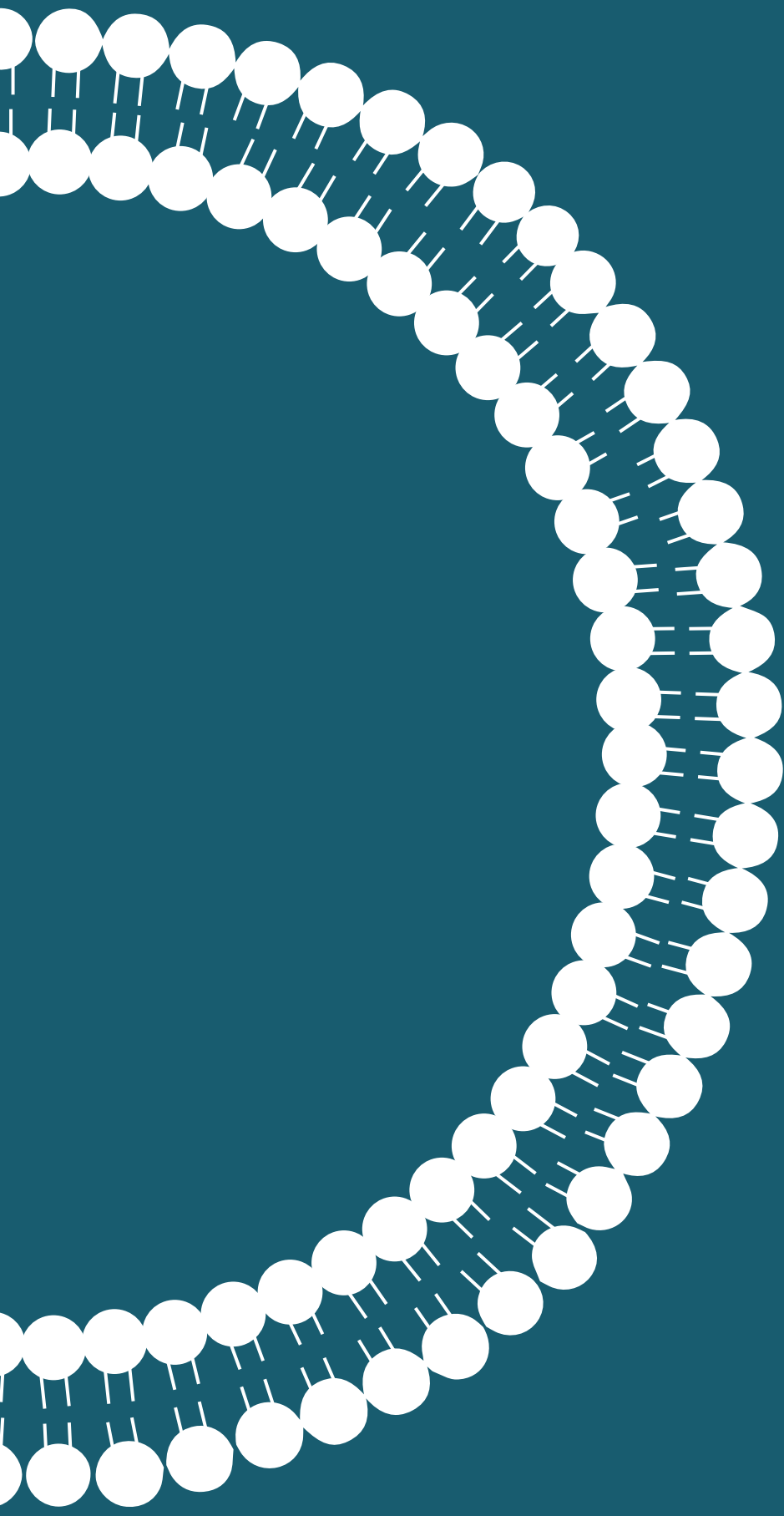
1. Herrington W, Lacey B, Sherliker P, Armitage J, Lewington S. Epidemiology of Atherosclerosis and the Potential to Reduce the Global Burden of Atherothrombotic Disease. *Circ Res*. 2016;118(4):535-46.
2. Libby P, Ridker PM, Hansson GK, Leducq Transatlantic Network on A. Inflammation in atherosclerosis: from pathophysiology to practice. *J Am Coll Cardiol*. 2009;54(23):2129-38.
3. Gistera A, Hansson GK. The immunology of atherosclerosis. *Nat Rev Nephrol*. 2017;13(6):368-80.
4. Chistiakov DA, Melnichenko AA, Myasoedova VA, Grechko AV, Orekhov AN. Mechanisms of foam cell formation in atherosclerosis. *J Mol Med (Berl)*. 2017;95(11):1153-65.
5. Witztum JL, Lichtman AH. The influence of innate and adaptive immune responses on atherosclerosis. *Annu Rev Pathol*. 2014;9(1):73-102.
6. Stemme S, Faber B, Holm J, Wiklund O, Witztum JL, Hansson GK. T lymphocytes from human atherosclerotic plaques recognize oxidized low density lipoprotein. *Proc Natl Acad Sci U S A*. 1995;92(9):3893-7.
7. van Duijn J, Kuiper J, Sluiter B. The many faces of CD8+ T cells in atherosclerosis. *Curr Opin Lipidol*. 2018;29(5):411-6.
8. Gronberg C, Nilsson J, Wigren M. Recent advances on CD4(+) T cells in atherosclerosis and its implications for therapy. *Eur J Pharmacol*. 2017;816(NA):58-66.
9. Zhu Z, Ye J, Ma Y, Hua P, Huang Y, Fu X, et al. Function of T regulatory type 1 cells is down-regulated and is associated with the clinical presentation of coronary artery disease. *Hum Immunol*. 2018;79(7):564-70.
10. Hasib L, Lundberg AK, Zachrisson H, Ernerudh J, Jonasson L. Functional and homeostatic defects of regulatory T cells in patients with coronary artery disease. *J Intern Med*. 2016;279(1):63-77.
11. Wolf D, Ley K. Immunity and Inflammation in Atherosclerosis. *Circ Res*. 2019;124(2):315-27.
12. Fredrikson GN, Hedblad B, Berglund G, Alm R, Ares M, Cercek B, et al. Identification of immune responses against aldehyde-modified peptide sequences in apoB associated with cardiovascular disease. *Arterioscler Thromb Vasc Biol*. 2003;23(5):872-8.
13. Sanjadi M, Rezvanie Sichanie Z, Totonchi H, Karami J, Rezaei R, Aslani S. Atherosclerosis and autoimmunity: a growing relationship. *Int J Rheum Dis*. 2018;21(5):908-21.
14. Crowson CS, Liao KP, Davis JM, 3rd, Solomon DH, Matteson EL, Knutson KL, et al. Rheumatoid arthritis and cardiovascular disease. *Am Heart J*. 2013;166(4):622-8 e1.
15. Ridker PM. Clinician's Guide to Reducing Inflammation to Reduce Atherothrombotic Risk: JACC Review Topic of the Week. *J Am Coll Cardiol*. 2018;72(25):3320-31.
16. Murphy SA, Cannon CP, Wiviott SD, McCabe CH, Braunwald E. Reduction in recurrent cardiovascular events with intensive lipid-lowering statin therapy compared with moderate lipid-lowering statin therapy after acute coronary syndromes from the PROVE IT-TIMI 22 (Pravastatin or Atorvastatin Evaluation and Infection Therapy-Thrombolysis In Myocardial Infarction 22) trial. *J Am Coll Cardiol*. 2009;54(25):2358-62.
17. Li Y, Zhong X, Cheng G, Zhao C, Zhang L, Hong Y, et al. Hs-CRP and all-cause, cardiovascular, and cancer mortality risk: A meta-analysis. *Atherosclerosis*. 2017;259(NA):75-82.

18. Ridker PM, Cannon CP, Morrow D, Rifai N, Rose LM, McCabe CH, et al. C-reactive protein levels and outcomes after statin therapy. *N Engl J Med*. 2005;352(1):20-8.
19. Bevilacqua MP, Pober JS, Wheeler ME, Cotran RS, Gimbrone MA, Jr. Interleukin-1 activation of vascular endothelium. Effects on procoagulant activity and leukocyte adhesion. *Am J Pathol*. 1985;121(3):394-403.
20. Eun SY, Ko YS, Park SW, Chang KC, Kim HJ. IL-1 β enhances vascular smooth muscle cell proliferation and migration via P2Y2 receptor-mediated RAGE expression and HMGB1 release. *Vascul Pharmacol*. 2015;72(NA):108-17.
21. Libby P. Interleukin-1 Beta as a Target for Atherosclerosis Therapy: Biological Basis of CANTOS and Beyond. *J Am Coll Cardiol*. 2017;70(18):2278-89.
22. Ridker PM, Everett BM, Thuren T, MacFadyen JG, Chang WH, Ballantyne C, et al. Antiinflammatory Therapy with Canakinumab for Atherosclerotic Disease. *N Engl J Med*. 2017;377(12):1119-31.
23. Tardif JC, Kouz S, Waters DD, Bertrand OF, Diaz R, Maggioni AP, et al. Efficacy and Safety of Low-Dose Colchicine after Myocardial Infarction. *N Engl J Med*. 2019;381(26):2497-505.
24. Micha R, Imamura F, Wyler von Ballmoos M, Solomon DH, Hernan MA, Ridker PM, Mozaffarian D. Systematic review and meta-analysis of methotrexate use and risk of cardiovascular disease. *Am J Cardiol*. 2011;108(9):1362-70.
25. Ridker PM, Everett BM, Pradhan A, MacFadyen JG, Solomon DH, Zaharris E, et al. Low-Dose Methotrexate for the Prevention of Atherosclerotic Events. *N Engl J Med*. 2019;380(8):752-62.
26. Bernatsky S, Hudson M, Suissa S. Anti-rheumatic drug use and risk of serious infections in rheumatoid arthritis. *Rheumatology (Oxford)*. 2007;46(7):1157-60.
27. Bell GM, Anderson AE, Diboll J, Reece R, Eltherington O, Harry RA, et al. Autologous tolerogenic dendritic cells for rheumatoid and inflammatory arthritis. *Ann Rheum Dis*. 2017;76(1):227-34.
28. Harry RA, Anderson AE, Isaacs JD, Hilken CM. Generation and characterisation of therapeutic tolerogenic dendritic cells for rheumatoid arthritis. *Ann Rheum Dis*. 2010;69(11):2042-50.
29. Benham H, Nel HJ, Law SC, Mehdi AM, Street S, Ramnorch N, et al. Citrullinated peptide dendritic cell immunotherapy in HLA risk genotype-positive rheumatoid arthritis patients. *Sci Transl Med*. 2015;7(290):290ra87.
30. Giannoukakis N, Phillips B, Finegold D, Harnaha J, Trucco M. Phase I (safety) study of autologous tolerogenic dendritic cells in type 1 diabetic patients. *Diabetes Care*. 2011;34(9):2026-32.
31. Bluestone JA, Buckner JH, Fitch M, Gitelman SE, Gupta S, Hellerstein MK, et al. Type 1 diabetes immunotherapy using polyclonal regulatory T cells. *Sci Transl Med*. 2015;7(315):315ra189.
32. Putnam AL, Brusko TM, Lee MR, Liu W, Szot GL, Ghosh T, et al. Expansion of human regulatory T-cells from patients with type 1 diabetes. *Diabetes*. 2009;58(3):652-62.
33. Kmiecik M, Gowda M, Graham L, Godder K, Bear HD, Marincola FM, Manjili MH. Human T cells express CD25 and Foxp3 upon activation and exhibit effector/memory phenotypes without any regulatory/suppressor function. *J Transl Med*. 2009;7(1):89.

34. van Eden W. Immune tolerance therapies for autoimmune diseases based on heat shock protein T-cell epitopes. *Philos Trans R Soc Lond B Biol Sci.* 2018;373(1738):20160531-NA.
35. Albani S, Keystone EC, Nelson JL, Ollier WE, La Cava A, Montemayor AC, et al. Positive selection in autoimmunity: abnormal immune responses to a bacterial dnaJ antigenic determinant in patients with early rheumatoid arthritis. *Nat Med.* 1995;1(5):448-52.
36. Koffeman EC, Genovese M, Amox D, Keogh E, Santana E, Matteson EL, et al. Epitope-specific immunotherapy of rheumatoid arthritis: clinical responsiveness occurs with immune deviation and relies on the expression of a cluster of molecules associated with T cell tolerance in a double-blind, placebo-controlled, pilot phase II trial. *Arthritis Rheum.* 2009;60(11):3207-16.
37. Alhadj Ali M, Liu YF, Arif S, Tatovic D, Shariff H, Gibson VB, et al. Metabolic and immune effects of immunotherapy with proinsulin peptide in human new-onset type 1 diabetes. *Sci Transl Med.* 2017;9(402).
38. Warren KG, Catz I, Ferenczi LZ, Krantz MJ. Intravenous synthetic peptide MBP8298 delayed disease progression in an HLA Class II-defined cohort of patients with progressive multiple sclerosis: results of a 24-month double-blind placebo-controlled clinical trial and 5 years of follow-up treatment. *Eur J Neurol.* 2006;13(8):887-95.
39. Freedman MS, Bar-Or A, Oger J, Traboulsee A, Patry D, Young C, et al. A phase III study evaluating the efficacy and safety of MBP8298 in secondary progressive MS. *Neurology.* 2011;77(16):1551-60.
40. Chataway J, Martin K, Barrell K, Sharrack B, Stolt P, Wraith DC, Group A-MS. Effects of ATX-MS-1467 immunotherapy over 16 weeks in relapsing multiple sclerosis. *Neurology.* 2018;90(11):e955-e62.
41. Tlaskalova-Hogenova H, Stepankova R, Hudcovic T, Tuckova L, Cukrowska B, Lodinova-Zadnikova R, et al. Commensal bacteria (normal microflora), mucosal immunity and chronic inflammatory and autoimmune diseases. *Immunol Lett.* 2004;93(2-3):97-108.
42. Jurynczyk M, Walczak A, Jurewicz A, Jesionek-Kupnicka D, Szczepanik M, Selmaj K. Immune regulation of multiple sclerosis by transdermally applied myelin peptides. *Ann Neurol.* 2010;68(5):593-601.
43. Yoo S, Ha SJ. Generation of Tolerogenic Dendritic Cells and Their Therapeutic Applications. *Immune Netw.* 2016;16(1):52-60.
44. Palinski W, Miller E, Witztum JL. Immunization of low density lipoprotein (LDL) receptor-deficient rabbits with homologous malondialdehyde-modified LDL reduces atherogenesis. *Proc Natl Acad Sci U S A.* 1995;92(3):821-5.
45. van Puijvelde GH, Hauer AD, de Vos P, van den Heuvel R, van Herwijnen MJ, van der Zee R, et al. Induction of oral tolerance to oxidized low-density lipoprotein ameliorates atherosclerosis. *Circulation.* 2006;114(18):1968-76.
46. van Puijvelde GH, van Es T, van Wanrooij EJ, Habets KL, de Vos P, van der Zee R, et al. Induction of oral tolerance to HSP60 or an HSP60-peptide activates T cell regulation and reduces atherosclerosis. *Arterioscler Thromb Vasc Biol.* 2007;27(12):2677-83.
47. Fredrikson GN, Bjorkbacka H, Soderberg I, Ljungcrantz I, Nilsson J. Treatment with apo B peptide vaccines inhibits atherosclerosis in human apo B-100 transgenic mice without inducing an increase in peptide-specific antibodies. *J Intern Med.* 2008;264(6):563-70.

48. Wigren M, Kolbus D, Duner P, Ljungcrantz I, Soderberg I, Bjorkbacka H, et al. Evidence for a role of regulatory T cells in mediating the atheroprotective effect of apolipoprotein B peptide vaccine. *J Intern Med.* 2011;269(5):546-56.
49. Herbin O, Ait-Oufella H, Yu W, Fredrikson GN, Aubier B, Perez N, et al. Regulatory T-cell response to apolipoprotein B100-derived peptides reduces the development and progression of atherosclerosis in mice. *Arterioscler Thromb Vasc Biol.* 2012;32(3):605-12.
50. Shaw MK, Tse KY, Zhao X, Welch K, Eitzman DT, Thipparthi RR, et al. T-Cells Specific for a Self-Peptide of ApoB-100 Exacerbate Aortic Atheroma in Murine Atherosclerosis. *Front Immunol.* 2017;8(NA):95.
51. Tse K, Gonen A, Sidney J, Ouyang H, Witztum JL, Sette A, et al. Atheroprotective Vaccination with MHC-II Restricted Peptides from ApoB-100. *Front Immunol.* 2013;4(NA):493.
52. Zamora A, Matejuk A, Silverman M, Vandenbark AA, Offner H. Inhibitory effects of incomplete Freund's adjuvant on experimental autoimmune encephalomyelitis. *Autoimmunity.* 2002;35(1):21-8.
53. Kobiyama K, Vassallo M, Mitzi J, Winkels H, Pei H, Kimura T, et al. A clinically applicable adjuvant for an atherosclerosis vaccine in mice. *Eur J Immunol.* 2018;48(9):1580-7.
54. Gistera A, Hermansson A, Strodthoff D, Klement ML, Hedin U, Fredrikson GN, et al. Vaccination against T-cell epitopes of native ApoB100 reduces vascular inflammation and disease in a humanized mouse model of atherosclerosis. *J Intern Med.* 2017;281(4):383-97.
55. Kimura T, Kobiyama K, Winkels H, Tse K, Miller J, Vassallo M, et al. Regulatory CD4(+) T Cells Recognize Major Histocompatibility Complex Class II Molecule-Restricted Peptide Epitopes of Apolipoprotein B. *Circulation.* 2018;138(11):1130-43.
56. Benne N, van Duijn J, Lozano Vigario F, Lebourg RJT, van Veelen P, Kuiper J, et al. Anionic 1,2-distearoyl-sn-glycero-3-phosphoglycerol (DSPG) liposomes induce antigen-specific regulatory T cells and prevent atherosclerosis in mice. *J Control Release.* 2018;291(NA):135-46.
57. Sedlackova L, Nguyen TT, Zlacka D, Sosna A, Hromadnikova I. Cell surface and relative mRNA expression of heat shock protein 70 in human synovial cells. *Autoimmunity.* 2009;42(1):17-24.
58. Almanzar G, Ollinger R, Leuenberger J, Onestingel E, Rantner B, Zehm S, et al. Autoreactive HSP60 epitope-specific T-cells in early human atherosclerotic lesions. *J Autoimmun.* 2012;39(4):441-50.
59. George J, Shoenfeld Y, Afek A, Gilburd B, Keren P, Shaish A, et al. Enhanced fatty streak formation in C57BL/6J mice by immunization with heat shock protein-65. *Arterioscler Thromb Vasc Biol.* 1999;19(3):505-10.
60. Xu Q, Dietrich H, Steiner HJ, Gown AM, Schoel B, Mikuz G, et al. Induction of arteriosclerosis in normocholesterolemic rabbits by immunization with heat shock protein 65. *Arterioscler Thromb.* 1992;12(7):789-99.
61. Klingenberg R, Ketelhuth DF, Strodthoff D, Gregori S, Hansson GK. Subcutaneous immunization with heat shock protein-65 reduces atherosclerosis in Apoe(-)/(-) mice. *Immunobiology.* 2012;217(5):540-7.
62. Long J, Lin J, Yang X, Yuan D, Wu J, Li T, et al. Nasal immunization with different forms of heat shock protein-65 reduced high-cholesterol-diet-driven rabbit atherosclerosis. *Int Immunopharmacol.* 2012;13(1):82-7.

63. Zhong Y, Tang H, Wang X, Zeng Q, Liu Y, Zhao XI, et al. Intranasal immunization with heat shock protein 60 induces CD4(+) CD25(+) GARP(+) and type 1 regulatory T cells and inhibits early atherosclerosis. *Clin Exp Immunol.* 2016;183(3):452-68.
64. Kita T, Yamashita T, Sasaki N, Kasahara K, Sasaki Y, Yodoi K, et al. Regression of atherosclerosis with anti-CD3 antibody via augmenting a regulatory T-cell response in mice. *Cardiovasc Res.* 2014;102(1):107-17.
65. Foks AC, Frodermann V, ter Borg M, Habets KL, Bot I, Zhao Y, et al. Differential effects of regulatory T cells on the initiation and regression of atherosclerosis. *Atherosclerosis.* 2011;218(1):53-60.
66. Wang X, Chauhan V, Nguyen AT, Schultz J, Davignon J, Young SG, et al. Immunochemical evidence that human apoB differs when expressed in rodent versus human cells. *J Lipid Res.* 2003;44(3):547-53.
67. Mestas J, Hughes CC. Of mice and not men: differences between mouse and human immunology. *J Immunol.* 2004;172(5):2731-8.
68. Proto JD, Doran AC, Subramanian M, Wang H, Zhang M, Sozen E, et al. Hypercholesterolemia induces T cell expansion in humanized immune mice. *J Clin Invest.* 2018;128(6):2370-5.
69. Paakkanen R, Lokki ML, Seppanen M, Tierala I, Nieminen MS, Sinisalo J. Proinflammatory HLA-DRB1*01-haplotype predisposes to ST-elevation myocardial infarction. *Atherosclerosis.* 2012;221(2):461-6.
70. Soeki T, Sata M. Inflammatory Biomarkers and Atherosclerosis. *Int Heart J.* 2016;57(2):134-9.



Chapter 3

Immunopectidomics analysis of human atherosclerosis plaques identifies antigenic drivers of atherosclerosis

F. Lozano Vigarío¹, I. Simó Vesperinas¹, N.S.A. Crone², M.J.M de Jong¹, E. Hemme¹, M.A.C. Depuydt¹, L. Delfos¹, J. de Mol¹, M.N. Bernabé Kleijn¹, J.A.H.M Peeters³, A. Wezel³, H.J. Smeets³, R.T.N. Tjokrodirjo⁴, A.H. de Ru⁴, A. Kros², P.H.A. Quax⁵, M.R. de Vries⁵, J. Kuiper¹, I. Bot¹, P. van Veelen⁴, B. Slütter¹

¹ Division of BioTherapeutics, Leiden Academic Centre for Drug Research, Leiden University, Leiden, the Netherlands

² Department of Supramolecular & Biomaterials Chemistry, Leiden Institute of Chemistry, Leiden University, the Netherlands

³ Department of Surgery, Haaglanden Medisch Centrum Westeinde, The Hague, the Netherlands

⁴ Center for Proteomics and Metabolomics, Leiden University Medical Center, Leiden, the Netherlands

⁵ Einthoven Laboratory for Experimental Vascular Medicine, Department of Surgery, Leiden University Medical Center, Leiden, the Netherlands

Manuscript under review

ABSTRACT

Atherosclerosis has an auto-immune component driven by self-reactive T and B cells. Identifying their antigenic drivers may lead to new diagnosis and treatment approaches. Here, we aim to identify immunogenic T cell epitopes derived from atherosclerosis-relevant proteins such as ApoB100 by studying the repertoire of peptides presented by HLA in human plaques.

We used immunopeptidomics to identify peptides presented by HLA-DR molecules in 51 plaques from patients that underwent endarterectomy surgery. We selected a set of 20 peptides derived from ApoB100 and studied the presence and cytokine profile of ApoB100-specific CD4⁺ T cells in peripheral blood mononuclear cells (PBMCs) from atherosclerosis patients. Results revealed significant CD4⁺ T cell activation in response to these ApoB100 peptides in 22.4% of the patients, and this T cell response correlated positively with plaque vulnerability. Furthermore, the cytokine profile of these cells was characterized by production of IL-10 and IL-17A but no IFN- γ .

Keywords

immunopeptidomics, PBMCs, antigen-specific T cells, ApoB100

INTRODUCTION

Atherosclerosis is an inflammatory disease of the arteries, and it is the main underlying cause of cardiovascular disease (CVD). Initially thought to be primarily a disease related to lipid metabolism, growing evidence has highlighted the important role of the immune system in the development of the disease.

The development of monoclonal antibody technology and immunohistochemistry allowed to study the cellular composition of atherosclerotic plaques. Initial studies showed the presence of activated CD8⁺ and CD4⁺ T lymphocytes and their distribution in human plaques, with about 20% of cells present in the shoulder region and the fibrous cap being T cells^{1,2}. More recently, the development of single cell sequencing technologies has allowed to identify the presence of clonally expanded T cells in atherosclerotic plaques, indicating an antigen-specific T cell response and an auto-immune component to this disease³. The interaction between the T cell receptor (TCR) and its cognate human leukocyte antigen (HLA)/peptide complex triggers the activation and proliferation of T cells, giving rise to a clonally expanded population of T cells with the same TCR. Furthermore, our lab has shown the increased expression of CD69 in CD4⁺ T cells in the plaque compared to circulation. This suggests recent antigen-specific T cell activation in the plaque and confirms the importance of antigen-specific CD4⁺ T cell immunity in atherosclerosis⁴.

Elucidating the antigen specificity of these interactions is important for the development of novel biomarkers for disease progression and novel therapeutic approaches such as therapeutic vaccines⁵. Previous work has shown that T cells in the plaque can proliferate and produce IFN- γ in response to native and oxidized LDL⁶. These data point towards the potential role of ApoB100, which is the main protein in LDL particles, as a driver of autoimmunity in atherosclerosis. Indeed, ApoB100 epitopes have been discovered using *in silico* approaches and ApoB100-specific CD4⁺ T cells have been detected in patients and associated with severity of CVD⁷. Here we propose a direct approach to identify ApoB100 epitopes that may drive CD4⁺ T cell expansion in the lesion, by performing immunopeptidomics on human atherosclerotic plaques derived from patients that underwent endarterectomy surgery. Using this approach, we established a peptide pool that allows detection of ApoB100-specific CD4⁺ T cells in PBMCs from non-HLA typed patients. Importantly, we show that the extent of the antigen-specific T cell responses associates with stability of atherosclerotic plaques.

MATERIALS & METHODS

Materials

Peptides used for proliferation experiments were synthesized in-house by solid-phase peptide synthesis (SPPS). Peptides used for CD40L expression experiments were custom-made by Genscript (Rijswijk, Netherlands). RPMI 1640 culture medium was obtained from Lonza (Basel, Switzerland). Fetal Bovine Serum (FBS) was purchased from Sigma-Aldrich (Zwijndrecht, Netherlands), penicillin/streptomycin from Fisher Scientific (Landsmeer, Netherlands) and L-glutamine was purchased from VWR (Amsterdam, Netherlands). CellTrace™ CFSE cell proliferation kit was obtained from ThermoFisher Scientific (MA, USA), concanavalinA was purchased from Invivogen (Toulouse, France), tetanus toxoid (*Clostridium tetani*) and *Staphylococcus* enterotoxin A (*Staphylococcus aureus*) were obtained from Sigma-Aldrich (Zwijndrecht, Netherlands). Recombinant human IL-2 was purchased from Roche (Mannheim, Germany).

Fluorescently labelled antibodies for flow cytometry antiCD3-PE (OK3), antiCD8-BrilliantViolet510 (SK1) and antiCD40L-APC (24-31) were purchased from Biolegend (CA, USA). AntiCD4-eFluor450 (OKT4) and Fixable Viability Dye APC-eFluor780 were obtained from eBioscience (ThermoFisher Scientific, MA, USA). AntiCD40 anti-human blocking antibody (HB14) was purchased from Miltenyi Biotec (Leiden, Netherlands).

LEGENDplex™ HU Th Cytokine Panel (12-plex) kit for quantification of IL-2, IL-4, IL-5, IL-6, IL-9, IL-10, IL-13, IL-17A, IL-17F, IL-22, IFN- γ and TNF- α was purchased from Biolegend (CA, USA).

Methods

Patient population

For immunopectidomics, human carotid and femoral atherosclerotic plaques were obtained from 51 anonymous patients that underwent primary endarterectomy surgery at the Haaglanden Medical Center, Westeinde, The Hague, The Netherlands (Cohort 1). Samples were handled in compliance with the “Code for Proper Secondary Use of Human Tissue”.

For the T cell proliferation assay, whole blood was collected from 17 patients that underwent carotid endarterectomy surgery at the Haaglanden Medical Center, Westeinde, The Hague, The Netherlands (Study approval number: 17-046, protocol number NL57482.098.17) (Cohort 2). For the CD40L expression experiment, whole blood and atherosclerotic plaques were obtained from 58 patients that underwent carotid endarterectomy surgery at the Haaglanden Medical Center, Westeinde, The Hague, The Netherlands (Study approval number: Z19.075, protocol number

NL71516.058.19). Both studies, all patients provide informed consent and were approved by the Medical Ethics Committee of the HMC, conforming to the principles outlined in the Declaration of Helsinki. All blood samples were collected by venipuncture prior to surgery. Atherosclerotic plaque specimens were obtained from primary endarterectomy surgeries, and restenotic plaques were excluded due to their different plaque composition as compared to primary atherosclerotic plaques⁸. Informed consent was obtained from all patients involved in cohort 2 and 3. Healthy volunteers were recruited from the Leiden Academic Center for Drug Research (Leiden, The Netherlands) and Sanquin Research (Amsterdam, The Netherlands) and provided informed consent.

Histology assessment

The culprit segment (5mm) of the atherosclerotic plaque (Cohort 3) was fixed in Shandon Zinc Formal-Fixx (Dilution 1:5; ThermoFisher) for 24h and subsequently stored in 70% Ethanol until further use. Plaque samples were graded in a semiquantitative scale as previously described⁹. Briefly, plaque samples were embedded in paraffin and subsequently sectioned in 5µm thick sections using a microtome. Sections were stained with Movat's pentachrome staining and three sections of each plaque were analysed for plaque features according to the semiquantitative scoring systems of AtheroExpress biobank¹⁰ and the Oxford Plaque Study¹¹.

The plaque vulnerability score of each patient was calculated as the average of the scores for necrotic core, calcification, foam cell content, cholesterol crystals, neovascularization and inflammatory cell content.

All patients underwent a CT-scan with arterial contrast pre-operatively. The degree of stenosis of the carotid arteries was measured using the formula of the North American Symptomatic Carotid Endarterectomy Trial (NASCET):

$$\% \text{ internal carotid artery (ICA) stenosis} = \left(1 - \frac{\text{Narrowest ICA diameter}}{\text{Diameter normal distal cervical ICA}}\right) \times 100$$

Isolation of HLA-peptide complexes by affinity chromatography

For the pilot feasibility study, a single plaque sample from one patient was used (Cohort 1). For the extended study plaque samples from 50 patients (Cohort 1) were pooled together and processed for immunopeptidomic analysis.

Carotid or femoral plaques were cut into small pieces and a total of 2.4 g of plaque material was processed further. Lysis buffer was added (50 mM Tris-Cl pH 8.0, 150

mM NaCl, 5 mM EDTA, 0.5% Zwittergent 3-12 (N-dodecyl-N,N-dimethyl-3-ammonio-1-propanesulfonate) and protease inhibitor (Complete, Roche Applied Science)) and the solution was probe sonicated on ice, followed by shaking on ice for 2 hours. The lysate was centrifuged for 10 min at $2500 \times g$ and for 45 min at $31,000 \times g$ to remove nuclei and other insoluble material, respectively. Next, lysates were passed through a 0.5 ml CL-4B Sepharose column to preclear the lysate. The cleared lysate was passed through a 0.2 ml column containing 2.5 mg anti-HLA-DR (B8.11.2) IgG coupled to protein A Sepharose¹². The antibody columns were washed with 1 ml of lysis buffer, 1 ml of low salt buffer (20 mM Tris-Cl pH 8.0, 120 mM NaCl), 1 ml of high salt buffer (20 mM Tris-Cl pH 8.0, 1 M NaCl), and finally with 1 ml of low salt buffer. Peptides were eluted with 1 ml of 10% acetic acid and purified on a 10kDa filter (Microcon, Millipore). The filtrate was diluted with 2 ml of 0.1% TFA and purified by SPE (Oasis HLB, Waters) using 20% and 30% acetonitrile in 0.1% trifluoroacetic acid (TFA) to elute the peptides.

Liquid chromatography-Mass spectrometry

Lyophilized peptides were dissolved in 95/3/0.1 (v/v/v) water/acetonitrile/formic acid (FA) and analysed in an online C18 nanoHPLC MS/MS consisting of an Ultimate3000nano gradient HPLC system (Thermo, Bremen, Germany), and an Exploris480 Mass Spectrometer (Thermo). Fractions were injected onto a cartridge precolumn (300 $\mu\text{m} \times 5 \text{ mm}$, C18 PepMap, 5 μm , 100 Å), and eluted using a homemade analytical nano-HPLC column (50 cm \times 75 μm ; Reprosil-Pur C18-AQ 1.9 μm , 120 Å) (Dr. Maisch, Ammerbuch, Germany). The gradient was run for 120 minutes from 2% to 40% solvent B (20/80/0.1 water/acetonitrile/FA v/v/v). The nano-HPLC column was drawn to a tip of $\square 5 \mu\text{m}$ that acted as the electrospray needle of the MS source. The mass spectrometer was operated in data-dependent MS/MS mode for a cycle of 20 MS/MS scans, with a HCD collision energy at 30 V and recording of the MS2 spectrum in the orbitrap, with a quadrupole isolation width of 1.2 Da. A resolution of 60,000 was used in the master scan (MS1), the scan range used was 300-1500, at standard AGC target at a maximum fill time of 50 ms. The lock mass correction on the background ion used was $m/z = 445.12$. Precursors were dynamically excluded after $n=1$ with an exclusion duration of 45 s, and with a precursor range of 20 ppm. Charge states 1-3 were included. Singly charged precursors were selected from the m/z in the range 800-1400, doubly charged precursors were selected from the m/z in the range 400-1000, and triply charged precursors were selected from the m/z in the range 300-900. For MS2 the first mass was set to 110 Da, with an MS2 scan resolution of 30,000 at an AGC target of 100% with a maximum fill time 'auto'.

For post-analysis, raw data were converted to peak lists using Proteome Discoverer version 2.1 (Thermo Electron), and subsequently submitted to the Uniprot *Homo sapiens* minimal database (20596 entries), using Mascot v2.2.07 (www.matrixscience.com) for peptide identification. Mascot searches were done with 10 ppm and 0.02 Da deviation for precursor and fragment mass, respectively, and no enzyme was specified. Methionine oxidation and cysteinylolation of cysteine were set as variable modifications. The false discovery rate was set < 1% and peptides with mascot ion scores < 35 were discarded.

The candidate peptides were synthesised, and the MS spectra of the synthetic peptides were compared to the MS spectra of their counterpart eluted from the plaque samples in order to confirm their identity.

Peptide synthesis

Peptides of the ApoB100 peptide pool 7 (PP7) used for the feasibility pilot study were synthesized in-house by Fmoc solid-phase peptide synthesis using the microwave-assisted automated peptide synthesizer Liberty Blue (CEM). Peptide synthesis was performed at 0.1mmol scale using a Tentagel S-RAM resin. After synthesis, peptides were acetylated in the C-terminus and cleaved from the resin using 95% TFA, 2.5% triisopropylsilane (TIPS) and 2.5% water. The resulting peptides were purified by reverse-phase high performance liquid chromatography (RP-HPLC) using a Kinetik Evo C18 column. Peptides were detected by absorbance at 220nm using an SPD-10AVP UV/Vis detector. Fractions were collected and analysed by liquid chromatography-mass spectrometry (LC-MS) to confirm peptide purity and identity. Purified peptides were freeze-dried and stored at -20°C until use. Peptides of the ApoB100 PP20 were synthesized by Genscript.

In silico prediction of peptide binding affinity for HLA-DR isotypes

The immune epitope database (IEDB) was used to predict the binding affinity of ApoB100 peptides identified in the immunopeptidomic analysis. The prediction was performed using the consensus approach that combines NN-align, SMM-align, CombLib and Sturniolo. If no predictor was available for a particular MHC class II molecule, NetMHCIIpan was used. Prediction was run for all 14 HLA-DR alleles available in IEDB.

T cell proliferation experiments

To assess T cell proliferation in response to the ApoB100 peptide pool, we used cryopreserved white blood cell (WBC) samples from patients that underwent carotid endarterectomy surgery (Cohort 2). Whole blood obtained from patients was lysed twice with ACK lysis buffer and cryopreserved as previously described⁴. For the assay, cryopreserved samples were defrosted, counted, and incubated overnight at

37°C and 5% CO₂ at a cell density of 1x10⁶ cells/ml. Next, cells were labelled with 0.5µM CFSE and again incubated overnight at 37°C and 5% CO₂. For stimulations, 200,000 cells per well were seeded in U-bottom 96-well plate and stimulated with either ApoB100 peptides, ConcanavalinA (ConA) or complete RPMI-1640 medium (RPMI-1640 supplemented with 10% (v/v) HI-FCS, 2mM L-glutamine, 100U/mL penicillin/streptomycin, 20µM β-mercaptoethanol). Human IL-2 was added to all conditions at a concentration of 20U/mL. Cells were stimulated for 5 days followed by 5 days of culture for a total of 10 days. Cell culture medium was refreshed every 2 days. On day 10, cells were labelled with anti-CD3, anti-CD4, anti-CD8 antibodies and the fixable viability dye eFluor780. Cell proliferation was assessed by the dilution of the CFSE label using flow cytometry in a Cytoflex S.

CD40L expression experiment

PBMCs were isolated from whole blood samples (Cohort 3) and cryopreserved until further use as previously described⁴. PBMCs were thawed, counted, and seeded in U-bottom 96-well plates at 500,000 cells per well. PBMCs were stimulated with ApoB100 peptide pool (5ug/mL each peptide), 2 ng/mL *Staphylococcus* enterotoxin B (SEB) or complete RPMI-1640 medium control. The peptide pool PepMix™ Human actine (PM-ACTS, JPT Peptide Technologies GmbH, Berlin, Germany) was also used as negative control at 5ug/mL of each peptide in the pool. Anti-CD40 blocking antibody was included in all conditions at 1µg/mL. PBMCs were incubated with stimulants for 18h and subsequently stained for flow cytometry with anti-CD3, anti-CD4, anti-CD8, anti-CD40L antibodies and fixable viability dye. Samples were measured using the Cytoflex S flow cytometer. For each patient, the stimulation index was calculated as:

$$\text{Stimulation index} = \frac{\% \text{ CD4}^+ \text{ CD40L}^+ \text{ T cells in peptide pool stimulation condition}}{\% \text{ CD4}^+ \text{ CD40L}^+ \text{ T cells in medium control}}$$

Cytokine profile by multiplex ELISA

To determine the cytokine profile of stimulated PBMCs (Cohort 3), 500,000 cells per well were seeded in U-bottom 96-well plate and stimulated for 3 days with ApoB100 peptide pool (5 µg/mL each peptide) or complete RPMI-1640 medium as control. During stimulation cells were incubated at 37°C and 5% CO₂. The level of IL-2, IL-4, IL-5, IL-6, IL-9, IL-10, IL-13, IL-17A, IL-17F, IL-22, IFN-γ and TNF-α in the conditioned medium was measured using bead-based multiplex ELISA LegendPlex (Biolegend, USA). Assay was performed according to manufacturer's instructions. Samples were measured using the Cytoflex S flow cytometer and data was analysed using LegendPlex software.

Statistics

Normal distribution of the data was assessed using Anderson-Darling test, D'Agostino & Pearson test, Shapiro-Wilk test and Kolmogorov-Smirnov test. Statistical difference between peptide-stimulated and unstimulated samples was analysed using two-tailed Wilcoxon matched-pairs signed rank test. Statistical correlation between variables was analysed using Pearson's correlation test. P-values lower than 0.05 were considered significant. Analyses were performed using GraphPad Prism version 9.3.1 for Windows (GraphPad Software, California, USA).

RESULTS

ApoB100-derived peptides eluted from one plaque induced CD4+ T cell proliferation in patients WBC

Immunopeptidomic aims to identify the set of peptides presented by HLA molecules in a given sample. To assess the feasibility of this technique for the identification of immunogenic epitopes from ApoB100, we studied the immunopeptidome of a single plaque sample from one patient. Briefly, the plaque sample was processed to isolate HLA/peptide complexes and peptides were subsequently eluted from the HLA molecules and identified by LC-MS/MS (Figure 1). The analysis identified 7 peptides derived from ApoB100 presented by HLA-DR molecules. An *in silico* analysis of the predicted binding affinity of these peptides for the most common HLA-DR alleles showed medium/high affinity ($IC_{50} < 1000nM$) for a wide range of alleles (Supplementary Figure 1).

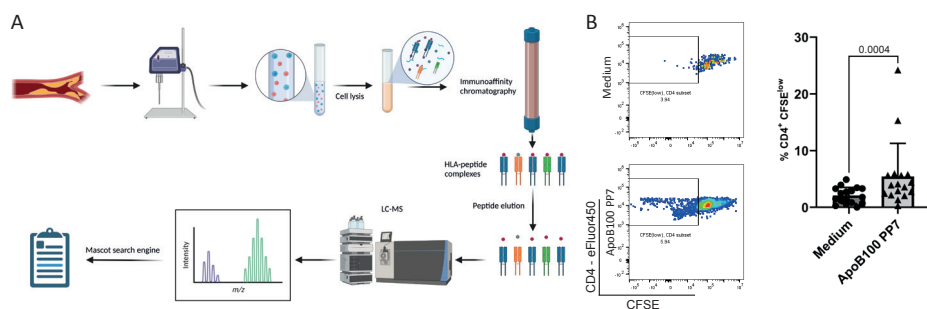


Figure 1. Immunopeptidomics experimental approach and feasibility study. (A) Immunopeptidomic workflow from a cryopreserved atherosclerosis plaque sample. Endarterectomy plaques were cut in small pieces and sonicated in lysis buffer. Subsequently, the HLA-peptide complexes were isolated by immunoaffinity chromatography. Peptides were eluted from the HLA molecules and LC-MS was used to separate and identify the peptides in the sample. Finally, the MS spectra of each potential peptide were assigned to a peptide sequence by searching the human proteome database with the Mascot™ engine. (B) Representative flow cytometry plots of proliferating CD4⁺ T cells from lysed blood in response to stimulation with preliminary ApoB100 peptide pool PP7 or medium control and dot plot (n=17) of the percentage of proliferating CD4⁺ T cells in each condition. P-value determined using two-tailed Wilcoxon matched-pairs signed rank test.

These 7 peptides were used to stimulate WBC samples from CVD patients. In order to have a better chance to detect a potentially rare CD4⁺ T cell population, we used a proliferation-based assay to expand the antigen-specific population. CFSE-labelled WBC samples were stimulated with this ApoB100 peptide pool (ApoB100 PP7) for 5 days in the presence of recombinant human IL-2, followed by 5 days of cell culture without peptides. Flow cytometry was used to determine CD4⁺ T cell proliferation based on the dilution of the CFSE label after cell division (Figure 1B). The results showed an increase in the proliferation of CD4⁺ T cells in the peptide pool condition compared to the medium control (p-value < 0.05) (Figure 1B). These results show that the immunopeptidomic approach can be applied for the identification of relevant immunogenic antigens presented in plaque samples.

Expanded analysis identified 13 potentially immunogenic ApoB100-derived peptides presented by HLA-DR

After the positive results from the pilot feasibility study, we used the same immunopeptidomic approach to elucidate the repertoire of peptides presented by HLA-DR molecules in 50 endarterectomy samples. A total of 2988 unique peptides were eluted from HLA-DR at a false discovery rate 1% and a mascot ion score > 35. Peptide length distribution, a common quality control check performed in

immunopeptidomic analysis¹³, showed that indeed the length of the peptides eluted from HLA-DR was centred around 15 amino acids, with the typical length distribution for HLA class II peptides between 10 and 25 amino acids¹⁴ (Figure 2A).

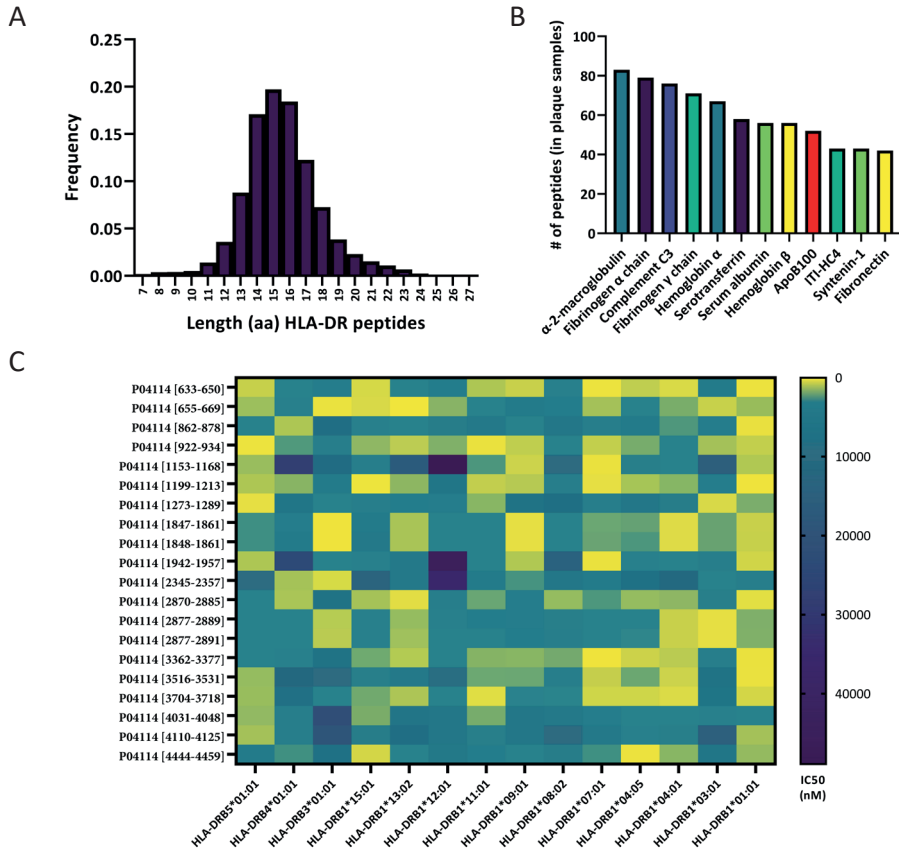


Figure 2. Immunopeptidomic analysis of n=50 atherosclerosis plaque samples. (A) Frequency distribution of the HLA-DR peptides lengths. (B) Number of peptides eluted from plaque samples grouped by source protein. (C) Heatmap representing the predicted binding affinity (IC₅₀ values in nM) of 20 selected peptides to different HLA-DR alleles. P04114 is the UniProt accession number for Apolipoprotein B100, number between brackets represent the position of the epitope in the amino acid sequence of the protein.

Next, we grouped the peptides eluted from HLA-DR by their parent protein and ranked the original proteins by their contribution to the peptide repertoire (Figure 2B). The main protein contributors to the immunopeptidome of the plaque were α -2-macroglobulin, fibrinogen α chain and complement C3. Interestingly, ApoB100 was the ninth source of peptides by number, with 52 peptides derived from this protein. Adaptive immune responses against ApoB100 have been previously linked to

atherosclerosis plaque development^{7, 15, 16}, therefore we focus on peptides derived from this protein to study atherosclerosis-specific immune responses. The amino acid sequences of the 52 ApoB100-derived peptides were uploaded to the Immune Epitope Database (IEDB) to predict the binding affinity to 14 alleles of HLA-DR. Based on this predicted binding affinity, we selected 13 peptides that had a medium to high affinity ($IC_{50} < 1000$ nM) for a wide range of HLA-DR alleles (Figure 2C and Supplementary Figure 2). We combined the 7 peptides identified in the pilot study with these 13 peptides in a peptide pool (ApoB100 PP20) for further experiments. The amino acid sequence and position within the ApoB100 protein of each peptide in the ApoB100 PP20 can be found in Supplementary Table 1. The identity of the eluted peptides was confirmed by comparing the MS spectra of synthetic peptides and the peptides eluted from plaque samples (data not shown).

ApoB100 peptide pool induced CD4⁺ T cell activation in a subset of atherosclerosis patients

With the peptide pool covering a wide number of HLA-DR variants, we hypothesized that this pool could be used to detect ApoB100 specific CD4⁺ T cells in CVD patients, regardless of their HLA type. In order to quantify the original ApoB100-specific CD4⁺ T cell population in CVD patients, we used an activation induced marker (AIM) assay based on the expression of CD40L by recently activated CD4⁺ T cells¹⁷. We stimulated PBMCs from a second cohort of patients with the ApoB100 PP20 peptide pool. Gating strategy for the flow cytometry data can be found on Supplementary Figure 3. For each patient we calculated the stimulation index. We observed a subgroup of patients (13/56, 22.4%) with a stimulation index equal or above the threshold of 2 (Figure 3A), suggesting this subgroup contained a detectable number of ApoB100 specific CD4⁺ T cells in the circulation. We defined the threshold for the stimulation index based CD40L response to ApoB100 PP20 of PBMCs from healthy volunteers (Figure 3A). Stimulation of patients PBMCs with a negative control peptide pool derived from human actin resulted in significantly lower response (Figure 3A).

We next addressed whether the quantity of ApoB100 specific CD4⁺ T cells is indicative of disease progression. As we have access to the endarterectomy material of PBMC donors, we scored these plaques based on the following histological features: necrotic core, calcification, foam cell, cholesterol crystals, inflammatory cells content and neovascularization (Figure 3B, Supplementary Table 2) and calculated a plaque vulnerability score as the average of these parameters. Next, we compared the stimulation index with the plaque vulnerability score, however the correlation did not reach statistical significance (Figure 3C) (p -value = 0.1). This correlation was significant (Pearson correlation coefficient (r) = 0.58, p -value = 0.049) in the subgroup of patients with higher stimulation index (Figure 3C). These data indicate that only

in patients with a significant CD4⁺ T cell response to ApoB100 the magnitude of the response correlate to the plaque vulnerability.

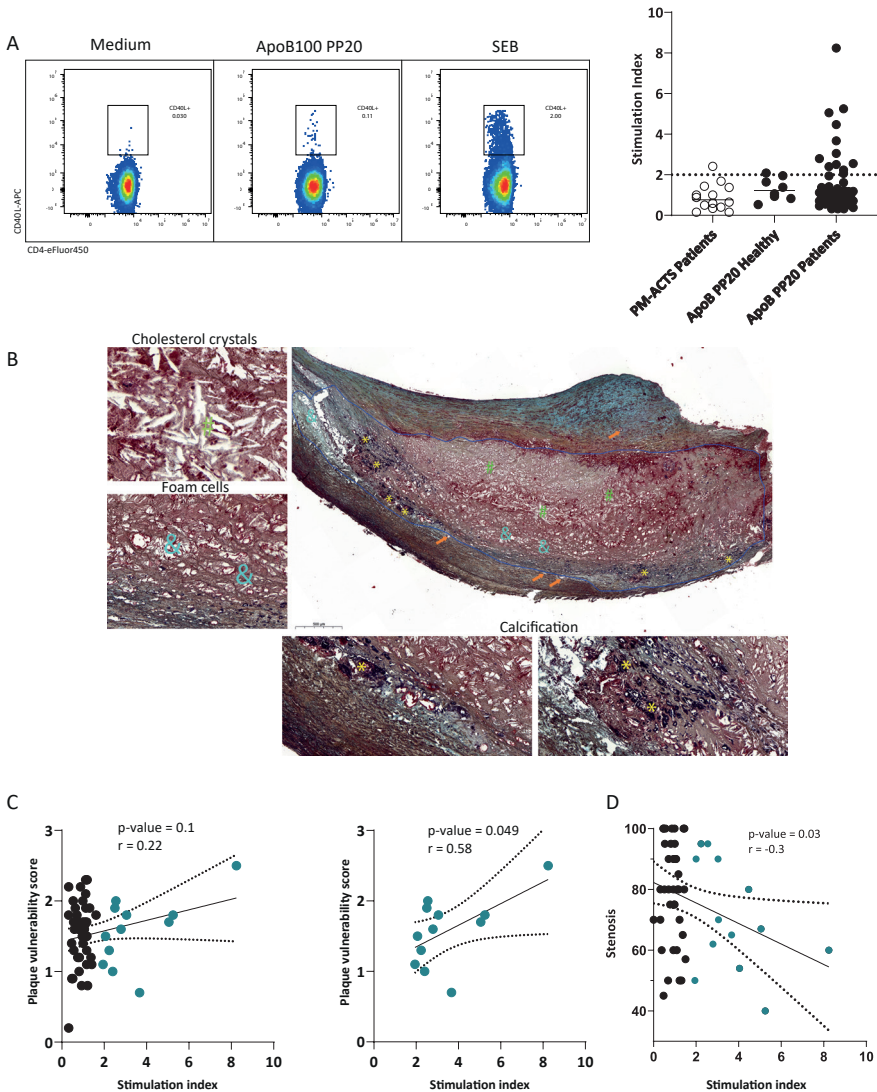


Figure 3. Expression of CD40L in CD4⁺ T cells from patient's PBMCs. (A) Representative flow cytometry plots of the gating of CD4⁺ CD40L⁺ cells in the live T cell population and dot plot with ApoB PP20 stimulation index per patient (n=58), PM-ACTS stimulation index per patient (n = 14) and ApoB PP20 stimulation index in healthy volunteers (n = 12). (B) Representative histology image of one of the plaque samples highlighting the different histological parameters taken into consideration to calculate the plaque vulnerability score. Blue line indicates the necrotic core, & depicts foam cells, # depicts cholesterol crystals, arrow and * indicate calcification. (C, left) Relationship between stimulation index and plaque vulnerability scores of all patients and (C, right) only subgroup with stimulation index ≥ 2 . (D) Relationship between stimulation index and stenosis. Statistical correlation between plaque vulnerability scores and stimulation index was determined using Pearson's correlation test.

Cytokine profile of PBMCs stimulated with ApoB100 peptide pool showed a IL17-driven proinflammatory response

The relatively high background of the AIM assay may limit its sensitivity to detect very low frequency populations of ApoB100-specific CD4⁺ T cells. Moreover, although the assay allows quantification of the number of ApoB100-specific CD4⁺ T cells, it does not give insight into the phenotype of these cells. As previous work on ApoB100-specific CD4⁺ T cell suggests, these cells can have atherogenic and atheroprotective functions based on their cytokine production^{18, 19}. Therefore, to obtain sensitive and functional information about this antigen-specific CD4⁺ T cell population we performed a multiplex bead-based ELISA assay to measure the cytokine profile of the PBMCs stimulated with ApoB100 PP20 peptide pool. For this, we stimulated patients PBMCs with either ApoB100 PP20 peptide pool or medium control for 3 days and performed multiplex ELISA with the conditioned medium. We observed that 31 out of 39 (79%) patients produced more IL-6 after peptide stimulation than their non-stimulated controls (Figure 4G), suggesting this protocol is more sensitive at detecting antigen-specific CD4⁺ T cell responses than the AIM approach. We observed a trend toward increased IL-2 production in the ApoB100 peptide stimulated condition compared to control ($p=0.066$, Figure 4B) and significant increases in IL-10, IL-17A, IL-5, IL-6 and IL-9 in the peptide pool condition compared to control (Figure 4C, 4D, 4F, 4G and 4H). Interestingly, we did not observe significant differences in the levels of IFN- γ produced in the peptide pool condition and the control (Figure 4E), suggesting that ApoB100-specific CD4⁺ T cells produce limited amounts of this Th1-related cytokine. While we do not observe a correlation between the level of individual cytokines and plaque vulnerability (Supplementary Figure 4), these data provide a clear indication that ApoB100-specific CD4⁺ T cells contain different functional subsets of T cells.

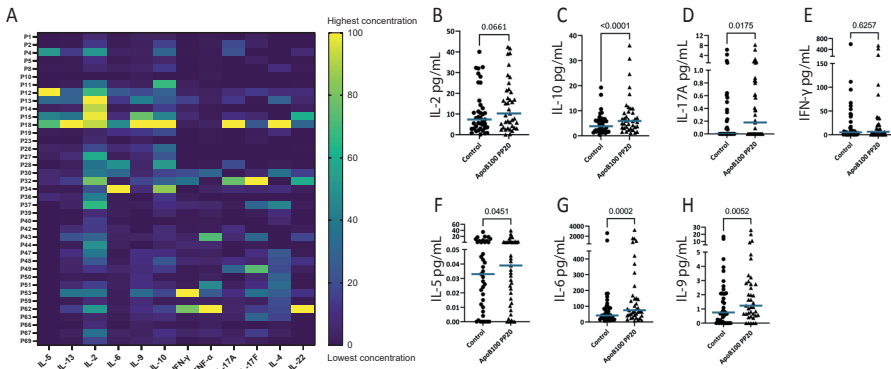


Figure 4. Cytokine profile of patient's PBMCs (n = 41) stimulated with ApoB100 PP20 peptide pool for 3 days. (A) Heatmap representing the concentration of 12 different cytokines (x axis) associated to T helper cell responses in conditioned medium of patients PBMCs (y axis). Data of each cytokine normalized to the highest concentration measured in all the patients. Concentration of IL-2 (B), IL-10 (C), IL-17A (D), IFN- γ (E), IL-5 (F), IL-6 (G) and IL-9 (H) in medium control and PBMCs stimulated with ApoB100 PP20. Blue bars in panels B-H represent median. P-values determined using two-tailed Wilcoxon matched-pairs signed rank test.

DISCUSSION

Several different approaches have been used in the last 20 years to try to identify ApoB100 immunogenic epitopes, mainly based on studies in mice and then translated to human²⁰ or by *in silico* screening of the ApoB100 sequence for strong binding motifs to the murine MHC-II isotype I-A^b 7, 21. However, whether ApoB100-specific autoreactive CD4⁺ T cell can directly contribute to atherosclerosis development and plaque instability will be dependent on them being able to recognize their cognate antigens in the plaque. Here we use an immunopeptidomic approach to show that ApoB100 epitopes are presented in the atherosclerotic lesions, which provides an important rationale for ApoB100-specific CD4⁺ T cells as drivers of autoimmunity in atherosclerosis. To the best of our knowledge, none of the ApoB100 peptides identified and selected in this study has been reported before.

Proliferation-based experiments show that CD4⁺ T cells from blood of CVD patients respond to these peptides, suggesting the immunopeptidomic approach is a viable method for antigen discovery in atherosclerosis. Proliferation assays, however, have limitations regarding long culture times, unspecific proliferation as a result of cell death^{22, 23} and the difficulty to precisely quantify the original population of antigen-specific T cells. The quantification of activation-induced markers such as CD40L on the other hand, allows the direct quantification of the original CD4⁺

T cell population responding to the peptides. The stimulation of PBMCs from patients with the ApoB100 peptide pool identified in the immunopeptidomic analysis showed that a subgroup of 22% of patients had detectable levels of ApoB100-specific CD4⁺ T cells. In this subgroup of patients, the stimulation index showed a positive correlation with histologically determined plaque vulnerability. However, when comparing the stimulation index with the percentage of maximal stenosis, a measurement of atherosclerosis plaque size, we observed a negative correlation, where patients with higher ApoB100-specific T cell responses showed lower levels of stenosis. Further research should be performed to determine the apparently opposing roles of ApoB100-specific T cells in plaque vulnerability and plaque size.

Multiple publications suggest the presence of ApoB100 specific CD4⁺ T cells in atherosclerotic lesions^{6, 7}. Moreover, a recent single-cell TCR sequencing study has shown the presence of clonally expanded, CD69⁺ CD4⁺ T cell populations in atherosclerotic lesions⁴, suggesting the presence of antigen-specific T cell responses in the lesion. Future studies should determine whether the ApoB100-specific T cell responses observed in PBMCs are also present in the plaque. However, the methodology employed in this study, which is based on flow cytometry determination of activation markers, may not be sufficiently sensitive for this task. The identification of TCR sequences associated to the ApoB100 epitopes described here would allow to determine the presence of ApoB100-specific CD4⁺ T cells in the lesion in a more sensitive manner. The identification of these TCRs in the single-cell sequencing data of human atherosclerotic plaques recently published by our lab would give a more comprehensive understanding on the characteristics of these antigen-specific T cells.

In order to obtain phenotypic information about the ApoB100-specific T cells, we also investigated the cytokines produced after ApoB100 stimulation. We observed an increased production of IL-10 and IL-17A but not in IL-2 or IFN- γ , the two signature cytokines of Th1 cells suggesting that these ApoB100-specific T cells present a Treg/Th17 phenotype. This data is in line with previous reports from Wolf et al. who showed the presence of ApoB100-specific CD4⁺ T cells that evolve from an anti-inflammatory Treg phenotype in initial stages of atherosclerosis to a more Th17 phenotype in later stages⁷. We also observed an increase in the production of a plethora of cytokines such as IL-9, IL-5 and IL-6, associated to different CD4⁺ T cell phenotypes^{24, 25}. This suggest that there is not a unique phenotype in the ApoB100-specific T cell population, but rather a diverse set of T cell phenotypes within the population. Although our data reinforces the hypothesis that a shift from IL-10 to IL-17 production in ApoB100-specific CD4⁺ T cells may be an important axis in the disease pathogenesis, we do not observe any correlations with plaque vulnerability. Cytokine levels, however, are difficult to interpret as we do not have

information on the cytokine production on a per cell basis, for which expansion of individual T cells coupled with TCR sequencing would be required.

The trend towards higher level of ApoB100-specific CD4⁺ T cells in more vulnerable plaques should be explored further by increasing the number of patients in follow up studies and it can lead to novel biomarkers for atherosclerosis progression or status based on the level or phenotype of antigen-specific CD4⁺ T cells.

Besides ApoB100 we also identified α -2-macroglobulin and fibrinogen alpha chain as the most prevalent proteins in the plaque's immunopeptidome. Both α -2-macroglobulin and fibrinogen are abundantly present in atherosclerosis lesions therefore their contribution to the immunopeptidome is not surprising. Fibrinogen has emerged as a candidate antigen driving autoimmune responses in rheumatoid arthritis²⁶ therefore high levels of antigen presentation of fibrinogen-derived peptides in atherosclerotic plaques might provide a link between atherosclerosis and rheumatoid arthritis²⁷. Other candidate proteins have been proposed as potential targets of autoimmunity in atherosclerosis such as heat-shock proteins^{28, 29}. In fact, proteins from the heat shock superfamily contributed with 18 peptides to the immunopeptidome. Therefore, this immunopeptidomic approach could be used to identify other important immunogenic epitopes from other proteins, which is key for the development of novel therapeutic strategies against atherosclerosis based on antigen-specific immune modulation.

CONCLUSIONS

In conclusion, here we show that immunopeptidomic-based analysis of atherosclerosis plaque tissue can be used to identify immunogenic epitopes of ApoB100. Using this approach, we identified 20 ApoB100 epitopes presented in human carotid and femoral atherosclerosis plaques and showed the presence of CD4⁺ T cell responses against these peptides in PBMCs of CVD patients. These ApoB100-specific CD4⁺ T cell responses showed a cytokine signature characterized by production of IL-17A, IL-10, IL-5, IL-6 and IL-9. Besides ApoB100, these data can be used to identify other immunogenic proteins and epitopes driving immune responses in atherosclerosis which is key for the development of new therapeutic strategies against CVDs.

AUTHORS CONTRIBUTIONS

FLV designed and performed experiments, analysed data and prepared and edited this manuscript and prepared figures. BS and PV designed the original concept and provided assistance regarding the experimental design. IS performed stimulation experiments, carried out peptide synthesis and aided with pilot studies. NSAC provided essential technical assistance with peptide synthesis. MJMJ, EH, MACD, LD, JM, MNBK processed patient material and performed PBMC isolation from patient's blood samples. JAHMP, AW, HJS performed endarterectomy surgery and collected patients' samples. RTNT performed peptide-HLA isolation from plaque samples, peptide elution and MS analysis. PHAQ, MRV performed the histology assessment of atherosclerosis plaque samples and contributed to the preparation of figures. AK, JK, IB provided valuable input during the preparation and edition of the manuscript.

FUNDING

This work was supported by the Dutch Heart Foundation and Health-Holland, grant number CVON2017-20: Generating the best evidence-based pharmaceutical targets and drugs for atherosclerosis (GENIUS II), and grant number LSHM18056-SGF: DC4Balance consortium. I.B. is an Established Investigator of the Dutch Heart Foundation (2019T067).

DATA AVAILABILITY STATEMENT

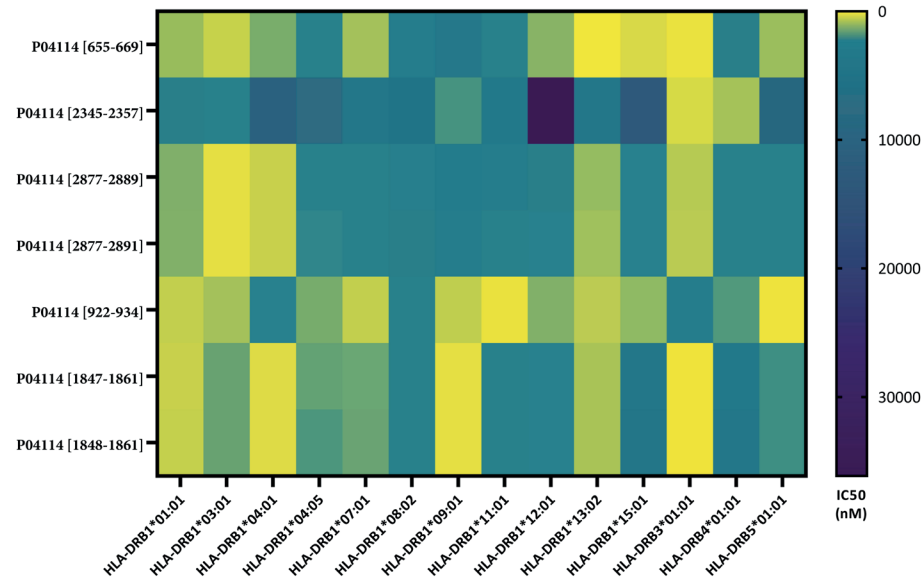
All non-patient related data is available upon request to the corresponding author (b.a.slutter@lacdr.leidenuniv.nl). Raw data of peptide discovery will be freely available from a repository after publication of this manuscript.

REFERENCES

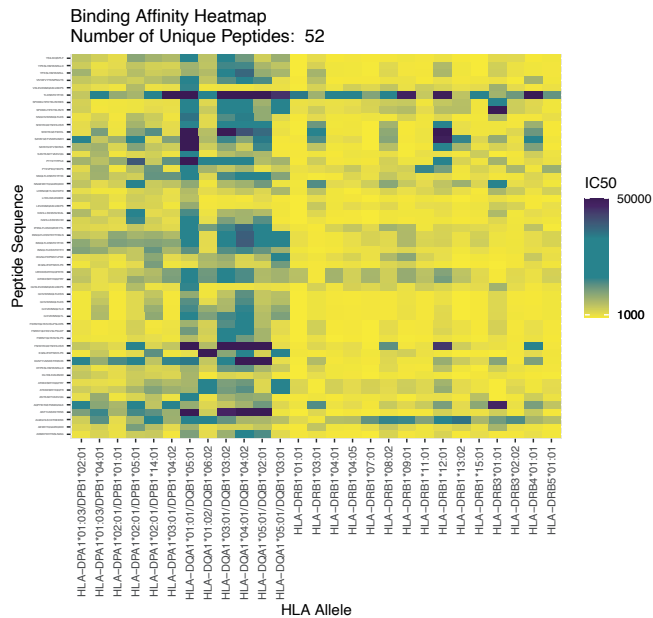
1. Hansson GK, Holm J, Jonasson L. Detection of activated T lymphocytes in the human atherosclerotic plaque. *Am J Pathol.* 1989;135(1):169-75.
2. Jonasson L, Holm J, Skalli O, Bondjers G, Hansson GK. Regional accumulations of T cells, macrophages, and smooth muscle cells in the human atherosclerotic plaque. *Arteriosclerosis.* 1986;6(2):131-8.
3. Chowdhury RR, D'Addabbo J, Huang X, Veizades S, Sasagawa K, Louis DM, et al. Human Coronary Plaque T Cells Are Clonal and Cross-React to Virus and Self. *Circ Res.* 2022;130(10):1510-30.
4. Depuydt MAC, Schaftenaar FH, Prange KHM, Boltjes A, Hemme E, Delfos L, et al. Single-cell T cell receptor sequencing of paired human atherosclerotic plaques and blood reveals autoimmune-like features of expanded effector T cells. *Nature Cardiovascular Research.* 2023.
5. Vigario FL, Kuiper J, Slutter B. Tolerogenic vaccines for the treatment of cardiovascular diseases. *EBioMedicine.* 2020;57:102827.
6. Stemme S, Faber B, Holm J, Wiklund O, Witztum JL, Hansson GK. T lymphocytes from human atherosclerotic plaques recognize oxidized low density lipoprotein. *Proc Natl Acad Sci U S A.* 1995;92(9):3893-7.
7. Wolf D, Gerhardt T, Winkels H, Michel NA, Pramod AB, Ghosheh Y, et al. Pathogenic Autoimmunity in Atherosclerosis Evolves From Initially Protective Apolipoprotein B(100)-Reactive CD4(+) T-Regulatory Cells. *Circulation.* 2020;142(13):1279-93.
8. Hellings WE, Moll FL, de Vries JP, de Bruin P, de Kleijn DP, Pasterkamp G. Histological characterization of restenotic carotid plaques in relation to recurrence interval and clinical presentation: a cohort study. *Stroke.* 2008;39(3):1029-32.
9. Kritikou E, Depuydt MAC, de Vries MR, Mulder KE, Govaert AM, Smit MD, et al. Flow Cytometry-Based Characterization of Mast Cells in Human Atherosclerosis. *Cells.* 2019;8(4).
10. Verhoeven B, Hellings WE, Moll FL, de Vries JP, de Kleijn DP, de Bruin P, et al. Carotid atherosclerotic plaques in patients with transient ischemic attacks and stroke have unstable characteristics compared with plaques in asymptomatic and amaurosis fugax patients. *J Vasc Surg.* 2005;42(6):1075-81.
11. Lovett JK, Gallagher PJ, Hands LJ, Walton J, Rothwell PM. Histological correlates of carotid plaque surface morphology on lumen contrast imaging. *Circulation.* 2004;110(15):2190-7.
12. Hassan C, Kester MG, de Ru AH, Hombrink P, Drijfhout JW, Nijveen H, et al. The human leukocyte antigen-presented ligandome of B lymphocytes. *Mol Cell Proteomics.* 2013;12(7):1829-43.
13. Purcell AW, Ramarathinam SH, Ternette N. Mass spectrometry-based identification of MHC-bound peptides for immunopeptidomics. *Nat Protoc.* 2019;14(6):1687-707.
14. Wieczorek M, Abualrous ET, Sticht J, Alvaro-Benito M, Stolzenberg S, Noe F, Freund C. Major Histocompatibility Complex (MHC) Class I and MHC Class II Proteins: Conformational Plasticity in Antigen Presentation. *Front Immunol.* 2017;8:292.
15. Wolf D, Ley K. Immunity and Inflammation in Atherosclerosis. *Circ Res.* 2019;124(2):315-27.

16. Kimura T, Kobiyama K, Winkels H, Tse K, Miller J, Vassallo M, et al. Regulatory CD4(+) T Cells Recognize Major Histocompatibility Complex Class II Molecule-Restricted Peptide Epitopes of Apolipoprotein B. *Circulation*. 2018;138(11):1130-43.
17. Yellin MJ, Sippel K, Inghirami G, Covey LR, Lee JJ, Sinning J, et al. CD40 molecules induce down-modulation and endocytosis of T cell surface T cell-B cell activating molecule/CD40-L. Potential role in regulating helper effector function. *J Immunol*. 1994;152(2):598-608.
18. Shaw MK, Tse KY, Zhao X, Welch K, Eitzman DT, Thipparthi RR, et al. T-Cells Specific for a Self-Peptide of ApoB-100 Exacerbate Aortic Atheroma in Murine Atherosclerosis. *Front Immunol*. 2017;8:95.
19. Herbin O, Ait-Oufella H, Yu W, Fredrikson GN, Aubier B, Perez N, et al. Regulatory T-cell response to apolipoprotein B100-derived peptides reduces the development and progression of atherosclerosis in mice. *Arterioscler Thromb Vasc Biol*. 2012;32(3):605-12.
20. Gistera A, Hermansson A, Strodthoff D, Klement ML, Hedin U, Fredrikson GN, et al. Vaccination against T-cell epitopes of native ApoB100 reduces vascular inflammation and disease in a humanized mouse model of atherosclerosis. *J Intern Med*. 2017;281(4):383-97.
21. Tse K, Gonen A, Sidney J, Ouyang H, Witztum JL, Sette A, et al. Atheroprotective Vaccination with MHC-II Restricted Peptides from ApoB-100. *Front Immunol*. 2013;4:493.
22. Amel Kashipaz MR, Huggins ML, Powell RJ, Todd I. Human autologous mixed lymphocyte reaction as an in vitro model for autoreactivity to apoptotic antigens. *Immunology*. 2002;107(3):358-65.
23. Kagan J, Choi YS. Failure of the human autologous mixed lymphocyte reaction in the absence of foreign antigens. *Eur J Immunol*. 1983;13(12):1031-6.
24. Nowak EC, Weaver CT, Turner H, Begum-Haque S, Becher B, Schreiner B, et al. IL-9 as a mediator of Th17-driven inflammatory disease. *J Exp Med*. 2009;206(8):1653-60.
25. Hirano T. Interleukin 6 in autoimmune and inflammatory diseases: a personal memoir. *Proc Jpn Acad Ser B Phys Biol Sci*. 2010;86(7):717-30.
26. Ho PP, Lee LY, Zhao X, Tomooka BH, Paniagua RT, Sharpe O, et al. Autoimmunity against fibrinogen mediates inflammatory arthritis in mice. *J Immunol*. 2010;184(1):379-90.
27. Cavagna L, Boffini N, Cagnotto G, Inverardi F, Grosso V, Caporali R. Atherosclerosis and rheumatoid arthritis: more than a simple association. *Mediators Inflamm*. 2012;2012:147354.
28. Rigano R, Profumo E, Buttari B, Tagliani A, Petrone L, D'Amati G, et al. Heat shock proteins and autoimmunity in patients with carotid atherosclerosis. *Ann N Y Acad Sci*. 2007;1107:1-10.
29. Wick G, Jakic B, Buszko M, Wick MC, Grundtman C. The role of heat shock proteins in atherosclerosis. *Nat Rev Cardiol*. 2014;11(9):516-29.

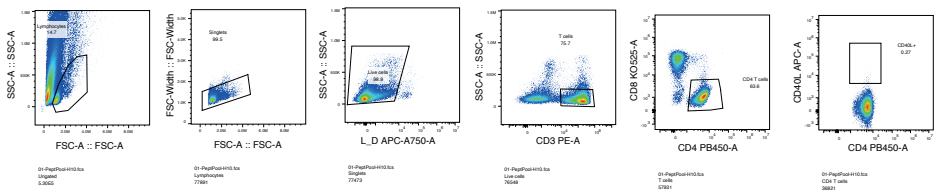
SUPPLEMENTARY DATA



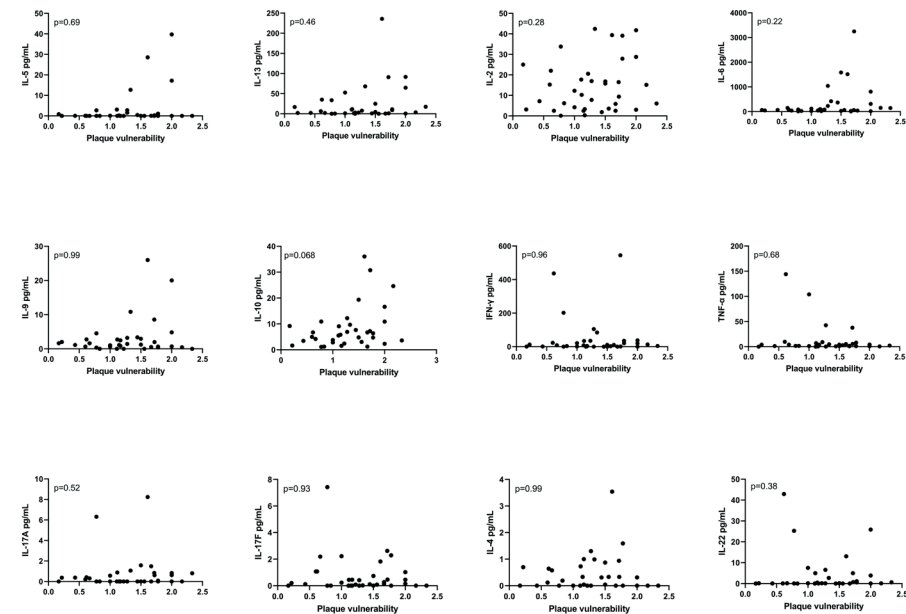
Supplementary Figure 1. Predicted binding affinity to HLA-DR alleles of ApoB100 peptides identified in feasibility study.



Supplementary Figure 2. Predicted binding affinity to HLA-DR alleles of ApoB100 peptides identified in immunopeptidomics of n=50 plaques.



Supplementary Figure 3. Gating strategy to define CD40L+ CD4 T cells in CD40L assay.



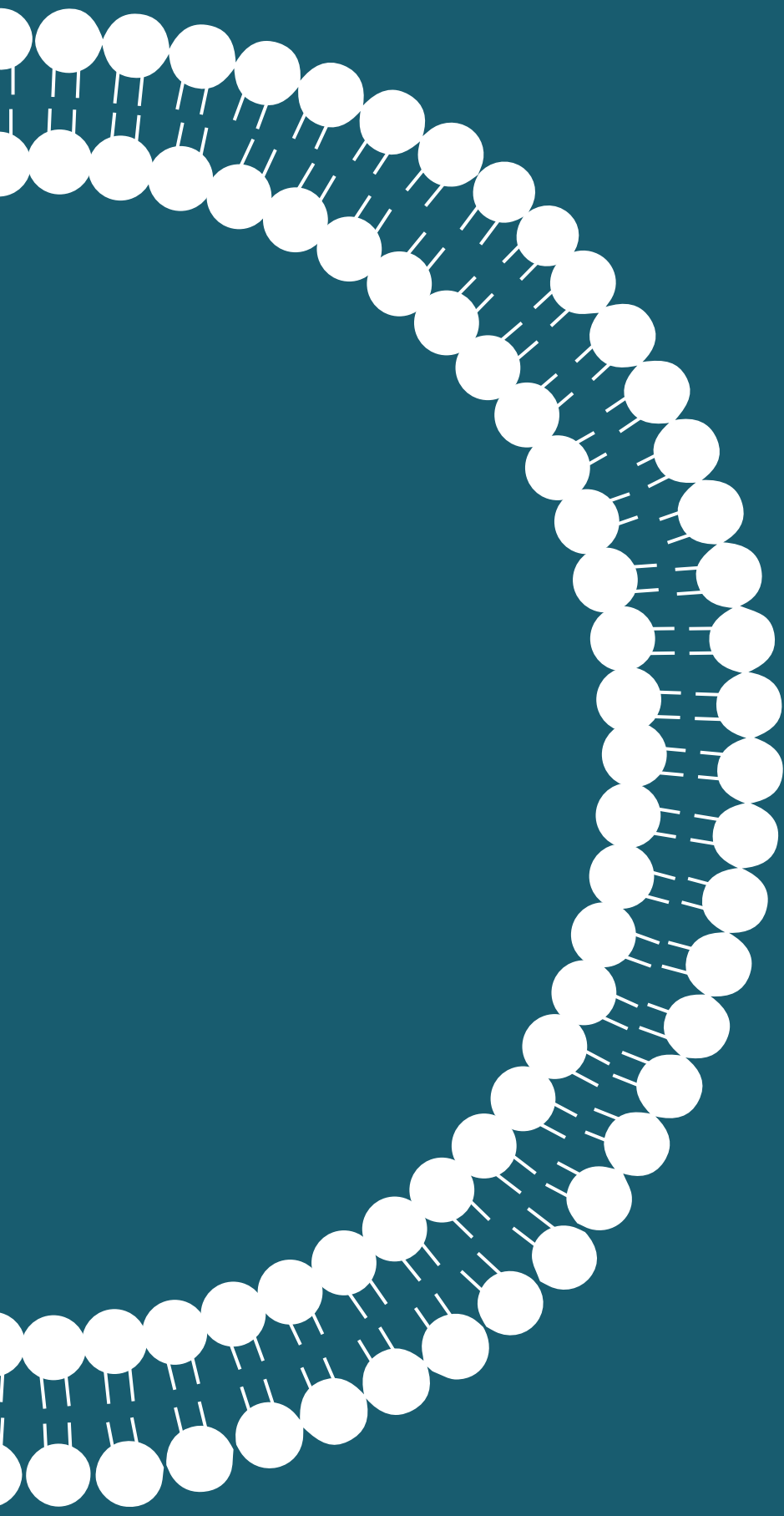
Supplementary Figure 4. Cytokine concentrations vs. plaque vulnerability score (n=30).

Supplementary Table 1. Amino acid sequence and position in ApoB100 protein (UniProt accession number = P04114) of peptides in ApoB PP20 peptide pool

ApoB PP20 peptide	Amino acid sequence	Position in ApoB100 protein
P1	IEGNLIFDPNNYLPK	P04114 [655-669]
P2	IERYEVDQQIQVL	P04114 [2345-2357]
P3	INNQLTLDSENTKY	P04114 [2877-2889]
P4	INNQLTLDSENTKYFH	P04114 [2877-2891]
P5	LKFIIPSPKRPVK	P04114 [922-934]
P6	LSASYKADTVAKVQG	P04114 [1847-1861]
P7	SASYKADTVAKVQG	P04114 [1848-1861]
P8	VSTAFVYTKPNPGYS	P04114 [3704-3718]
P9	VKLEVANMQAELVAKPS	P04114 [862-878]
P10	FSRNYQLYKSVSLPSLDP	P04114 [633-650]
P11	FSHDYKGSTSHHLVSR	P04114 [1942-1957]
P12	NNAEWVYQGAIQIDD	P04114 [4110-4125]
P13	SNGVIVKINNQLTLD	P04114 [2870-2885]
P14	IVAHLLSSSSVIDAL	P04114 [3362-3377]
P15	SPDKKLTIFKTEL RVRES	P04114 [4031-4048]
P16	DYPKSLHMYANRLD	P04114 [1199-1213]
P17	SATAYGSTVSKRVAWH	P04114 [1153-1168]
P18	LHRNIQEYLSILDPD	P04114 [4444-4459]
P19	EANTYLNKSTRSSVK	P04114 [3516-3531]
P20	IPENLFLKSDGRVKYTL	P04114 [1273-1289]

Supplementary Table 2. Semiquantitative scoring of histological features of carotid plaques.

Feature	Grade 0	Grade 1	Grade 2	Grade 3	Grade 4
Necrotic core	Not present	<20% of arterial area	20-40% of arterial area	40-70% of arterial area	>70% of arterial area
Calcification	Not present	<10% of arterial area	10-40% of arterial area	>40% of arterial area	-
Foam cell content	Not present	Few small size (5 cells) clusters	Multiple small or medium (10 cells) size clusters	One large size (15 cells) cluster or foam cells present around 70% of the arterial area	-
Cholesterol crystal content	Not present	<10% of necrotic core area	10-40% of necrotic core area	>40% of necrotic core area	-
Inflammatory cells content	Not present	Few small size clusters (50 cells) or a few cells scatter in the arterial area	Multiple small size clusters	One large size cluster (100 cells) or inflammatory cells scattered around 70% of the arterial area	-
Neovascularization	Not present	< 25 neovessels	25-50 neovessels	> 50 neovessels	-



Chapter 4

Liposomal Formulations loaded with Vitamin D3 Induce Regulatory Circuits in Human Dendritic Cells

N.A. Nagy¹, F. Lozano Vigario², R. Sparrius¹, T. M. M. van Capel¹, R. van Ree^{1,3}, S.W. Tas^{1,4}, T. B. H. Geijtenbeek¹, B. Slütter², E.C. de Jong¹

¹ Amsterdam UMC, University of Amsterdam, Department of Experimental Immunology, Amsterdam Institute for Infection & Immunity, Meibergdreef 9, 1105 AZ, Amsterdam, the Netherlands

² Division of BioTherapeutics, Leiden Academic Centre for Drug Research, Einsteinweg 55, 2333 CC, Leiden, the Netherlands

³ Amsterdam UMC, University of Amsterdam, Department of Otorhinolaryngology, Meibergdreef 9, 1105 AZ, Amsterdam, the Netherlands

⁴ Amsterdam UMC, University of Amsterdam, Department of Rheumatology and Clinical Immunology, Meibergdreef 9, 1105 AZ, Amsterdam, the Netherlands

Frontiers in Immunology, Volume 14 -2023, 9 June 2023; DOI: 10.3389/fimmu.2023.1137538

ABSTRACT

Nanomedicine provides a promising platform for manipulating dendritic cells (DCs) and the ensuing adaptive immune response. For the induction of regulatory responses, DCs can be targeted *in vivo* with nanoparticles incorporating tolerogenic adjuvants and auto-antigens or allergens. Here, we investigated the tolerogenic effect of different liposome formulations loaded with vitamin D3 (VD3). We extensively phenotyped monocyte-derived DCs (moDCs) and skin DCs and assessed DC-induced regulatory CD4⁺ T cells in coculture. Liposomal VD3 primed-moDCs induced the development of regulatory CD4⁺ T cells (Tregs) that inhibited bystander memory T cell proliferation. Induced Tregs were of the FoxP3⁺ CD127^{low} phenotype, also expressing TIGIT. Additionally, liposome-VD3 primed moDCs inhibited the development of T helper 1 (Th1) and T helper 17 (Th17) cells. Skin injection of VD3 liposomes selectively stimulated the migration of CD14⁺ skin DCs. These results suggest that nanoparticulate VD3 is a tolerogenic tool for DC-mediated induction of regulatory T cell responses.

INTRODUCTION

With a worldwide rise in prevalence of both allergic and autoimmune conditions, the need for developing specific and efficient tolerizing immunotherapies is more relevant than ever¹. To date, the only tolerizing treatment with curative potential is allergen immunotherapy (AIT), but some well-known disadvantages afflict it. Sustained efficacy of AIT is dependent on at least 3 years of monthly injections that carry the risk of potentially life-threatening side effects, both factors negatively affecting patient adherence²⁻⁴. In contrast to allergy treatment, no curative options exist for autoimmune conditions, and more specific alternatives to broadly immune suppressive therapies are required.

Dendritic cells (DCs) are immune cells under scrutiny for dictating a therapeutic tolerogenic response, as they can foster peripheral tolerance through promoting deletion of effector T cells and the induction of regulatory T cells (Tregs)⁵⁻⁷. DCs can be manipulated by tolerogenic adjuvants to induce immune regulation. Several forms of vitamin D, including the active vitamin D metabolite 1,25 α -dihydroxy vitamin D3 (VD3), are endowed with pluripotent immunosuppressive activity, and clinical evidence suggests beneficial effects in rheumatoid arthritis, psoriasis, or as an additive to allergen immunotherapy⁸⁻¹⁰. VD3 can directly stimulate forkhead box protein (FoxP3)⁺ Treg development¹¹ or mediates tolerogenic effects through the interaction with DCs¹²⁻¹⁵. VD3 inhibits maturation of and IL-12 production by DCs but also induces the expression of tolerogenic molecules and cytokines, such as Ig-like transcript 3 (ILT3), as well as IL-10^{16, 17}. Most importantly, VD3-treated DCs demonstrate exceptional resistance to proinflammatory stimulation after repeated rechallenge, making VD3 a robust tolerance-promoting adjuvant⁸.

Given the crucial role of DCs in immune tolerance, several phase I clinical trials are now applying *ex vivo* DC therapy with an ultimate curative aim for rheumatoid arthritis and multiple sclerosis, using, amongst other components, VD3 to create tolerogenic DCs¹⁸⁻²². However, *ex vivo* DC therapy is costly and requires personalized application²³. A different approach is targeting DCs *in vivo* using a tolerogenic vaccine formulation, passing the necessity of personalization. Nanoparticles could be of aid in this approach as they offer the possibility to unite adjuvant, disease-relevant antigen, and cell-specific targeting molecules in one spatial unit^{24, 25}. In addition, nanoparticles protect their content from degradation and causing harmful effects in bystander cells. This advantage is relevant for a compound such as VD3, given its instability and toxic effects in high doses^{10, 26}. Liposomes are biocompatible nanoparticles with a lipid bilayer, adjustable in size, rigidity, and surface electric charge with relative ease²⁵. For this study, we selected an anionic and a cationic formulation with similar size and rigidity from a larger

array of liposomal formulations that we previously evaluated as putative tolerogenic vaccine carriers²⁷.

One readily accessible site for delivery of a liposomal vaccine is the skin, where several subsets of DCs reside. Due to continuous exposure to harmless bacterial flora, Langerhans cells (LCs) in the epidermis and the dermal CD1a⁺ or CD14⁺ skin DC subsets are equipped with efficient tolerogenic properties in steady state^{28, 29}, and can be targeted with intradermal injection of liposomes³⁰.

It is currently unknown how VD3-loaded liposomes affect DCs and the ensuing adaptive T cell response. Therefore, to deliver *in vitro* proof of concept for a DC-targeted tolerogenic nanoparticle therapy, we investigated the effects of VD3-loaded liposomal formulations on monocyte-derived DCs (moDCs) and the ensuing T cell response. Additionally, we applied an *ex vivo* human skin model to examine the effect of liposomal VD3 injection on skin DC crawl-outs. We demonstrate that liposomal VD3 efficiently induces tolerogenic DCs that promote the outgrowth of functional Tregs and suppress T helper 1 (Th1) and T helper 17 (Th17) responses. When injected in *ex vivo* human skin, VD3-loaded liposomes selectively enhance the migration of CD14⁺ DDCs, suggesting ongoing tolerogenic processes *in situ*. Taken together, these data demonstrate proof-of-concept for the efficacy of VD3-loaded liposomes in tolerizing DCs, resulting in the regulation of T cell responses.

MATERIALS AND METHODS

Liposome preparation

Anionic liposomes containing 1,2-distearoyl-sn-glycero-3-phosphoglycerol (DSPG) and cationic liposomes containing 1,2-dipalmitoyl-3-trimethylammonium-propane (DPTAP) (Table 1) were manufactured using the thin film dehydration-rehydration method, as described elsewhere^{27, 31, 32}. For the vitamin-loaded formulations, 150 µg VD3 (Sigma Aldrich, St Louis, Missouri) dissolved in ethanol was added to approximately 3 mg of lipids in the lipid mix. VD3-loaded liposomes were dialyzed overnight using a Spectra-Por® Float-A-lyzer® dialysis kit (MWCO 100,000 Da) against 400 ml 10 mM phosphate buffer (PB) pH 7.4 to separate non-encapsulated VD3. Liposomes were stored at 4 °C in PB and used for further experiments within 3 months.

Table 1. Physicochemical properties of VD3-loaded liposomal formulations. Characteristics are shown as mean \pm SD of n=3 different batches. LE, loading efficiency of VD3.

Formulation	Lipid composition	Z-ave. (nm) \pm SD	Pdl \pm SD	ζ potential (mV) \pm SD	LE (%) \pm SD
DSPG(-) VD3	DSPC:DSPG:CHOL	183 \pm 12.63	0.14 \pm 0.07	-39.5 \pm 11.6	1.86 \pm 0.02
DSPG(-) VD3	DOPC:DSPG:CHOL	168 \pm 11.55	0.16 \pm 0.04	-46.33 \pm 4.92	63 \pm 3.65
DPTAP(+) VD3	DSPC:DPTAP:CHOL	205 \pm 28.9	0.13 \pm 0.03	29.0 \pm 2.33	2.37 \pm 3.30
DPTAP(+) VD3	DOPC:DPTAP:CHOL	184 \pm 11.6	0.19 \pm 0.04	25.9 \pm 2.64	62 \pm 2.69

Quality control of liposomes

Quality control was performed as previously described²⁷. For stability testing, measurements were repeated each month after liposome preparation (Table 2). To confirm lipid concentration of the formulations and VD3 concentration encapsulated in the liposomes, reversed-phase ultra-performance liquid chromatography (Waters ACQUITY UPLC, Waters, Massachusetts) was used, as described²⁷. VD3 was detected by absorbance at 252 nm using an ACQUITY UPLC TUV detector (Waters). Loading efficiency (LE) of VD3 was calculated as

$$LE(\%) = \frac{VD3 \text{ concentration after dialysis}}{VD3 \text{ concentration before extrusion}} * 100$$

As the loading efficiency of VD3 proved marginal with the head lipid DSPC in the formulations, the head lipid was replaced by DOPC, leading to markedly improved loading efficiency (Table 1). All formulations had a size of less than 250 nm and a Pdl of less than 0.2, indicating a monodisperse quality (Table 1). Measured ζ -potential corresponded to the expected surface charge of the formulations. Formulations were stable throughout their use (Table 2).

Table 2. Stability measurements of DSPG and DPTAP VD3-loaded liposomal formulations.

DSPG(-) VD3			
Time (months)	Z-ave. (nm) \pm SD	Pdl \pm SD	Z-potential (mV) \pm SD
0	168 \pm 9.78	0.16 \pm 0.03	-48.33 \pm 5.57
1	169 \pm 11.40	0.14 \pm 0.03	-40.49 \pm 5.78
2	180 \pm 6.81	0.16 \pm 0.03	-42.30 \pm 3.85
3	170 \pm 7.20	0.18 \pm 0.01	-49.29 \pm 5.41
DPTAP(+) VD3			
Time (months)	Z-ave. (nm) \pm SD	Pdl \pm SD	Z-potential (mV) \pm SD
0	180 \pm 9.69	0.18 \pm 0.04	27.01 \pm 3.00
1	183 \pm 15.11	0.19 \pm 0.03	27.46 \pm 4.45
2	197 \pm 13.23	0.20 \pm 0.02	26.90 \pm 5.02
3	175 \pm 19.70	0.18 \pm 0.04	28.52 \pm 2.62

***In vitro* generation and activation of moDCs**

MoDCs were differentiated from peripheral blood monocytes obtained from buffy coats or fresh blood as described elsewhere³³. Briefly, monocytes were isolated from peripheral blood mononuclear cells (PBMCs) via density centrifugation and subsequently cultured for 5-7 days in Iscove's Modified Dulbecco's Medium (IMDM, Gibco, Paisley, UK) supplemented with gentamicin (86 μ g/ml; Duchefa, Haarlem, The Netherlands), 5 % fetal calf serum (FCS) (Gibco), granulocyte-macrophage colony-stimulating factor (GM-CSF, 500 U/ml; Schering-Plough, Uden, The Netherlands) and IL-4 (10 IU/ml; Miltenyi Biotech, Bergisch Gladbach, Germany). Healthy volunteers for blood sampling were recruited per the Academic Medical Center Medical Ethical Committee (protocol nr. 2015_074). For assessment of moDC surface markers, cells were matured for 48 hours with IL-1 β (25 ng/ml) and TNF- α (50 ng/ml) (both purchased from PBH, Hannover, Germany; this combination will be referred to as maturation factor or 'MF') and Escherichia coli lipopolysaccharide (LPS) with or without liposomal or soluble VD3 (0.01-2.5 μ M) and with or without empty liposomes DSPG or DPTAP as control. Lipid concentration in empty liposome conditions was adjusted to the lipid concentration of VD3-loaded liposomes used in the experiments. As each batch of liposomes differed in LE of VD3, lipid concentrations of empty batches used in the experiments had to be adjusted accordingly. For extensive assessment of co-stimulatory and co-inhibitory markers, moDCs were surface stained with anti-HLA-DR-BV421, anti-ILT2 (CD85J)-BV480, anti-ILT3 (CD85k)-BV510, anti-B7H3 (CD276)- BV750, anti-CD86-FITC, anti-ICOSL-PE-CF594, anti-CD83-PE-Cy5 (all BD Biosciences), and anti-ILT4 (CD85d)-PE, as well as anti-PD-L1 (CD274)-PE-Cy7 (all eBioscience, Thermo Fisher) and 10.000 DCs (3) acquired on the SP6800 Spectral Analyzer (Sony).

Isolation of naïve and memory CD4⁺ T cells

The total CD4⁺ T cell population was isolated from PBMCs by negative magnetic selection using the MACS CD4⁺ T cell isolation kit (Miltenyi Biotech). Subsequently, naïve CD4⁺CD45RA⁺ cells were purified by negative selection, and CD4⁺CD45RO⁺ memory cells by positive selection using anti-PE beads (Miltenyi Biotech). Purity of isolated populations exceeded 95 % and was analyzed by flow cytometry using anti-CD4-APC, anti-CD45RA-FITC (all BD), and anti-CD45RO-PE (DAKO, Agilent, Santa Clara, California).

Stimulation and analysis of CD4⁺ T cells

For phenotypic analysis, 20.000 allogeneic naïve CD4⁺ T cells were stimulated in 200 µl IMDM with 10 % FCS with 10 pg/ml *Staphylococcus aureus* enterotoxin B (Sigma-Aldrich) as described³³, and 5000 MF+LPS-activated DCs that were previously matured for 48 hours with or without liposomal or soluble VD3. DCs were washed three times with 3 ml medium prior to use in culture, given that VD3 has been demonstrated to have a profound direct effect on T cells^{34, 35}. On day 5 of the coculture, effector T cells were gently harvested and incubated in a new culture plate with human rIL-2 (10 U/ml, Cetus, Emeryville, CA), leaving moDCs attached in the wells of the original culture plate. When resting (coculture day 10-12), a maximum of 500.000 effector T cells was restimulated for 5 hours with phorbol 12-myristate 13-acetate (100ng/ml)/ionomycin (1 µg/ml, Sigma) + brefeldin (10 µg/ml, Sigma) followed by intracellular staining for IFN-γ-FITC (BD) and IL-13-PE (BD), as described previously^{33, 36}. Additionally, 100.000 CD4⁺ T cells were stimulated with soluble murine mAb to human CD3 (0.5 µg/mL; Sanquin Research, Amsterdam, The Netherlands) and CD28 (1 µg/mL, Sanquin Research) in 200 µL of IMDM for analysis of IL-10 in 24-hour supernatants. To phenotype Tregs, resting T cells were stained for CD25, CD127, FoxP3, or with a panel of antibodies for CD39, CD49b, CD69, programmed cell death 1 (PD-1), T-cell immunoglobulin and ITIM domain (TIGIT), T cell immunoglobulin and mucin domain 3 (TIM-3), CD127, CD25, inducible-co-stimulator (ICOS), cytotoxic T lymphocyte associated protein (CTLA-4), FoxP3, and LAG-3 as described elsewhere³⁷. Cells were acquired in the live gate on a FACS Canto A (BD) or the SP6800 Spectral Analyzer (Sony). For suppressor assays, 300.000 allogeneic naïve CD4⁺ T cells were cocultured for 6 days with 30.000 MF+ LPS-activated, soluble, or liposomal VD3-treated moDCs. After 6 days of coculture with moDCs, the emerging effector T cells were gently harvested, and irradiated at 30 Gray to prevent further expansion. 50.000 effector T cells were subsequently used with 25.000 memory CD4⁺ T cells labeled with carboxyfluorescein diacetate succinimidyl ester (CFSE) (0.5 mM; Molecular Probes, Eugene, Oregon) as target cells³⁶.

Autologous coculture of naïve CD4⁺ T cells with moDCs and neutrophils

On day 6 of DC generation, immature DCs were primed for 2 hours with 2.5 μ M VD3 or 2.5 μ M VD3-containing DSPG liposomes before harvesting. Co-cultures with DCs, autologous neutrophils, and CD4⁺ T cells were done in *C. albicans* hyphae-coated plates in IMDM medium containing 5 % human serum, as described elsewhere³⁷⁻³⁹. Neutrophils were isolated fresh on the first day of co-culture, from the erythrocyte pellet of Lymphoprep density centrifugation, as described³⁹. The pellet was lysed for 15 minutes on ice with 0.155 mol NH₄Cl (Sigma-Aldrich), 1mM KHCO₃ (Merck, Darmstadt, Germany), and 80 μ M EDTA (Merck) dissolved in pH 7.3 sterile water. After centrifugation and repeated lysis of 5 minutes, neutrophils were resuspended in IMDM 5 % human serum.

Extraction and priming of skin DCs

Ex vivo DCs were obtained from healthy human skin as described elsewhere⁴⁰. Intradermal injections were carried out with 50 μ l of phosphate-buffered saline, LPS+MF, VD3 (25 μ M), and liposomes DSPG or DPTAP with or without VD3 in concentrations corresponding to the soluble vitamin control. Migrating cells were stained for the skin DC markers with anti-CD11c-PE-Cy7 (eBioscience, Thermo Fisher), anti-HLA-DR-PercP (BD), anti-CD1a-FITC (BD), and anti-CD14-APC-Cy7(BD).

Data analysis and statistics

Flow cytometric data were analyzed using FlowJo™ Software (for Windows, Version 10.6.2., Ashland). Heatmaps were generated using Tercen™. Statistical analyses were conducted using GraphPad Prism software (GraphPad, La Jolla, CA).

RESULTS

Priming of DCs with VD3-loaded liposomes induces CD4⁺ T cells with regulatory function

To investigate whether VD3-liposome primed DCs induce functional Tregs, we primed naïve CD4⁺ T cells with moDCs exposed to VD3-containing DSPG or DPTAP liposomes and determined regulatory T cell capacity in a T-cell suppressor assay. Allogeneic naïve CD4⁺ T cells were cocultured with VD3 or VD3-liposome primed moDCs and subsequently cocultured with CFSE-labeled CD4⁺ T memory cells (Figure 1A). The maximum concentration of liposome-incorporated VD3 in the suppressor assays was 1 μ M, as in the liposome batches used for these experiments, loading efficiency of VD3 was less than 3 % (Table 1).

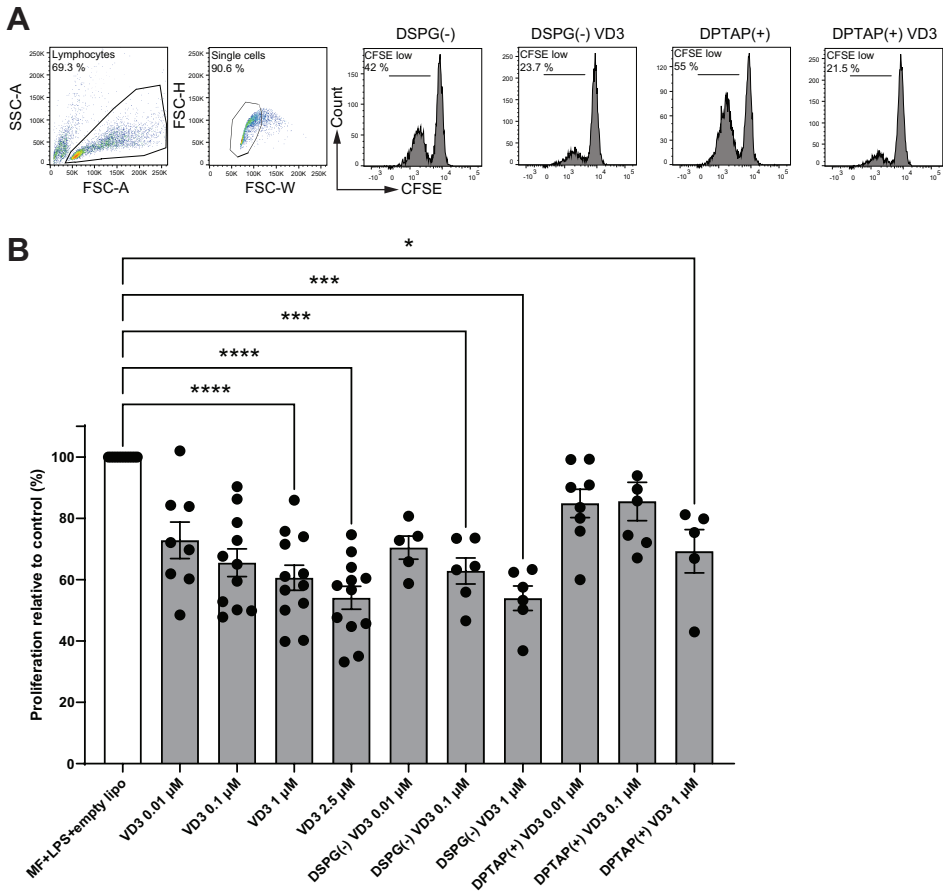


Figure 1. VD3-liposome-treated DCs induce functional Tregs. Allogeneic naïve CD4⁺ T cells were co-cultured with MF+LPS-activated DCs, or DCs activated with MF+LPS and soluble VD3 or VD3-loaded liposomes for 6 days and subsequently used as T cells in co-culture with CFSE-labeled CD4⁺ T memory cells. After 6 days of coculture, proliferation of CD4⁺ T memory cells was measured with flow cytometry. (A) Example gating of CD4⁺ T memory proliferation after coculture with MF+LPS and liposome DC-primed or MF+LPS and VD3-liposome DC-primed T cells (from left to right). (B) CD4⁺ bystander T memory proliferation normalized to the proliferation induced by MF+LPS and empty DSPG and DPTAP liposome DC-primed T cells, which was set to 100 %. Lipid concentrations of empty DSPG batches ranged from 1-2.6 μ g/ml, 10-26 μ g/ml, 50-260 μ g/ml, and of empty DPTAP batches 0.5-1 μ g/ml, 2.5-15 μ g/ml, 14-40 μ g/ml, adjusted to the lipid concentration added when using 0.01, 0.1 or 1 μ M liposome-incorporated VD3, respectively. N=5-12 independent experiments. Mean \pm SD of proliferation in the control condition was 36 % \pm 12.4 %. Error bars indicate mean \pm SEM. * p \leq 0.05. *** p \leq 0.001. **** p \leq 0.0001. Statistical significance was calculated using a mixed-effects model of one-way ANOVA, with Dunnett's correction for multiple comparisons.

T cells primed by VD3-exposed DCs suppressed the proliferation of bystander T cells in a dose-dependent fashion, most pronounced at 2.5 μM of VD3 (Figure 1B). Interestingly, DCs primed with either negatively charged DSPG-VD3 or positively charged DPTAP-VD3 induced suppressive Tregs (Figures 1A, B). At a VD3 concentration of 1 μM , DCs primed by negatively charged DSPG-VD3 liposomes induced suppressive T cells that inhibited bystander T cell proliferation to similar levels as soluble VD3 at 2.5 μM . DCs treated with positively charged DPTAP-VD3 liposomes also induced suppressive T cells, but to levels seen with 0.01-0.1 μM soluble VD3. In conclusion, our data indicate that DCs primed with 1 μM VD3-loaded liposomes induce functional Tregs, irrespective of liposome type, comparable to soluble VD3-treated DCs.

DCs activated in the presence of liposomal VD3 induce both FoxP3⁺ and IL-10-expressing Tregs

As Tregs consist of several subsets, we analyzed the phenotype of functional Tregs induced by liposomal VD3-primed DCs. We first determined the presence of two heterogeneous T cell populations associated with Tregs in human, FoxP3⁺ CD25⁺ CD127^{low} CD4⁺ T cells, as well as IL-10-producing CD4⁺ T cells. Frequencies of FoxP3⁺ CD127^{low} CD4⁺ T cells were strongly increased in coculture with DCs activated in the presence of anionic DSPG liposomes containing 2.5 μM VD3 (Figures 2A, B). After treatment with DPTAP liposomes containing 2.5 μM VD3, DCs also induced FoxP3⁺ CD127^{low} cells. Stimulation of DCs with a lower concentration of 1 μM liposomal VD3 or with soluble VD3 did not result in significant induction of Foxp3⁺ CD127^{low} CD4⁺ T cells.

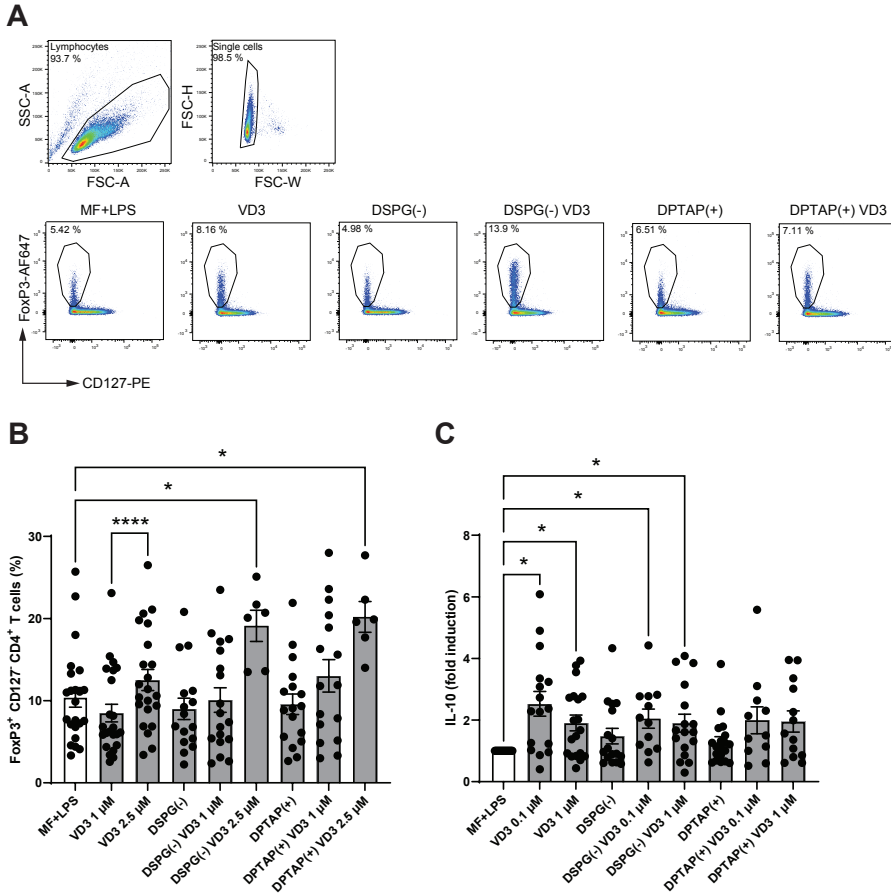


Figure 2. VD3-liposome treated DCs prime for the development of FoxP3⁺ CD127⁻ CD4⁺ T cells and IL-10-producing CD4⁺ T cells. Allogeneic naïve CD4⁺ T cells were cocultured with MF+LPS activated, VD3 or VD3-liposome primed moDCs for 10-12 days, and frequencies of FoxP3⁺ CD25⁺ CD127^{low} cells were measured by FACS. For IL-10 measurement with ELISA, CD4⁺ T cells were re-stimulated with aCD3, aCD28. (A) FoxP3⁺ CD127^{low} T cells were gated from the single-cell gate. Example dot plots of gating FoxP3⁺ CD127^{low} T cells and frequencies in example conditions are shown. (B) Frequency of FoxP3⁺ CD127^{low} T cells after stimulation with differently primed moDCs. N=6-23 independent experiments. (C) IL-10 production by co-cultured T cells after overnight stimulation with aCD3, aCD28 normalized to MF+LPS DC condition, which was set to 1. Lipid concentration of empty DSPG batches shown ranges from 50-260 μ g/ml and of empty DPTAP batches 14-86 μ g/ml, adjusted to the lipid concentration added when using 1-2.5 μ M liposome-incorporated VD3. Mean \pm SD of LPS-stimulated IL-10 production in the control condition was 289 pg/ml \pm 333 pg/ml. N=11-19 independent experiments. Error bars indicate mean \pm SEM. * p \leq 0.05. **** p \leq 0.0001. Statistical significance was calculated using a mixed-effects model of one-way ANOVA, with Dunnett's correction for multiple comparisons.

Foxp3⁺ CD4⁺ T cells also rely on IL-10 production as a means of suppressing inflammation, together with type 1 regulatory T cells (Tr1), which have been shown to be induced by VD3-treated DCs⁴¹. IL-10 production was increased in T cells primed by DCs treated with 0.1 μ M VD3 (Figure 2C). Interestingly, only DCs primed with VD3-containing DSPG liposomes significantly stimulated IL-10 production compared to the control condition, while with DPTAP-VD3 primed moDCs, only a trend of IL-10 induction was visible. Our data suggest that VD3-liposome-treated moDCs at a concentration of 2.5 μ M VD3 induce FoxP3⁺ T cells in coculture, while IL-10 producing T cells are significantly fostered by 0.1-1 μ M VD3-stimulated or 0.1-1 μ M VD3-containing DSPG liposome stimulated moDCs.

A heterogeneous marker profile is induced in FoxP3⁺ and FoxP3⁻ CD4⁺ T cells by VD3-liposome-treated DCs

As we observed both induction of FoxP3⁺ CD127⁻ T cells and IL-10 producers, we phenotyped these heterogeneous cell populations with a flow cytometry panel of different T cell activation and regulatory markers (Figures 3A-E). The expression profiles are displayed in a heatmap (Figure 3F), indicating enhanced expression of CTLA-4 and TIGIT within the FoxP3⁺ population of CD4⁺ T cells, as well as an increased expression of ICOS⁺ CTLA-4⁺ FoxP3⁺ T cells (ICOS⁺ Tregs) in VD3-DC primed conditions. Priming of DCs with liposomal VD3 led to significantly higher frequencies of cells expressing the co-inhibitory receptor TIGIT within FoxP3⁺ CD127^{low} CD25⁺ T cells and the FoxP3⁺ bulk population (Figure 4A, Supplementary Figure 1A), compared to the activated DC control condition. In contrast, in the same population, no significant changes in CTLA-4⁺ cells were observed (Supplementary Figure 1B). Even though the co-inhibitory receptor TIM-3, the ectonucleotidase CD39, and the early T cell activation marker CD69 have been described as functional Treg markers^{42, 43}, these markers were significantly decreased in VD3-liposome treated conditions (Figure 3F, Figures 4B, C, D). Although the VD3-DC-induced expression changes in ICOS⁺ Tregs were not significant (Supplementary Figure 1C), cells expressing ICOS increased in frequency within the resting CD69⁻ FoxP3⁺ T cell population (Figure 3F, Figure 4E). CTLA-4⁺ cells and CTLA-4 ICOS co-expressing cells, on the other hand, were only increased in the activated CD69⁺ FoxP3⁺ T cell population upon coculture with VD3-treated DCs (Figures 4F, G). Interestingly, non-activated CD69⁻ FoxP3⁺ T cells were significantly induced by VD3-liposome-treated DCs but not CD69 co-expressing FoxP3⁺ T cells (Figures 4H, I), suggesting that the VD3-DC stimulated increase in FoxP3⁺ Tregs is not due to an increase in activated effector T cells. In VD3-DC instructed FoxP3⁻ T cells, we also observed reduced frequencies of TIM-3, CD39, or PD-1⁺ cells (Figure 3F, Supplementary Figures 1D-F). We examined the expression of LAG-3 and CD49b, two markers considered essential for defining Tr1 cells. However, we could

not measure reliable changes in this population due to low expression levels of the most critical marker, LAG-3 (data not shown). Even though CD49b appeared differentially expressed in the VD3-DC primed conditions (Figure 3F), this change was not significant (Supplementary Figure 1G). Taken together, compared to activated DCs, DCs primed with liposomal VD3 induced FoxP3⁺ CD127⁻ T cells with enhanced expression of TIGIT, while we could not demonstrate induction of FoxP3⁻ Tr1 cells. Interestingly, several functional Treg markers were decreased in soluble and liposomal VD3-primed T cells.

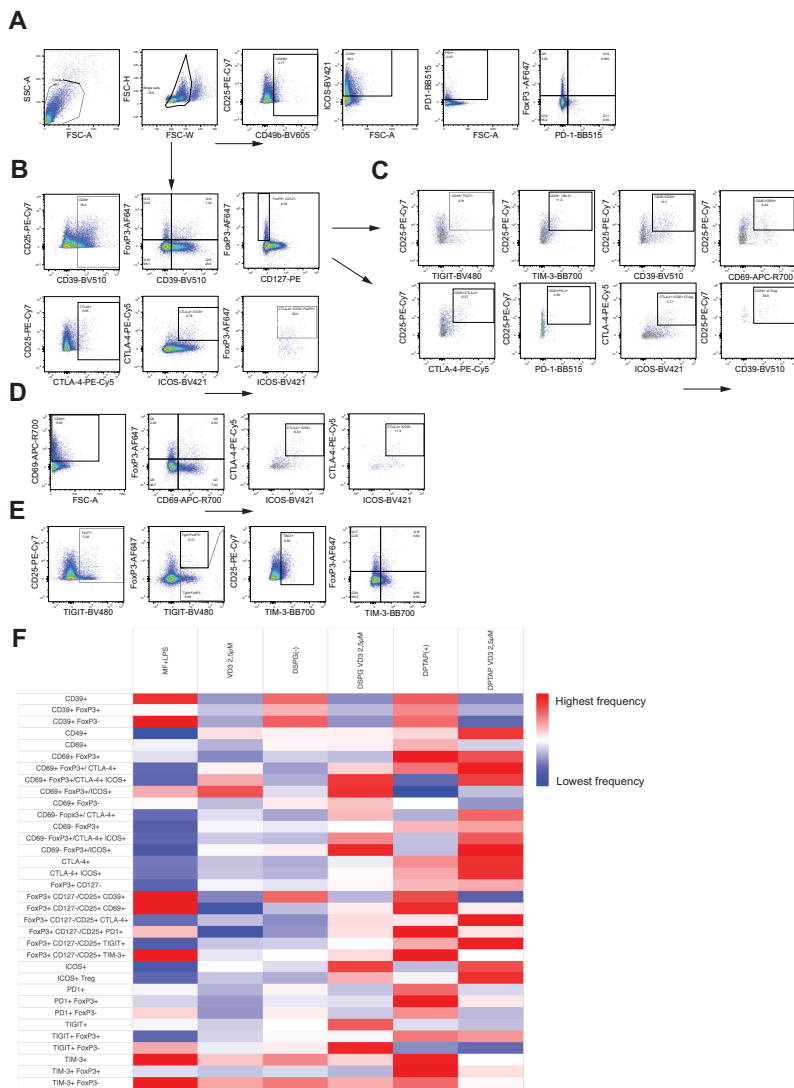


Figure 3. Phenotypic analysis of Tregs induced by VD3-liposome treated DCs. After 10-12 days coculture with differently primed moDCs, CD4+ T cells were stained for Treg subset and functional markers. Arrows indicate which parent population the subpopulation of cells was derived from. (A) CD4+ T cells expressing CD49b, ICOS or PD-1 were gated from the single cell gate. PD-1 and FoxP3+ co-expressing cells were gated, as shown in the right panel. (B) CD4+ T cells expressing CD39, CD25, CTLA-4, or ICOS were also derived from the single-cell gate. FoxP3+ cells were further examined for CD39 co-expression and CD127 expression. CTLA-4+ cells were gated together with ICOS, and FoxP3+ cells were determined within the double positive population. (C) Example gating for assessing expression of TIGIT, TIM-3, CD39, CD69, CTLA-4, PD-1 and ICOS within the FoxP3+ CD127low CD25+ population of CD4+ T cells. CTLA-4 ICOS co-expressing cells within this popu-

lation were identified as iTregs and further examined for CD39 expression. (D) After gating CD69+ cells from single CD4+ T cells, CD69 expression against FoxP3 expression was assessed with a quadrant gate, and CTLA-4 ICOS co-expression determined within both CD69- (Q5) and CD69+ (Q6) FoxP3+ cells. (E) TIGIT and TIM-3 expressing cells were gated from the single cell population of CD4+ T cells and assessed for FoxP3 expression as shown. (F) Heatmap representing frequency of indicated T cell populations per DC-activation condition is shown.

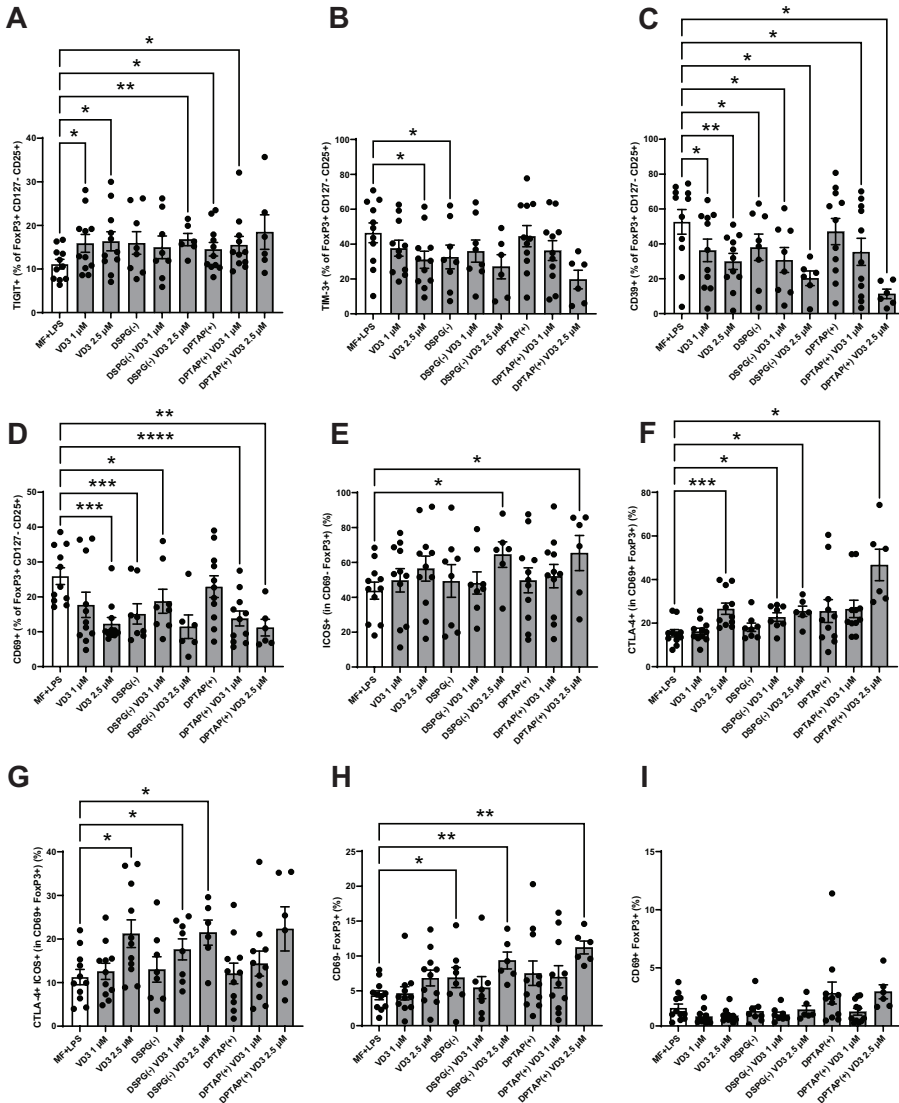


Figure 4. VD3-liposome-treated DCs induce Tregs with a distinct phenotype. (A) Frequency of TIGIT+ or (B) TIM-3+ cells within the FoxP3+ CD127- CD25+ population of T cells. (C) Frequencies of CD39+ cells within FoxP3+ CD127- CD25+ cells. (D) Frequencies of CD69+ cells within FoxP3+ CD127- CD25+ cells. (E) Frequencies of ICOS+ cells within the CD69- FoxP3+ cell population. (F)

Frequencies of CTLA-4+ cells within the CD69+ FoxP3+ population. (G) Frequencies of CTLA-4+ ICOS+ cells within CD69+ FoxP3+ T cells. (H) Frequencies of CD69- FoxP3+ T cells. (I) Frequencies of CD69+ FoxP3+ T cells. Lipid concentration of empty DSPG batches shown ranges from 50-260 µg/ml and of empty DPTAP batches 14-86 µg/ml, adjusted to the lipid concentration added when using 1-2.5 µM liposome-incorporated VD3. N=5-11 independent experiments. Error bars indicate mean ± SEM. *p≤0.05. **p≤0.01. ***p≤0.001. ****p≤0.0001. Statistical significance was calculated using a mixed-effects model of one-way ANOVA, with Dunnett's correction for multiple comparisons.

VD3-liposome primed DCs influence directionality of CD4⁺ T cell polarization

When Treg generation is fostered in coculture, polarization of other CD4⁺ T helper subsets may be inhibited. To determine whether VD3-liposome-primed DCs affect T cell polarization, we assessed Th1 or Th2 polarization with intracellular staining for IFN-γ (Th1 polarization) or IL-13 (Th2 polarization). Interestingly, liposome-primed moDCs significantly inhibited Th1 polarization at a concentration of 2.5 µM VD3, similar to soluble VD3-primed DCs (Figures 5A, B). Neither liposomes nor VD3 affected Th2 cell polarization. Hence, VD3-liposome-primed moDCs demonstrate the capacity to suppress pro-inflammatory Th1 polarization in coculture without favoring Th2 polarization. IL-17-producing CD4⁺ T cells (Th17 cells) are an essential hallmark of chronic inflammatory diseases, as they are involved in the pathophysiology and disease progression in several of these conditions⁴⁴⁻⁴⁶. Accordingly, we aimed to investigate the effect of VD3-liposome primed moDCs on Th17 polarization. As stimulation by neutrophils is required for the development of Th17 cells from naïve precursors in humans³⁹, for these experiments, we pre-incubated DCs with soluble or DSPG liposomal VD3 and cocultured with autologous naïve CD4⁺ T cells and neutrophils. Strikingly, in this solid Th17-favoring coculture environment, both soluble and DSPG-VD3 liposome-primed DCs abrogated the development of Th17 cells (Figures 5C, D). Significant changes in Th17 induction were not seen in conditions without neutrophils (Supplementary Figure 2). Thus, our data suggest that liposomal VD3 treatment of DCs results in T helper polarization favoring anti-inflammatory, tolerogenic conditions.

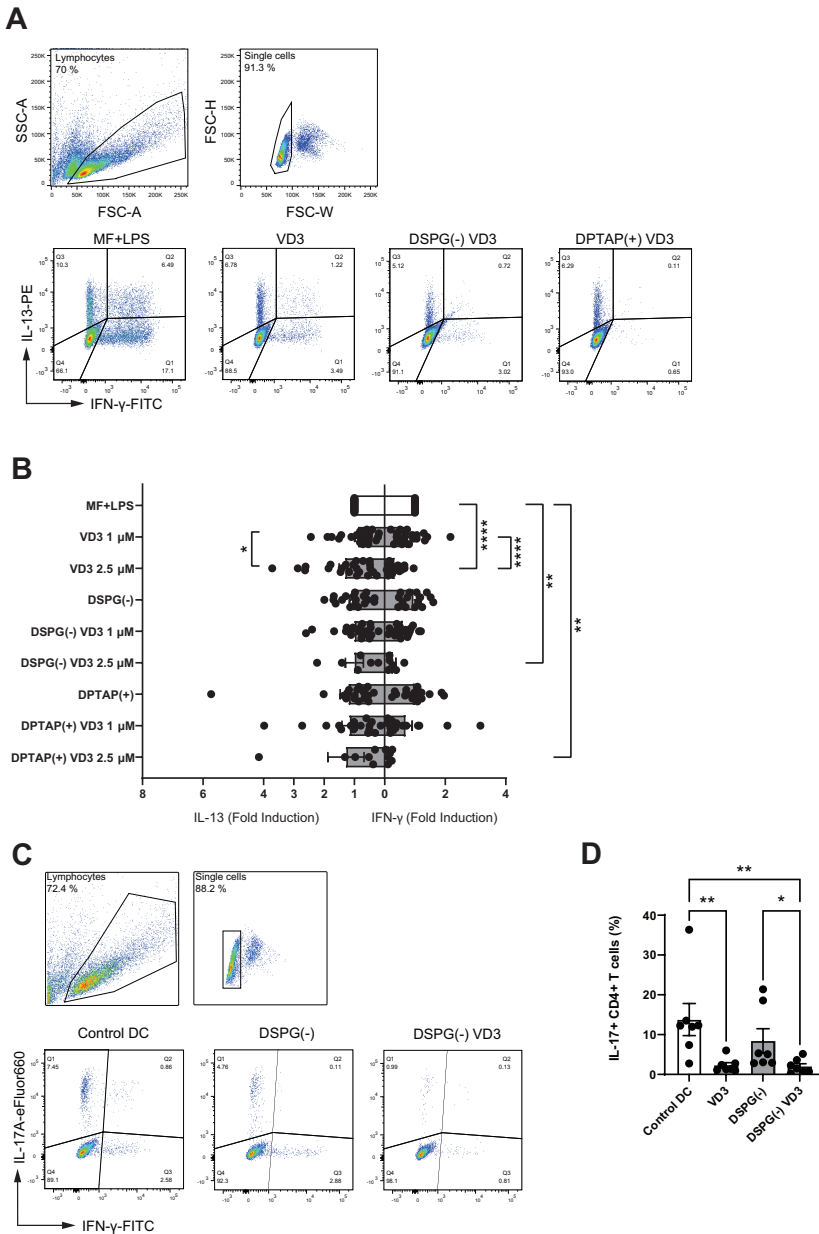


Figure 5. VD3-liposome-treated DCs reduce Th1 and Th17 polarization. (A) Example dot plots of gating IFN- γ + and IL-13+ CD4+ T cells from the single-cell population in MF+LPS DC or VD3-stimulated DC conditions. Allogeneic naïve CD4+ T cells were co-cultured with MF+LPS activated, VD3 or VD3-liposome primed moDCs for 10-12 days and stained for IFN- γ + and IL-13+ after 5-hour

stimulation with PMA+Ionomycin. (B) Fold-induction of IL-13+ and IFN- γ + CD4+ T cells in different moDC-priming conditions. Lipid concentration of empty DSPG batches shown ranges from 50-260 $\mu\text{g/ml}$ and of empty DPTAP batches 14-86 $\mu\text{g/ml}$, adjusted to the lipid concentration added when using 1-2.5 μM liposome-incorporated VD3. Mean \pm SD of IFN- γ + T cells stimulated by MF+LPS DCs was 22.5 % \pm 8.9 %, while of IL-13+ T cells, 10.68 % \pm 7.34 %. N= 6-23 independent experiments. Error bars indicate mean \pm SEM. * $p \leq 0.05$. ** $p \leq 0.01$. *** $p \leq 0.0001$. Statistical significance was calculated using a mixed-effects model of one-way ANOVA, with Dunnett's correction for multiple comparisons. (C) Example gating of IL-17 and IFN- γ expressing CD4+ T cells in different priming conditions. (D) Frequencies of IL-17+ CD4+ T cells after autologous co-culture with neutrophils and differently primed moDCs. Soluble and liposome-incorporated VD3 concentration was 2.5 μM . N=7 independent experiments. Error bars indicate mean \pm SEM. * $p \leq 0.05$. ** $p \leq 0.01$. Statistical significance was calculated using Friedman test with Dunn's correction for multiple comparisons.

Priming of moDCs with liposomal VD3 distinctly changes expression of tolerogenic surface markers

To further our knowledge of the mechanism by which VD3-treated DCs can induce suppressive T cells, we phenotyped DCs after 48-hour maturation with a flow cytometry panel containing DC maturation and tolerogenic DC markers. Frequencies of marker-positive DC populations are displayed in a heatmap (Figure 6A). Immature DCs showed lower expression levels of most markers, compared to the rest of the activated conditions, except for the markers B7H3 and ICOSL, whereas frequencies of ICOSL⁺ DCs were higher in immature cells (Figure 6A, Supplementary Figure 3A). Compared to activated DCs, VD3 priming led to enhanced expression of ILT3 (Figures 6A, B), whereas the other tolerogenic markers examined were not significantly different in expression between activated and VD3 (liposome)-treated DCs (Figure 6A, Supplementary Figures 3B-E). Similarly, DCs activated in the presence of DSPG-loaded VD3 showed higher ILT3 expression. However, DPTAP-VD3 primed DCs displayed an opposite trend, where ILT3 expression was highest in DCs activated in presence of DPTAP empty liposomes (Figures 6A, B). Treatment of DCs with soluble and liposomal VD3 decreased the frequency of CD83⁺ cells (Figure 6C). Compared to activated DCs, CD86 and HLA-DR expression did not change significantly upon VD3 treatment of the cells (Figure 6A, Supplementary Figures 3F, G). Taken together, these findings suggest that DSPG-VD3 loaded and DPTAP-VD3 loaded liposomes have a differential effect on ILT3 expression of DCs, whereas all forms of VD3-priming lead to reduced expression of CD83.

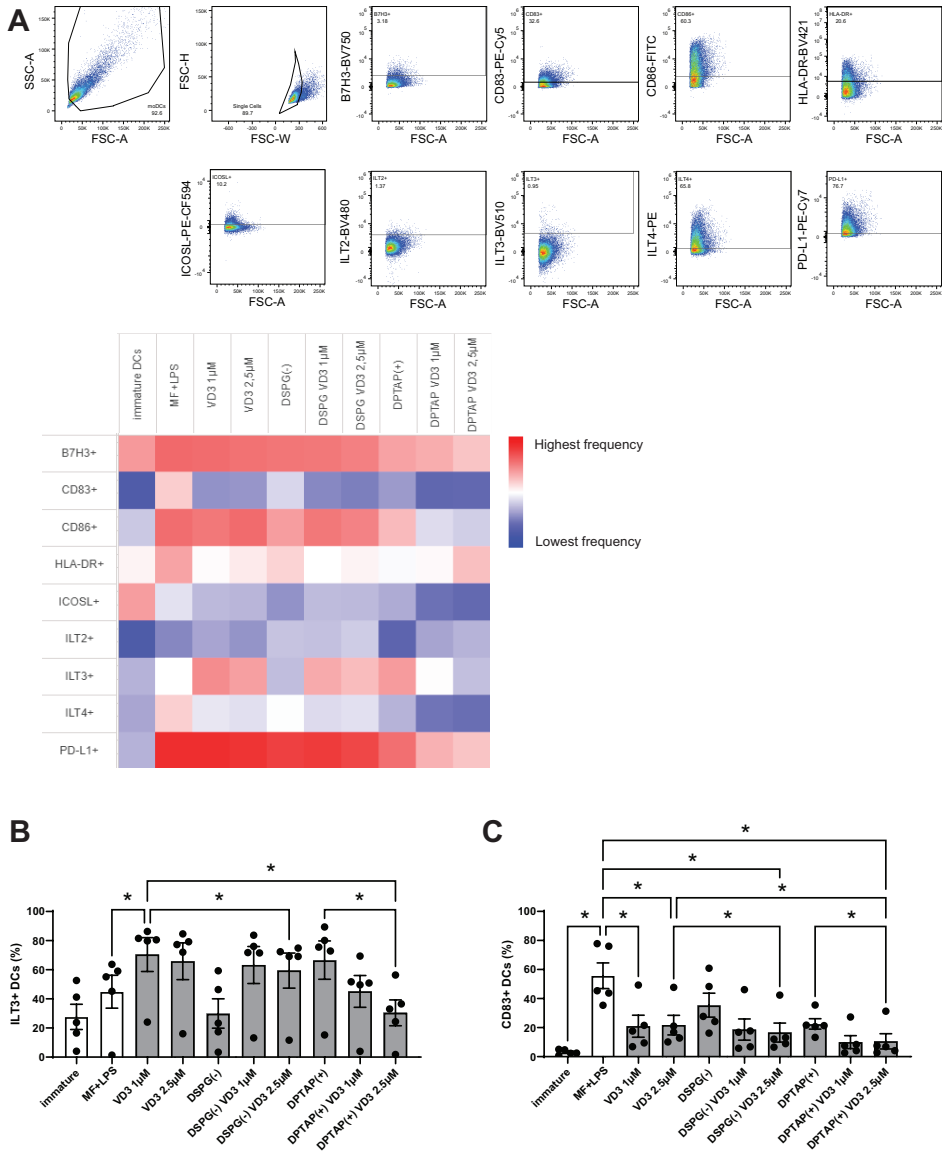


Figure 6. VD3-liposome treatment induces expression of ILT3 and reduces expression of CD83 on DCs. (A) Gating strategy and heatmap representing frequency of marker positive populations. All marker positive populations were derived from the single-cell gate. (B) Frequencies of ILT3 expressing DCs per condition. (C) Frequencies of CD83 expressing DCs per condition. Lipid concentration of empty DSPG batches shown ranges from 50-260 µg/ml and of empty DPTAP batches 14-86 µg/ml, adjusted to the lipid concentration added when using 1-2.5 µM liposome-incorporated VD3. N=5 independent experiments. Error bars indicate mean ± SEM. *p≤ 0.05. Statistical significance was

calculated using one-way ANOVA with Dunnett's correction for multiple comparisons.

Injection of VD3-loaded DSPG or DPTAP liposomes enhances migration of CD14⁺ DDCs from skin biopsies

As intradermal application of liposome-loaded VD3 is an attractive mode of administering therapy, we injected 25 μ M soluble VD3, anionic DSPG liposome-loaded VD3, or cationic DPTAP liposomes loaded with VD3 in *ex vivo* human skin, consistent with the approach of our previous study⁴⁰. Migratory effect of liposomal VD3 injection on (CD1a⁺⁺) LCs, CD1a⁺ DDCs, and CD14⁺ DDCs was determined using flow cytometry (Figure 7A). The average counts of crawl-out DCs per injection condition did not differ significantly (Figure 7B). Compared to injection of PBS or empty liposome controls, both soluble VD3 and liposomal VD3 injection resulted in selective migration of CD14⁺ DDCs out of the skin biopsies (Figure 7C). CD14⁺ DDCs were present among crawl-outs in higher frequencies (Figure 7C top panel) and higher absolute counts (Figure 7C bottom panel). The observed increase in CD14⁺ DDC efflux mediated by VD3-liposome injections was accompanied by a decrease in percentages and counts of CD1a⁺ DDCs (Figure 7D), while percentages and counts of CD1a⁺⁺ LCs remained unaltered (Figure 7E). Hence, we establish that liposomal VD3 injection (both loaded in anionic DSPG or cationic DPTAP liposomes) induces a similar effect on differential migration of crawl-out DCs as previously seen with soluble VD3⁴⁰.

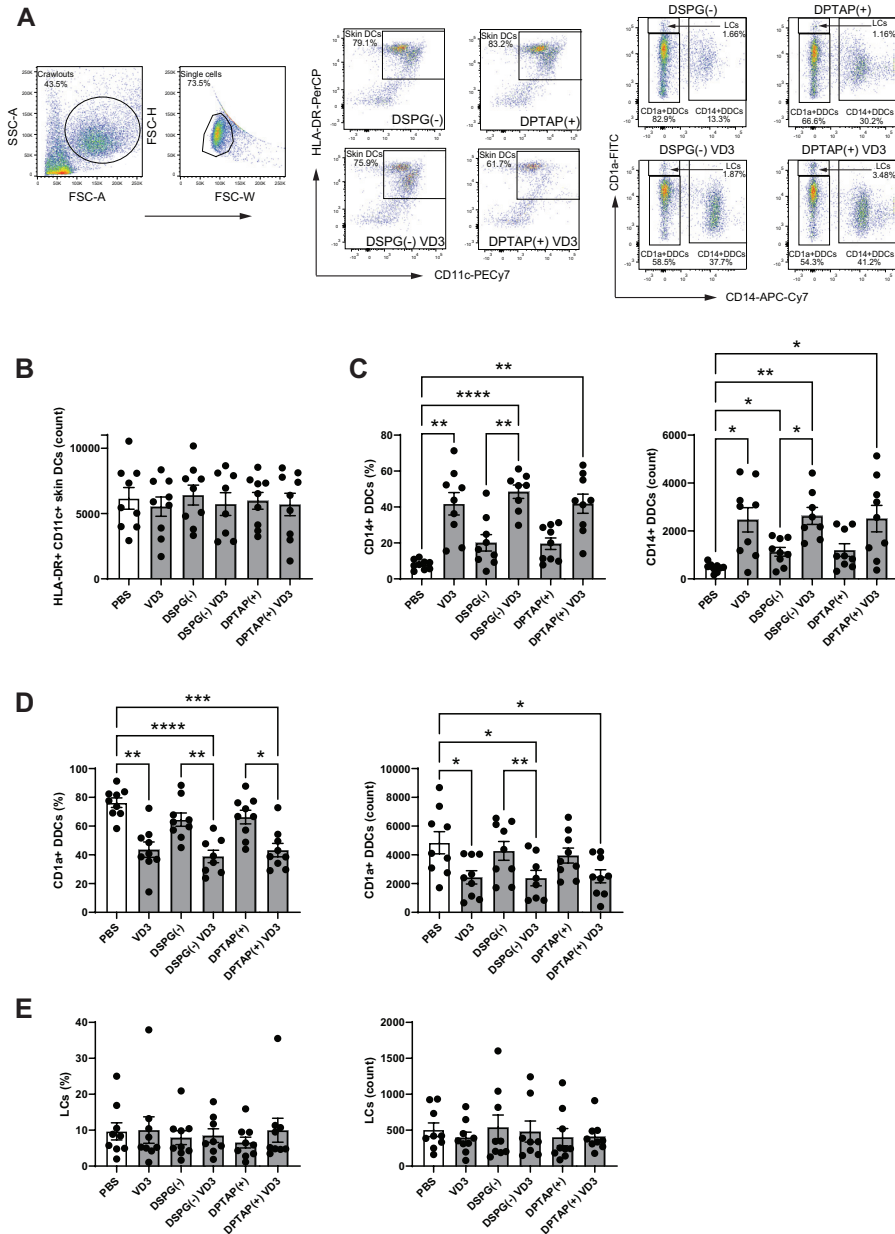


Figure 7. Injection of VD3-loaded DSPG or DPTAP liposomes enhances migration of CD14+ DDCs from human skin ex vivo. (A) Gating example for skin DCs (CD11c+ HLA-DR+ crawl-out DCs) and identification of subsets based on CD1a and CD14 staining. (B) Counts of CD11c+ HLA-DR+ crawl-out DCs. (C) Percentages (top panel) and counts (bottom panel) of CD14a+ DDCs, (D) CD1a+ DCs,

and (E) CD1a⁺⁺ LCs present in crawl-out DCs, per injection condition. Soluble and liposomal VD3 concentration injected was 25 μ M. Lipid concentration of empty DSPG batches ranged from 1000-2600 μ g/ml and of empty DPTAP batches 860-2500 μ g/ml, adjusted to the lipid concentration added when using 25 μ M liposome-incorporated VD3. N=8-9 independent experiments. Error bars indicate mean \pm SEM. * $p \leq 0.05$. ** $p \leq 0.01$. *** $p \leq 0.001$. **** $p \leq 0.0001$. Statistical significance was calculated using mixed-effects analysis with Dunnett's correction for multiple comparisons.

DISCUSSION

In this study, we embarked upon the development of a DC-tolerizing nanoparticulate product. We show that liposomal VD3 induces tolerogenic DCs that enhance the development of functional Tregs from naïve precursors, comparable to the effect of soluble VD3-treated DCs. We demonstrate that the T cells instructed by liposomal VD3-primed DCs have the phenotype of FoxP3⁺ CD127^{low} CD25⁺ CD4⁺ T cells expressing TIGIT. Furthermore, VD3-liposome primed DCs silence Th1 and Th17-type responses. As an additional laboratory proof-of-concept, we tested the VD3-liposome formulations in an *ex vivo* human skin model and showed that they enhance migration of CD14⁺ DDCs from skin biopsies, similar to soluble VD3.

To our knowledge, we are the first group to add VD3-loaded liposomes to human DCs and examine the *in vitro* T cell response in detail to deliver proof-of-concept for an *in vivo* DC-targeting tolerizing therapy as a promising alternative to *ex vivo* DC vaccination. Even though we did not observe differences in tolerogenic properties of DCs treated with soluble VD3 or liposome-loaded VD3, we demonstrate comparable effects between the two treatment approaches. These findings present the *de novo* observation that VD3-loaded liposomes are suitable carriers for targeting DCs with VD3. Furthermore, we establish tolerogenic precedent for loading disease-specific antigens together with VD3 in liposomes, with the prospect of developing a non-personalized vaccine against autoimmune and allergic diseases. Additional pharmacological benefits of encapsulating VD3 in liposomes include protection from degradation and the channeling of VD3 towards APCs to establish immune tolerance without causing toxic side effects in bystander cells^{10, 26}.

As suppression of effector T cell proliferation is a defining hallmark of Tregs, we used a T cell suppressor assay as proof-of-concept for inducing tolerogenic DCs with VD3-loaded liposomes. Irrespective of the choice of liposome formulation, VD3-primed moDCs induced CD4⁺ T cells with a proliferation-suppressing regulatory capacity. This finding is strengthened by an *in vivo* study where VD3- and OVA-loaded polymer nanoparticles injected in mice significantly suppressed target cytotoxic lymphocyte proliferation, inducing OVA-specific immune tolerance⁴⁷.

A recently published phase I clinical trial delivered an even stronger precedent in which liposomes containing a collagen-derived self-peptide and VD3 were subcutaneously injected in anti-citrullinated protein antibody + rheumatoid arthritis patients⁴⁸. The treatment resulted in improved disease activity, associated with an expansion of auto-antigen-specific T cells, coupled with a reduction in inflammatory myeloid cell populations and anti-citrullinated antibodies.

Upon phenotyping the Tregs resulting from VD3-DC treatment, we demonstrate a VD3-DC-induced increase in TIGIT⁺ FoxP3⁺ CD127^{low} T cells. Furthermore, we show that the CD69⁺ FoxP3⁺ population contains higher frequencies of ICOS⁺ CTLA-4⁺ T cells. TIGIT and CTLA-4 are inhibitory receptors that corroborate the Treg identity of VD3-liposome DC-induced FoxP3⁺ CD127^{low} CD25⁺ T cells or CD69⁺ FoxP3⁺ T cells^{49, 50}, while ICOS-ICOSL interactions between T cells and DCs have also been described to lead to Treg formation⁵¹. In previous research, VD3-treatment of CD4⁺ T cells induced the ectonucleotidase CD39 and the T cell activation marker CD69⁴⁴. CD39 converts extracellular ATP to immunosuppressive adenosine⁴², while CD69 is emerging as a crucial protein in regulating immune responses⁵². CD39, CD69, and TIM-3 enhance efficient differentiation and establishment of FoxP3⁺ T cells, conveying suppressive function to these cells^{42, 43, 50, 53-55}. Moreover, CD39 and CD69 have been linked to effective suppression of Th17 polarization^{43, 44, 56}. Unexpectedly, we observed a decrease in expression of these functional markers when applying VD3-treated DCs. Fast turnover, as well as intracellular instead of extracellular presence of these receptors, could be a possible explanation for these counterintuitive observations⁴¹. However, as CD69 is also an early activation marker of memory T cells⁵⁷, decreased expression in VD3-DC treated conditions suggests that VD3-primed DCs lead to the outgrowth of less activated effector T cells. Induction of FoxP3⁺ T cells by VD3-DC treatment in the CD69⁻ resting T cell population also indicates that these induced FoxP3⁺ cells are not activated effector T cells but Tregs.

As we observed an induction of IL-10 production of T cells stimulated with soluble or DSPG-VD3 primed DCs, which points, albeit not exclusively, to the induction of Tr1 type Tregs, we measured two important markers considered characteristic of this Treg subset, LAG-3, and CD49b⁵⁸. However, we did not succeed at reliable measurement of LAG-3 due to deficient expression levels and found no differences in expression of CD49b. Repeatedly, in the FoxP3⁺ population of T cells, CD39 and CD69 were decreased in VD3-liposome DC conditions while expression levels of the other markers were unchanged. Hence, we could not unequivocally establish that VD3-liposome-treated DCs induced Tr1 Tregs in our cocultures.

Furthermore, we cannot exclude the possibility that VD3-treated DCs induce an altogether different Treg subset which is not fully characterized yet.

We chose two previously published formulations in this study, DSPG, and DPTAP, anionic and cationic counterparts, respectively, to load VD3. Confirming our previous results, empty DSPG or DPTAP liposomes had no tolerogenic or activating effects on moDCs, or the ensuing allogeneic T cell response and could therefore serve as internal controls in our experiments. Even though suppressive and FoxP3⁺ CD127^{low} T cells were significantly induced by both DSPG-VD3 and DPTAP-VD3 treated DCs, IL-10 producing T cells were only induced by DSPG-VD3 treated DCs. In previous research, we demonstrated that DPTAP liposomes are poorly internalized by moDCs and instead adhere to the DC membrane²⁷. Together with the data in the current manuscript, our findings suggest that negatively charged liposomes are more suitable as delivery systems of adjuvants for future tolerance-promoting treatments.

A crucial function of Tregs is supplanting effector T cells. VD3-DCs are generally known to prevent Th1 polarization while they induce Th2 development and IL-10-producing Tregs^{14, 16, 36, 40}. In this study, VD3-liposome primed DCs inhibited Th1 cell development, yet they did not enhance Th2 development. This finding suggests that liposomal VD3 treatment may be preferable over soluble VD3-treated DCs in treating allergies, while autoimmune conditions may benefit from soluble and liposomal VD3.

As a disbalance between Th17 cells and Tregs is often pinpointed as pathogenetic in several inflammatory diseases^{46, 59, 60}, the effect of VD3-liposome treated DCs on Th17 polarization was also essential to observe. In an autologous coculture setting with neutrophils, VD3-liposome-treated DCs markedly abrogated Th17 cell development. We, and others, recently showed that DCs treated with soluble VD3 reduce Th17 development in human cell culture^{37, 61, 62}, adding a further argument for the suitability of VD3 for treating inflammation.

Several mechanisms of tolerance induction by VD3-treatment of DCs have been described. VD3 has been shown to downmodulate maturation of DCs, including the expression of CD83, CD86, and HLA-DR⁸. Furthermore, VD3 is associated with upregulation of several surface markers considered hallmarks of tolerogenic DCs, such as ILT2, ILT3, and PD-L1^{8, 63}. Together with ILT4, B7-H3, and ICOSL, these markers were demonstrated to exert tolerogenic functions via cognate interaction with effector T cells, rendering them anergic or transforming them into Tregs^{51, 64-66}. Interestingly, we only found enhanced frequencies of ILT3⁺ DCs upon soluble and DSPG anionic liposome VD3 treatment. Further analysis showed that only frequencies of CD83⁺ cells were significantly reduced by soluble or liposomal VD3-

treatment of DCs, but not of HLA-DR or CD86⁺ cells. This contrasts with earlier studies where VD3-treatment of DCs leads to a reduction of all three markers of DC activation^{8, 67}. Unmeasured markers or production of a soluble factor, such as IL-10, could provide an alternative explanation for the mechanism of DC-mediated tolerance in our experiments.

When developing a DC-tolerizing vaccine, the administration route must be considered. Dermal injection of a therapeutic compound is patient-friendly, and would provide easy access to skin DCs, which can migrate to proximal lymph nodes to exert tolerogenic functions there. Hence, we have chosen an *ex vivo* skin model to investigate the suitability of the liposome carriers loaded with VD3 for a tolerogenic vaccine. Confirming previous results with soluble VD3 injection, both DSPG and DPTAP VD3-liposome injection led to selective enhancement of CD14⁺ DDC migration⁴⁰. In the same study, VD3-treated crawl-out skin DCs stimulated the outgrowth of suppressive Tregs, which produced less IFN- γ and contained higher frequencies of FoxP3⁺ cells, indicating a tolerogenic quality to CD14⁺ DDCs. A plausible explanation for VD3-induced CD14⁺ DDCs is that the other subsets present in skin start expressing CD14 upon VD3 stimulation. This explanation is supported by several studies demonstrating enhanced CD14 expression on DCs by VD3-treatment^{36, 68}. The DC identity and capacity of CD14⁺ DDCs to migrate to lymph nodes is currently under debate⁶⁹, yet CD14⁺ DDCs co-expressing CD141 have been described as constitutive IL-10 producers dampening skin inflammation by inducing Tregs⁷⁰. Several other studies characterized CD14⁺ DDCs as less immunogenic, with the capability to transform into LCs under the influence of TGF- β ⁷¹⁻⁷³. Thus, the CD14⁺ DDC subset appears to consist of a heterogeneous mix of skin DCs, which can be molded by adjuvants, such as VD3, towards tolerogenic plasticity.

Collectively, we establish VD3-loaded liposomes as efficient therapeutic vehicles that induce DCs capable of promoting T cell tolerance *in vitro*. Together with the current findings in our study, a plethora of evidence points towards a beneficial effect of VD3 treatment on autoimmune and allergic conditions, supporting ongoing development of a DC-targeted vaccine platform using VD3 as its tolerance-promoting adjuvant.

DATA AVAILABILITY STATEMENT

The original contributions presented in the study are included in the article/Supplementary Material. Further inquiries can be directed to the corresponding author.

ETHICS STATEMENT

The studies involving human participants were reviewed and approved by the Institutional Review Board of the Amsterdam University Medical Center, per protocol nr. METC 2015_074. The patients/participants provided their written informed consent to participate in this study.

AUTHOR CONTRIBUTIONS

NN manufactured liposomes, performed experiments, conceptualized, and validated the study, performed formal analysis and wrote the manuscript. FLV provided valuable input on liposome manufacturing and helped reviewing and editing the manuscript. RS performed experiments and manufactured liposomes. TvC performed experiments. RvR provided valuable input on data analysis and writing of the manuscript. ST provided valuable input on data analysis and writing of the manuscript. IdV provided valuable conceptual input on research methodology. TG provided valuable input on data analysis, and carefully reviewed and edited the manuscript. BS provided valuable input on liposome manufacturing, analysis of data and carefully reviewed the manuscript. EdJ conceptualized the research, provided methodology, resources and manner of data analysis for cellular assays, supervised the research, and carefully assessed the manuscript. All authors contributed to the article and approved the submitted version.

FUNDING

This work was supported by Health Holland and “Samenwerkende Gezondheidsfondsen” (SGF), with the LSH-TKI project the LSH-TKI project DC4Balance LSHM18056-SGF. The sponsors had no role in the study design, collection, analysis, interpretation of data, report writing, or decision to submit the manuscript for publication.

ACKNOWLEDGMENTS

The authors thank Florianne Hafkamp, Rico Bas, Esther Taanman-Kueter, Charlotte Castenmiller, and Romain Lebox for technical assistance with experiments, Wim Jiskoot, Joke Bouwstra, and Alexander Kros for stimulating liposomal discussions, members of the DC4Balance consortium, and members of the DC4Balance consortium.

CONFLICT OF INTEREST

Authors BS and EdJ: Payment to institute by Health Holland and Samenwerkende Gezondheidsorganisaties SGF Grantnr: LSHM18065-SGF. Author RvR: Payment to institute by Health Holland and Samenwerkende Gezondheidsorganisaties SGF Grantnr: LSHM18065-SGF, Payment to institute by Health Holland – TKI-LSH PPP Allowance – Grant nr. LSHM19073, European Commission, NWO-TKI, AB Enzymes, Angany Inc., payment to self-consulting fees received from HAL Allergy, Citeq BV, Angany Inc, Reacta Healthcare, and Mission MightyMe, payment to self for lectures, speakers bureaus, or educational events by HAL Allergy BV, ALK and ThermoFisher Scientific.

The remaining authors declare that the research was conducted in the absence of any commercial or financial relationships that could be construed as a potential conflict of interest.

REFERENCES

1. Okada H, Kuhn C, Feillet H, Bach JF. The 'hygiene hypothesis' for autoimmune and allergic diseases: an update. *Clin Exp Immunol*. 2010;160(1):1-9.
2. Bernstein DI, Epstein T, Murphy-Berendts K, Liss GM. Surveillance of systemic reactions to subcutaneous immunotherapy injections: year 1 outcomes of the ACAAI and AAAAI collaborative study. *Ann Allergy Asthma Immunol*. 2010;104(6):530-5.
3. Larsen JN, Broge L, Jacobi H. Allergy immunotherapy: the future of allergy treatment. *Drug Discov Today*. 2016;21(1):26-37.
4. Berings M, Karaaslan C, Altunbulakli C, Gevaert P, Akdis M, Bachert C, Akdis CA. Advances and highlights in allergen immunotherapy: On the way to sustained clinical and immunologic tolerance. *J Allergy Clin Immunol*. 2017;140(5):1250-67.
5. Waisman A, Lukas D, Clausen BE, Yogev N. Dendritic cells as gatekeepers of tolerance. *Semin Immunopathol*. 2017;39(2):153-63.
6. Hawiger D, Inaba K, Dorsett Y, Guo M, Mahnke K, Rivera M, et al. Dendritic cells induce peripheral T cell unresponsiveness under steady state conditions in vivo. *J Exp Med*. 2001;194(6):769-79.
7. Hasegawa H, Matsumoto T. Mechanisms of Tolerance Induction by Dendritic Cells In Vivo. *Front Immunol*. 2018;9(NA):350.
8. Nikolic T, Roep BO. Regulatory multitasking of tolerogenic dendritic cells - lessons taken from vitamin d3-treated tolerogenic dendritic cells. *Front Immunol*. 2013;4(NA):113.
9. Jerzynska J, Stelmach W, Rychlik B, Lechanska J, Podlecka D, Stelmach I. The clinical effect of vitamin D supplementation combined with grass-specific sublingual immunotherapy in children with allergic rhinitis. *Allergy Asthma Proc*. 2016;37(2):105-14.
10. Heine G, Francuzik W, Doelle-Bierke S, Drozdenko G, Frischbutter S, Schumacher N, et al. Immunomodulation of high-dose vitamin D supplementation during allergen-specific immunotherapy. *Allergy*. 2021;76(3):930-3.
11. Jeffery LE, Burke F, Mura M, Zheng Y, Qureshi OS, Hewison M, et al. 1,25-Dihydroxyvitamin D3 and IL-2 combine to inhibit T cell production of inflammatory cytokines and promote development of regulatory T cells expressing CTLA-4 and FoxP3. *J Immunol*. 2009;183(9):5458-67.
12. Wang G, Zhang J, Fang Y, Cao W, Xu B, Chen X. Stimulation of tolerogenic dendritic cells using dexamethasone and 1,25-dihydroxyvitamin D3 represses autologous T cell activation and chondrocyte inflammation. *Exp Ther Med*. 2019;17(1):679-88.
13. Adnan E, Matsumoto T, Ishizaki J, Onishi S, Suemori K, Yasukawa M, Hasegawa H. Human tolerogenic dendritic cells generated with protein kinase C inhibitor are optimal for functional regulatory T cell induction - A comparative study. *Clin Immunol*. 2016;173(NA):96-108.
14. Vanherwegen AS, Eelen G, Ferreira GB, Ghesquiere B, Cook DP, Nikolic T, et al. Vitamin D controls the capacity of human dendritic cells to induce functional regulatory T cells by regulation of glucose metabolism. *J Steroid Biochem Mol Biol*. 2019;187(NA):134-45.
15. Mora JR, Iwata M, von Andrian UH. Vitamin effects on the immune system: vitamins A and D take centre stage. *Nat Rev Immunol*. 2008;8(9):685-98.

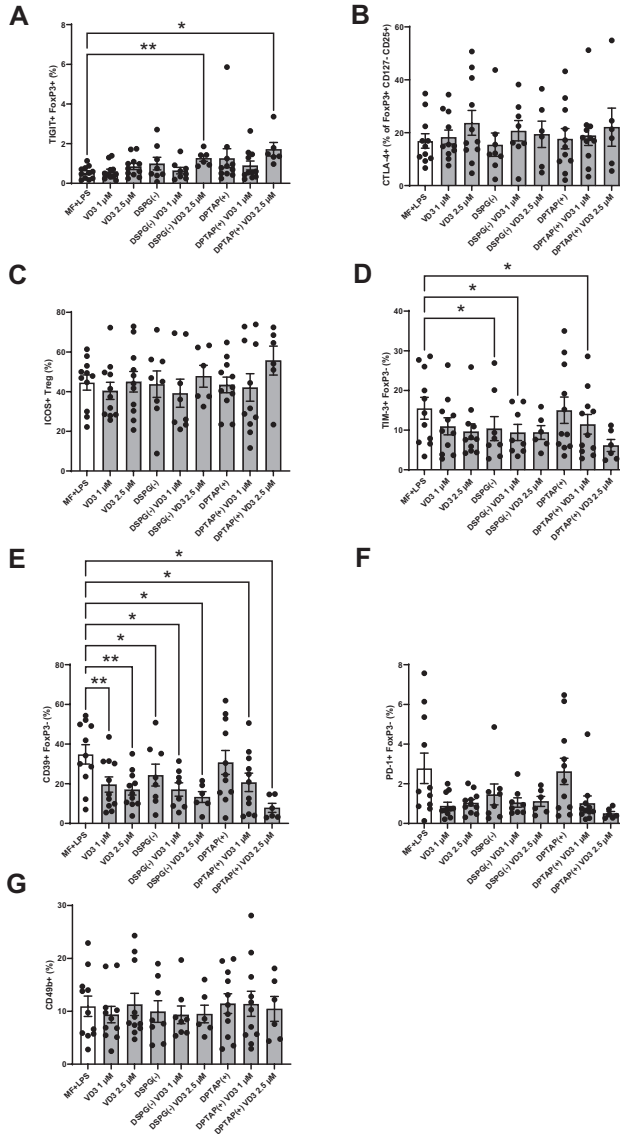
16. Penna G, Amuchastegui S, Giarratana N, Daniel KC, Vulcano M, Sozzani S, Adorini L. 1,25-Dihydroxyvitamin D3 selectively modulates tolerogenic properties in myeloid but not plasmacytoid dendritic cells. *J Immunol.* 2007;178(1):145-53.
17. Penna G, Adorini L. 1 α ,25-dihydroxyvitamin D3 inhibits differentiation, maturation, activation, and survival of dendritic cells leading to impaired alloreactive T cell activation. *J Immunol.* 2000;164(5):2405-11.
18. Willekens B, Presas-Rodriguez S, Mansilla MJ, Derdelinckx J, Lee WP, Nijs G, et al. Tolerogenic dendritic cell-based treatment for multiple sclerosis (MS): a harmonised study protocol for two phase I clinical trials comparing intradermal and intranodal cell administration. *BMJ Open.* 2019;9(9):e030309.
19. Anderson AE, Swan DJ, Wong OY, Buck M, Eltherington O, Harry RA, et al. Tolerogenic dendritic cells generated with dexamethasone and vitamin D3 regulate rheumatoid arthritis CD4(+) T cells partly via transforming growth factor-beta1. *Clin Exp Immunol.* 2017;187(1):113-23.
20. Bell GM, Anderson AE, Diboll J, Reece R, Eltherington O, Harry RA, et al. Autologous tolerogenic dendritic cells for rheumatoid and inflammatory arthritis. *Ann Rheum Dis.* 2017;76(1):227-34.
21. Benham H, Nel HJ, Law SC, Mehdi AM, Street S, Ramnarth N, et al. Citrullinated peptide dendritic cell immunotherapy in HLA risk genotype-positive rheumatoid arthritis patients. *Sci Transl Med.* 2015;7(290):290ra87.
22. Ten Brinke A, Martinez-Llordella M, Cools N, Hilken CMU, van Ham SM, Sawitzki B, et al. Ways Forward for Tolerance-Inducing Cellular Therapies- an AFACTT Perspective. *Front Immunol.* 2019;10(NA):181.
23. Baldin AV, Savvateeva LV, Bazhin AV, Zamyatnin AA, Jr. Dendritic Cells in Anticancer Vaccination: Rationale for Ex Vivo Loading or In Vivo Targeting. *Cancers (Basel).* 2020;12(3):590-NA.
24. Unger WW, van Beelen AJ, Bruijns SC, Joshi M, Fehres CM, van Bloois L, et al. Glycan-modified liposomes boost CD4+ and CD8+ T-cell responses by targeting DC-SIGN on dendritic cells. *J Control Release.* 2012;160(1):88-95.
25. Benne N, van Duijn J, Kuiper J, Jiskoot W, Slutter B. Orchestrating immune responses: How size, shape and rigidity affect the immunogenicity of particulate vaccines. *J Control Release.* 2016;234:124-34.
26. Taylor PN, Davies JS. A review of the growing risk of vitamin D toxicity from inappropriate practice. *Br J Clin Pharmacol.* 2018;84(6):1121-7.
27. Nagy NA, Castenmiller C, Vigario FL, Sparrius R, van Capel TMM, de Haas AM, et al. Uptake Kinetics Of Liposomal Formulations of Differing Charge Influences Development of in Vivo Dendritic Cell Immunotherapy. *J Pharm Sci.* 2022;111(4):1081-91.
28. van der Aar AM, Sylva-Steenland RM, Bos JD, Kapsenberg ML, de Jong EC, Teunissen MB. Loss of TLR2, TLR4, and TLR5 on Langerhans cells abolishes bacterial recognition. *J Immunol.* 2007;178(4):1986-90.
29. Stoitzner P, Schaffenrath S, Tripp CH, Reider D, Komenda K, Del Frari B, et al. Human skin dendritic cells can be targeted in situ by intradermal injection of antibodies against lectin receptors. *Exp Dermatol.* 2014;23(12):909-15.

30. Stolk DA, de Haas A, Vree J, Duinkerken S, Lubbers J, van de Ven R, et al. Lipo-Based Vaccines as an Approach to Target Dendritic Cells for Induction of T- and iNKT Cell Responses. *Front Immunol.* 2020;11(NA):990.
31. Varypataki EM, van der Maaden K, Bouwstra J, Ossendorp F, Jiskoot W. Cationic liposomes loaded with a synthetic long peptide and poly(I:C): a defined adjuvanted vaccine for induction of antigen-specific T cell cytotoxicity. *AAPS J.* 2015;17(1):216-26.
32. Benne N, van Duijn J, Lozano Vigario F, Lebourg RJT, van Veelen P, Kuiper J, et al. Anionic 1,2-distearoyl-sn-glycero-3-phosphoglycerol (DSPG) liposomes induce antigen-specific regulatory T cells and prevent atherosclerosis in mice. *J Control Release.* 2018;291:135-46.
33. de Jong EC, Vieira PL, Kalinski P, Schuitemaker JH, Tanaka Y, Wierenga EA, et al. Microbial compounds selectively induce Th1 cell-promoting or Th2 cell-promoting dendritic cells in vitro with diverse th cell-polarizing signals. *J Immunol.* 2002;168(4):1704-9.
34. Dankers W, Davelaar N, van Hamburg JP, van de Peppel J, Colin EM, Lubberts E. Human Memory Th17 Cell Populations Change Into Anti-inflammatory Cells With Regulatory Capacity Upon Exposure to Active Vitamin D. *Front Immunol.* 2019;10(NA):1504.
35. Sheikh V, Kasapoglu P, Zamani A, Basiri Z, Tahamoli-Roudsari A, Alahgholi-Hajibehzad M. Vitamin D3 inhibits the proliferation of T helper cells, downregulate CD4(+) T cell cytokines and upregulate inhibitory markers. *Hum Immunol.* 2018;79(6):439-45.
36. van der Aar AM, Sibiryak DS, Bakdash G, van Capel TM, van der Kleij HP, Opstelten DJ, et al. Vitamin D3 targets epidermal and dermal dendritic cells for induction of distinct regulatory T cells. *J Allergy Clin Immunol.* 2011;127(6):1532-40 e7.
37. Hafkamp FMJ, Taanman-Kueter EWM, van Capel TMM, Kormelink TG, de Jong EC. Vitamin D3 Priming of Dendritic Cells Shifts Human Neutrophil-Dependent Th17 Cell Development to Regulatory T Cells. *Front Immunol.* 2022;13(NA):872665.
38. Volpe E, Servant N, Zollinger R, Bogiatzi SI, Hupe P, Barillot E, Soumelis V. A critical function for transforming growth factor-beta, interleukin 23 and proinflammatory cytokines in driving and modulating human T(H)-17 responses. *Nat Immunol.* 2008;9(6):650-7.
39. Souwer Y, Groot Kormelink T, Taanman-Kueter EW, Muller FJ, van Capel TMM, Varga DV, et al. Human T(H)17 cell development requires processing of dendritic cell-derived CXCL8 by neutrophil elastase. *J Allergy Clin Immunol.* 2018;141(6):2286-9 e5.
40. Bakdash G, Schneider LP, van Capel TM, Kapsenberg ML, Teunissen MB, de Jong EC. Intradermal application of vitamin D3 increases migration of CD14+ dermal dendritic cells and promotes the development of Foxp3+ regulatory T cells. *Hum Vaccin Immunother.* 2013;9(2):250-8.
41. White AM, Wraith DC. Tr1-Like T Cells - An Enigmatic Regulatory T Cell Lineage. *Front Immunol.* 2016;7(NA):355.
42. Borsellino G, Kleinewietfeld M, Di Mitri D, Sternjak A, Diamantini A, Giometto R, et al. Expression of ectonucleotidase CD39 by Foxp3+ Treg cells: hydrolysis of extracellular ATP and immune suppression. *Blood.* 2007;110(4):1225-32.
43. Fletcher JM, Lonergan R, Costelloe L, Kinsella K, Moran B, O'Farrelly C, et al. CD39+Foxp3+ regulatory T Cells suppress pathogenic Th17 cells and are impaired in multiple sclerosis. *J Immunol.* 2009;183(11):7602-10.

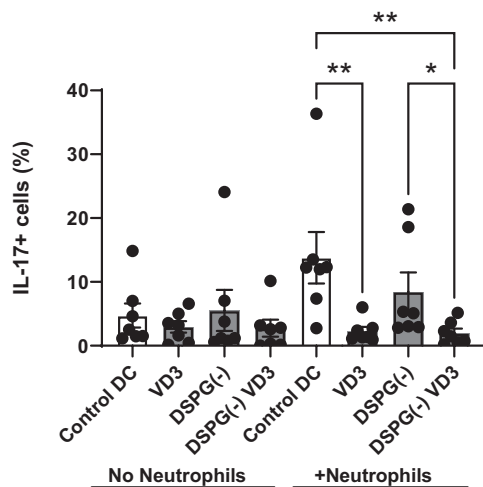
44. Nanzer AM, Chambers ES, Ryanna K, Richards DF, Black C, Timms PM, et al. Enhanced production of IL-17A in patients with severe asthma is inhibited by 1 α ,25-dihydroxyvitamin D3 in a glucocorticoid-independent fashion. *J Allergy Clin Immunol.* 2013;132(2):297-304 e3.
45. Harrison SR, Li D, Jeffery LE, Raza K, Hewison M. Vitamin D, Autoimmune Disease and Rheumatoid Arthritis. *Calcif Tissue Int.* 2020;106(1):58-75.
46. Wolf D, Gerhardt T, Winkels H, Michel NA, Pramod AB, Ghosheh Y, et al. Pathogenic Autoimmunity in Atherosclerosis Evolves From Initially Protective Apolipoprotein B(100)-Reactive CD4(+) T-Regulatory Cells. *Circulation.* 2020;142(13):1279-93.
47. Jung HH, Kim SH, Moon JH, Jeong SU, Jang S, Park CS, Lee CK. Polymeric Nanoparticles Containing Both Antigen and Vitamin D(3) Induce Antigen-Specific Immune Suppression. *Immune Netw.* 2019;19(3):e19.
48. Sonigra A, Nel HJ, Wehr P, Ramnorruth N, Patel S, van Schie KA, et al. Randomized phase I trial of antigen-specific tolerizing immunotherapy with peptide/calcitriol liposomes in ACPA+ rheumatoid arthritis. *JCI Insight.* 2022;7(20):NA-NA.
49. Harjunpää H, Guilleroy C. TIGIT as an emerging immune checkpoint. *Clin Exp Immunol.* 2020;200(2):108-19.
50. Cortés JR, Sánchez-Díaz R, Bovolenta ER, Barreiro O, Lasarte S, Matesanz-Marin A, et al. Maintenance of immune tolerance by Foxp3+ regulatory T cells requires CD69 expression. *J Autoimmun.* 2014;55(NA):51-62.
51. Akbari O, Freeman GJ, Meyer EH, Greenfield EA, Chang TT, Sharpe AH, et al. Antigen-specific regulatory T cells develop via the ICOS-ICOS-ligand pathway and inhibit allergen-induced airway hyperreactivity. *Nat Med.* 2002;8(9):1024-32.
52. Cibrián D, Sánchez-Madrid F. CD69: from activation marker to metabolic gatekeeper. *Eur J Immunol.* 2017;47(6):946-53.
53. Ahlmanner F, Sundstrom P, Akeus P, Eklof J, Borjesson L, Gustavsson B, et al. CD39(+) regulatory T cells accumulate in colon adenocarcinomas and display markers of increased suppressive function. *Oncotarget.* 2018;9(97):36993-7007.
54. Yu L, Yang F, Zhang F, Guo D, Li L, Wang X, et al. CD69 enhances immunosuppressive function of regulatory T-cells and attenuates colitis by prompting IL-10 production. *Cell Death Dis.* 2018;9(9):905.
55. Gautron AS, Dominguez-Villar M, de Marcken M, Hafler DA. Enhanced suppressor function of TIM-3+ FoxP3+ regulatory T cells. *Eur J Immunol.* 2014;44(9):2703-11.
56. Martin P, Sanchez-Madrid F. CD69: an unexpected regulator of TH17 cell-driven inflammatory responses. *Sci Signal.* 2011;4(165):pe14.
57. Chen ZY, Wang L, Gu L, Qu R, Lowrie DB, Hu Z, et al. Decreased Expression of CD69 on T Cells in Tuberculosis Infection Resisters. *Front Microbiol.* 2020;11(NA):1901.
58. Gagliani N, Magnani CF, Huber S, Gianolini ME, Pala M, Licona-Limon P, et al. Coexpression of CD49b and LAG-3 identifies human and mouse T regulatory type 1 cells. *Nat Med.* 2013;19(6):739-46.
59. Veldhoen M. Interleukin 17 is a chief orchestrator of immunity. *Nat Immunol.* 2017;18(6):612-21.

60. Su Y, Huang J, Zhao X, Lu H, Wang W, Yang XO, et al. Interleukin-17 receptor D constitutes an alternative receptor for interleukin-17A important in psoriasis-like skin inflammation. *Sci Immunol*. 2019;4(36):NA-NA.
61. Hamzaoui A, Berraies A, Hamdi B, Kaabachi W, Ammar J, Hamzaoui K. Vitamin D reduces the differentiation and expansion of Th17 cells in young asthmatic children. *Immunobiology*. 2014;219(11):873-9.
62. Mann EH, Ho TR, Pfeffer PE, Matthews NC, Chevetton E, Mudway I, et al. Vitamin D Counteracts an IL-23-Dependent IL-17A(+)IFN-gamma(+) Response Driven by Urban Particulate Matter. *Am J Respir Cell Mol Biol*. 2017;57(3):355-66.
63. Svaiger U, Rozman PJ. Synergistic Effects of Interferon-gamma and Vitamin D(3) Signaling in Induction of ILT-3(high)PDL-1(high) Tolerogenic Dendritic Cells. *Front Immunol*. 2019;10(NA):2627.
64. Manavalan JS, Rossi PC, Vlad G, Piazza F, Yamilina A, Cortesini R, et al. High expression of ILT3 and ILT4 is a general feature of tolerogenic dendritic cells. *Transpl Immunol*. 2003;11(3-4):245-58.
65. Zheng X, Xiao ZX, Hu L, Fang X, Luo L, Chen L. Dendritic cell-associated B7-H3 suppresses the production of autoantibodies and renal inflammation in a mouse model of systemic lupus erythematosus. *Cell Death Dis*. 2019;10(6):393.
66. Peng Q, Qiu X, Zhang Z, Zhang S, Zhang Y, Liang Y, et al. PD-L1 on dendritic cells attenuates T cell activation and regulates response to immune checkpoint blockade. *Nat Commun*. 2020;11(1):4835.
67. Bartels LE, Hvas CL, Agnholt J, Dahlerup JF, Agger R. Human dendritic cell antigen presentation and chemotaxis are inhibited by intrinsic 25-hydroxy vitamin D activation. *Int Immunopharmacol*. 2010;10(8):922-8.
68. Unger WW, Laban S, Kleijwegt FS, van der Slik AR, Roep BO. Induction of Treg by monocyte-derived DC modulated by vitamin D3 or dexamethasone: differential role for PD-L1. *Eur J Immunol*. 2009;39(11):3147-59.
69. McGovern N, Schlitzer A, Gunawan M, Jardine L, Shin A, Poyner E, et al. Human dermal CD14(+) cells are a transient population of monocyte-derived macrophages. *Immunity*. 2014;41(3):465-77.
70. Chu CC, Ali N, Karagiannis P, Di Meglio P, Skowera A, Napolitano L, et al. Resident CD141 (BDCA3)+ dendritic cells in human skin produce IL-10 and induce regulatory T cells that suppress skin inflammation. *J Exp Med*. 2012;209(5):935-45.
71. Caux C, Vanbervliet B, Massacrier C, Dezutter-Dambuyant C, de Saint-Vis B, Jacquet C, et al. CD34+ hematopoietic progenitors from human cord blood differentiate along two independent dendritic cell pathways in response to GM-CSF+TNF alpha. *J Exp Med*. 1996;184(2):695-706.
72. Larregina AT, Morelli AE, Spencer LA, Logar AJ, Watkins SC, Thomson AW, Falo LD, Jr. Dermal-resident CD14+ cells differentiate into Langerhans cells. *Nat Immunol*. 2001;2(12):1151-8.
73. Klechevsky E, Morita R, Liu M, Cao Y, Coquery S, Thompson-Snipes L, et al. Functional specializations of human epidermal Langerhans cells and CD14+ dermal dendritic cells. *Immunity*. 2008;29(3):497-510.

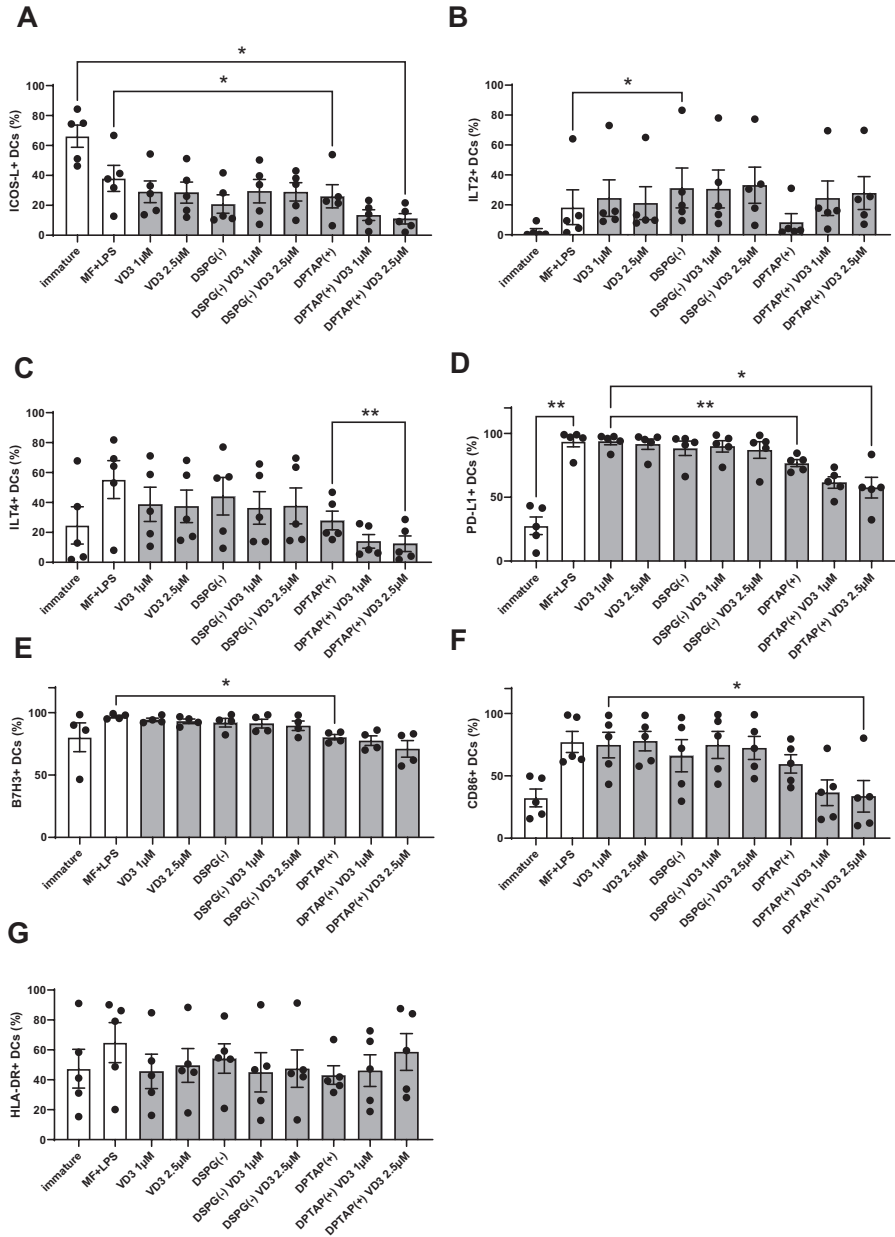
SUPPLEMENTARY FIGURES



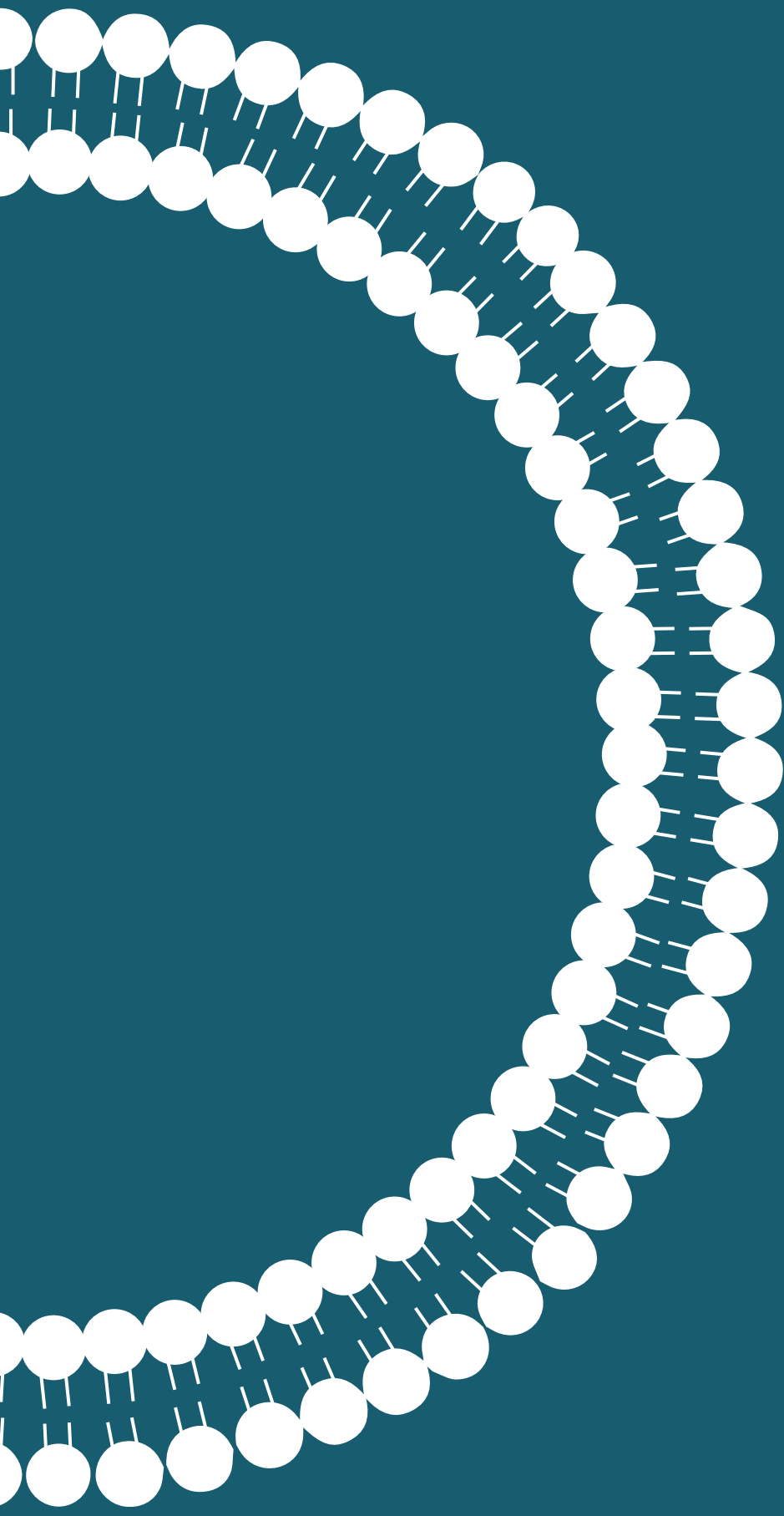
Supplementary Figure 1. VD3-liposome treated DCs stimulate the development of CD4⁺ T cells with a distinct footprint of Treg markers. After 10-12-day co-culture with differently primed moDCs, CD4⁺ T cells were stained for Treg subset and functional markers. (A-G) Frequencies of TIGIT⁺ FoxP3⁺, CTLA-4⁺ within FoxP3⁺ CD127^{low} CD25⁺, ICOS⁺ Treg (ICOS⁺ CTLA-4⁺ FoxP3⁺), TIM-3⁺ FoxP3⁺, CD39⁺ FoxP3⁺, PD-1⁺ FoxP3⁺, and CD49b⁺ CD4⁺ T cells. N=5-11 independent experiments. Error bars indicate mean \pm SEM. * $p \leq 0.05$. ** $p \leq 0.01$. Statistical significance was calculated using mixed-effects analysis with Dunnett's correction for multiple comparisons.



Supplementary Figure 2. Frequencies of IL-17+ CD4+ T cells after autologous co-culture without or with neutrophils and differently primed moDCs. N=7 independent experiments. Error bars indicate mean \pm SEM. * $p \leq 0.05$. ** $p \leq 0.01$. Statistical significance was calculated using Friedman test with Dunn's correction for multiple comparisons.



Supplementary Figure 3. Effect of VD3-liposome treatment on tolerogenic and maturation markers of DCs. (A-G) Frequencies of marker+ DCs are shown. N=4-5 independent experiments. Error bars indicate mean \pm SEM. * $p \leq 0.05$. ** $p \leq 0.01$.



Chapter 5

The Use of a Staggered Herringbone Micromixer for the Preparation of Rigid Liposomal Formulations Allows Efficient Encapsulation of Antigen and Adjuvant

F. Lozano Vigario¹, N.A. Nagy², M.H. The¹, R. Sparrius², J.A. Bouwstra¹, A. Kros³, W. Jiskoot¹, E.C. de Jong², B. Slütter¹

¹ Division of BioTherapeutics, Leiden Academic Centre for Drug Research, Leiden University, The Netherlands

² Department of Experimental Immunology, Amsterdam University Medical Centre, Amsterdam Institute for Infection & Immunity, University of Amsterdam, Amsterdam, Netherlands.

³ Department of Supramolecular & Biomaterials Chemistry, Leiden Institute of Chemistry, Leiden University, The Netherlands

Adapted from Journal of Pharmaceutical Science, Volume 111, Issue 4, April 2022;
DOI: 10.1016/j.xphs.2022.01.029

ABSTRACT

Anionic liposomal formulations have previously shown to have intrinsic tolerogenic capacity and these properties have been related to the rigidity of the particles. The combination of highly rigid anionic liposomes to deliver tolerogenic adjuvants and antigen peptides has potential applications for the treatment of autoimmune and inflammatory diseases. However, the preparation of these highly rigid anionic liposomes using traditional methods such as lipid film hydration presents problems in terms of scalability and loading efficiency of some costly tolerogenic adjuvants like 1- α ,25-dihydroxyvitaminD3. Here we propose the use of an off-the-shelf staggered herringbone micromixer for the preparation of these formulations and perform a systematic study on the effect of temperature and flow conditions on the size and polydispersity index of the formulations. Furthermore, we show that the system allows for the encapsulation of a wide variety of peptides and significantly higher loading efficiency of 1- α ,25-dihydroxyvitaminD3 compared to the traditional lipid film hydration method, without compromising their non-inflammatory interaction with dendritic cells. Therefore, the microfluidics method presented here is a valuable tool for the preparation of highly rigid tolerogenic liposomes in a fast, size-tuneable, and scalable manner.

Keywords

liposomes, rigidity, herringbone micromixer, microfluidics, vitaminD3, tolerance

Abbreviations

DiD, DiI18(5); 1,1'-dioctadecyl-3,3,3',3'- tetramethylindodicarbocyanine, 4-chlorobenzenesulfonate; DLS, dynamic light scattering; DSPC, 1,2-distearoyl-*sn*-glycero-3-phosphocholine; DSPG, 1,2-Distearoyl-*sn*-glycero-3-phosphoglycerol; FRR, flow rate ratio; GRAVY, grand average of hydropathy; HPLC, high-performance liquid chromatography; LE%, loading efficiency; LFH, lipid film hydration; MWCO, molecular weight cut-out; PB, phosphate buffer; Pdl, polydispersity index; TEM, transmission electron microscopy; TFA, trifluoroacetic acid; TFR, total flow rate; TIPS, triisopropylsilane; UPLC, ultra-high performance liquid chromatography; VD3, 1- α ,25-dihydroxyvitaminD3

INTRODUCTION

Liposomes are nanometre-sized vesicles formed by a lipid bilayer enclosing an aqueous core and are used for various applications, including vaccination. Whereas cationic liposomes and lipid nanoparticle formulations have shown to have immune stimulatory properties¹ anionic liposomes might induce immune tolerance. We have previously shown that 1,2-Distearoyl-*sn*-glycero-3-phosphoglycerol (DSPG)-containing liposomes carrying peptide antigens are able to induce T regulatory cells, which are key mediators of peripheral tolerance, and was able to arrest development of atherosclerosis in mice². The tolerogenic capacity of these DSPG formulations is, in part, due to the high rigidity of these liposomes as this impacts both the uptake of the formulation by professional antigen presenting cells, such as dendritic cells, and on the capacity of the formulation to induce tolerogenic immune responses³.

Although the physicochemical properties of liposomal formulations can influence their capacity to induce a tolerogenic immune response, the generation of a strong tolerogenic response might require the inclusion of tolerogenic adjuvants. Immune modulatory molecules such as 1- α ,25-dihydroxyvitaminD3 (VD3), rapamycin or retinoic acid have been widely studied for their capacity to induce tolerogenic dendritic cells and may therefore represent interesting adjuvants for tolerogenic vaccines⁴⁻⁶. However, despite their high hydrophobicity index, the loading efficiency of these molecules, specially VD3, into highly rigid anionic liposomes using the traditional lipid film hydration method is surprisingly low (Table 1) with only a small fraction (<10%) of the VD3 being loaded into the liposomes. Moreover, the traditional liposome preparation of lipid film hydration also has limitations regarding the scalability and batch to batch variability.

Table 1. Loading efficiency of tolerogenic adjuvants into anionic rigid liposomes using the lipid film hydration method. The table summarizes the average loading efficiency of at least 2 separate batches of liposomes (n=2)

	Loading efficiency % (\pm SD)
Rapamycin	7.1 (\pm 5.1)
Retinoic acid	38.6 (\pm 0.9)
1- α ,25-dihydroxyvitaminD3	8.08 (\pm 10.1)

Due to the promising application of highly rigid anionic liposomes in the field of antigen-specific tolerance and the need for methods to efficiently load tolerogenic adjuvants, we developed a microfluidics-based approach.

Microfluidics allows the high-throughput and scalable manufacture of liposomal formulations. In these systems, the sudden change in solvent polarity in a

micrometre-sized channel triggers the nanoprecipitation of the phospholipids, forming lipid bilayers with more thermodynamically stable structures⁷ and may encapsulate more antigen and adjuvant in the process. However, the available commercial microfluidics systems have limitations for the preparation of highly rigid liposomal formulations. These formulations need to be prepared above the transition temperature of the phospholipids, which in the case of liposomes containing 1,2-distearoyl-*sn*-glycero-3-phosphocholine (DSPC) and DSPG is 55°C. The design of the microfluidics systems makes difficult to accurately define the temperature in the microchannel. Here we described a method with an off-the-shelf glass staggered herringbone micromixer that allows the preparation of highly rigid anionic liposomes loaded with VD3. This system offers significant advantages over the lipid film hydration method including a markedly improved loading efficiency of VD3.

MATERIALS AND METHODS

Materials

Staggered herringbone micromixer was purchased from Darwin Microfluidics (Paris, France) cat# LTF-012.00-4264. Both the aqueous and organic phases were loaded into Hamilton glass syringes obtained from Sigma-Aldrich (Zwijndrecht, The Netherlands) and the inlet flow was controlled by two single channel syringe pumps (ProSense, Oosterhout, The Netherlands). 1,2-distearoyl-*sn*-glycero-3-phosphocholine (DSPC) and 1,2-distearoyl-*sn*-glycero-3-phospho-(1'-rac-glycerol) (DSPG) were purchased from Avanti Polar Lipids (Alabaster, USA). Cholesterol was obtained from Sigma-Aldrich (Zwijndrecht, The Netherlands). 1- α ,25-dihydroxyvitaminD3 was purchased from Sigma-Aldrich (Zwijndrecht, The Netherlands). Peptides were synthesized in house by solid-phase peptide synthesis (SPPS) using the CEM microwave-assisted automated peptide synthesizer Liberty Blue. Ethanol absolute was purchased from Biosolve (Valkenswaard, The Netherlands). Float-A-lyzers 100,000Da MWCO dialysis tubes were purchased from Sigma-Aldrich (Zwijndrecht, The Netherlands). Whatman Nucleopore polycarbonate track-etched membranes were obtained from Sigma-Aldrich (Zwijndrecht, The Netherlands).

Methods

Preparation of highly rigid anionic liposomes using staggered herringbone micromixer

The organic phase for the preparation of anionic liposomal formations consisted on DSPC:DSPG:Cholesterol dissolved in ethanol absolute in a molar ratio 4:1:2.

The lipid concentration on the organic phase was 10 mg/mL unless specified otherwise. The aqueous phase consisted of Phosphate Buffer (PB) 10 mM pH 7.4, in the case of peptide-loaded liposomes, the peptides were included in the aqueous phase at a concentration of 100 $\mu\text{g/mL}$. In the case of liposomes loaded with 1 α ,25-dihydroxyvitaminD3 or labelled with the lipophilic dye DiD, the adjuvant or fluorescent label were included in the organic phase together with the lipids. The concentration of 1 α ,25-dihydroxyvitaminD3 in the organic phase was 150 $\mu\text{g/mL}$. The organic and aqueous phases were injected into the herringbone micromixer as schematically depicted in Figure 1. The flow rate ratio (FRR) between the aqueous and the organic phase was varied from 2:1 to 5:1 (Table S1) and the total flow rate (TFR), defined as the sum of the aqueous flow rate and the organic flow rate, was also varied from 100 $\mu\text{L/min}$ to 900 $\mu\text{L/min}$ in order to determine the effect of flow conditions on particle size and polydispersity index (Pdl). All formulations were prepared at a temperature above the gel-liquid phase transition temperature of the phospholipids in the formulation unless mentioned otherwise. The temperature was set by submerging the micromixer in a water bath at 60°C. The temperature of the water bath was controlled by using a temperature probe connected to a heating plate. Formulations were dialyzed against 400 mL of PB 10 mM pH 7.4 overnight with constant stirring using Float-A-lyzer dialysis kit (MWCO 100,000 Da) to remove traces of ethanol and non-encapsulated molecules.

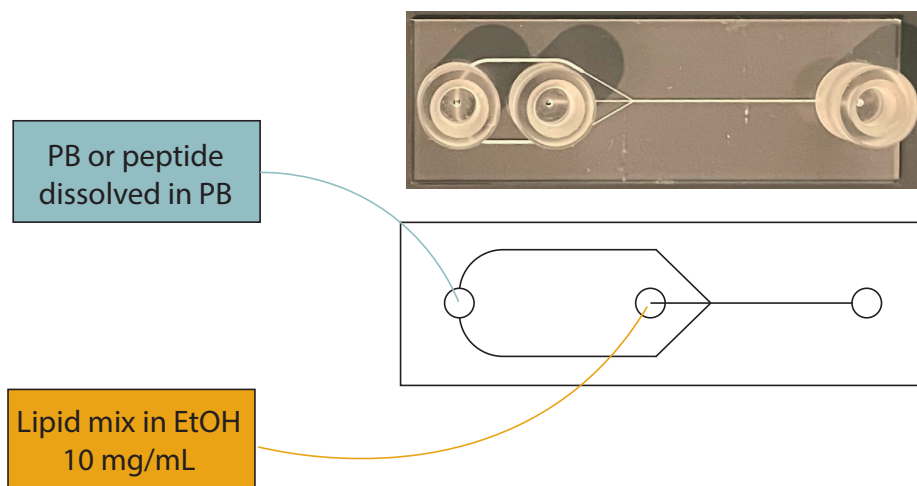


Figure 1. Microfluidics system setup. The staggered herringbone micromixer consists of a glass chip with two inlet ports, one for the organic phase and another for the aqueous phase. The organic and the aqueous phase are mixed in a microchannel of 200 μm width and 80 μm depth. The microchannel presents a series of chevrons (mixing element) with a short arm (1/3 channel width) and a long arm (2/3 of channel width). The height of each chevron is 30 μm . The microchannel presents a total of 180 chevron elements and the length of the mixing channel is 28.7mm.

Preparation of liposomes using lipid film hydration method

For VD3-loaded liposomes, a total of 5 mg phospholipids and cholesterol dissolved in chloroform and 50 μ g VD3 were mixed in a round bottom flask in a molar ratio of 4:1:2 (DSPC:DSPG:Cholesterol). In the case of DiD-labelled liposomes, a total of 6.6 mg of phospholipids and cholesterol at a molar ratio of 4:1:2 (DSPC:DSPG:Cholesterol) and 0.1 mol% of DiD dissolved in chloroform were mixed in a round bottom flask. A dry lipid film was formed by removing the chloroform in a rotary evaporator (180 mbar, 15 minutes) at 40°C. The dry lipid film was hydrated with 1 mL PB 10 mM pH 7.4 in a rotary evaporator (atmospheric pressure, rotation only) at 60°C for 30 minutes. The product of the lipid film hydration is a suspension of large multilamellar vesicles. Samples were extruded 4 times through 400 nm and 200 nm stacked track-etch polycarbonate membranes (Whatman® Nucleopore™, GE Healthcare, Little Chalfont, UK) at high pressure using an extruder (LIPEX Extruder, Northern Lipids Inc., Canada) connected to a water bath at 60°C. The formulations were dialyzed overnight against 400 mL of PB 10 mM pH 7.4 using Flot-A-lyzer dialysis kit (MWCO 100,000 Da).

Liposome characterization – DLS

Dynamic Light Scattering (DLS) was performed using a Zetasizer NanoZS (Malvern Panalytical, UK) to measure the z-average hydrodynamic diameter and Pdl of the formulations. The same instrument was used to determine the ζ -potential by means of laser doppler electrophoresis. When the measurement was performed prior to dialysis, the method was adjusted to consider the changes in the viscosity and refractive index of the dispersant due to the presence of ethanol in the samples (Table S2).

Liposome characterization – UPLC

Reverse phase ultra-high performance liquid chromatography (UPLC) was used for the quantification of the encapsulated peptide, VD3 and total lipids. For quantification of the lipophilic compound VD3, a sample of the formulation was dried under a N₂ stream, resuspended in the same volume of ethanol, and subsequently injected into a 1.7 μ m BEH C18 column (2.1 x 50 mm, Water ACQUITY UPLC, Waters, MA, USA). For the measurement, 10 μ L of sample was injected into the UPLC column. Column temperature was set at 40°C. The mobile phases consisted of milliQ water with 0.1% TFA (solvent A) and acetonitrile with 0.1% TFA (solvent B). After sample injection, a linear gradient of solvent B from 5% to 95% was applied to the column for 7 minutes at a flow rate of 0.5 mL/min, followed by 95% solvent B for 2 minutes and 5% solvent B 95% solvent A for 3 minutes. Peptides were detected by absorbance at 220 nm, VD3 was detected by absorbance at 252 nm using ACQUITY UPLC TUV detector and lipids were detected using ACQUITY UPLC Evaporative Light

Scattering detector (ELSD). Loading efficiency was calculated as the total amount of peptide or VD3 after dialysis divided by the total amount of peptide before dialysis (for formulations prepared with microfluidics) or before extrusion (for formulations prepared with lipid film hydration method).

Liposome characterization – Negative staining Transmission Electron Microscopy (TEM)

For the characterization of liposomes loaded with VD3 by Transmission Electron Microscopy (TEM), a sample of liposomal formulation was deposited on carbon-Formvar coated 200 mesh copper grids (Electron Microscopy Sciences, USA) for 30 seconds and subsequently stained with a contrast solution of 1% uranyl acetate for 30 seconds. The coated grids were left to dry overnight at room temperature before imaging. Images were taken in a JEM1400 plus Transmission Electron Microscope operating at 80 kV and fitted with a CCD camera.

Peptide synthesis

Peptides were synthesized in-house by solid-phase peptide synthesis (SPPS) using a Liberty Blue microwave-assisted automated peptide synthesizer. Synthesis scale was 0.1 mmol using an S-RAM Tentagel resin. Fmoc-deprotection was done with dimethylformamide (DMF) containing 20% piperidine. After synthesis peptides were acetylated using pyridine and acetic anhydride (1:1 v/v). Peptide cleavage from the resin was performed by incubating the resin for 1h with a mixture of 95% (v/v) trifluoroacetic acid (TFA), 2.5% (v/v) triisopropylsilane (TIPS) and 2.5% (v/v) water. Peptides were precipitated using ice-cold diethyl ether followed by centrifugation. Peptides were subsequently purified by reverse-phase high performance liquid chromatography (HPLC) using a Kinetic Evo C18 column. Purity was assessed by liquid chromatography-mass spectrometry (LC-MS).

Net charge of peptides at pH 7.4 was calculated using Innovagen peptide property calculator. The grand average of hydropathy (GRAVY) of peptides was calculated as the sum of hydropathy values of the amino acids divided by the peptide length. The sequences and physicochemical properties of the peptides can be found in Table S3.

Human monocyte-derived dendritic cell culture and activation

Peripheral blood monocytes were isolated from buffy coats or fresh blood and differentiated into monocyte-derived dendritic cells (moDCs) as previously described⁸. To assess moDC liposome uptake 50-200 x 10³ immature DCs were incubated with DiD-labelled formulations prepared by either the lipid-film hydration method or the staggered herringbone micromixer at a lipid concentration of 10 µg/mL or 30 µg/mL for 4 hours in IMDM (Thermo Fisher Scientific) 5% FCS (Sigma-

Aldrich, St Louis, Missouri). Cells were washed and liposome uptake was measured by flow cytometry on a FACS Canto. Uptake was quantified using percentages of DiD-positive moDCs. For determination of moDC maturation, immature DCs were cultured in IMDM (Thermo Fisher Scientific) 5% FCS (Sigma-Aldrich, St Louis, Missouri) supplemented with 500 U/mL granular-macrophage colony stimulating factor (GM-CSF) only, or with 100 ng/mL lipopolysaccharide (LPS) derived from *E. coli* strain O111-B4 (Sigma-Aldrich) and GM-CSF, in the presence or absence of 10 or 30 µg/mL liposomes for 24 hours. Stimuli were washed away and DCs were stained with a cocktail of the following markers: anti-CD83-phycoerythrin (PE) (BD Biosciences, Franklin Lake, New Jersey), anti-CD86-brilliant violet 421 (BV421) (BD), anti-HLA-DR-peridinin-chlorophyll-protein-Cy5.5 (PerCP-Cy5.5) (BD), and anti-CD14-PE-Cy7 (Biolegend, San Diego, California). Activation of moDCs was determined by flow cytometric analysis on a FACS Fortessa (BD). For compensation, single marker-fluorochrome stainings were included. Flow cytometry data was analysed using FlowJo software (Treestar, Ashland, Oregon).

Statistics

Statistical differences between groups were analysed by either unpaired T-test or one-way ANOVA followed by Tukey's multiple comparisons test. Statistical correlation was tested using Pearson's correlation test. P-values below 0.05 were considered significant. All analysis were performed using GraphPad Prism 8.1.1 for Windows (GraphPad Software, San Diego, California, USA).

RESULTS

Temperature of the system is a key parameter for the preparation of monodisperse highly rigid anionic liposomes by microfluidics

One of the challenges of the preparation of highly rigid liposomes is the relatively high transition temperature of the phospholipids in these formulations. Therefore, during the preparation of these liposomes using microfluidics, the aqueous and organic phases need to be above this temperature. A drawback of most microfluidic systems is the inability to properly control the temperature, complicating the controlled nanoprecipitation of lipids with a high transition temperature. Indeed, DSPC:DSPG:Cholesterol liposome prepared at room temperature resulted in relatively large liposomes (Figure 2A) and high Pdl (Figure 2B). Merely heating the inlet solutions before injection in the micromixer did not correct this issue (Figure 2A, B), however submerging the micromixer in water bath at 60°C resulted in monodisperse liposomes with an average size of 120 nm and a Pdl below 0.2

(Figure 2A, B). This shows that controlling the temperature of the entire system allows the production highly rigid liposomes with great reproducibility.

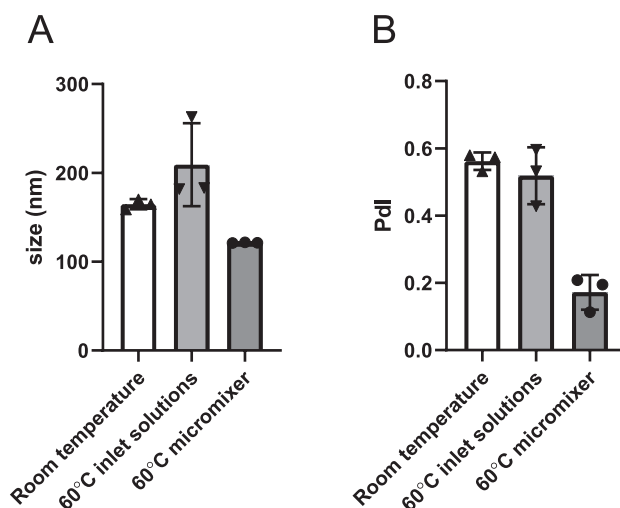


Figure 2. Importance of temperature control in micromixer. Effect of temperature on (A) size and (B) Pdl of DSPC:DSPG:Cholesterol liposomes prepared in staggered herringbone micromixer. Formulations were either prepared at room temperature, by heating the inlet solutions at 60°C before injections or by submerging the micromixer in a temperature-controlled water bath at 60°C. All formulations were prepared at a TFR of 500 $\mu\text{L}/\text{min}$ and a FRR of 2:1. Graphs show three replicate measurements from the same batch of formulation.

The flow rate ratio and not the total flow rate determine the particle size during preparation

Having established that the microfluidics system allows for the formation of monodisperse rigid liposomes, we next addressed whether this is scalable and tuneable. To increase the output, we varied the total flow rate (TFR) of the system from 100 $\mu\text{L}/\text{min}$ to 900 $\mu\text{L}/\text{min}$. Remarkably, the average size of the liposomes and Pdl were not significantly influenced by the TFR (Figure 3A and 3B). This suggests that our system is robust even at higher flow rates, which may increase the scale-up potential of the system since higher volumes of formulations can be prepared in a short period of time.

Next, we adjusted the flow rate ratio (FRR) of water and organic phase while keeping the TFR constant at 500 $\mu\text{L}/\text{min}$. We observed that by increasing the flow rate in favour of the aqueous phase, the resulting liposomes exhibited a smaller average hydrodynamic diameter (Figure 3C) while remaining monodisperse (Figure

3D). Thus, the average size of liposomes is tuneable with our system by adjusting the FRR.

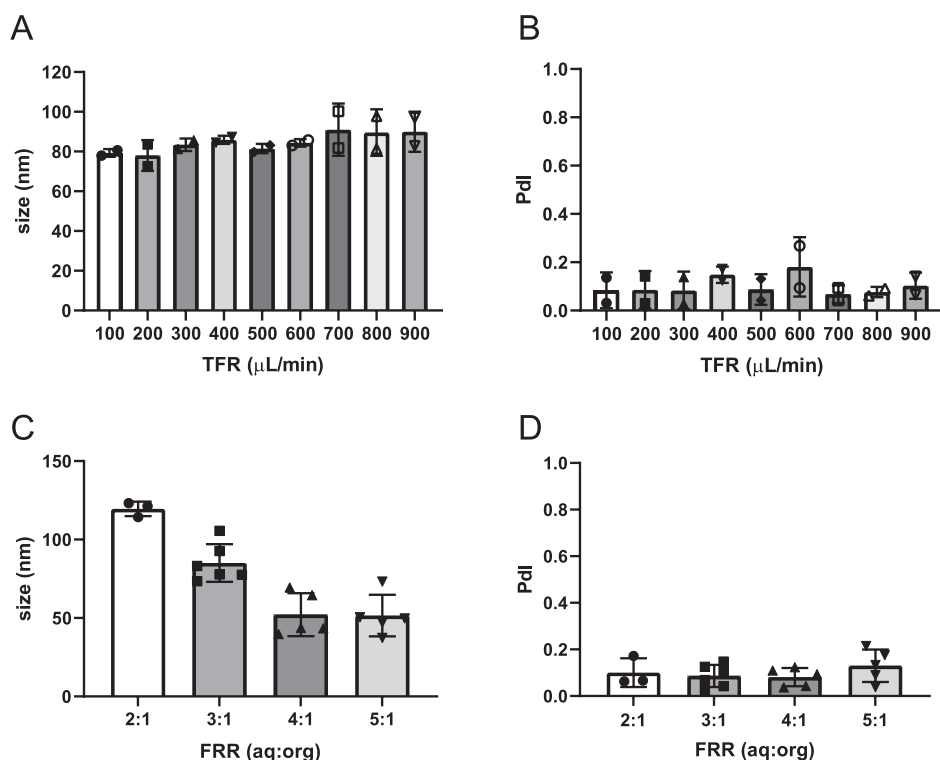


Figure 3. Effect of flow conditions on liposome characteristics. Effect of TFR on (A) average particle size and (B) PdI of DSPC:DSPG:Cholesterol formulations. To study the effect of TFR, formulations were prepared at a fixed FRR of 3:1. Effect of FRR on (C) average particle size and (D) PdI of DSPC:DSPG:Cholesterol formulations. To study the effect of the FRR, formulations were prepared using a fixed TFR of 500 $\mu\text{L}/\text{min}$. Each data point represents a separate batch of formulation. Graphs show data from independent batches of formulation and the mean of that data.

Loading efficiency of peptide antigen across a wide spectrum of charge and hydrophobicity

Next, we addressed whether the microfluidics system allows for incorporation of peptide antigens and adjuvants. Encapsulation of peptides can be particularly challenging as they can have a wide range of physicochemical properties. To address this, we selected 7 peptides (Table S3) with a wide range of net charge and hydrophobicity (expressed as the grand average of hydropathicity index, GRAVY) and determined the loading efficiency. We observed a wide variability in loading efficiency (Figure 4) and no statistical correlation between the loading

efficiency and the net charge ($r = 0.65$, p -value = 0.11) or GRAVY ($r = 0.44$, p -value = 0.32), however none of the peptides show a lower encapsulation than 10%.

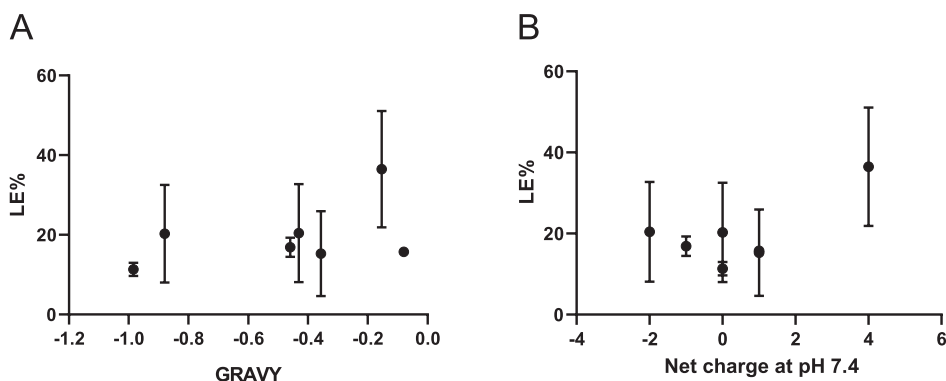


Figure 4. Effect of GRAVY and net charge of peptides in the loading efficiency (LE). (A) Loading efficiency of different peptides into DSPC:DSPG:Cholesterol liposomes vs GRAVY. (B) Loading efficiency vs net charge of peptides. The flow conditions for these formulations were set at 400 μ L/min and a FRR of 2:1. Each data point represents the mean loading efficiency (\pm SD) of two independent batches of formulation.

The loading efficiency of VD3 is significantly improved when the highly rigid liposomes are prepared using the herringbone micromixer

A major drawback of the lipid film hydration method is the poor encapsulation of tolerogenic adjuvants into liposomes with a high phase transition temperature (Table 1). Therefore, we next addressed if the encapsulation efficiency of VD3 can be improved by using the staggered herringbone micromixer. Addition of VD3 to production process increased the size of the liposomes (Figure 5A) and the Pdl (Figure 5B) compared to unloaded liposomes (Figure 2A), however size was comparable to the lipid film hydration equivalent (Figure 5A). Formulations prepared using the microfluidics system showed an increase in Pdl and a slight decrease in the ζ -potential (Figure 5B and 5C) compared to the formulations prepared with lipid film hydration method. The microfluidics method, however, was vastly superior to the lipid film hydration method in the loading efficiency of VD3 (Figure 5C, 60% vs 2% $p < 0.0001$). Therefore, the changes in Pdl and ζ -potential could be explained by the incorporation of VD3 into the liposomes. Importantly, TEM imaging suggests the high encapsulation efficiency is not a result of formation of VD3 micelles or aggregates (Figure 5E).

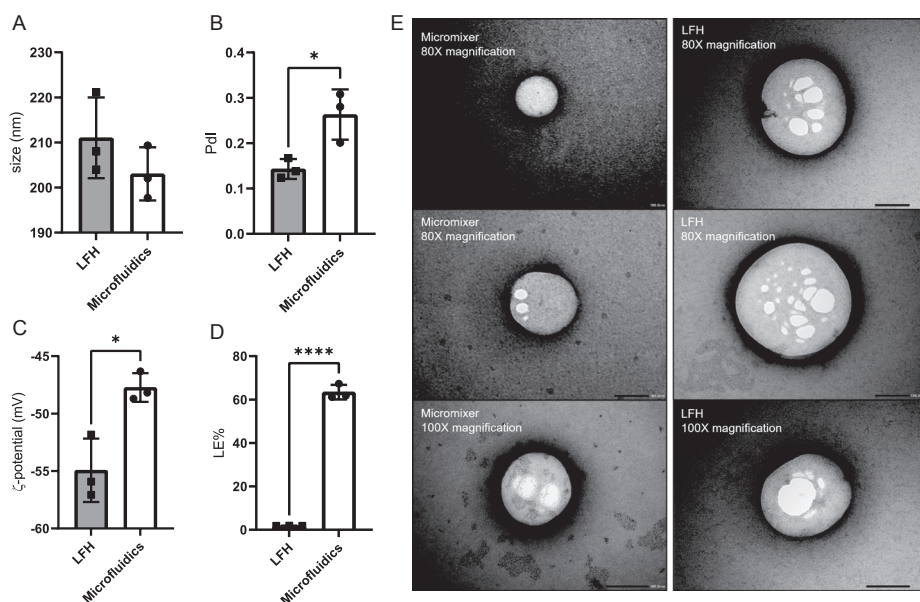


Figure 5. Comparison of VD3 incorporation into liposomes using lipid film hydration method vs microfluidics. (A) Average particle size, (B) Pdl and (C) ζ-potential of DSPC:DSPG:Cholesterol liposome loaded with VD3 prepared using either the staggered herringbone micromixer or the gold-standard lipid-film hydration method (LFH) ($n = 3$). (D) Loading efficiency of VD3 for both methods. The flow conditions in the microfluidics system were set at TFR of 500 $\mu\text{L}/\text{min}$ and a FRR of 3:1 (Aqueous:Organic). The final lipid and VD3 concentration in the formulations was 5 mg/ml and 50 $\mu\text{g}/\text{mL}$ respectively for both the microfluidics and LFH formulations. (E) Transmission Electron Microscopy (TEM) images of VD3-loaded liposomes prepared with either the staggered herringbone micromixer or the lipid film hydration method. Black scale bars represent 100 nm. Graphs show mean, each data point represents an independent batch of formulation * $p < 0.05$, **** $p < 0.0001$ determined by unpaired t-test.

Exposure of monocyte-derived dendritic cells to the highly rigid anionic liposomes prepared with the micromixer does not induce DCs activation

We have previously shown that rigid anionic liposomes are more easily taken up by antigen presenting cells than fluid liposomes and have a propensity to induce tolerance³. In order for liposomes to affect the immune response, the uptake of the nanoparticles by dendritic cells is essential. We used monocyte-derived dendritic cells (moDCs) to assess if liposomes prepared using the traditional lipid film hydration method and the staggered herringbone micromixer are comparable in terms of cell uptake and biological effect. To assess cell uptake, we exposed moDCs to liposomes prepared with either lipid-film hydration method or the

staggered herringbone micromixer at two different lipid concentrations (10 and 30 $\mu\text{g/mL}$) for 4h. Both lipid film hydration prepared as well as microfluidics prepared liposomes were readily taken up by moDC. Albeit we observed a reduction in cell uptake for one of the batches prepared with microfluidics compared to the lipid film hydration method after 4h of incubation, we did not observe significant differences in uptake when a second batch of liposomes was tested (Figure 6A). Furthermore, we studied the capacity of the formulations to induce activation of moDCs. For this, cells were exposed to the formulations for 24h and CD86 and CD83 expression was assessed by flow cytometry. Results showed no significant differences in the activation makers studied (Figure 7C and 7D), indicating that these formulations prepared with either the lipid film hydration method or microfluidics, do not have immune-stimulatory or pro-inflammatory properties.

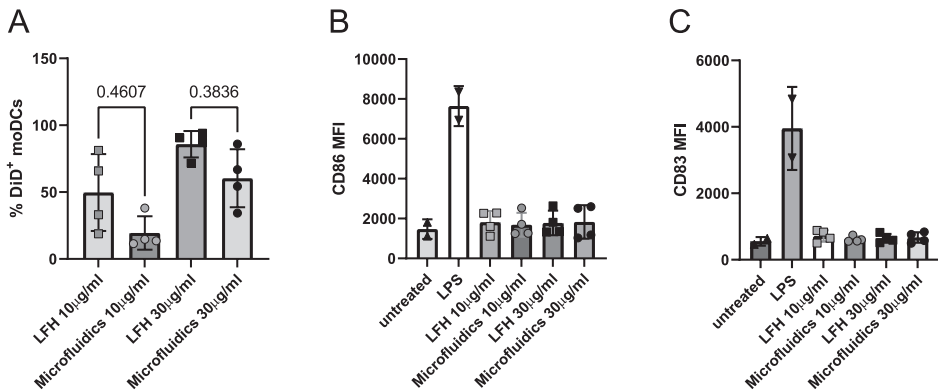


Figure 6. Effect of preparation method on uptake and cell activation. (A) Uptake by monocyte derived DC of DiD-labelled anionic liposomes (DSPC:DSPG:Cholesterol) prepared using lipid-film hydration method (LFH) or microfluidics after 4h and (B, C) resulting DC maturation after 24h of incubation. Panels B and C show the mean fluorescence intensity (MFI) of the activation markers (B) CD86 and (C) CD83. Data represent 2 moDC donors treated with two independently prepared batches at two different lipid concentrations (10 and 30 $\mu\text{g/mL}$). P-value determined by one-way ANOVA followed by Tukey's multiple comparisons test.

DISCUSSION

Physicochemical parameters of liposomal formulations such as the rigidity can affect their ability to induce certain immune responses. In previous studies we have shown that highly rigid anionic liposomal formulations containing distearoyl-sn-glycero-3-phosphoglycerol (DSPG) are more efficient at delivering their cargo and inducing T regulatory cells³. The inclusion of tolerogenic adjuvants, such as VD3, in these formulations may potentiate the tolerogenic capacity of the liposomes. However, the loading of these molecules into highly rigid liposomes has proven to

be challenging using traditional liposome preparation methods. These liposome production methods also present other drawbacks, for example, formulations need to be prepared in batches, which is time consuming and leads to variability between batches^{9,10}. On the other hand, they require sizing-down the multilamellar vesicles formed after the hydration of the dry lipid film in order to generate monodisperse unilamellar liposomal formulations. Sizing methods commonly used, such as extrusion, are not suitable for large-scale production due to the amount of energy required to pass litres of formulations through nm-size filters¹¹. Furthermore, liposomes composed of phospholipids with high transition temperature also require temperature control during extrusion, which would increase the energy consumption of the manufacture process. Extrusion can also lead to the loss of costly material such as lipids, antigen and/or adjuvants. Microfluidics methods for the preparation of liposomes have the ability to overcome some of these limitations. In general, the formation of liposomes in these systems occurs when phospholipids dissolved in a water-miscible organic solvent mixes with an aqueous solution in a microchannel. The controlled mix of the organic and aqueous solvents triggers the nanoprecipitation of phospholipids that will first form lipid bilayer discs and then vesicles⁷. Highly rigid liposomes are composed of phospholipids with high transition temperature (55°C or higher) and the solubility of these phospholipids in organic solvents is often poor at room temperature. Therefore, the control of temperature is a key parameter during liposome manufacture process both for the lipid film hydration method and microfluidics-based methods. Temperature control in commercial microfluidics systems often consist of heating the aqueous and organic solutions in the inlet syringes. However, this might not ensure that the temperature in the microchannel is the required working temperature and can lead to formulations¹² with high polydispersity or high inter-day variability due to changes in ambient temperature. The material and relatively small dimensions of the staggered herringbone micromixer used here allowed the tight control of the temperature during mixing by submerging the glass chip in a water bath at the desired temperature. We observed that a proper control of the mixing temperature is necessary in order to obtain monodisperse liposomal formulations and that these conditions cannot be achieved by heating the inlet solutions prior to injection.

Apart from liposomal rigidity, other parameters such as average particle size also have an impact on the biological activity of nanoparticle formulations. Liposome particle size can affect the biodistribution, cell uptake and immune responses¹³. For instance, studies have shown that particles with a size of 50 nm can induce different types of immune responses compared to those with an average particle size of 120 nm¹⁴. Therefore, the ability to prepare liposomal formulations with a controllable particle size is essential for any liposome preparation method.

We showed that the particle size of the liposomes prepared using the microfluidics method proposed here can be altered by changing the flow conditions, specifically the FRR between the aqueous solvent and the organic solvent. By increasing the proportion of the aqueous solvent, the average particle size of the formulations can be reduced without significantly affecting the Pdl. The other flow parameter under study, the TFR, did not significantly affect the average particle size or Pdl of the formulation, which highlights the scale up potential of this preparation method since up to 900 μL of formulation can be prepared per minute.

The ability to efficiently load cargo into liposomal formulations is also essential in a liposome preparation method. Loading peptide antigens into highly rigid liposomal formulations could allow the induction of an antigen-specific tolerogenic response since these formulations have previously shown to be more efficient at delivering their cargo³. We studied the loading efficiency of peptides with different net charges at pH 7.4 and different levels of hydrophilicity. Although no correlation was observed between the loading efficiency of the peptides and their net charge or GRAVY value, it is worth noting that the peptide with the higher positive charge (+4) also showed the highest loading efficiency, possibly related to the favourable electrostatic interaction between the peptide and the anionic liposomes. In any case, the loading efficiency above 10% observed for all the peptides is in line with what we have previously observed using the lipid film hydration method². Contrary to what could be expected, the loading of lipophilic molecules with tolerogenic properties such as VD3 into rigid anionic liposomes has proven to be relatively inefficient using traditional liposome preparation methods (Figure 5). Interestingly, we observed that the loading efficiency of VD3 into DSPC:DSPG:Cholesterol liposomes increases dramatically from 1.9% (± 0.02) to 63.4% (± 3.4) when the formulations are prepared using the staggered herringbone micromixer compared to the lipid film hydration method. The increased in loading efficiency was not accompanied by a change in liposome morphology as assessed by TEM neither aggregates of VD3 could be found in the TEM microscopy images. This data indicates that our microfluidics-based method is an excellent tool for encapsulation of both a wide range of peptide antigens as well as a tolerogenic adjuvant like VD3. Importantly, we show that preparation on rigid liposomes with microfluidics does not compromise its previously reported non-inflammatory uptake by dendritic cells and does not lead to dendritic cells activation. Therefore, the presented microfluidics method may be very useful for the production of liposomal formulations to induce immune tolerance.

Thus, in conclusion, here we describe the use of an off-the-shelf staggered herringbone micromixer for the preparation of highly rigid liposomal formulations in a size-tuneable and scalable manner. This system presents important advantages in terms of loading efficiency of the tolerogenic molecule VD3 compared to the

gold-standard lipid film hydration method. Highly rigid anionic liposomes can have intrinsic tolerogenic capacity and combined with tolerogenic molecules represent promising nanotherapeutics for the treatment of autoimmune and inflammatory diseases.

AUTHOR CONTRIBUTIONS

FLV conceptualised, designed, and carried out experiments, wrote the manuscript and prepared the figures. BS conceptualised and edited the manuscript. NAN performed uptake and DC activation experiments. MHT and RS performed part of the experiments. JAB, AK, WJ, ECJ provided valuable input for the experimental design and edited the draft manuscript.

ACKNOWLEDGMENTS

We thank D. Wu for the technical assistance during transmission electron microscopy experiments. We also thank I. Simó Vesperinas and N.S.A. Crone for the peptide synthesis.

This work is part of the DC4balance consortium and is supported by Health-Holland, the Dutch Cooperation of Health Foundations (SGF) and the Dutch Heart Foundation, grant nr. LSHM18056-SGF.

REFERENCES

1. Christensen D, Korsholm KS, Rosenkrands I, Lindenstrøm T, Andersen P, Agger EM. Cationic liposomes as vaccine adjuvants. *Expert Rev Vaccines*. 2007;6(5):785-796. doi:10.1586/14760584.6.5.785
2. Benne N, van Duijn J, Lozano Vigario F, et al. Anionic 1,2-distearoyl-sn-glycero-3-phosphoglycerol (DSPG) liposomes induce antigen-specific regulatory T cells and prevent atherosclerosis in mice. *J Control Release*. 2018;291:135-146. doi:10.1016/j.jconrel.2018.10.028
3. Benne N, Lebourg RJT, Glandrup M, et al. Atomic force microscopy measurements of anionic liposomes reveal the effect of liposomal rigidity on antigen-specific regulatory T cell responses. *J Control Release*. 2020;318(October 2019):246-255. doi:10.1016/j.jconrel.2019.12.003
4. Ferreira GB, Vanherwegen A-S, Eelen G, et al. Vitamin D3 Induces Tolerance in Human Dendritic Cells by Activation of Intracellular Metabolic Pathways. *Cell Rep*. 2015;10(5):711-725. doi:10.1016/j.celrep.2015.01.013
5. Maldonado RA, LaMothe RA, Ferrari JD, et al. Polymeric synthetic nanoparticles for the induction of antigen-specific immunological tolerance. *Proc Natl Acad Sci*. 2015;112(2):E156-E165. doi:10.1073/pnas.1408686111
6. Bakdash G, Vogelpoel LTC, Van Capel TMM, Kapsenberg ML, De Jong EC. Retinoic acid primes human dendritic cells to induce gut-homing, IL-10-producing regulatory T cells. *Mucosal Immunol*. 2015;8(2):265-278. doi:10.1038/mi.2014.64
7. Maeki M, Fujishima Y, Sato Y, et al. Understanding the formation mechanism of lipid nanoparticles in microfluidic devices with chaotic micromixers. Choi J, ed. *PLoS One*. 2017;12(11):e0187962. doi:10.1371/journal.pone.0187962
8. Van Der Aar AMG, Sibiryak DS, Bakdash G, et al. Vitamin D3 targets epidermal and dermal dendritic cells for induction of distinct regulatory T cells. *J Allergy Clin Immunol*. 2011;127(6):1532-1540.e7. doi:10.1016/j.jaci.2011.01.068
9. Al-Amin M, Bellato F, Mastrotto F, et al. Dexamethasone Loaded Liposomes by Thin-Film Hydration and Microfluidic Procedures: Formulation Challenges. *Int J Mol Sci*. 2020;21(5):1611. doi:10.3390/ijms21051611
10. Yu B, Lee RJ, Lee LJ. Microfluidic Methods for Production of Liposomes. In: *Methods in Enzymology*. Vol 465. ; 2009:129-141. doi:10.1016/S0076-6879(09)65007-2
11. Wagner A, Vorauer-Uhl K. Liposome Technology for Industrial Purposes. *J Drug Deliv*. 2011;2011:1-9. doi:10.1155/2011/591325
12. Ross D, Gaitan M, Locascio LE. Temperature Measurement in Microfluidic Systems Using a Temperature-Dependent Fluorescent Dye. *Anal Chem*. 2001;73(17):4117-4123. doi:10.1021/ac010370l
13. Benne N, van Duijn J, Kuiper J, Jiskoot W, Slütter B. Orchestrating immune responses: How size, shape and rigidity affect the immunogenicity of particulate vaccines. *J Control Release*. 2016;234:124-134. doi:10.1016/j.jconrel.2016.05.033
14. Mottram PL, Leong D, Crimeen-Irwin B, et al. Type 1 and 2 Immunity Following Vaccination Is Influenced by Nanoparticle Size: Formulation of a Model Vaccine for Respiratory Syncytial Virus. *Mol Pharm*. 2007;4(1):73-84. doi:10.1021/mp060096p

SUPPLEMENTARY DATA

Table S1. Flow conditions

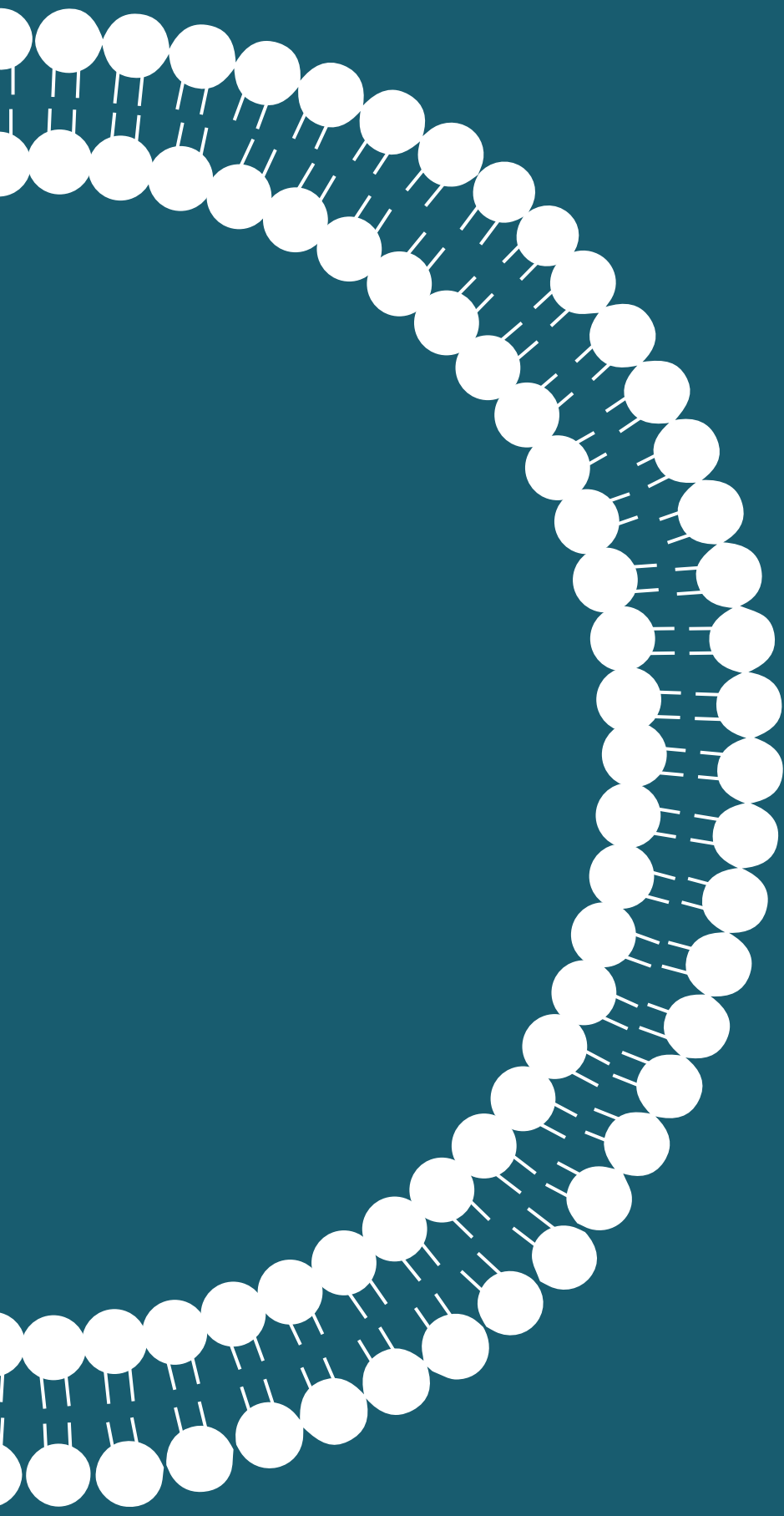
Formulation#	Total Flow Rate ($\mu\text{L}/\text{min}$)	Flow Rate Ratio (Aqueous : Organic)	Aqueous flow rate ($\mu\text{L}/\text{min}$)	Organic flow rate ($\mu\text{L}/\text{min}$)
1	500	2:1	333.3	166.7
2		3:1	375	125
3		4:1	400	100
4		5:1	416.7	83.3

Table S2. Viscosity values and Refractive Index of the dispersant used in DLS method for samples measured before dialysis

Flow Rate Ratio (Aqueous : Organic)	% (v/v) of ethanol in formulation	Viscosity of dispersant (cP)	Refractive Index
2:1	33.4	2.4128	1.349
3:1	25	1.9970	1.344
4:1	20	1.8318	1.342
5:1	16.7	1.6398	1.339

Table S3. Peptide sequence and physicochemical properties of peptides used

Peptide name	Peptide sequence	Molecular weight (g/mol)	Net charge (at pH 7.4)	GRAVY
Peptide 1	INNQLTLDSENTKY	1565.69	0	-0.985
Peptide 2	INNQLTLDSENTKYFH	1850	0	-0.880
Peptide 3	IEGNLIFDPNNYLPK	1789	-1	-0.460
Peptide 4	SASYKADTVAKVQG	1466.6	1	-0.357
Peptide 5	LSASYKADTVAKVQG	1579.76	1	-0.080
Peptide 6	LKFIIPSPKRPVK	1564.96	4	-0.154
Peptide 7	IERYEVDQIQVL	1674.86	-2	-0.431



Chapter 6

Surface composition of nanoparticles rather than its rigidity, affects tolerogenic behaviour *in vivo*

F. Lozano Vigario¹, M.A. Neustrup¹, L. H. M. Burgmeijer¹, W.E. van der Heijden¹, A. Kros², J.A. Bouwstra¹, B.A. Slütter¹

¹ Division of BioTherapeutics, Leiden Academic Centre for Drug Research, Leiden University, The Netherlands

² Supramolecular & Biomaterials Chemistry, Leiden Institute of Chemistry, Leiden University, The Netherlands

ABSTRACT

The induction of antigen-specific immune tolerance using nanoparticles is a promising therapeutic strategy to arrest pathogenic immune responses in atherosclerosis. Previous research has shown that anionic liposomes containing 1,2-Distearoyl-sn-glycero-3-phosphoglycerol (DSPG) have intrinsic capacity to induce tolerogenic immune responses in mice. The tolerogenic properties of these liposomes has been associated to their high rigidity since saturated phospholipids form tightly packed lipid bilayers and rigid liposomes. However, the phospholipid composition can also determine the protein corona formed around the nanoparticles when in a biological fluid. Here, we made use of DOPG/PLGA hybrid nanoparticles with a poly(lactic-co-glycolic acid) (PLGA) core, that provides rigidity, surrounded by loosely packed DOPC:DOPG lipid bilayer to determine the contribution of nanoparticle rigidity to tolerogenic immune responses *in vitro* and *in vivo*. We show that although the DOPG/PLGA hybrid nanoparticles are able to deliver the antigen to dendritic cells and induce antigen-specific T cell responses *in vitro*, they fail to replicate the same effect *in vivo*. We hypothesize that these differences might be due to the different protein coronas formed around the particles and that, at least *in vivo*, the protein corona might play a bigger role than the nanoparticle rigidity in the efficacy of lipid-based formulations. We show that while the uptake of DSPG liposomes is mediated by C1q, the uptake of the DOPG/PLGA hybrid nanoparticles might be mediated by ApoB100. In conclusion, our data suggests that the lipid bilayer composition and the set of proteins attracted to the nanoparticle surface might be more important than the particle rigidity to determine their *in vivo* behaviour.

INTRODUCTION

Nanoparticles can be used for the delivery of antigens to antigen presenting cells (APCs), such as dendritic cells. The use of liposomes and other lipid-based nanoparticles for the induction of immune tolerance has been explored in previous studies and it is a promising novel therapeutic approach to treat inflammatory and autoimmune diseases^{1, 2}. Atherosclerosis is an example of such a disease, where the inflammatory response accelerates the growth of atherosclerotic plaques that eventually leads to cardiovascular events³.

The physicochemical characteristics of nanoparticles are key for their capacity to induce tolerogenic responses⁴. For example, liposome formulations with anionic ζ -potential have shown to have better capacity to induce T regulatory cells (Tregs)¹, the main mediators of peripheral tolerance, while cationic nanoparticles stir the immune response towards a pro-inflammatory T helper 1 or cytotoxic CD8⁺ T cell response⁵. Furthermore, the liposomal rigidity has also shown to be important in the tolerogenic capacity of liposomal formulations⁶. Previous work in our group has shown that the rigidity of liposomes measured by atomic force microscopy correlates with their capacity to induce Tregs⁶ and that highly rigid anionic liposomes containing the saturated anionic phospholipid 1,2-distearoyl-sn-glycero-3-phospho-(1'-rac-glycerol) (DSPG) are able to induce Tregs and to attenuate the development of atherosclerosis in mice¹. The tolerogenic capacity of these formulations has also been studied in both *in vitro* and *ex vivo* human models⁷.

The main determinant of liposome rigidity is the phospholipid composition, more specifically the level of saturation in the acyl chains of phospholipids and the presence of cholesterol in the bilayer⁸. The presence of saturated acyl chains will lead to more tightly packed bilayers and therefore higher particle rigidity⁹. However, the phospholipid organization in the bilayer and the presence of cholesterol can also alter the protein corona of the nanoparticles¹⁰. Therefore, when studying the relationship between nanoparticle rigidity and their immune modulating properties, the different lipid composition can be a confounding factor.

Here, we make use of DOPG/PLGA hybrid nanoparticles to determine the contribution of nanoparticle rigidity to tolerogenic immune responses *in vitro* and *in vivo*. These hybrid nanoparticles will have a high rigidity due to the solid PLGA polymeric core, but they also have the surface characteristics of a loosely packed lipid bilayer. We therefore compare the tolerogenic capacity of three different lipid-based formulations with different rigidity. One formulation consisting of the unsaturated phospholipids 1,2-dioleoyl-sn-glycero-3-phosphocholine (DOPC) and 1,2-dioleoyl-sn-glycero-3-phospho-(1'-rac-glycerol) (DOPG) (Figure 1A), forming more disordered and fluid liposome bilayer at physiological temperature

(37°C). Another formulation containing the saturated phospholipids 1,2-distearoyl-sn-glycero-3-phosphocholine (DSPC), 1,2-distearoyl-sn-glycero-3-phospho-(1'-rac-glycerol) (DSPG) and cholesterol (Figure 1B) forming a more ordered and tightly packed liposome bilayer and therefore more rigid. The presence of unsaturated vs saturated phospholipids in these two formulations makes the rigidity of these liposomes very different⁶. The DOPG/PLGA hybrid nanoparticle formulation (Figure 1C) consists of a poly(lactic-co-glycolic acid) (PLGA) polymeric nanoparticle surrounded by DOPC:DOPG lipid bilayer. To follow the antigen-specific immune response to these formulations, we loaded the particles with the model antigen OVA₃₂₃₋₃₃₉ (OVA323), that can be recognized by CD4⁺ T cells isolated from OT-II transgenic mice. Previous research has shown that the inclusion of the tolerogenic adjuvant 1 α ,25-Dihydroxyvitamin D3 (vitaminD3) is key for the translation of these tolerogenic formulations from pre-clinical research to the patients⁷, therefore all formulations studied here included vitaminD3.

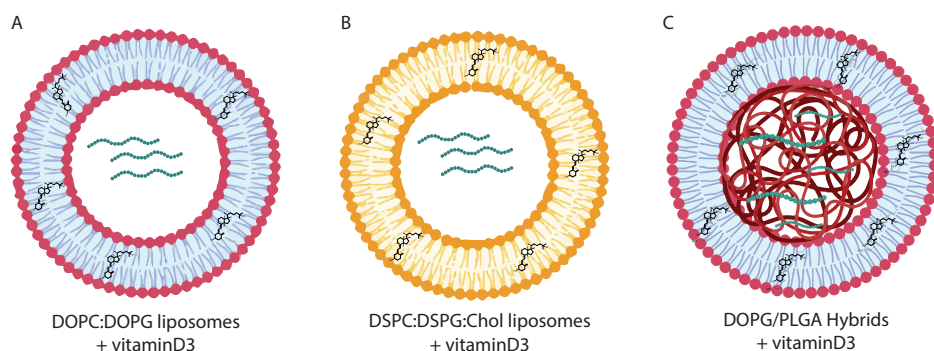


Figure 1. Schematic representation of nanoparticle formulations compared in this study. (A) Less rigid DOPC:DOPG liposome formulation with vitaminD3 in the lipid bilayer and OVA323-339 in the aqueous core. (B) Highly rigid DSPC:DSPG:Cholesterol liposomes with vitaminD3 and OVA323-339. (C) DOPG/PLGA hybrid nanoparticle with vitaminD3 in lipid bilayer and OVA323-339 in PLGA core.

MATERIAL AND METHODS

Materials

Phospholipids DOPC, DOPG, DSPC, DSPG and 1,2-dipalmitoyl-sn-glycero-3-phosphoethanolamine-N-(lissamine rhodamine B sulfonyl) (Liss-Rho-DPPE) were purchased from Avanti Polar Lipids (Birmingham, AL, USA). Cholesterol and poly(D,L-lactide-co-glycolide) (PLGA) were purchased from Sigma-Aldrich. T116-203 Interconnect Tee junctions were obtained from Mengel Engineering (Virum, Denmark). Staggered herringbone micromixer was purchased from Darwin

Microfluidics (Paris, France). Spectra-Por® Float-A-Lyzer were obtained from Sigma-Aldrich. 1 α ,25-Dihydroxyvitamin D3 (vitaminD3) was purchased from Sigma-Aldrich. OVA₃₂₃₋₃₃₉ (OVA323) was purchased from Invivogen (Toulouse, France). RPMI 1640 culture medium was obtained from Lonza (Basel, Switzerland). Fetal Bovine Serum (FBS) was purchased from Sigma-Aldrich (Zwijndrecht, Netherlands), penicillin/streptomycin from Fisher Scientific (Landsmeer, Netherlands) and L-glutamine was purchased from VWR (Amsterdam, Netherlands). CellTrace™ CFSE cell proliferation kit was obtained from ThermoFisher Scientific (MA, USA). Granulocytes-macrophages colony stimulating factor (GM-CSF) was purchased from ImmunoTools (Friesoythe, Germany). CD4 T cells isolation kit was obtained from Miltenyi Biotec (Leiden, the Netherlands). Anti-mouse CD3e (clone 145-2C11) and anti-mouse CD28 (clone 37.51) antibodies were purchased from Invitrogen (Waltham, Massachusetts, USA). *E. coli*-derived lipopolysaccharide (LPS) was purchased from Invivogen (Toulouse, France). Tissue-Tek® O.C.T. Compound was purchased from Sakura Finetek (CA, USA). 12-myristate 13-acetate (PMA) and ionomycin were purchased from Sigma Aldrich. BrefeldinA was obtained from ThermoFisher Scientific. Human C1q and human apolipoprotein B (ApoB) were purchased from Millipore (Merck, Darmstadt, Germany). Human apolipoprotein E (ApoE) was purchased from Sigma Aldrich (Zwijndrecht, Netherlands).

Animals

C57Bl/6, OT-II and ApoB100-OVA LDLr^{-/-} mice were bred in-house under standard laboratory conditions. ApoB100-OVA LDLr^{-/-} transgenic mice were generated in collaboration with the Department of Molecular Genetics and Translational Biology at University Medical Center Groningen. These mice were genetically modified using CRISPR/Cas9 technology to express a heterozygous genetic insertion of the two immunodominant epitopes of chicken ovalbumin, OVA₃₂₃₋₃₃₉ and OVA₂₅₇₋₂₆₄ in the C-terminal domain of ApoB100. All animals received water and food *ad libitum*. All experiments were approved by Animal Welfare Body of Leiden University and were performed in accordance with the Dutch government guidelines and Directive 2010/63/EU of the European Parliament.

Preparation of DOPG liposomes

DOPC:DOPG liposomes were prepared using a co-flow microfluidics system. Phospholipids DOPC and DOPG dissolved in ethanol absolute were mixed in a 4:1 molar ratio. Organic phase consisted on DOPC:DOPG lipid mix in ethanol at a concentration of 10 mg/mL. In formulations containing vitaminD3, this adjuvant was included in the organic phase. For fluorescently labelled formulations, 0.1 mol% of DOPC was substituted with Liss-Rho-DPPE. Aqueous phase consisted of PBS 1x containing OVA323 antigen. The organic and aqueous phases were combined in a

flow rate ratio of 2:1 using a T116-203 Interconnect Tee using NE300 syringe pumps (ProSense B.V., Oosterhout, The Netherlands) and Hamilton gastight glass syringes (Brunschiwig Chemie B.V., Amsterdam, The Netherlands). The two phases passively mix in a 40 cm loop PEEK tube with an internal diameter of 0.5 mm. Formulations were dialyzed overnight against PBS 1x under constant stirring using Float-A-lyzer dialysis tube (MWCO 100,000Da) to remove organic solvent and non-encapsulated peptides and/or adjuvant.

Preparation of DSPG liposomes

DSPG:DSPG:CHOL liposomes were prepared as previously described¹¹. Briefly, DSPC, DSPG and cholesterol dissolved in ethanol absolute were combined in a 4:1:2 molar ratio at a total lipid concentration of 10 mg/mL. For the formulations containing vitaminD3, this was included in the organic phase together with the lipids. The aqueous phase consisted of phosphate buffer (PB) 10mM pH 7.4. For fluorescently labelled formulations, 0.1 mol% of DSPC was substituted with Liss-Rho-DPPE. The antigen OVA323 was included in the aqueous phase. The aqueous and organic phases were mixed using a staggered herringbone micromixer submerged in a water bath at 60°C. The two phases were mixed at a 2:1 (aqueous:organic) flow rate ratio and a total flow rate of 500 μ L/min. Formulations were dialyzed overnight using a Float-A-lyzed dialysis tube (MWCO 100,000 Da) under constant stirring against PB 10 mM pH 7.4.

Preparation of DOPG/PLGA hybrid nanoparticles

Hybrid nanoparticles were prepared using a custom-made three-syringe microfluidics system. Particles were prepared in two consecutive steps, in the first step PLGA dissolved in acetonitrile at 3 mg/mL was mixed with an aqueous phase consisting of either milliQ water or OVA323 dissolved in milliQ water. This initial mixing step was performed using a T116-203 Interconnect Tee. The output of this mixing step is PLGA particles that mix in another T116-203 Interconnect Tee with an organic phase consisting on DOPC:DOPG (4:1 molar ratio) at 3 mg/mL concentration in ethanol absolute. For fluorescently labelled formulations, 0.1 mol% of DOPC was substituted with Liss-Rho-DPPE. The flow rate ratio used was 3:1:1 (Aqueous:PLGA:lipids) and a total flow rate of 6250 μ L/min. Flow rate was controlled using NE300 syringe pumps and the aqueous, PLGA and lipid phases were loaded in Hamilton gastight glass syringes. After preparation, the organic solvent was partially evaporated for 30 minutes under an N₂ stream, and the formulations were dialyzed overnight using a Float-A-lyzed dialysis tube (MWCO 100,000Da) against milliQ water under constant stirring.

Characterization of formulations

Average hydrodynamic diameter (z-average) and polydispersity index (Pdl) of the formulations were determined using Dynamic Light Scattering (DLS) using a Zetasizer NanoZS (Malvern Panalytical, UK). The ζ -potential of the nanoparticles was determined by laser doppler electrophoresis using the same instrument.

Bone marrow derived dendritic cell culture

Immature dendritic cells were differentiated from pluripotent bone marrow cells isolated from femur and tibias of C57Bl/6 mice. Mice were sacrificed by cervical dislocation and femurs and tibias were collected. Bone marrow cells were extracted, and a single cell suspension was obtained by flushing the bone marrow out of the bones with PBS over a 70 μ m cell strainer. Cells were cultured for 10 days at 37°C and 5% CO₂ at a cell density of 2x10⁶ cells in 95 mm Petri dishes in complete RPMI (cRPMI). cRPMI consisted of RPMI supplemented with 10% v/v fetal bovine serum (FBS), 2 mM L-glutamine, 100 U/mL penicillin/streptomycin and 50 μ M β -mercaptoethanol. Furthermore, the medium was supplemented with 20 ng/mL granulocytes-macrophages colony stimulating factor (GM-CSF). Cell medium was refreshed every 2 days.

CD45.1 CD4 OT-II T cells isolation

OT-II transgenic mice were sacrificed by cervical dislocation and spleens collected. Spleens were strained through 70 mm cell strainer to obtain a single cell suspension. Red blood cells were lysed using ACK lysis buffer and CD4⁺ T cells were isolated using CD4 T cells isolation kit.

Effect of formulations on bone marrow-derived dendritic cells

Immature DCs were collected from 95 mm Petri dishes and 50,000 cells/well were seeded in U-bottom 96-well plates. Cells were exposed to the formulations for 4h, after which the formulations were removed from the wells and the DCs were thoroughly washed with PBS to remove the nanoparticles that were not taken up. Cells were incubated overnight with cRPMI medium supplemented with 20 ng/mL GM-CSF and 100 ng/mL *E. coli*-derived lipopolysaccharide (LPS). Cells were stained for MHC-II-eFluor450, CD11c-FITC, CD40-PE, CD86-APC and Fixable Viability Dye-APC-eFluor780 followed by flow cytometry analysis using a Cytoflex flow cytometer (Beckman Coulter, CA, USA).

Effect of primed dendritic cells on T cell polarization

Immature DCs were cultured and exposed to formulations as described above. Cells were seeded in 96-well U-bottom plates at 25,000 cells/well and exposed to

the formulations for 4 hours. The dose of OVA323 was 1 nmol for those conditions receiving OVA-loaded particles or free OVA controls. Formulations were washed away, and cells were incubated overnight with 100 ng/mL LPS and 20 ng/mL GM-CSF in cRPMI medium. After overnight incubation, medium was removed and 100,000 CFSE-labelled OT-II CD4⁺ T cells per well were added. DCs and OT-II T cells were co-culture for 72 hours at 37°C and 5% CO₂. Cells were stained for Thy1.2-PE-Cy7, CD4-eFLuor450, FoxP3-PE, Tbet-APC, RORγT-Brilliant Violet 650 and Fixable Viability Dye-APC-eFLuor780.

Analysis of antigen-specific CD4⁺ T cell responses in vivo

Eight- to twelve-week-old mice were weighted and randomly allocated into groups of 5 mice. RandoMice® software (v1.1.1) was used for randomization and allocation of the mice to the experimental groups using weight as blocking factor¹². On day 0, all animals received an intravenous (IV) injection via tail vein of 500,000 OT-II CD4⁺ T cells. On day 1, animals received an IV injection in the tail vein of DOPC:DOPG liposomes, DSPC:DSPG:CHOL liposomes or DOPG/PLGA hybrid nanoparticles containing 1 nmol of OVA323 and 1-6.5 µg of vitaminD3. Empty DOPG/PLGA hybrid nanoparticles and 1 nmol free OVA323 and 6.5 µg vitaminD3 were used as control. On day 7, animals were sacrificed by cervical dislocation and spleens were collected. Single-cell suspension of the spleens was obtained by mashing them through a 70 µm cell strainer. Red blood cells were lysed using ACK lysis buffer, and the splenocytes were transfer to U-bottom 96-well plates for *ex vivo* re-stimulation and flow cytometry staining. Cells were stained for Thy1.2-AlexaFluor700, CD4-Brilliant Violet 510, CD45.1-eFLuor450, FoxP3-PE, Tbet-APC, RORγT-Brilliant Violet 650, CTLA4-Brilliant Violet 605, CD73-PE-Cy7, CD69-PE and Fixable Viability Dye-APC-eFLuor780. Stained cells were analysed by flow cytometry on a Cytoflex S (Beckman Coulter).

Effect of DOPG/PLGA hybrid nanoparticles in atherosclerosis

LDLr^{-/-} x ApoB100-OVA transgenic mice between 8 and 12 weeks old were weighted and randomly allocated to either treatment (n =15) or control group (n = 15) using RandoMice® software (v1.1.1) and weight as blocking factor for the randomization¹². At the start of the experiment animals are put on western-type diet consisting of 0.25% cholesterol and 15% cocoa butter (Special Diet Services, Essex, UK). On day 0, all animals received an IV injection of 1 x 10⁶ OT-II CD4⁺ T cells via the tail vein. Before adoptive transfer, OT-II CD4 T cells were activated by overnight incubation with 0.5 µg/ml antiCD3 and antiCD28 antibodies. On day 1, animals in the treatment group received an IV injection of DOPG/PLGA hybrid nanoparticles

loaded with 1 nmol OVA323 and 3.5–8 μg of vitaminD3, while animals in the control group received DOPG/PLGA hybrid nanoparticles with the same dose of vitaminD3 but no OVA323 antigen. Immunizations were repeated on days 22 and 43 of the experiment. Blood samples were collected 1 week after each immunization and animals were weighted weekly. On day 70, animals were weighted and anesthetized with an intraperitoneal injection of 10 mg/kg xylazine and 100 mg/kg ketamine. Anesthetized mice were exsanguinated and perfused by transcardiac perfusion using PBS. Spleen, aorta, hearts, and heart lymph nodes were collected. Spleens were processed as described above. Aortas were digested for 30 minutes at 37°C with collagenase I, collagenase XI, DNase and hyaluronidase. Single-cell suspensions of the aortas were obtained by passing the digested tissue through 70 μm cell strainer. Cells were transferred to U-bottom 96-well plates and stained for Thy1.2-Alexa Fluor 700, CD8a-Brilliant Violet 510, CD4-Brilliant Violet 650, CD45.1-eFluor450, CD45-FITC, CD11b-PE-Dazzle594, FoxP3-PE, Tbet-APC and Fixable Viability Dye-APC-eFluor780. Hearts were embedded and frozen in Tissue-Tek® O.C.T. Compound and 7 μm cryosections of the trivalve area were obtained using a Leica CM1950 (Leica Biosystems, Wetzlar, Germany). Sections were stained for Oil-Red-O (ORO) to visualize lipid-rich areas and Masson's trichrome staining to determine collagen content. Microscopy images of the stained slides were taken using Pannoramic 250 Flash III slide scanner (3DHistech, Budapest, Hungary) and images were analysed using a custom-made macro in Fiji image processing software¹³.

Quantification of plasma cholesterol levels

Plasma was obtained by centrifugation of EDTA-treated blood at 2000 G for 10 minutes at 4°C and stored at -20°C until cholesterol quantification. Total cholesterol was determined using Roche/Hitachi enzymatic colorimetric assay and using Precipath standardized serum (Roche Diagnostics) as standard.

Effect of protein corona on particle size distribution and ζ -potential

Formulations were mixed at a lipid concentration of 0.5 mg/mL with 10% (v/v) mouse serum, 10% (v/v) FBS, 2 μg /mL ApoE, 10 μg /mL ApoB or 10 μg /mL C1q. Protein concentrations used in this study are physiologically relevant and based on previous protein corona studies^{1, 14, 15}. Formulations at 0.5 mg/mL diluted in either PBS (DOPC:DOPG liposomes) or PB (DSPC:DSPG:Cholesterol liposomes and DOPG/PLGA hybrids) without protein were used as control. Formulations with or without protein were incubated for 1h at 37°C and unbound proteins were subsequently washed twice using a Vivaspin 500 centrifugal concentrator (MWCO 300 kDa, Sartorius, Göttingen, Germany). Z-average, Pdl and ζ -potential were determined

by DLS and laser doppler electrophoresis in a Zetasizer Ultra (Malvern Panalytical Ltd., UK).

Effect of protein corona on particle uptake by BMDCs

Bone marrow-derived dendritic cells (BMDCs) were seeded in a U-bottom 96-well plate at a concentration of 30,000 cells/well. DOPC:DOPG liposomes, DSPC:DSPG:Cholesterol liposomes or DOPG/PLGA hybrids labelled with Liss-Rho-PPPE were added to the wells at a lipid concentration of 20 $\mu\text{g/mL}$. The cell culture medium in the wells was either serum free (no protein control) or contained 10% mouse serum, 10% FBS, 2 $\mu\text{g/mL}$ ApoE, 10 $\mu\text{g/mL}$ ApoB or 10 $\mu\text{g/mL}$ C1q. BMDCs were exposed to formulations for 3.5h at 37°C and 5% CO_2 , or at 4°C (control). Excess nanoparticles and proteins were removed by washing the cells twice with PBS and BMDCs were incubated overnight with cRPMI medium supplemented with 20 ng/mL GM-CSF at 37°C and 5% CO_2 . Cells were subsequently stained with CD11c-FITC and Fixable Viability Dye-APC-eFluor780 for flow cytometry analysis. Stained cells were analysed on a Cytoflex S (Beckman Coulter).

Statistics

Statistical differences between groups were determined by one-way or two-way ANOVA followed by Tukey's or by Dunnett's multiple comparison test. P-values lower than 0.05 were considered statistically significant. Analysis was performed using GraphPad Prism for Windows (GraphPad Software, San Diego, California, USA).

RESULTS

Nanoparticle characterization

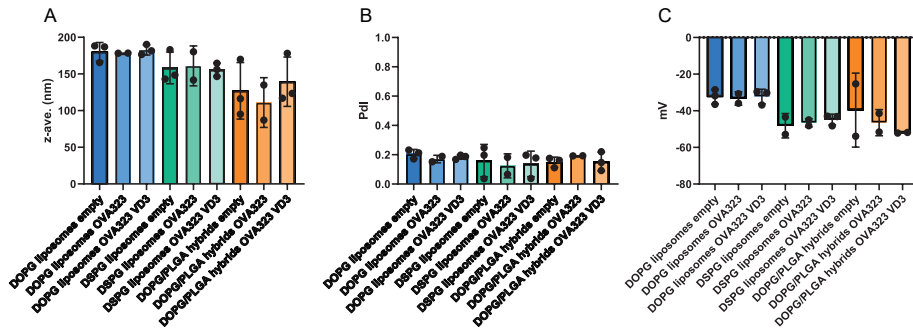


Figure 2. Characterization of nanoparticles by dynamic light scattering and laser Doppler electrophoresis. (A) Average hydrodynamic diameter of the nanoparticles (Z-average) in nm, (B) Polydispersity Index and (C) ζ -potential in mV of DOPG liposomes, DSPG liposomes and DOPG/PLGA hybrid nanoparticles either empty, loaded with the antigen OVA323 or both OVA323 and the adjuvant vitaminD3 (VD3). Data shown is mean \pm SD from at least two independent formulation batches ($n \geq 2$).

Nanoparticle size has an impact in the biological effect and biodistribution of the formulations, with a particle size between 100 and 200 nm being the most optimal for the induction of DCs-mediated antigen-specific immune responses⁴. All generated formulations have an average hydrodynamic diameter (z-ave.) within this size range, with DOPG/PLGA hybrid nanoparticles closer to 100 nm and the slightly larger DOPG liposomes around 180 nm (Figure 2A). Polydispersity index (Pdl) of the formulations is a quality attribute that indicates the width of the size distribution. All formulations have a Pdl around 0.2 or lower, indicating a monodisperse size distribution (Figure 2B). Finally, the ζ -potential of the formulations, a measurement of the surface charge of the nanoparticles, is between -25 mV and -55 mV (Figure 2C), indicating that all formulations are strongly negatively charged.

Anionic nanoparticles have a tolerogenic effect on dendritic cells in vitro

To assess the tolerogenic effect of the formulations on DCs, we cultured dendritic cells from murine bone marrow (BMDCs) and exposed them to the formulations. Tolerogenic DCs are characterized by the expression of lower levels of co-stimulatory molecules such as CD86 or CD40 upon pro-inflammatory stimulation, therefore maintaining an immature phenotype¹⁶. The immature DCs were exposed to DOPG liposomes, DSPG liposomes or DOPG/PLGA hybrid nanoparticles loaded with vitaminD3 for 4 hours. Subsequently, formulations were thoroughly

washed away, and cells were incubated overnight with 100 ng/mL of LPS. Next, the expression of CD86 and CD40 was measured by flow cytometry (Figure 3A). We observed a significant decrease in the percentage of DCs expressing both CD86 and CD40 (Figure 3B) in the DSPG liposomes and DOPG/PLGA hybrid nanoparticles conditions compared to the medium control with this reduction being more pronounced in the DOPG/PLGA hybrids condition. Furthermore, the geometric mean fluorescence intensity (gMFI) of CD86 was significantly reduced in all formulations compared to medium control but also to the free vitaminD3 control (Figure 3C), indicating that the formulation of vitaminD3 in liposomes boosts its tolerogenic potential. The expression of the co-stimulatory molecule CD40 was also lower in all formulations compared to medium control, but in this case the free vitaminD3 also affected CD40 expression (Figure 3D). Thus, on the DCs level, the most rigid DOPG/PLGA particles showed the most potent tolerogenic properties.

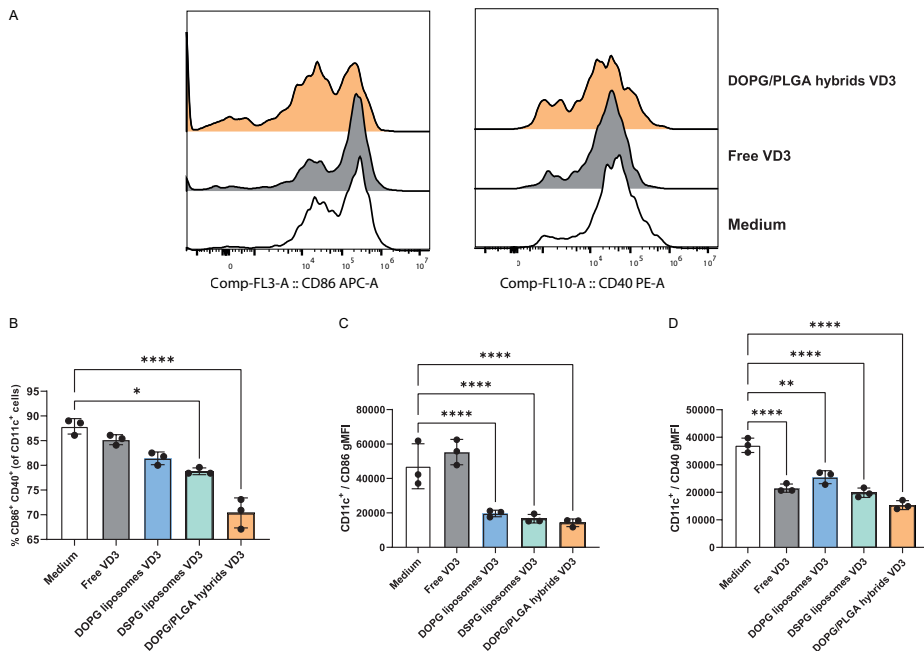


Figure 3. Effect of nanoparticle in expression of activation markers in BMDCs after pro-inflammatory stimulus. (A) Representative histograms of CD86 and CD40 expression in BMDCs treated with DOPG/PLGA hybrids loaded with VD3, free VD3 control or medium control. (B) Percentage of CD11c⁺ cells expressing both CD86 and CD40. (C) Geometric mean fluorescence intensity (gMFI) of antiCD86 within the CD11c⁺ population. (D) Geometric mean fluorescence intensity (gMFI) of antiCD40 within the CD11c⁺ population. **** $p \leq 0.0001$, *** $p \leq 0.001$, ** $p \leq 0.01$, * $p \leq 0.05$ determined by one-way ANOVA and Tukey's multiple comparison test.

DOPG/PLGA hybrid nanoparticles induce antigen-specific T cell proliferation and increase FoxP3, ROR γ T and Tbet expression compared to liposomes

Since the induction of immature DCs by the formulations suggests the initiation of tolerogenic responses, we next studied the effect of nanoparticle-primed DCs on T cell proliferation and polarization. For that, BMDCs were exposed to nanoparticles either empty, loaded with the model antigen OVA323 or loaded with OVA323 and vitaminD3. Primed DCs were co-culture for 72 hours with OVA323-specific CD4⁺ T cells isolated from the spleen of OT-II mice. All three nanoparticle formulations loaded with antigen were able to induce T cell proliferation to a level similar as the positive control, free OVA323 condition (Figures 4A, B). When looking further into the population of proliferating cells, we observed that only the DCs primed with OVA-loaded DOPG/PLGA hybrid nanoparticles were able to induce significant upregulation of the transcription factor FoxP3, which is the main driver of a Treg phenotype (Figure 4C). However, for the DOPG/PLGA hybrid nanoparticle conditions we also observed an increase in expression of transcription factors ROR γ T and Tbet (Figure 4D and 4E), associated to Th17 and Th1 cells respectively, which was suppressed by inclusion of vitaminD3. Interestingly, both DOPG liposomes and DSPG liposomes loaded with OVA323 and vitaminD3 led to a significant lower expression of the Th1-associated transcription factor Tbet compared to the free antigen control (Figure 4E), suggesting that although these particles did not trigger strong Treg responses, they did reduce the overall inflammatory phenotype of the CD4⁺ T cells.

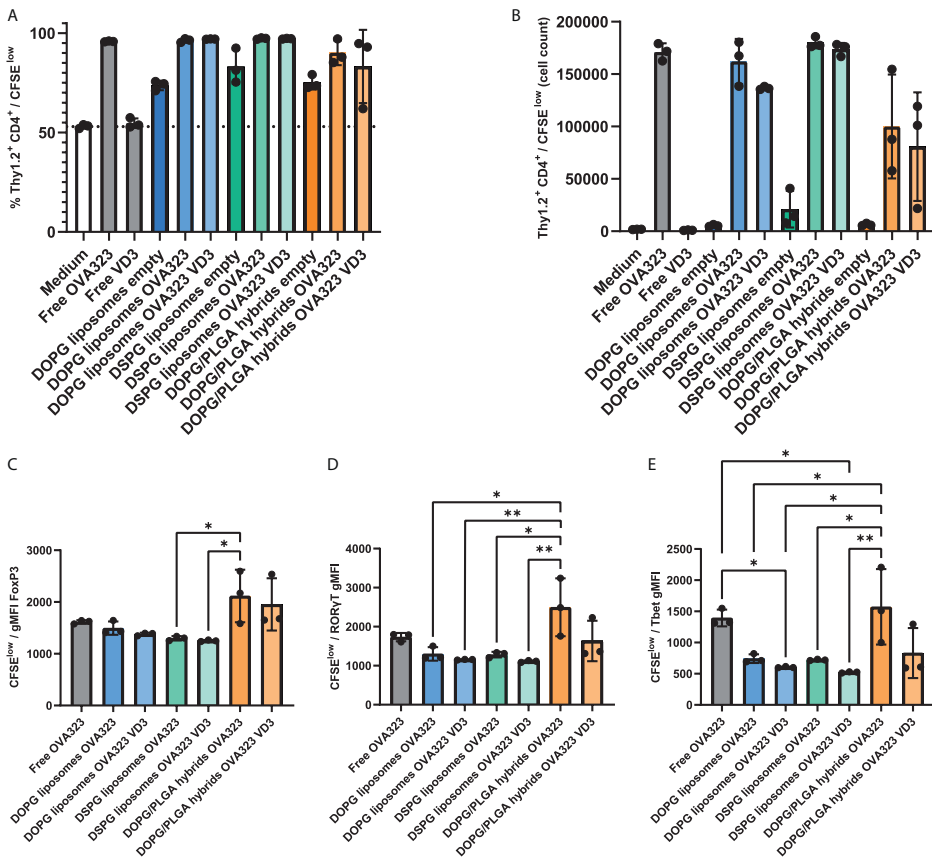


Figure 4. Effect of nanoparticle-primed BMDCs on T cells proliferation and differentiation in vitro. (A) Percentage of CD4⁺ T cells (Thy1.2⁺ CD4⁺) that proliferated (CFSE^{low}) during BMDC and T cell co-culture. (B) Number of proliferated CFSE^{low} CD4⁺ T cells after coculture with BMDCs. (C) Geometric mean fluorescence (gMFI) of (C) anti-FoxP3, (D) anti-RORγT and (E) anti-Tbet antibodies in the population of proliferated CD4⁺ T cells. ** $p \leq 0.01$, * $p \leq 0.05$ determined by one-way ANOVA and Tukey's multiple comparison test.

Administration of DOPG/PLGA hybrid nanoparticles loaded with antigen and vitaminD3 has no effect on atherosclerosis development

Since *in vitro* data showed that vitaminD3 loaded DOPG/PLGA hybrid nanoparticles induced higher FoxP3 expression than DSPG liposomes, we next assessed whether these nanoparticle formulations could affect the development of atherosclerosis. We used LDLR^{-/-} mice with an additional genetic modification to express a ApoB100

tagged with the epitope OVA323, therefore we could use OVA323 as the target antigen for the vaccine formulation.

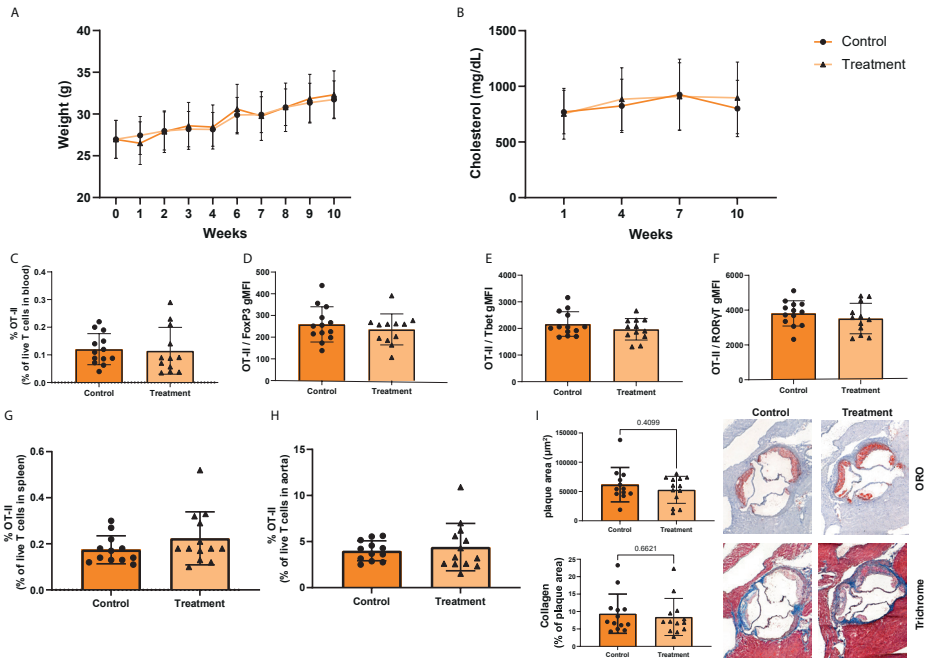


Figure 5. Effect of DOPG/PLGA hybrid nanoparticles on atherosclerosis development. (A) Weight and (B) plasma cholesterol levels of mice during the experiment. (C) Percentage of OT-II CD4+ T cells in blood of immunized mice at the end of the experiment. Geometric mean fluorescence intensity (gMFI) of (D) FoxP3, (E) Tbet and (F) RORγT in the OT-II T cell population in blood. Percentage of OT-II CD4+ T cells in (G) spleen and (H) aorta of mice at the end of the experiment. (I) Plaque area in μm^2 and collagen content as a percentage of total plaque area, and representative images of Oil-Red-O and trichrome staining of trivalve area slides. Significant differences between control and treatment groups were tested using unpaired two-tailed t test.

We transferred activated OT-II CD4⁺ T cells to the LDLR^{-/-} mice and subsequently immunize the mice with either DOPG/PLGA hybrid nanoparticles loaded with OVA323 and vitaminD3 or DOPG/PLGA hybrids loaded with vitaminD3 but no antigen as control (mock vaccination). Average particle size, Pdl and ζ -potential of formulations can be found in Supplementary Figure 1. We performed a total of 3 IV injections of the formulations over the course of 10 weeks. Animals were fed a western-type diet during the 10 weeks of experiment. As expected, weight of the animals steadily increased over the experiment, with no significant differences between the vaccinated and mock vaccinated group (Figure 5A). Furthermore, the concentration of cholesterol in plasma were also not different between the

two groups and remained high throughout the duration of the study (Figure 5B). Surprisingly, we did not observe any difference between the groups in the number or phenotype of OT-II T cells in blood (Figure 5C), spleen (Figure 5G) or aorta (Figure 5H). The Oil-Red-O and trichrome histochemical staining also did not show differences in plaque area or collagen content of the plaques (Figure 5I) between control and treatment groups. These data suggest that the DOPG/PLGA hybrid nanoparticles are not able to induce antigen-specific T cell responses *in vivo* and therefore the treatment has no effect on atherosclerosis development.

Only the DSPG liposomes but not the DOPG/PLGA hybrid nanoparticles are able to induce an antigen-specific T cell response *in vivo*

Due to the lack of *in vivo* response to the immunization with DOPG/PLGA hybrid nanoparticles in the atherosclerosis experiment, we assessed how DOPG/PLGA hybrid nanoparticles compared to the previously reported DSPG liposome formulation and to DOPG liposomes *in vivo*. All formulations were loaded with OVA323 and vitaminD3. Briefly, we transferred 500,000 OT-II OVA-specific CD4⁺ T cells to C57Bl/6 mice and subsequently immunized those mice with the nanoparticle formulations. Empty DOPG/PLGA hybrid nanoparticles or free OVA323 and vitaminD3 were used as controls.

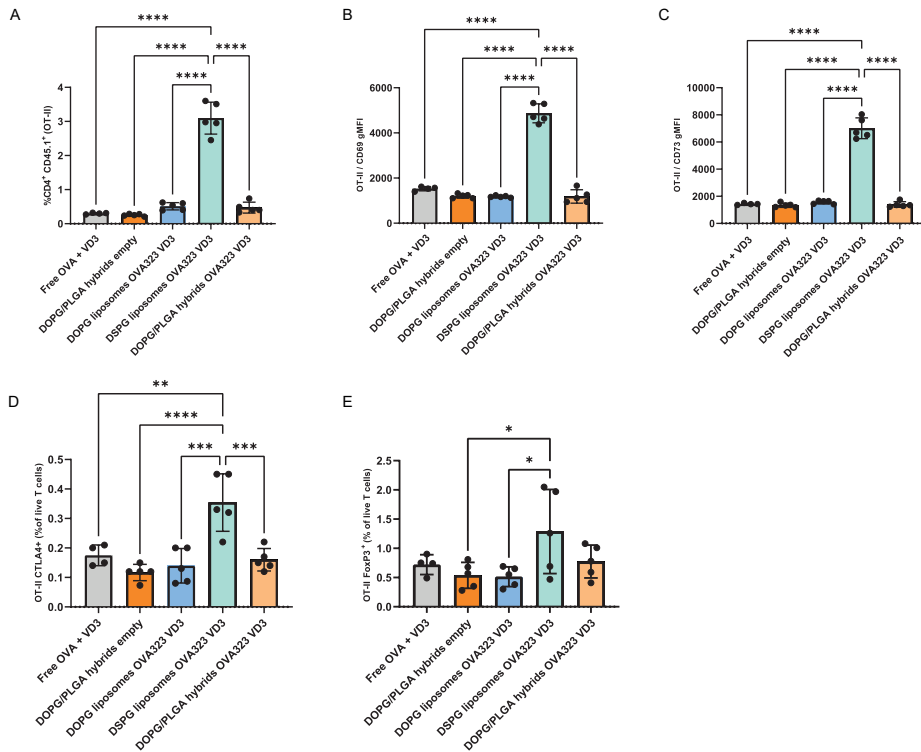


Figure 6. Induction of antigen-specific T cells by nanoparticles in spleen of mice 7 days after intravenous immunization. (A) Percentage of transferred OT-II CD4⁺ T cells in spleens of immunized mice. (B) Geometric mean fluorescence intensity (gMFI) of anti-CD69 antibody in the OT-II CD4⁺ T cell population in spleen. (C) gMFI of anti-CD73 antibody in the OT-II CD4⁺ T cell population in spleen. (D) Percentage of OT-II CD4⁺ T cells expressing CTLA4 and (E) FoxP3 in the live T cell population of the spleen. **** $p \leq 0.0001$, *** $p \leq 0.001$, ** $p \leq 0.01$, * $p \leq 0.05$ determined by one-way ANOVA and Tukey's multiple comparison test.

On day 7 after immunization, we isolated the spleen of the mice and studied the presence of the OVA-specific T cells and their phenotype. In line with the previous *in vivo* experiment, we observed that the DOPG/PLGA hybrid nanoparticles did not induce significantly higher levels of OT-II CD4⁺ T cells compared to the free antigen or the empty DOPG/PLGA hybrid nanoparticle controls, and only the DSPG liposome formulation was able to induce significant antigen-specific T cell proliferation (Figure 6A). Furthermore, only the group immunized with DSPG liposomes showed higher expression of CD69, a marker of recent T cell activation, in the OT-II T cell population (Figure 6B). We also observed an increase in the expression of CD73 (Figure 6C), CTLA4 (Figure 6D) and FoxP3 (Figure 6E), markers

that indicate CD4⁺ Treg activation in the DSPG liposome group. No statistically significant differences between groups were observed in the percentage of OT-II T cells expressing Tbet or ROR γ T (Supplementary Figure 2). These data explain the lack therapeutic efficacy of DOPG/PLGA nanoparticles and underline the importance of *in vivo* testing.

Lipid bilayer composition affects protein corona formation and alters cellular uptake of nanoparticles

Our data shows that although the rigid DOPG/PLGA hybrid particles induce Tregs *in vitro*, their ability to induce them *in vivo* is lost. Interestingly, the same goes for the most fluid particle, the DOPG liposome, whose lipid composition is different to the DSPG liposome but similar to the DOPG/PLGA hybrid particles. We have previously shown that the capacity to induce Tregs of DSPG liposomes depends on the attraction of a protein corona, labelling the particles for uptake via scavenger receptors¹. We hypothesized that potentially the protein corona attracted to DOPG-containing bilayers may differ from DSPG-containing ones, despite both phospholipid classes sharing the same polar headgroup. To determine if these 3 formulations have different capacity to attract proteins to their surface, we first incubated DOPG liposomes, DSPG liposomes and DOPG/PLGA hybrids with mouse serum, FBS or the serum proteins ApoE, ApoB or C1q and determined the effect on particle size (Figure 7A), Pdl (Figure 7B) and ζ -potential (Figure 7C) using DLS. Mouse serum induced a clear increase in particle size of the DSPG liposomes but no significant increase in Pdl, while it only induced a slight increase in particle size in the case of the DOPG/PLGA hybrid nanoparticles but with a bigger effect on Pdl (Figure 7A and 7B).

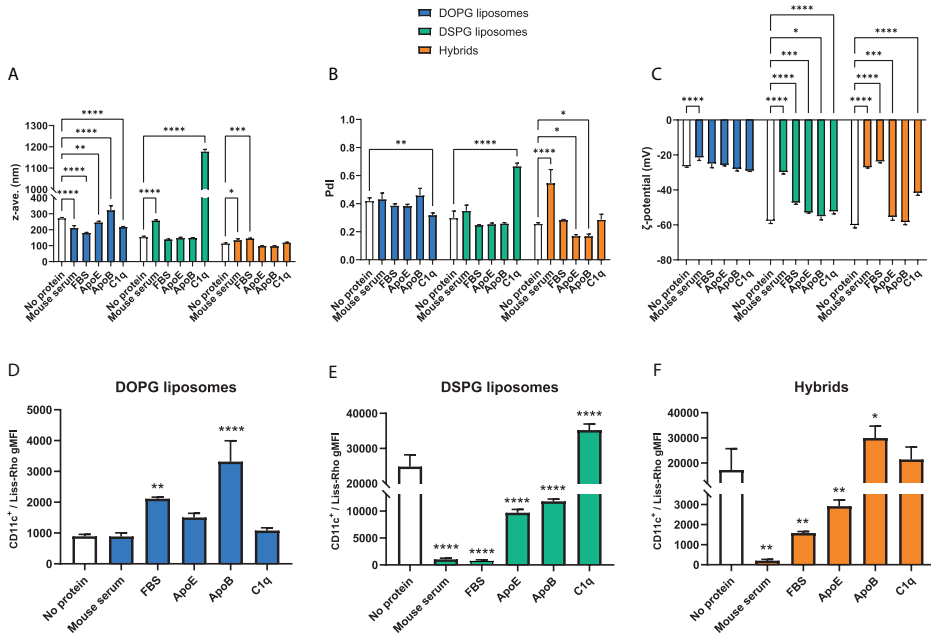


Figure 7. Effect of protein corona on particle characteristics and uptake by BMDCs. Effect of mouse serum, fetal bovine serum (FBS), ApoE, ApoB or C1q on (A) average particle size, (B) polydispersity index and (C) ζ -potential of DOPG liposomes, DSPG liposomes or DOPG/PLGA hybrid nanoparticles. Effect of mouse serum, FBS, ApoE, ApoB or C1q on the uptake of lissamine-rhodamine-labelled (D) DOPG liposomes, (E) DSPG liposomes and (F) DOPG/PLGA hybrid nanoparticles by bone marrow-derived dendritic cells (BMDCs). Geometric mean fluorescent intensity (gmFI) data normalized by subtracting the background fluorescence in nanoparticle-free control. Graphs show mean \pm SD. **** $p \leq 0.0001$, *** $p \leq 0.001$, ** $p \leq 0.01$, * $p \leq 0.05$ compared to no protein condition and determined by (A-C) two-way ANOVA or (D-F) one-way ANOVA followed by Dunnett's multiple comparison test.

This may indicate that DSPG liposomes generate a protein corona when in contact with mouse serum while the DOPG/PLGA hybrid nanoparticles tend to aggregate. There is a clear effect of the Vivaspin purification step in particle size and Pdl of DOPG liposomes since the average particle size before Vivaspin is below 200 nm and the Pdl is around 0.2 (Supplementary Figure 3), while the Pdl is around 0.4 for this formulation after the Vivaspin step (Figure 7B). In the case of particles incubated with FBS, the protein source in cell culture medium used in *in vitro* experiments, there was no significant effect on the particle size and Pdl of DSPG liposomes while DOPG/PLGA hybrid nanoparticles increased in average size without affecting Pdl. ApoB induced an increase in particle size of DOPG liposomes suggesting the formation of an ApoB protein corona. For DSPG liposomes, only C1q has an impact in particle size (Figure 7A) and Pdl (Figure 7B) with a dramatic increase in

both parameters that indicates aggregation of the formulation. In the case of the DOPG/PLGA hybrid nanoparticles the incubation with ApoE, ApoB or C1q did not increase particle size (Figure 7A) or Pdl (Figure 7B). Changes in ζ -potential are also indicative of the adsorption of proteins to the nanoparticle surface. In the case of DOPG liposomes only the incubation with mouse serum led to slightly less negative surface charge (Figure 7C). For DSPG liposomes, all the protein conditions tested led to less negative surface charge, with mouse serum having the biggest effect (Figure 7C). For DOPG/PLGA hybrid nanoparticles, all protein conditions except for ApoB led to less negative ζ -potential with the largest effect caused by mouse serum and FBS (Figure 7C).

After studying the effect of protein corona formation on physicochemical properties of the nanoparticles, we next compared the uptake of nanoparticles with and without the different protein coronas by BMDCs. For DOPG liposomes, the protein corona formed after incubation with FBS or ApoB significantly increased the cell uptake (Figure 7D). In the case of DSPG liposomes, only the presence of C1q in the medium led to an enhance uptake by DCs while the rest of the proteins studied significantly reduced cellular uptake (Figure 7E). For DOPG/PLGA hybrid nanoparticles, only the presence of ApoB in the medium led to a significant increase in uptake by DCs (Figure 7F). Interestingly, the presence of mouse serum in the medium abrogated the uptake of DOPG/PLGA hybrids almost completely (Figure 7F). These data show that the DSPG-containing and the DOPG-containing bilayers have different capacity to attract proteins, and this has consequences for the uptake of nanoparticle by DCs, which is the first step in the initiation of an antigen-specific immune response.

DISCUSSION

Phospholipid composition affects the physicochemical characteristics of lipid-based nanoparticles such as ζ -potential and rigidity but also determines the interaction with biomolecules in the environment, i.e. the protein corona. Here, we studied the capacity of “fluid” anionic liposomes (DOPG liposomes), “rigid” anionic liposomes (DSPG liposomes) and DOPG/PLGA hybrid particles covered with a fluid DOPG phospholipid bilayer to deliver antigens to DCs and induce tolerogenic antigen-specific CD4⁺ T cells both *in vitro* and *in vivo*. The use of DOPG/PLGA hybrid nanoparticles allows us to determine the contribution of nanoparticle rigidity independently from the lipid composition. Although the Young’s module of the hybrid nanoparticles has not been determined experimentally, similar lipid-wrapped PLGA nanoparticles have shown to have a Young’s module of 60 ± 32 MPa, in contrast with DOPC:DOPG liposomes (0.493 ± 0.365 MPa) and DSPC:DSPG:CHOL liposomes (1.498 ± 0.530 MPa)^{6, 17}.

We observed that the exposure of BMDCs to empty DOPG/PLGA hybrid nanoparticles leads to a reduced activation level, measured by the expression of CD86 and CD40, upon pro-inflammatory stimulation with LPS. This effect was also observed in both DOPG and DSPG liposomes when the tolerogenic adjuvant vitaminD3 was included in the formulation. These results are in line with previous reports showing that delivery of vitaminD3 using anionic liposomes is able to induce regulatory or tolerogenic phenotype on DCs⁷. Interestingly, DSPG liposomes without vitaminD3 did not seem to induce this tolerogenic phenotype, although these liposome formulations have previously shown to be able to induce a Treg response in mice¹. The mechanism of action of Treg induction by DSPG liposomes has not been elucidated yet, although our data suggests that it is not through the inhibition of CD86 and CD40 expression. Similarly, a report from Braake & Benne et al. (2021) showed no effect of non-adjuvated DSPG liposomes on the expression of CD86 and CD40, only when the tolerogenic adjuvant retinoic acid was included in the formulation it was able to induce tolerogenic DCs¹⁸.

We also studied the capacity of nanoparticle-primed DCs to induce antigen-specific T cell responses. We observed that all nanoparticle formulations were able to induce CD4⁺ T cell proliferation (Figure 3A and 3B) demonstrating that the antigen was successfully delivered and presented to T cells. We further characterized the phenotype of the proliferating T cells. The DCs primed with DOPG/PLGA hybrid nanoparticles induced the expression of FoxP3, RORγT and Tbet on T cells, transcription factors associated to Tregs, Th17 and Th1 cells respectively, compared to liposome-primed DCs. In contrast to previous reports, DCs primed with DSPG liposomes loaded with antigen or with antigen and vitaminD3 did not induce FoxP3 in the proliferating cells population, however these formulations seemed to reduce expression of Tbet compared to free antigen, indicating a less pro-inflammatory phenotype.

In vitro exposure of DCs to nanoparticles does not fully capture the complexity of biological systems and it does not recapitulate the effect of biodistribution or biological barriers to reach the target cells¹⁹. We therefore studied the effect of the nanoparticles *in vivo*. The DSPG liposomes were able to successfully induce an OVA-specific T cell response as it has been reported in previous studies^{1, 18}. These antigen-specific CD4⁺ T cells also showed higher expression of CTLA4, a co-inhibitory molecule that is key for peripheral tolerance²⁰. On the other hand, the DOPG/PLGA hybrid nanoparticles did not induce antigen-specific T cell responses in neither the atherosclerosis nor the adoptive transfer experiments, explaining its inability to reduce atherosclerosis in the LDLR^{-/-} x ApoB-OVA model. In fact, the *in vivo* behaviour of hybrid DOPG/PLGA particles seemed to be very similar to the fluid DOPG liposomes.

Both DOPG liposomes and DOPG/PLGA hybrids share the same lipid bilayer, and it is the main difference between these formulations and DSPG liposomes. We hypothesized that the difference in lipid bilayer composition might lead to differences in the protein corona, previous research has shown that bilayers composed of unsaturated phospholipids can form lipid domains while the presence of cholesterol in the bilayer disrupts these domains, favours a more homogeneous distribution of the different phospholipids in the bilayer and increases binding of proteins to the nanoparticle surface¹⁰. Therefore, the lack of cholesterol and the unsaturated phospholipid composition in both the DOPG liposomes and the DOPG/PLGA hybrids could lead to quantitative and/or qualitative differences in protein corona and explain the lack of *in vivo* effect of these two formulations. We indeed observed that the incubation of DOPG liposomes, DSPG liposomes and DOPG/PLGA hybrids with mouse serum or FBS influenced their physicochemical characteristics (Figure 7A, B and C). Increase in particle size and Pdl as well as partial neutralization of the surface charge are all clear signs of the formation of a protein corona²¹. There was a clear difference in ζ -potential between DOPG liposomes and DOPG/PLGA hybrids although both formulations have the same lipid bilayer composition. This difference could be due to the use of PBS for the formulation of DOPG liposomes while PB was used for the preparation of DOPG/PLGA hybrids. The clear abrogation of the uptake of DOPG/PLGA hybrids by BMDCs in the presence of mouse serum suggests that the protein corona formed *in vivo* hinders the uptake of these particles by APCs, explaining the lack of antigen-specific immune responses in the mouse experiments. When looking at the effect of individual proteins on the uptake, we observed that C1q greatly enhances the uptake of DSPG liposomes. The role of this complement protein on DSPG liposome uptake has been reported before¹. The increased uptake in this condition can also be potentiated by the particle aggregation observed, since nanoparticle aggregation can lead to enhanced uptake by APCs²². On the other hand, for DOPG liposomes, ApoB seems to play a bigger role in mediating the liposome uptake. The same effect can be observed for the DOPG/PLGA hybrids, however there were no signs of ApoB deposition on these particles in the DLS data. A weaker interaction between ApoB and the DOPG/PLGA hybrids could result in the wash-out of the protein during the purification step before DLS explaining the limited impact of ApoB incubation in the physicochemical properties of DOPG/PLGA hybrids. The lack of *in vivo* effect of the DOPG/PLGA hybrid nanoparticles compared to the DSPG liposomes could therefore be explained by the availability of the different proteins mediating the uptake of these different nanoparticles, in the circulation. While C1q is a complement protein that is freely available in circulation²³, ApoB100 is an amphipathic protein that travels in the bloodstream associated with cholesterol and lipids forming LDL and VLDL

particles²⁴. Furthermore, unlike other lipoproteins ApoB is non-exchangeable so it cannot transfer between different lipoprotein particles²⁵, therefore it is not freely available to adsorb to the nanoparticle surface and mediate their cellular uptake. All in all, our data point towards a more prevalent role of the lipid bilayer composition compared to the particle rigidity in the biological effect of nanoparticles, and those differences in the biological effect seem to be mediated by the protein corona.

CONCLUSIONS

Physicochemical properties of liposomes such as negative surface charge and high rigidity have been previously linked to tolerogenic capacity of these formulations. However, liposome rigidity is mostly determined by the phospholipid composition of the bilayer, which can also determine the protein corona of the particle in a biological environment. The data presented here suggests that the phospholipid composition associated with highly rigid liposomes, i.e. saturated phospholipids, and cholesterol, may be more important in determining the *in vivo* effect of liposomes than the particle rigidity itself.

AUTHOR CONTRIBUTIONS

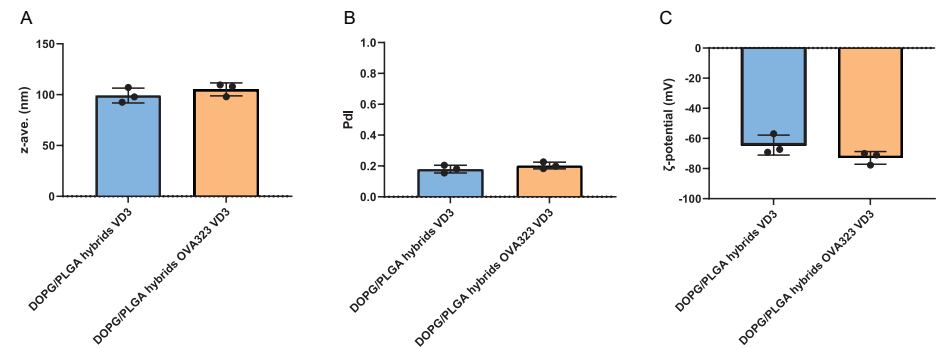
FLV conceptualised the project, designed and carried out experiments, drafted this chapter and prepared the figures. MAN conceptualised the hybrid nanoparticles and developed the formulation method. LHMB and WEH performed part of the experiments. AK, JAB and BS provided valuable input in the experimental design and edited the draft chapter.

REFERENCES

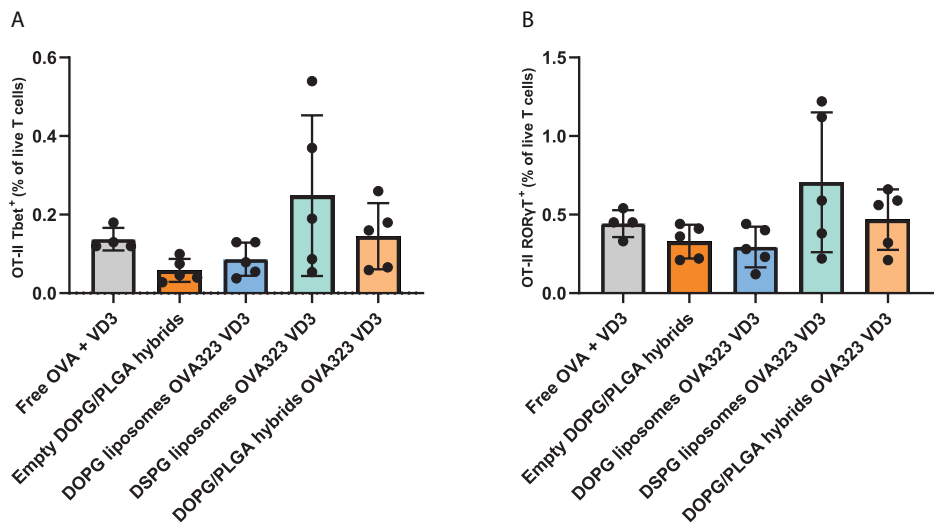
1. Benne N, van Duijn J, Lozano Vigario F, Lebourg RJT, van Veelen P, Kuiper J, et al. Anionic 1,2-distearoyl-sn-glycero-3-phosphoglycerol (DSPG) liposomes induce antigen-specific regulatory T cells and prevent atherosclerosis in mice. *J Control Release*. 2018;291:135-46.
2. Pujol-Autonell I, Serracant-Prat A, Cano-Sarabia M, Ampudia RM, Rodriguez-Fernandez S, Sanchez A, et al. Use of autoantigen-loaded phosphatidylserine-liposomes to arrest autoimmunity in type 1 diabetes. *PLoS One*. 2015;10(6):e0127057.
3. Libby P. The changing landscape of atherosclerosis. *Nature*. 2021;592(7855):524-33.
4. Benne N, van Duijn J, Kuiper J, Jiskoot W, Slutter B. Orchestrating immune responses: How size, shape and rigidity affect the immunogenicity of particulate vaccines. *J Control Release*. 2016;234:124-34.
5. Korsholm KS, Hansen J, Karlén K, Filskov J, Mikkelsen M, Lindénstrom T, et al. Induction of CD8⁺ T-cell responses against subunit antigens by the novel cationic liposomal CAF09 adjuvant. *Vaccine*. 2014;32(31):3927-35.
6. Benne N, Lebourg RJT, Glandrup M, van Duijn J, Lozano Vigario F, Neustrup MA, et al. Atomic force microscopy measurements of anionic liposomes reveal the effect of liposomal rigidity on antigen-specific regulatory T cell responses. *J Control Release*. 2020;318:246-55.
7. Nagy NA, Lozano Vigario F, Sparrius R, van Capel TMM, van Ree R, Tas SW, et al. Liposomes loaded with vitamin D3 induce regulatory circuits in human dendritic cells. *Front Immunol*. 2023;14:1137538.
8. Nakano K, Tozuka Y, Yamamoto H, Kawashima Y, Takeuchi H. A novel method for measuring rigidity of submicron-size liposomes with atomic force microscopy. *Int J Pharm*. 2008;355(1-2):203-9.
9. Beckers D, Urbancic D, Sezgin E. Impact of Nanoscale Hindrances on the Relationship between Lipid Packing and Diffusion in Model Membranes. *J Phys Chem B*. 2020;124(8):1487-94.
10. Nele V, D'Aria F, Campani V, Silvestri T, Biondi M, Giancola C, De Rosa G. Unravelling the role of lipid composition on liposome-protein interactions. *J Liposome Res*. 2023;1-9.
11. Lozano Vigario F, Nagy NA, The MH, Sparrius R, Bouwstra JA, Kros A, et al. The Use of a Staggered Herringbone Micromixer for the Preparation of Rigid Liposomal Formulations Allows Efficient Encapsulation of Antigen and Adjuvant. *J Pharm Sci*. 2022;111(4):1050-7.
12. van Eenige R, Verhave PS, Koemans PJ, Tiebosch I, Rensen PCN, Kooijman S. RandoMice, a novel, user-friendly randomization tool in animal research. *PLoS One*. 2020;15(8):e0237096.
13. Schindelin J, Arganda-Carreras I, Frise E, Kaynig V, Longair M, Pietzsch T, et al. Fiji: an open-source platform for biological-image analysis. *Nat Methods*. 2012;9(7):676-82.
14. Pattipeiluhu R, Crielaard S, Klein-Schiphorst I, Florea BI, Kros A, Campbell F. Unbiased Identification of the Liposome Protein Corona using Photoaffinity-based Chemoproteomics. *ACS Cent Sci*. 2020;6(4):535-45.
15. Viney NJ, Yeang C, Yang X, Xia S, Witztum JL, Tsimikas S. Relationship between "LDL-C", estimated true LDL-C, apolipoprotein B-100, and PCSK9 levels following lipoprotein(a) lowering with an antisense oligonucleotide. *J Clin Lipidol*. 2018;12(3):702-10.

16. Domogalla MP, Rostan PV, Raker VK, Steinbrink K. Tolerance through Education: How Tolerogenic Dendritic Cells Shape Immunity. *Front Immunol.* 2017;8:1764.
17. Eshaghi B, Alsharif N, An X, Akiyama H, Brown KA, Gummuluru S, Reinhard BM. Stiffness of HIV-1 Mimicking Polymer Nanoparticles Modulates Ganglioside-Mediated Cellular Uptake and Trafficking. *Adv Sci (Weinh).* 2020;7(18):2000649.
18. Ter Braake D, Benne N, Lau CYJ, Mastrobattista E, Broere F. Retinoic Acid-Containing Liposomes for the Induction of Antigen-Specific Regulatory T Cells as a Treatment for Autoimmune Diseases. *Pharmaceutics.* 2021;13(11).
19. Ishida T, Harashima H, Kiwada H. Interactions of liposomes with cells in vitro and in vivo: opsonins and receptors. *Curr Drug Metab.* 2001;2(4):397-409.
20. Wing K, Onishi Y, Prieto-Martin P, Yamaguchi T, Miyara M, Fehervari Z, et al. CTLA-4 control over Foxp3+ regulatory T cell function. *Science.* 2008;322(5899):271-5.
21. Xiao Q, Zoulikha M, Qiu M, Teng C, Lin C, Li X, et al. The effects of protein corona on in vivo fate of nanocarriers. *Adv Drug Deliv Rev.* 2022;186:114356.
22. Liu X, Chen Y, Li H, Huang N, Jin Q, Ren K, Ji J. Enhanced retention and cellular uptake of nanoparticles in tumors by controlling their aggregation behavior. *ACS Nano.* 2013;7(7):6244-57.
23. van de Bovenkamp FS, Dijkstra DJ, van Kooten C, Gelderman KA, Trouw LA. Circulating C1q levels in health and disease, more than just a biomarker. *Mol Immunol.* 2021;140:206-16.
24. Segrest JP, Jones MK, De Loof H, Dashti N. Structure of apolipoprotein B-100 in low density lipoproteins. *J Lipid Res.* 2001;42(9):1346-67.
25. Gordon SM, Pourmousa M, Sampson M, Sviridov D, Islam R, Perrin BS, Jr., et al. Identification of a novel lipid binding motif in apolipoprotein B by the analysis of hydrophobic cluster domains. *Biochim Biophys Acta Biomembr.* 2017;1859(2):135-45.

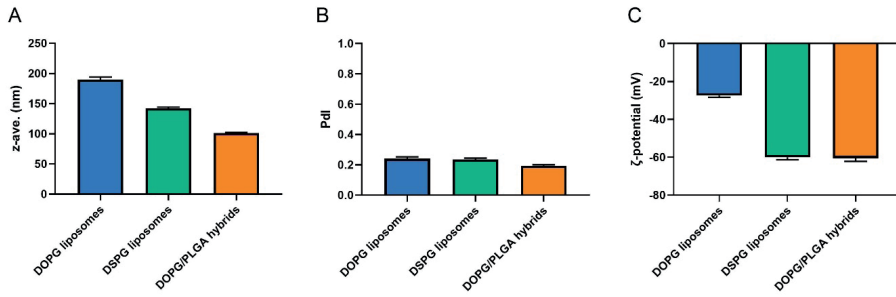
SUPPLEMENTARY DATA



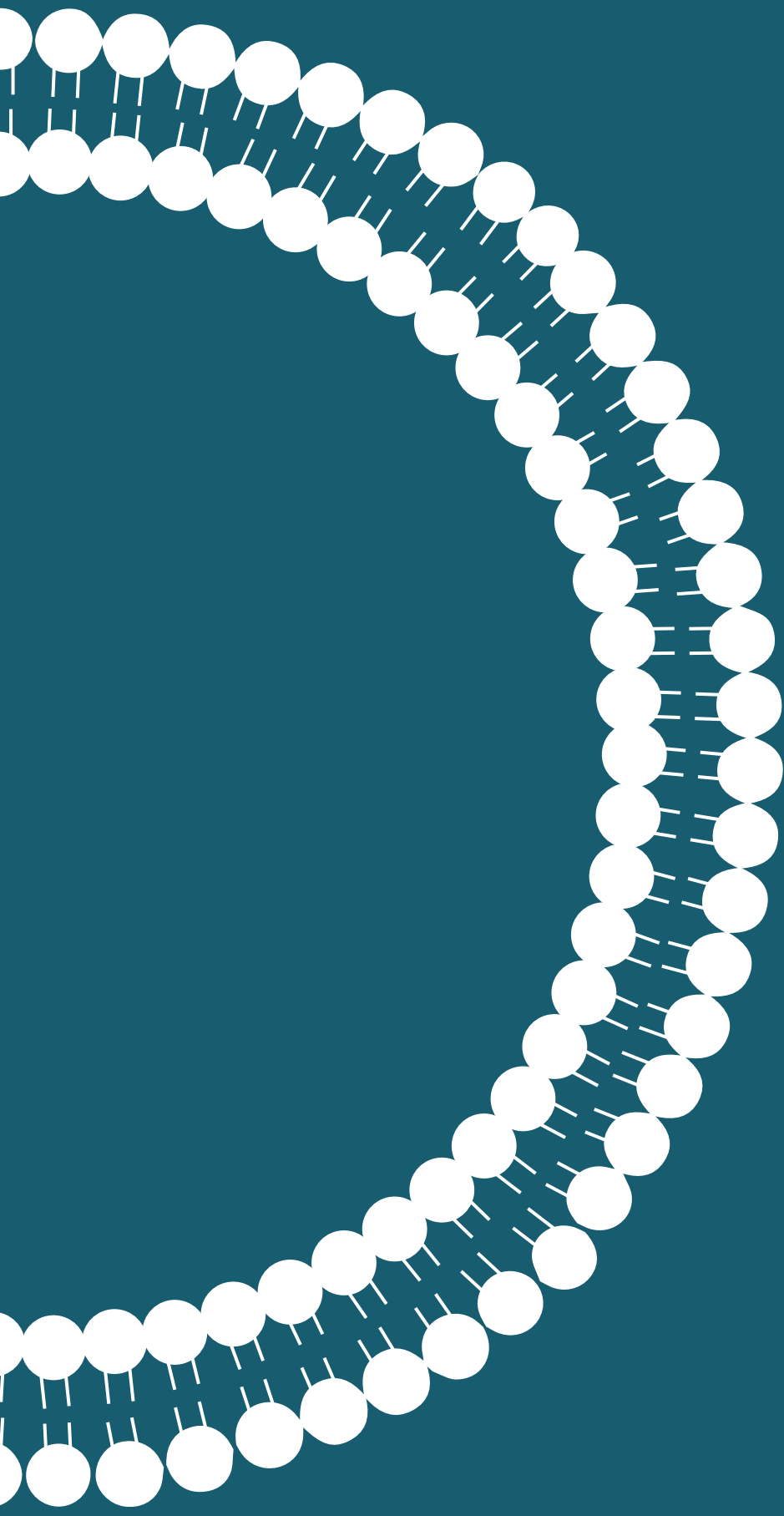
Supplementary Figure 1. Physicochemical characteristics of formulations used in atherosclerosis experiment. (A) Average hydrodynamic diameter of the nanoparticles (Z-average) in nm, (B) Polydispersity Index and (C) ζ -potential in mV of DOPG/PLGA hybrids nanoparticles loaded with vitaminD3 only and with vitaminD3 and OVA323. Data shown is mean \pm SD.



Supplementary Figure 2. Th1 and Th17 OT-II T cells in spleen of mice 7 days after immunization. (A) Percentage of OT-II T cells expressing the Th1 transcription factor Tbet and (B) the Th17 transcription factor ROR γ T in the live T cell population of the spleen. Statistically significant differences between groups tested by one-way ANOVA and Tukey's multiple comparison test.



Supplementary Figure 3. Physicochemical characteristics of nanoparticle formulations before the Vivaspin centrifugation step in the protein corona study. (A) Average particle size, (B) Polydispersity Index and (C) ζ -potential of the formulations incubated in buffer at 37°C for 1h. Data shown is mean \pm SD.



Chapter 7

Nasal subunit vaccination with cationic liposomes induces Influenza-specific resident CD8⁺ T cells in the airways and reduces viral burden upon infection

F. Lozano Vigario¹, D. Ostroumov², J.A. Bouwstra¹, A. Kros³, T.C. Wirth², B. Slütter¹

¹ Division of BioTherapeutics, Leiden Academic Centre for Drug Research, Leiden University, The Netherlands

² Department of Gastroenterology, Hepatology, Infectious Diseases and Endocrinology, Hannover Medical School, Hannover, Germany

³ Supramolecular & Biomaterials Chemistry, Leiden Institute of Chemistry, Leiden University, The Netherlands

Manuscript under review

ABSTRACT

The induction of anti-viral CD8⁺ T cell immunity in the respiratory tract is key for protection against infections such as Influenza or SARS-CoV2, however most vaccines are optimized for the induction of systemic humoral immune responses. The induction of tissue-resident memory CD8⁺ T cells via immunization can be achieved using live attenuated vaccines and it often requires a prime-boost regime with a long interval between both immunizations. Therefore, the use of safer and easier to manufacture subunit vaccines to elicit potent tissue-resident cellular immune responses is an unmet need in the vaccine field. Here, we show that intranasal immunization followed by a rapid systemic boost with a subunit vaccine based on cationic liposomes loaded with a single-epitope influenza antigen, PA224, and the adjuvant cyclic dimeric guanosine monophosphate (c-di-GMP) induces a potent and long lasting CD8⁺ T cell response systemically and locally in the lungs. This immunization regime led to a significant reduction in viral load in lungs of influenza-infected mice. The accelerated induction of lung-resident memory CD8⁺ T cells using a subunit vaccine can have advantages for the deployment of effective vaccines against rapidly spreading respiratory viruses.

INTRODUCTION

Respiratory viruses such as coronaviruses and influenza are a global threat for public health as seen during SARS-CoV2 pandemic and the annual epidemics of influenza. The World Health Organization (WHO) and scientific literature estimate that seasonal influenza viruses severely affect up to 5 million people every year and result in between 290,000 and 650,000 deaths¹.

Vaccination is the most effective intervention to reduce morbidity and mortality of infectious diseases. Currently used vaccines can be broadly divided into inactivated, live attenuated and subunit vaccines². The focus of current vaccines is the induction of strong antibody responses, however cellular immunity is also critical for protection against viral infections^{3,4}. In the case of influenza, the generation of T cell responses against viral antigens conserved across different strains might overcome the need for annual vaccination. CD8⁺ T cells, also called cytotoxic T cells, can recognize virus-infected cells that present viral epitopes via MHC-I molecules⁵ and therefore can target antigens that are not accessible for antibodies, such as nucleoprotein- or polymerase-derived epitopes, which are substantially less prone to mutations than hemagglutinin⁶. The induction of long-term memory CD8⁺ T cells through vaccination is therefore a key step towards the development of broadly protective influenza vaccines that do not require annual vaccination. However, the induction of immunological memory often requires a prime-boost vaccination regime with a long interval between the two immunizations, which can be an important hurdle in emergency situations such as rapidly spreading pandemics.

Additionally, in the case of respiratory viruses the induction of robust local immune responses in the respiratory mucosa is particularly important⁷. This is highlighted by the poor correlation observed between serum antibody titers and protection against influenza in a challenge study with volunteers⁸. Furthermore, despite the high efficacy in the reduction of morbidity and mortality observed for the SARS-CoV2 vaccines, these systemically administered vaccines are less effective at preventing transmission^{9,10}. One possible explanation is the low levels of local responses induced in the respiratory tract, which is the first site of infection and viral replication. Therefore, the induction of a robust tissue-resident memory T cell (T_{rm}) response in the respiratory tract can not only improve vaccine protection but also reduce viral shedding and transmission¹⁰.

The induction of a strong local immune response in the lungs has only been achieved using live attenuated vaccines but subunit vaccines have a better safety profile, are more stable and easier to manufacture than live attenuated vaccines¹¹. Furthermore, live attenuated vaccines cannot be administered to all demographic groups as they are contraindicated for immunosuppressed individuals¹². Therefore,

the development of subunit vaccines able to induce strong and long-lasting immune responses in the respiratory tract is of urgent need.

In this study, we propose a vaccination strategy to induce influenza-specific CD8⁺ T cells in the lungs using cationic liposomes loaded with influenza-derived CD8⁺ T cell epitopes and bis-(3'-5')-cyclic diguanylate monophosphate (c-di-GMP). C-di-GMP is cyclic dinucleotide that can induce type I interferon production by activating the stimulator of interferon genes (STING) signal pathway and it has been studied as an adjuvant in cancer vaccines^{13, 14}. Cationic liposomes have previously been shown to induce strong antigen-specific CD8⁺ T cell responses¹⁵. Apart from their immune activating properties, cationic liposomes present advantages for intranasal vaccination such as the favourable electrostatic interaction with the negatively charged mucosal lining that promotes mucoadhesion¹⁶. Previous studies showed that the delivery of an intranasal influenza vaccine using a mucoadhesive gel induced stronger and faster antibody responses both in the mucosa and systemically compared to soluble controls¹⁷.

Here, we show that the c-di-GMP-loaded cationic liposomes can be used as a platform to induce strong CD8⁺ T cell responses against a variety of peptide antigens derived from SARS-CoV2 and influenza. Furthermore, we use liposomes loaded with an influenza-derived antigen in an accelerated prime-boost regime^{18, 19} consisting of a nasal prime followed by a systemic boost and show that this immunization strategy induces a strong and durable CD8⁺ T cell response both systemically and in the lungs and it leads to a reduction of viral load in lungs of mice after influenza challenge.

MATERIALS

Lipids 1,2-distearoyl-sn-glycero-3-phosphocholine (DSPC), 1,2-dipalmitoyl-3-trimethylammonium-propane (DPTAP) were purchased from Avanti Polar Lipids (Alabaster, AL, USA). Cholesterol was obtained from Sigma-Aldrich (Zwijndrecht, the Netherlands). Adjuvant bis-(3'-5')-cyclic dimeric guanosine monophosphate (c-di-GMP) was purchased from Invivogen (San Diego, CA, USA). Peptides were purchased from GenScript Biotech (Rijswijk, the Netherlands). The agonistic anti-CD40 antibody (clone 1C10, hybridoma) was kindly provided by Frances Lund, Department of Microbiology, University of Alabama at Birmingham, AL, USA. The antibodies Thy1.2 (CD90.2)-PE-Cy7, CD8a-PE-Dazzle 594, CD8a-Brilliant Violet 510, CD8a-FITC, IFN γ -APC, CD69-PE, CD103-Brilliant Violet 510, CD4-APC, Ly6G-PerCP, F4/80-Brilliant Violet 650 were purchased from Biolegend (CA, USA). The antibodies CD8a-FITC, CD8a-PE, IFN γ -eFluor450, TNF- α -PE, CD69-FITC, CD103-FITC, CD4-eFluor450, Ly6G-PE, CD11b-APC, CD19-FITC and Fixable

Viability Dye-APC-eFluor780 were purchased from eBioscience (ThermoFisher Scientific, MA, USA).

A/PR/8/34 H1N1 (PR8 H1N1) virus was a kind gift from Dr. A. Huckriede (UMC Groningen, NL)²⁰. Stock solutions in allantoic fluid (2.7×10^9 TCID₅₀/ml) were thawed on ice and diluted in cold PBS to 20,000 TCID₅₀/ml before nasal administration into mice.

METHODS

SARS-CoV2 peptide antigen selection

For the selection of SARS-CoV2-derived peptides to load into the cationic liposomes, we screened the amino acid sequence of the virus surface glycoprotein (NCBI Reference Sequence: YP_009724390.1) and the nucleocapsid phosphoprotein (NCBI Reference Sequence: YP_009724397.2) and selected previously described²¹, conserved epitopes with high predicted binding affinity for HLA-A*11:01.

Preparation of cationic liposomal formulations

Liposomes were prepared using the lipid film hydration method as previously described²². Briefly, a total of 10mg of DSPC, DPTAP and cholesterol dissolved in chloroform were mixed in a round-bottom flask in a molar ratio of 4:2:1 (DSPC:DPTAP:CHOL). The lipids were mixed with 200 μ g of bis-(3'-5')-cyclic dimeric guanosine monophosphate (c-di-GMP). The organic solvent was removed by means of a rotary evaporator with pressure set at 180 mbar and connected to a water bath at 40°C. The dry lipid film was hydrated with 1 mL of either milliQ water or 500 μ g of peptide dissolved in milliQ water. The resulting suspension of multilamellar vesicles was snap-frozen using liquid N₂ and freeze-dried overnight using a Christ alpha 1-2 freeze-dryer (Osterode, Germany). The dry product was re-hydrated stepwise by first adding 25% of the final volume of phosphate buffer (PB) 10 mM pH 7.4 followed by vortex and 30 minutes incubation at 60°C in a water bath. This step was repeated one more time. A final re-hydration step involves the addition of the remaining 50% of the final volume of PB 10mM pH 7.4, vortex and incubation in 60°C water bath for at least 1 hour. The lipid concentration after re-hydration was 5 mg/mL. The formulation was down-sized by means of high-pressure extrusion using a LIPEX Extruder (Northern Lipids Inc., Canada) connected to a water bath at 60°C. Formulations were extruded 4x through 400nm and 200nm stacked track-etched polycarbonate membranes (Whatman® Nucleopore™, GE Healthcare, Little Chalfont, UK). The resulting monodisperse formulations were purified using Vivaspinn centrifugal concentrators (MWCO 100 kDa, Sartorius, Göttingen, Germany) to remove non-encapsulated peptides and c-di-GMP. Finally,

formulations for intranasal administration were further concentrated using a N₂ gas flow.

Characterization of the formulations

The z-average hydrodynamic diameter (Z_{ave}), polydispersity index (Pdl) and ζ -potential of the formulations were determined using dynamic light scattering (DLS) and laser Doppler electrophoresis in a Zetasizer NanoZS (Malvern Panalytical, UK).

Peptide and c-di-GMP concentrations were determined by reverse-phase ultra-high performance liquid chromatography (UPLC). For quantification of the peptides, a modified Bligh-Dyer method was used to extract and separate the peptide from the liposomes. In short, 100 μ L of formulation was mixed with 250 μ L of methanol, 250 μ L of 0.1M hydrochloric acid 0.1M and 250 μ L of chloroform. The mix was vortexed for 30 seconds and centrifuged for 10 minutes at 1000G. A sample was taken from the water-methanol upper phase containing the peptides. The extracted sample was analysed by injecting 10 μ L of sample into a 1.7 μ m BEH C18 column (2.1 x 50 mm, Waters ACQUITY UPLC, Waters, MA, USA). Column temperature was set at 40°C. A mobile phase linear gradient was applied to the column starting with 95% milliQ water with 0.1% TFA (solvent A) and 5% acetonitrile with 0.1% TFA (solvent B) and going to 95% solvent B in 7 minutes. The gradient was followed by 95% solvent B for 2 minutes and back to 95% solvent A for 3 minutes. Flow rate of the mobile phase was set at 0.5 mL/min. Peptides were detected by absorbance at 220 nm using ACQUITY UPLC TUV detector. To quantify the c-di-GMP concentration in the formulations, 10 μ L of the liposomal formulation was directly injected into a 1.7 μ m BEH C18 column (2.1 x 50 mm, Waters ACQUITY UPLC, Waters, MA, USA), without previous sample pre-treatment. The mobile phases and the gradient applied were the same as for quantification of the peptides. The detection of c-di-GMP was done by absorbance at 254 nm using ACQUITY UPLC TUV detector.

Animals

Mice were bred in the Animal Research Facility of Leiden University, Faculty of Science, The Netherlands or the Animal Care Facility of Hannover Medical School, Germany, under standard laboratory conditions. Animals were provided with food and water *ad libitum*. Animal experiments were reviewed and approved by the Ethics Committee for animal experiments of Leiden University or by German institutional and government boards (LAVES). Animal work was performed according to Dutch and/or German Government regulations and Directive 2010/63/EU of the European Parliament.

***In vivo* screening of antigen-specific immune responses to SARS-CoV2-derived antigens**

Transgenic mice expressing human HLA-A11 were immunized intravenously with a mix of liposomes loaded with 5 μ g of c-di-GMP and 10 nmol of the SARS-CoV2-derived peptides COVN361, COV1020, COVN134, COVS757 and COVN310 (peptides details in Supplementary Table 1). After 1 week, mice received an intravenous boost with a mix consisting of 50 nmol of each of the SARS-CoV2 peptides, 5 μ g c-di-GMP and 50 μ g of agonistic anti-CD40 antibody. Blood was collected via submandibular bleeding on day 7 (after prime) and day 27 (after boost) for *ex vivo* restimulation with the individual peptides and flow cytometry analysis. Epitope-specific CD8⁺ T cell response was investigated by intracellular IFN γ staining as previously described^{23, 24}. Briefly, stimulation of peptide-specific T cells was performed by incubation of cell suspensions with the respective SARS-CoV2-derived peptides (2 μ g/ml) in presence of GolgiPlug (1/1000 dilution) (Becton Dickinson, San José, CA, USA) in RPMI medium (Gibco), supplemented with 10% FCS (Gibco), penicillin (50 U/ml), streptomycin (50 μ g/ml) (Bio&Sell). Unstimulated T cells in presence of GolgiPlug were used as control for background cytokine production. Cells were incubated overnight at 37°C and 5% CO₂. Prior to staining, cells were treated with TruStain FcX (Biolegend) to block Fc-receptors for 15 minutes at 4°C, then stained for CD8a-FITC (53–6.7), IFN γ -APC (XMG1.2), TruStain FcX (anti-mouse CD16/32) and CD90.2 (53-2.1). Samples were analysed by flow cytometry data in a FACSCanto II (BD Bioscience, Heidelberg, Germany).

***In vivo* evaluation of Influenza-specific immune responses**

C57Bl6/J mice between 8 and 12 weeks old were weighted before the start of the experiments and randomly allocated to the different control or experimental groups using the randomization software RandoMice® and using weight as a blocking factor for the randomization method²⁵. On day 1, animals were immunized with DSPC:DPTAP:Cholesterol liposomes containing 10 nmol of the murine immunodominant influenza epitopes PA₂₂₄₋₂₃₃ (PA224)²⁶ and NP₃₆₆₋₃₇₄ (NP366)²⁷ peptides and 5 μ g of c-di-GMP. Animals received 10 μ L of formulation intranasally, 100 μ L of formulation intravenously through the tail vein or subcutaneous under the skin over the neck. For intranasal immunizations mice were lightly anaesthetized with 0.6 L/min of 4% isoflurane. On day 7, a blood sample of 50-100 μ L was taken from the animals by tail vein cut, and 200 μ L of either DSPC:DPTAP:Cholesterol liposomes containing the peptide(s) antigen(s) and c-di-GMP or a boost mix containing antiCD40 agonistic antibody (clone 1C10, hybridoma provided by Frances Lund, Department of Microbiology, University of Alabama

at Birmingham, AL, USA), c-di-GMP, and peptides was administered intravenously through the tail vein. At the end of the experiment, mice received an intravenous injection of 3 μ g of anti-mouse antiCD45.2-Allophycocyanin (antiCD45.2-APC) in order to label all T cells in circulation, therefore allowing the identification of tissue-infiltrated T cells from circulating T cells as previously described²⁸. Mice were sacrificed by cervical dislocation 3 minutes after antiCD45.2-APC injection. After sacrifice, spleen, lungs, and inguinal lymph nodes were collected for *ex vivo* restimulation and flow cytometry analysis.

***In vivo* challenge of vaccinated mice with PR8 H1N1**

Based on the results from the previous experiment, we chose the most optimal prime immunization route, antigen and boost formulation to vaccinate mice and subsequently challenge them with influenza virus. Mice between 8 and 12 weeks old were weighted and randomly allocated to either treatment or control group. Mice in treatment group received an intranasal or subcutaneous immunization DSPC:DPTAP:Cholesterol liposomes containing 10 nmol of PA224 antigen peptide and 5 μ g of c-di-GMP, while mice in the control group received an intranasal immunization with the same cationic liposomal formulation containing 5 μ g c-di-GMP but no antigen peptide or intranasal PBS. Intranasal immunizations were performed as described above. On day 7 after prime immunization, a blood sample was drawn via tail vein cut and mice received an intravenous injection of DSPC:DPTAP:Cholesterol liposomes containing either 10 nmol of PA224 and 5 μ g of c-di-GMP (treatment group) or 5 μ g c-di-GMP only or PBS (control group). On day 14, 50-100 μ L blood sample was taken via tail vein cut. On day 35 mice were weighted to determine baseline weight before viral challenge. For the viral challenge, mice were lightly anaesthetized with 0.6 L/min of 4% isoflurane and a 50 μ L suspension containing 1000 TCID₅₀ (median tissue culture infectious dose) of PR8 H1N1 was applied to the nostrils. After viral challenge mice were weighted daily and sacrificed on day 39 by cervical dislocation. Lungs were collected for viral titer quantification and *ex vivo* T cell restimulation. Lung samples were mechanically disrupted and digested with collagenase and DNAase I enzymes for 30 minutes at 37°C. Digested samples were passed through a cell strainer and immune cells were isolated using 35% Percoll density gradient centrifugation, followed by *ex vivo* restimulation with PA224 and flow cytometry staining. Spleens were restimulated *ex vivo* with PA224, stained for flow cytometry. BAL samples were directly stained for Thy1.2-PE-Cy7, CD8a-Brilliant Violet 510, CD4-eFluor450, Ly6G-PerCP, Ly6C-PE, CD11b-APC, CD19-FITC and fixable viability dye APC-eFluor 780 and analysed by flow cytometry in Cytotflex S (Beckman Coulter, CA, USA).

Ex vivo restimulation and flow cytometry analysis of samples

Prior to restimulation, organ samples were processed into a single cell suspension. Spleen, lungs and blood samples were lysed using Ammonium-Chloride-Potassium (ACK) lysing buffer. Samples were stimulated with either 5 $\mu\text{g/mL}$ of peptide and 3 $\mu\text{g/mL}$ of Brefeldin A (BrefA) or only 3 $\mu\text{g/mL}$ of BrefA (unstimulated control) for 5 hours at 37°C and using bone marrow derived dendritic cells as feeder cells. After stimulation, blood samples were stained for Thy1.2-PE-Cy7, CD8a-FITC, IFN γ -eFluor450 and fixable viability dye APC-eFluor780 and analysed by flow cytometry in Cytotflex S (Beckman Coulter, CA, USA). Spleen, lymph nodes and lung samples were stained for Thy1.2-PE-Cy7, CD8a-PE, CD4-APC, CD69-FITC, CD103-Brilliant Violet 510, IFN γ -eFluor450 and fixable viability dye APC-eFluor780 and analysed by flow cytometry in Cytotflex S (Beckman Coulter, CA, USA).

Measurement of viral titers

Lung samples for measurement of viral titer were mechanically homogenized using glass mortar and pestle in guanidine thiocyanate (GTC) immediately after collection of the organ and store at -80°C until the quantification of viral titers was performed. RNA was isolated from samples using phenol/chloroform extraction. The RNA was concentrated further using a mini-prep column. RNA to cDNA transcription was performed using RevertAid M-MuLV reverse transcriptase according to manufacturer instructions. Quantitative viral gene determination was performed using SYBR Green Master Mix on QuantStudio 6 Flex (Applied Biosystems, Life Technologies). Standard curve was prepared with known viral titers and used to quantify the viral load in lung tissue.

Statistical analysis

Statistically significant difference between conditions was assessed by one-way ANOVA followed by Tukey's multiple comparison test, two-way ANOVA followed by Sidak multiple comparisons test or two-tailed unpaired t-test. P-values lower than 0.05 were considered significant. Software used for statistical analysis was GraphPad Prism 9.3.1 for Windows (GraphPad Software, California, USA).

RESULTS

Intravenous prime-boost regime induces a potent antigen-specific CD8⁺ T cell response to a variety of peptide antigens

Table 1. Physicochemical characteristics of liposomal formulations. Data shown represents the average \pm standard deviation of at least two separate batches of formulation ($n \geq 2$).

Formulation	Z _{ave} (nm)	PDI	ζ-potential (mV)	LE% peptide
DSPC:DPTAP:CHOL:cdiGMP	178.1 \pm 2.68	0.11 \pm 0.031	33.25 \pm 2.53	-
DSPC:DPTAP:CHOL:cdiGMP:PA224	194.0 \pm 15.62	0.097 \pm 0.053	29.01 \pm 5.29	2.51
DSPC:DPTAP:CHOL:cdiGMP:NP366	223.1 \pm 8.75	0.064 \pm 0.024	27.90 \pm 1.18	8.12
DSPC:DPTAP:CHOL:cdiGMP:COVN361	218.0 \pm 16.26	0.085 \pm 0.056	32.39 \pm 0.68	4.97
DSPC:DPTAP:CHOL:cdiGMP:COVS1020	206.4 \pm 11.58	0.062 \pm 0.018	31.52 \pm 0.88	7.66
DSPC:DPTAP:CHOL:cdiGMP:COVN134	202.6 \pm 16.64	0.083 \pm 0.020	30.26 \pm 2.27	6.15
DSPC:DPTAP:CHOL:cdiGMP:COVS757	201.2 \pm 20.45	0.15 \pm 0.082	30.28 \pm 1.18	8.71
DSPC:DPTAP:CHOL:cdiGMP:COVN310	207.1 \pm 8.225	0.11 \pm 0.034	31.12 \pm 2.67	3.23

To study the capacity of the cationic liposomal formulations (physicochemical properties in Table 1) to induce virus-specific CD8⁺ T cell responses *in vivo*, we immunized mice with cationic liposomes loaded with a variety of different peptide antigens derived from SARS-CoV2 or H1N1 influenza. One week after prime immunization mice received a boost with a mix of antiCD40 antibody, c-di-GMP and free peptides, to expand potential low frequency responses¹⁹. We observed a strong CD8⁺ T cell response against the epitopes COVN361 and COVN134 from SARS-CoV2 in blood of vaccinated mice after prime-boost regime but only weak or no detectable responses against the other three antigens COVS1020, COVS757 and COVN310 (Figure 1C). In the case of mice immunized with cationic liposomes loaded with the influenza peptides PA224 and NP366, we observed a strong CD8⁺ T cell response against PA224 but only a minimal response for NP366 after prime immunization. Following boost immunization with antiCD40, c-di-GMP and free peptides, the PA224-specific CD8⁺ T cell response had massively expanded, however again the NP366-specific response in spleen of mice after prime and boost was close to undetectable (Figure 1D). Thus, this subunit vaccine formulation allows expansion of a selection of SARS-CoV2 and influenza specific CD8⁺ T cells.

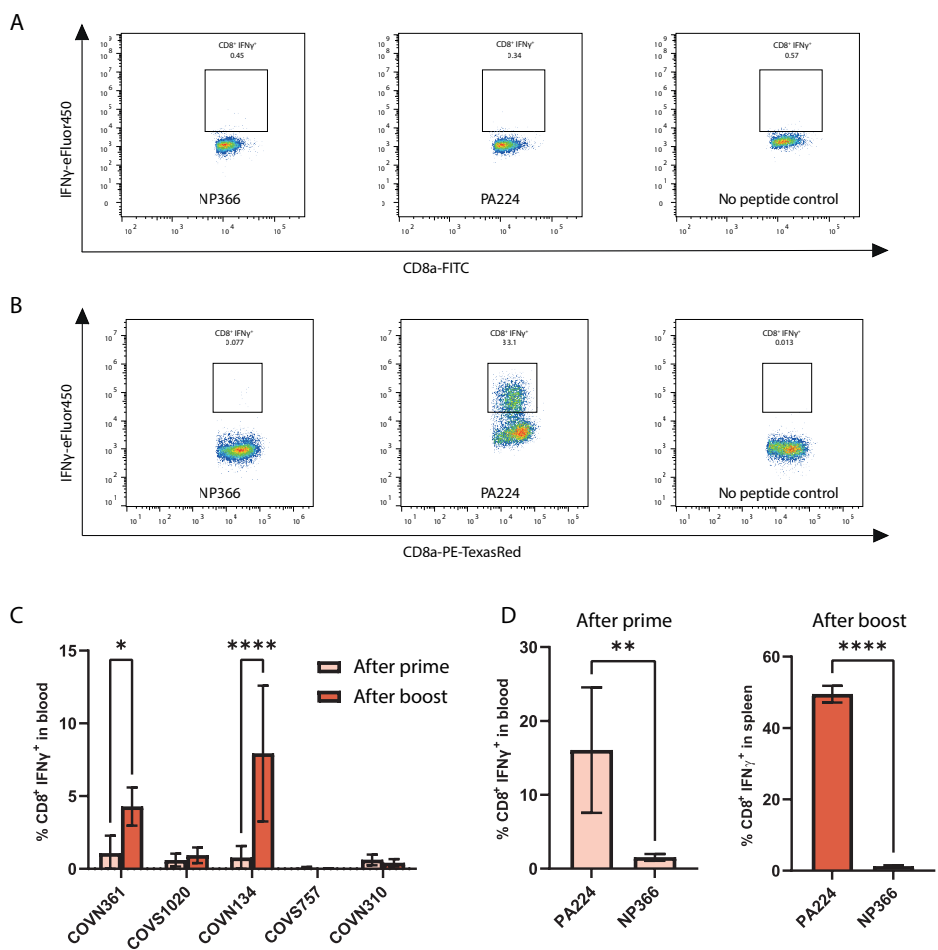


Figure 1. Immune responses after immunization with viral peptide-loaded cationic liposomes. (A) Representative flow cytometry plots of blood-derived CD8 $^{+}$ T cells after prime and before boost restimulated with NP366, PA224 or no peptide as control. (B) Representative flow cytometry plots of spleen-derived CD8 $^{+}$ T cells on day 27 after boost restimulated with NP366, PA224 or no peptide as control. (C) SARS-CoV2-specific CD8 $^{+}$ T cell response in blood after prime and after 27 days after boost with antiCD40, peptide and c-di-GMP. (D) Influenza-specific CD8 $^{+}$ T cell response in blood after prime and in spleen on day 30 after boost. * $p < 0.05$, ** $p < 0.01$, **** $p < 0.0001$ determined using (A) two-way ANOVA followed by Sidak multiple comparisons test or (B) two-tailed unpaired t-test.

Intravenous, intranasal and subcutaneous prime immunization followed by systemic boost induce a potent and long lasting CD8⁺ T cell response

As systemic intravenous (IV) administration is not a preferred administration route and does not lead to effective establishment of lung T_{rm} ²⁹, we next aimed to address whether the cationic subunit vaccine may induce antigen-specific CD8⁺ T cells response through local administration routes. We compared IV, intranasal (IN) and subcutaneous (SC) prime with c-di-GMP and PA224-loaded cationic liposomes. Control mice received empty liposomes intranasally. After prime immunization, all mice (including the control group) received an IV boost with antiCD40 antibody, c-di-GMP and PA224. After IV priming, only the IV and SC route induced detectable CD8⁺ T cell response in blood. Thirty days after boosting, all groups showed massive expansion of PA224-specific CD8⁺ T cells in the spleen (Figure 2B), lungs (Figure 2C) and lymph node (Figure 2D), revealing that the liposomal formulation is not restricted to IV use. Interestingly, the percentage of PA224-specific T cells expressing CD103 was significantly higher in the IN-immunized mice compared to SC or IV groups (Figure 2E), suggesting that a larger fraction of the cells are T_{rm} cells. As we have previously shown that IV boosting may expand the number of locally induced T_{rm} ³⁰, we evaluated the number of PA224-specific CD8⁺ T cells in the lung parenchyma after boosting, using the intravascular staining protocol to exclude CD8⁺ T cells in the capillary beds. Indeed, the percentage of lung-infiltrated CD8⁺ T cells was significantly higher in the IN prime group compared to systemic immunization (Figure 2F). Overall, this data indicates that an IN prime with cationic liposomes induces a systemic CD8⁺ T cell response and a local response in the lungs with characteristics of tissue-resident CD8⁺ T cells.

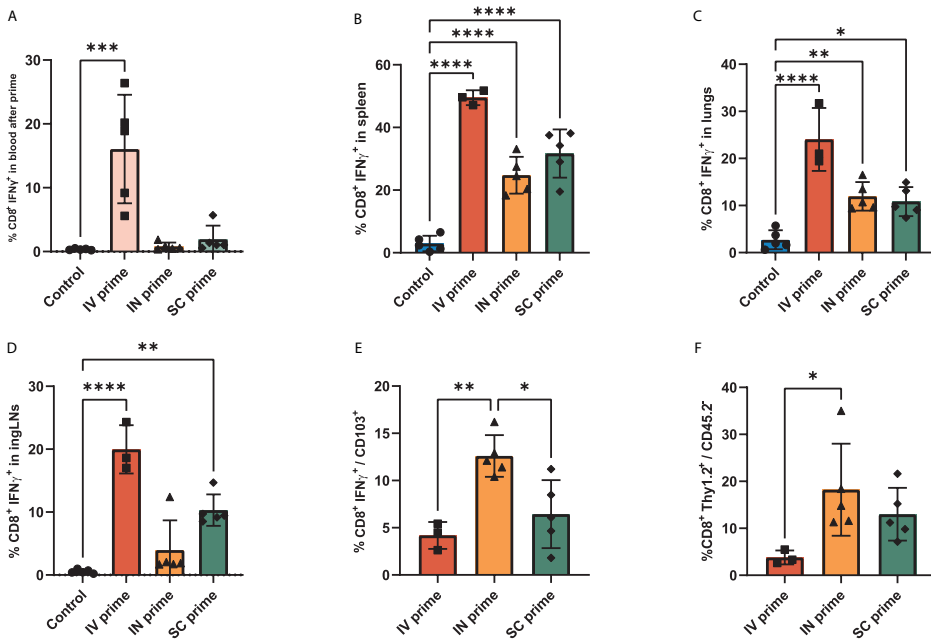


Figure 2. CD8⁺ T cell responses to PA224 after prime through different administration routes. (A) PA224-specific CD8⁺ T cell responses in blood after prime and before boost immunization. PA224-specific CD8⁺ T cell response in (B) spleen, (C) lungs and (D) inguinal lymph nodes on day 30 after boost. (E) PA224-specific CD8⁺ T cells expressing CD103 in lungs. (F) Lung-resident CD8⁺ T cells identified by lack of staining with antiCD45.2-APC administered IV shortly before sacrifice. * $p < 0.05$, ** $p < 0.01$, *** $p < 0.001$, **** $p < 0.0001$ determined using one-way ANOVA followed by Tukey's multiple comparison test.

Both heterologous and homologous prime-boost strategies induce strong CD8⁺ T cell responses

Although the antiCD40-based boost mix was able to induce a potent CD8⁺ T cell response, the use of monoclonal antibodies in prophylactic vaccines has several limitations in terms of cost, manufacture and side effects³¹. Therefore, we next compared the CD8⁺ T cell response elicited by this heterologous prime-boost regime versus a homologous prime-boost regime where both prime and boost consist of the cationic liposomal formulation. Control mice did not receive prime or boost immunizations. We observed that both immunization regimes were able to induce a potent PA224-specific CD8⁺ T cell response in both spleen (Figure 3A) and lungs (Figure 3B) after intranasal prime followed by intravenous boost, however higher variation in the response was observed in the liposome boost group (SD = 15.92) compared to the antiCD40 boost group (SD = 4.89). No significant differences

were found between the two prime-boost regimes in the frequency of CD103 in the PA224-specific CD8⁺ T cell population (Figure 3C). This data indicates that both homologous and heterologous prime-boost strategies induce similar CD8⁺ T cell responses systemically and locally in the lungs.

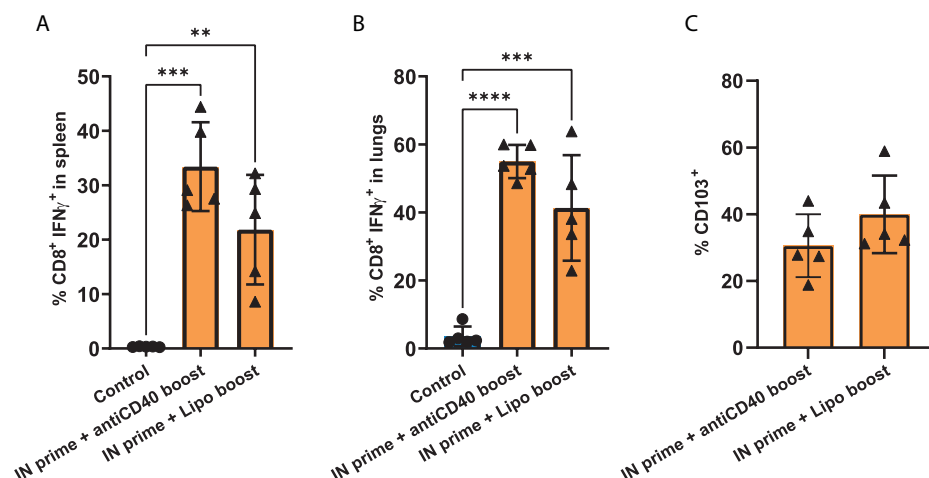


Figure 3. Comparison of boost immunization with either antiCD40 boost mix or cationic liposomes after intranasal prime. PA224-specific CD8⁺ T cell response in (A) spleen and (B) lungs on day 7 after boost. (C) Frequency of CD103 in PA224-specific (IFN γ ⁺) CD8⁺ T cells in the lungs. ** $p < 0.01$, *** $p < 0.001$, **** $p < 0.0001$ determined using one-way ANOVA followed by Tukey's multiple comparison test.

Response to intranasal immunization correlates with a reduction in lung viral titers upon Influenza infection

After confirming that the prime and boost immunizations with cationic liposomes was able to induce a systemic PA224-specific CD8⁺ T cell response, including a strong response in the lungs, we aimed to determine if these CD8⁺ T cells are able to reduce the viral load in the lungs after challenge with PR8 H1N1 virus. Mice received an IN prime immunization with either cationic liposomes loaded with c-di-GMP (control) or liposomes loaded with PA224 and c-di-GMP (vaccinated), followed by systemic boost with the same formulation 7 days later. On day 35 of the experiment (27 days after boost immunization), mice were challenged with a lethal dose of H1N1 PR8 (1000 TCID₅₀) and 4 days later they were sacrificed. The results from blood samples taken before (Figure 4A) and after (Figure 4B) boost confirm a significant increase in PA224-specific CD8⁺ T cells in the vaccinated group compared to control at 7 days after boost. Furthermore, the vaccinated group showed a strong PA224-specific CD8⁺ T cell response in the lungs (Figure 4C). The reduction in body weight

in all the mice confirmed that the infection was successful, with no significant differences in weight loss between groups (Figure 4D). Lung viral titers on day 4 after infection trended downward but were not significantly different between vaccinated and control groups, due to 3 non-responders in vaccinated group (Figure 4E). Viral titers however showed a clear negative correlation with the CD8⁺ T cell response elicited after booster immunization (Figure 4F).

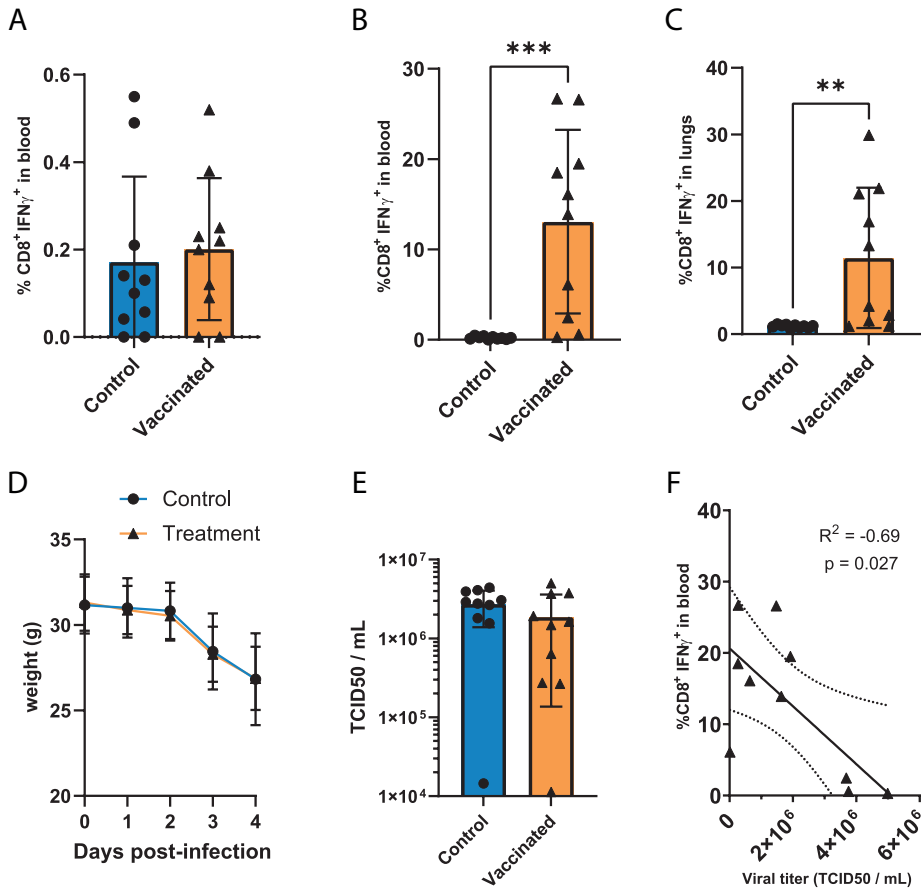


Figure 4. Challenge experiment. (A) CD8⁺ T cell response before and (B) after boost. (C) PA224-specific CD8⁺ T cell response in lungs. (D) Weight post infection. (E) Viral titers in lungs 4 days after infection and (F) correlation between lung viral titers and systemic CD8⁺ T cell response after boost. ** p < 0.01, *** p < 0.001 determined using one-way ANOVA followed by Tukey's multiple comparison test. Correlation p-value and r correlation coefficient determined using Person's correlation test.

Local CD8⁺ T cell response after intranasal immunization reduces viral burden upon influenza infection

To determine the role of the local and systemic influenza specific CD8⁺ T cell response in the viral burden reduction, we next compared the viral loads 4 days after infection in intranasally primed versus subcutaneously primed mice. Control mice were primed with intranasal PBS and boost IV with PBS. Mice primed subcutaneously showed a stronger systemic immune response both one week after boost (Figure 5A) and immediately before the infection (Figure 5B) compared to the intranasal group, suggesting the systemic PA224-specific memory CD8⁺ T cell response was larger in the SC versus the IN vaccinated mice. After infection animals in all groups lost a significant percentage of body weight (Figure 5C), indicating a successful viral infection. Interestingly, we observed a significant decrease in viral load in the group that received cationic liposomes intranasally compared to the control, but this protective effect was not observed in mice primed subcutaneously (Figure 5D). When comparing the viral load to the PA224-specific CD8⁺ T cell response elicited by the formulations in the IN group, we observed an inverse correlation (Figure 5E) while no correlation was present in the group immunized subcutaneously (Figure 5F). Thus, although the IN vaccination led to a smaller systemic virus-specific CD8⁺ T cell response, the induction of local T_{rm} appear to provide superior protection against H1N1 PR8 infection. Indeed, the bronchoalveolar lavage (BAL) fluid, which can be used as a proxy to study the inflammatory state of lungs upon infection³², showed change in the leukocyte composition. The cell composition of the BAL of immunized mice on day 4 after infection showed no differences between control and vaccinated mice in terms of granulocytes (Figure 6A) or monocytes/macrophages (Figure 6B). A significant increase in B cell content of in the SC prime group could be observed compared to both control and IN groups (Figure 6C). Similarly, the BAL showed an increase in lymphocytes in the SC group compared to control (Figure 6D). When looking at the two major T cell subsets, we observed an increase in CD4⁺ T cells in the IN group compared to SC primed mice (Figure 6E). Finally, both IN and SC groups showed significantly higher percentages of CD8⁺ T cells in the BAL compared to control (Figure 6F). Overall, this data shows that immunized mice present an enhanced recruitment of T cells to the lungs upon infection, with the response mainly driven by CD8⁺ T cells.

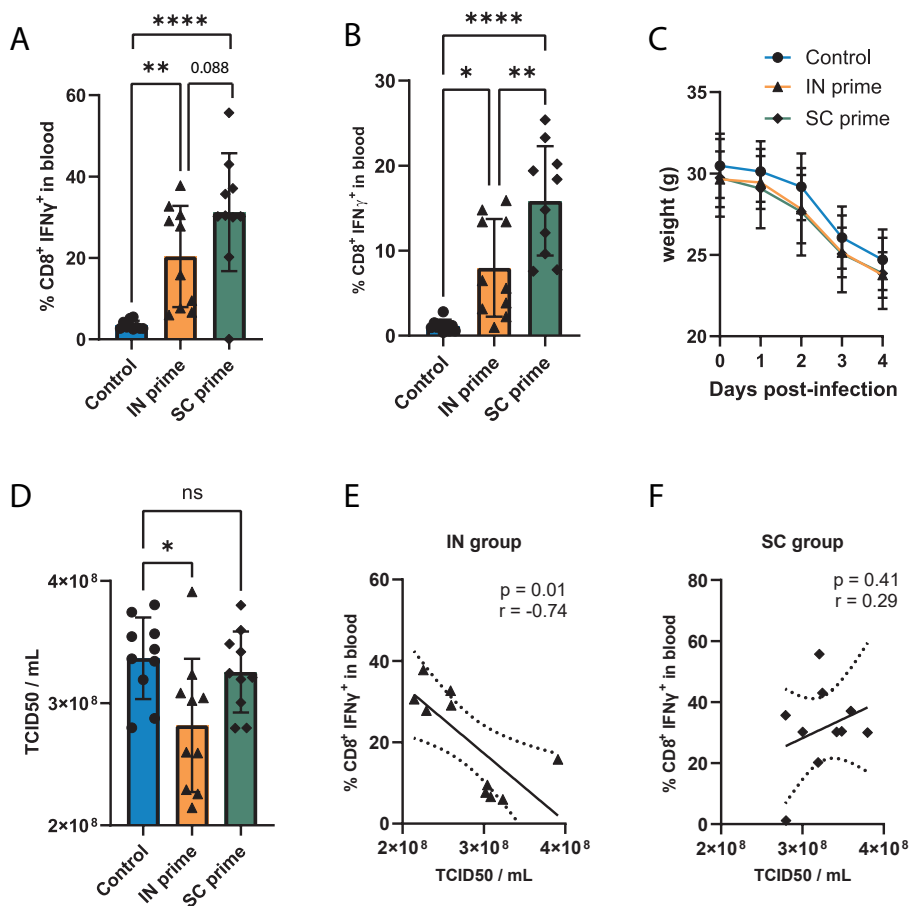


Figure 5. Viral challenge after intranasal and subcutaneous immunizations. PA224-specific CD8⁺ T cell responses in blood (A) on day 7 and (B) before infection on day 27 after boost. (C) Mice weight post infection. (D) Viral titers in lungs 4 days after infection. Correlation between lung viral titers and PA224-specific CD8⁺ T response after boost in (E) intranasal group and (F) subcutaneous group. * $p < 0.05$, ** $p < 0.01$, **** $p < 0.0001$ determined using one-way ANOVA followed by Tukey's multiple comparison test. P-value and r correlation coefficient determined using Person's correlation test.

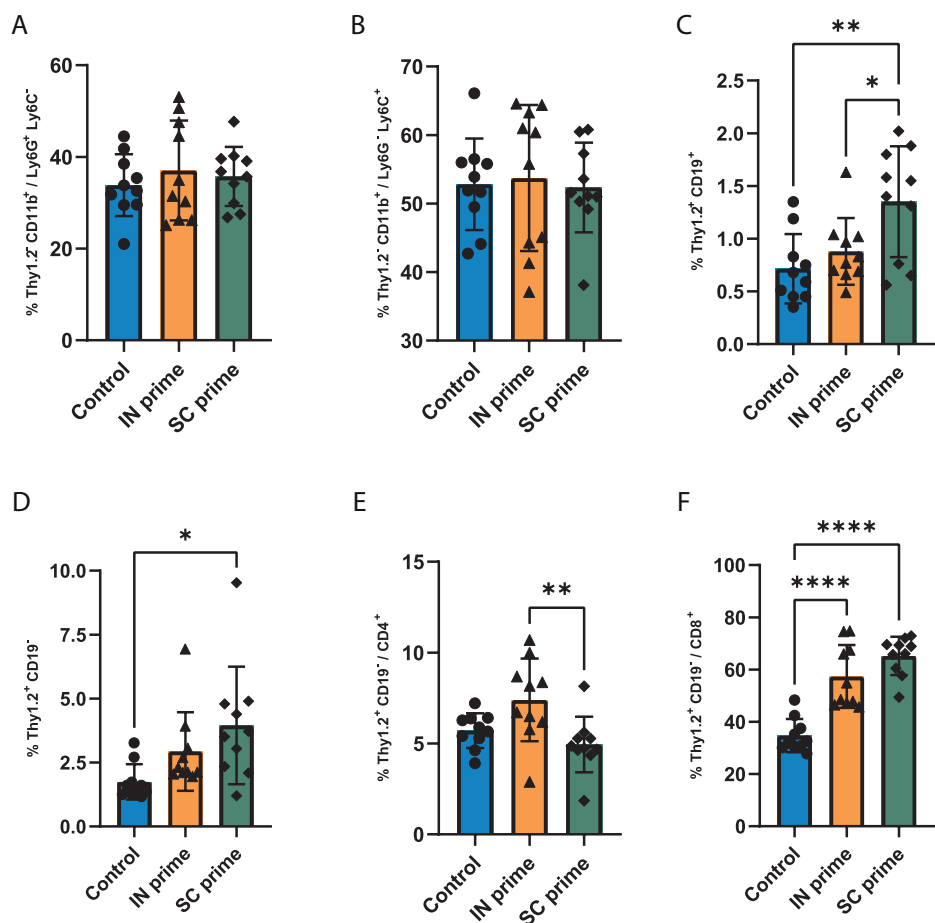


Figure 6. Cell composition of bronchoalveolar lavage (BAL) of immunized and control mice. Percentage of (A) granulocytes (Ly6G⁺ Ly6C⁻) and (B) monocytes (Ly6G⁻ Ly6C⁺) in the myeloid cell compartment in BAL. (C) Percentage of B cells. (D) Percentage of T cells in live cell population in BAL. Percentage of (E) CD4⁺ T cell subset and (F) CD8⁺ T cell subset within the T cell population. * p < 0.05, ** p < 0.01, **** p < 0.0001 determined using one-way ANOVA followed by Tukey's multiple comparison test.

DISCUSSION

Vaccine efficacy has traditionally been measured by the capacity to induce potent antibody responses, while the induction of cellular immunity has been a secondary goal. However, recent studies have highlighted the importance of T cell responses for long-lasting protection against viral infections^{3, 33}. The induction of cellular

immunity in addition to the antibody response could overcome the problem of virus variants that escape humoral immunity due to the high mutation rates of certain proteins such as hemagglutinin in Influenza virus³⁴. Cytotoxic CD8⁺ T cells are key players in anti-viral cellular immunity since they can directly kill infected cells. CD8⁺ T cells can recognize antigenic epitopes that are usually not accessible to antibodies, and they often target more conserved epitopes of the virus, such as those derived from the nucleoprotein or the virus polymerase³⁴. Furthermore, the generation of these immune responses locally in the respiratory tract, in the form of virus-specific T_{rm} responses, is crucial for protection and could reduce transmission of respiratory viruses like influenza and coronaviruses¹⁰. Cellular immunity can be achieved through vaccination with live attenuated vaccines, however the safer and easier to manufacture subunit vaccines are not so efficient at inducing T cell responses.

Here, we show that a subunit vaccine consisting of cationic liposomes loaded with c-di-GMP and a single-epitope antigen induces a potent, long-lasting and antigen-specific CD8⁺ T cell response both systemically and locally in the lungs against different antigen peptides derived from SARS-CoV2 and influenza. Furthermore, CD8⁺ T cells in the lungs of intranasally primed mice showed higher expression of CD103 (Figure 2F and 3C), a common marker of memory CD8⁺ T cells and we showed an increase in lung-resident CD8⁺ T cells in this group using intravascular CD45.2 staining (Figure 2E). While the generation of this type of cellular immunity often requires long intervals between prime and boost^{35, 36}, we show that this vaccine formulation can induce long-lasting memory CD8⁺ T cells after an accelerated prime-boost regime. Translated to humans, this rapid induction of a potent memory T cell response can have logistics advantages for prompt and efficient immunization against new pandemic virus strains of influenza or SARS-CoV2.

The lack of response against some of the peptides tested (Figure 1) indicates that the selection of appropriate viral epitopes during early stages of vaccine design is key. In this study, we compared two different epitopes from influenza virus, PA224 derived from the virus polymerase acidic protein, and NP366 derived from the viral nucleoprotein. Although T cell immunity in primary influenza infections in C57Bl/6 mice seems to be almost equally divided between NP366-specific CD8⁺ T cells and PA224-specific CD8⁺ T cells³⁷, in our experiments PA224 epitope induced stronger CD8⁺ T cell responses compared to NP366. Antigenic competition might explain the weak immune responses towards some of the SARS-CoV2 epitopes and previously reported immunogenic epitopes such as NP366³⁸. Future studies should take in to account this effect of antigenic competition for the selection of peptide antigens and the design of administration strategies³⁹.

In previous studies, a heterologous prime-boost regime where prime immunization consisted of cationic liposomes and boost was performed with agonistic antiCD40 monoclonal antibody mixed with antigens and adjuvants has proven to induce a strong CD8⁺ T cell response against tumour antigens⁴⁰. Here, we show that prime and boost can be performed with the same liposomal formulations leading to a comparable immune response (Figure 3). This could have advantages in terms of affordability of such vaccines for both viral infections and cancer since it circumvents the need to use costly monoclonal antibodies. Furthermore, side effects associated to antiCD40 antibodies, such as cytokine storm, could be acceptable in the context of anti-cancer therapies but not for prophylactic vaccination⁴¹. Future research should investigate the source of the increased variability on the elicited immune response when boost was performed with cationic liposomes in comparison to the agonistic antiCD40 boost mix and the formulation should be optimized further to reduce this variability.

We show that intranasal prime is key for this viral burden reduction (Figure 5D and 5E) since subcutaneously primed mice showed comparable viral titers to the control group despite the stronger systemic immune response in this group (Figure 5A and 5B). These results are in line with previous studies that have shown that CD8⁺ T cell responses induced by intranasal vaccination with non-replicating adjuvanted vaccine are protective against influenza infections, in contrast with the CD8⁺ T cell responses induced through subcutaneous immunization³⁵. The improved capacity of intranasally administered formulation to induce this lung-resident memory CD8⁺ T cells can lead to a faster response upon infection and a better control of the viral infection in the lungs.

Finally, the study of the cell composition of the bronchoalveolar lavage (BAL) of immunized and infected mice showed an increased recruitment of T cells to the lungs in all vaccinated mice compared to control (Figure 6). Infected mice immunized subcutaneously showed a better recruitment of B cells while intranasal prime had an increased recruitment of CD4⁺ T cells. Previous studies have shown that CD4⁺ T cells can act synergistically with CD8⁺ T cells to control influenza infections^{42, 43}, and perhaps contributed to the improved control of the infection in this group. Cationic liposomes have shown to be able to induce strong CD4⁺ T cell responses as well as CD8⁺ T cell responses²². Future research should study the delivery of both CD8⁺ and CD4⁺ T cell epitopes from influenza in cationic liposomes to induce a complete cellular immune response.

All in all, our work suggests that prime-boost vaccination strategies against respiratory viral infections could be more effective and powerful if the first immunization is administered intranasally.

CONCLUSION

Our study shows that intranasal immunization followed by a rapid systemic boost with a single-epitope liposomal subunit vaccine induces a potent CD8⁺ T cell response both systemically and locally in the lungs. The local CD8⁺ T cells elicited by vaccination expressed higher levels of CD103, associated to tissue-resident memory phenotype, and led to lower viral titers in lungs of influenza-infected mice compared to control.

AUTHOR CONTRIBUTIONS

FLV designed and carried out experiments, analysed the data, wrote the manuscript, and prepared the figures. DO performed experiments, analysed data, wrote and edited part of the manuscript. JAB and AK revised and edited the draft manuscript. BS and TCW conceptualised the project, provided input in the experimental design, revised, and edited the manuscript.

REFERENCES

1. Iuliano AD, Roguski KM, Chang HH, Muscatello DJ, Palekar R, Tempia S, et al. Estimates of global seasonal influenza-associated respiratory mortality: a modelling study. *Lancet*. 2018;391(10127):1285-300.
2. Pollard AJ, Bijker EM. A guide to vaccinology: from basic principles to new developments. *Nat Rev Immunol*. 2021;21(2):83-100.
3. Janssens Y, Joye J, Waerlop G, Clement F, Leroux-Roels G, Leroux-Roels I. The role of cell-mediated immunity against influenza and its implications for vaccine evaluation. *Front Immunol*. 2022;13:959379.
4. Sridhar S, Begom S, Bermingham A, Hoschler K, Adamson W, Carman W, et al. Cellular immune correlates of protection against symptomatic pandemic influenza. *Nat Med*. 2013;19(10):1305-12.
5. Rosendahl Huber S, van Beek J, de Jonge J, Luytjes W, van Baarle D. T cell responses to viral infections - opportunities for Peptide vaccination. *Front Immunol*. 2014;5:171.
6. Hu Y, Sneyd H, Dekant R, Wang J. Influenza A Virus Nucleoprotein: A Highly Conserved Multi-Functional Viral Protein as a Hot Antiviral Drug Target. *Curr Top Med Chem*. 2017;17(20):2271-85.
7. Mettelman RC, Allen EK, Thomas PG. Mucosal immune responses to infection and vaccination in the respiratory tract. *Immunity*. 2022;55(5):749-80.
8. Gould VMW, Francis JN, Anderson KJ, Georges B, Cope AV, Tregoning JS. Nasal IgA Provides Protection against Human Influenza Challenge in Volunteers with Low Serum Influenza Antibody Titre. *Front Microbiol*. 2017;8:900.
9. van Doremalen N, Lambe T, Spencer A, Belij-Rammerstorfer S, Purushotham JN, Port JR, et al. ChAdOx1 nCoV-19 vaccine prevents SARS-CoV-2 pneumonia in rhesus macaques. *Nature*. 2020;586(7830):578-82.
10. van Doremalen N, Purushotham JN, Schulz JE, Holbrook MG, Bushmaker T, Carmody A, et al. Intranasal ChAdOx1 nCoV-19/AZD1222 vaccination reduces viral shedding after SARS-CoV-2 D614G challenge in preclinical models. *Sci Transl Med*. 2021;13(607).
11. Burchill MA, Tamburini BA, Pennock ND, White JT, Kurche JS, Kedl RM. T cell vaccinology: exploring the known unknowns. *Vaccine*. 2013;31(2):297-305.
12. Rubin LG, Levin MJ, Ljungman P, Davies EG, Avery R, Tomblyn M, et al. 2013 IDSA clinical practice guideline for vaccination of the immunocompromised host. *Clin Infect Dis*. 2014;58(3):e44-100.
13. Nakamura T, Miyabe H, Hyodo M, Sato Y, Hayakawa Y, Harashima H. Liposomes loaded with a STING pathway ligand, cyclic di-GMP, enhance cancer immunotherapy against metastatic melanoma. *J Control Release*. 2015;216:149-57.
14. Karaolis DK, Means TK, Yang D, Takahashi M, Yoshimura T, Muraille E, et al. Bacterial c-di-GMP is an immunostimulatory molecule. *J Immunol*. 2007;178(4):2171-81.
15. Varypataki EM, Benne N, Bouwstra J, Jiskoot W, Ossendorp F. Efficient Eradication of Established Tumors in Mice with Cationic Liposome-Based Synthetic Long-Peptide Vaccines. *Cancer Immunol Res*. 2017;5(3):222-33.
16. Leal J, Smyth HDC, Ghosh D. Physicochemical properties of mucus and their impact on transmucosal drug delivery. *Int J Pharm*. 2017;532(1):555-72.

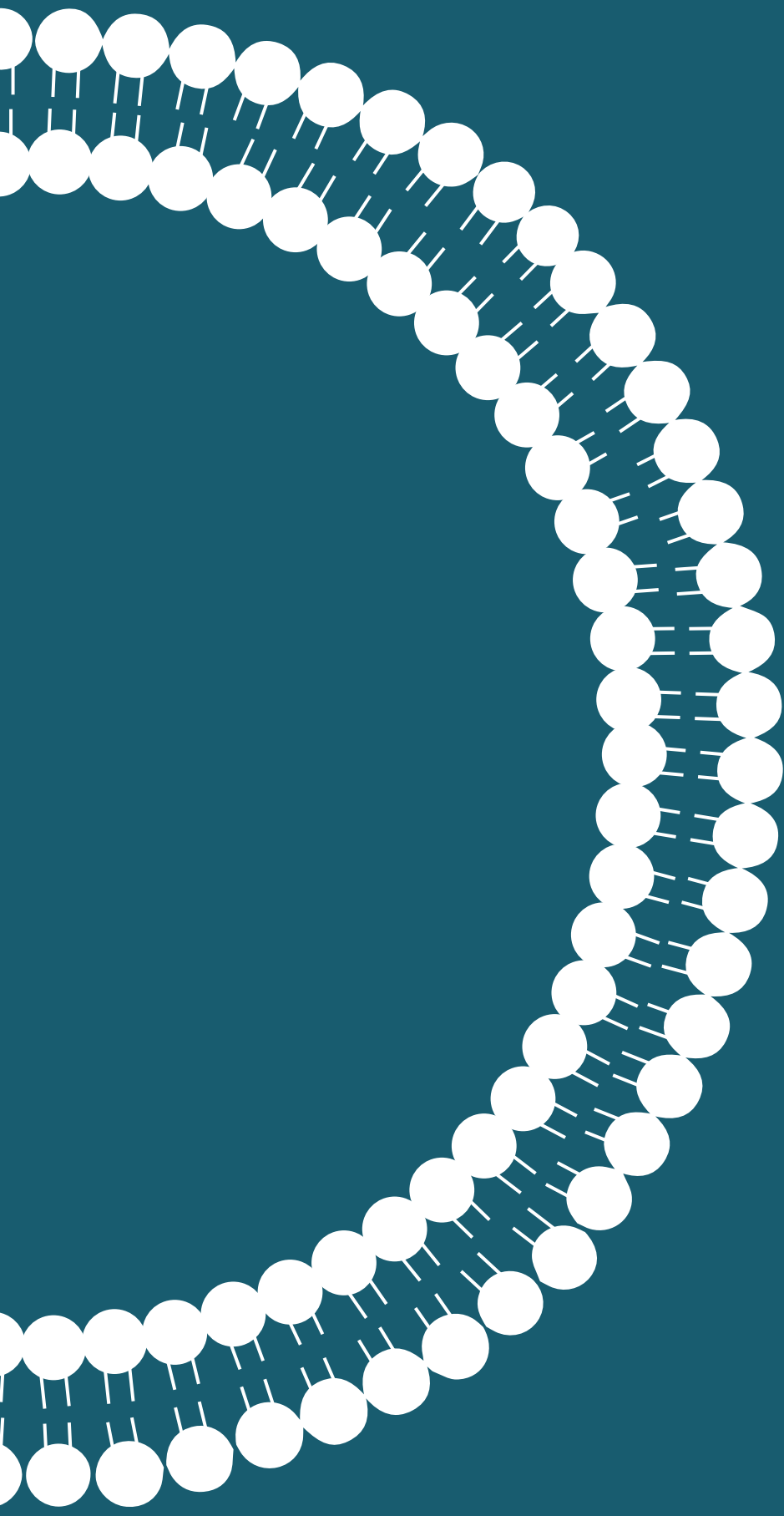
17. Varma DM, Batty CJ, Stiepel RT, Graham-Gurysh EG, Roque JA, 3rd, Pena ES, et al. Development of an Intranasal Gel for the Delivery of a Broadly Acting Subunit Influenza Vaccine. *ACS Biomater Sci Eng*. 2022;8(4):1573-82.
18. Slutten B, Pewe LL, Lauer P, Harty JT. Cutting edge: rapid boosting of cross-reactive memory CD8 T cells broadens the protective capacity of the Flumist vaccine. *J Immunol*. 2013;190(8):3854-8.
19. Pham NL, Pewe LL, Fleenor CJ, Langlois RA, Legge KL, Badovinac VP, Harty JT. Exploiting cross-priming to generate protective CD8 T-cell immunity rapidly. *Proc Natl Acad Sci U S A*. 2010;107(27):12198-203.
20. Budimir N, Meijerhof T, Wilschut J, Huckriede A, de Haan A. The role of membrane fusion activity of a whole inactivated influenza virus vaccine in (re)activation of influenza-specific cytotoxic T lymphocytes. *Vaccine*. 2010;28(52):8280-7.
21. Ahmed SF, Quadeer AA, McKay MR. Preliminary Identification of Potential Vaccine Targets for the COVID-19 Coronavirus (SARS-CoV-2) Based on SARS-CoV Immunological Studies. *Viruses*. 2020;12(3).
22. Benne N, van Duijn J, Lozano Vigario F, Lebox RJT, van Veelen P, Kuiper J, et al. Anionic 1,2-distearoyl-sn-glycero-3-phosphoglycerol (DSPG) liposomes induce antigen-specific regulatory T cells and prevent atherosclerosis in mice. *J Control Release*. 2018;291:135-46.
23. Badovinac VP, Messingham KA, Jabbari A, Haring JS, Harty JT. Accelerated CD8+ T-cell memory and prime-boost response after dendritic-cell vaccination. *Nat Med*. 2005;11(7):748-56.
24. Badovinac VP, Harty JT. Intracellular staining for TNF and IFN-gamma detects different frequencies of antigen-specific CD8(+) T cells. *J Immunol Methods*. 2000;238(1-2):107-17.
25. van Eenige R, Verhave PS, Koemans PJ, Tiebosch I, Rensen PCN, Kooijman S. RandoMice, a novel, user-friendly randomization tool in animal research. *PLoS One*. 2020;15(8):e0237096.
26. Belz GT, Xie W, Altman JD, Doherty PC. A previously unrecognized H-2D(b)-restricted peptide prominent in the primary influenza A virus-specific CD8(+) T-cell response is much less apparent following secondary challenge. *J Virol*. 2000;74(8):3486-93.
27. Townsend AR, Rothbard J, Gotch FM, Bahadur G, Wraith D, McMichael AJ. The epitopes of influenza nucleoprotein recognized by cytotoxic T lymphocytes can be defined with short synthetic peptides. *Cell*. 1986;44(6):959-68.
28. Anderson KG, Mayer-Barber K, Sung H, Beura L, James BR, Taylor JJ, et al. Intravascular staining for discrimination of vascular and tissue leukocytes. *Nat Protoc*. 2014;9(1):209-22.
29. Rotrosen E, Kupper TS. Assessing the generation of tissue resident memory T cells by vaccines. *Nat Rev Immunol*. 2023;23(10):655-65.
30. Slutten B, Van Braeckel-Budimir N, Abboud G, Varga SM, Salek-Ardakani S, Harty JT. Dynamics of influenza-induced lung-resident memory T cells underlie waning heterosubtypic immunity. *Sci Immunol*. 2017;2(7).
31. Chung C, Kudchodkar SB, Chung CN, Park YK, Xu Z, Pardi N, et al. Expanding the Reach of Monoclonal Antibodies: A Review of Synthetic Nucleic Acid Delivery in Immunotherapy. *Antibodies (Basel)*. 2023;12(3).
32. Van Hoecke L, Job ER, Saelens X, Roose K. Bronchoalveolar Lavage of Murine Lungs to Analyze Inflammatory Cell Infiltration. *J Vis Exp*. 2017(123).

33. Naranbhai V, Nathan A, Kaseke C, Berrios C, Khatri A, Choi S, et al. T cell reactivity to the SARS-CoV-2 Omicron variant is preserved in most but not all individuals. *Cell*. 2022;185(6):1041-51 e6.
34. Koutsakos M, Illing PT, Nguyen THO, Mifsud NA, Crawford JC, Rizzetto S, et al. Human CD8(+) T cell cross-reactivity across influenza A, B and C viruses. *Nat Immunol*. 2019;20(5):613-25.
35. Gasper DJ, Neldner B, Plisch EH, Rustom H, Carrow E, Imai H, et al. Effective Respiratory CD8 T-Cell Immunity to Influenza Virus Induced by Intranasal Carbomer-Lecithin-Adjuvanted Non-replicating Vaccines. *PLoS Pathog*. 2016;12(12):e1006064.
36. Natalini A, Simonetti S, Favaretto G, Lucantonio L, Peruzzi G, Munoz-Ruiz M, et al. Improved memory CD8 T cell response to delayed vaccine boost is associated with a distinct molecular signature. *Front Immunol*. 2023;14:1043631.
37. Crowe SR, Turner SJ, Miller SC, Roberts AD, Rappolo RA, Doherty PC, et al. Differential antigen presentation regulates the changing patterns of CD8+ T cell immunodominance in primary and secondary influenza virus infections. *J Exp Med*. 2003;198(3):399-410.
38. Kallas EG, Grunenberg NA, Yu C, Manso B, Pantaleo G, Casapia M, et al. Antigenic competition in CD4(+) T cell responses in a randomized, multicenter, double-blind clinical HIV vaccine trial. *Sci Transl Med*. 2019;11(519).
39. Blobel NJ, Ramirez-Valdez A, Ishizuka AS, Lynn GM, Seder RA. Antigenic competition affects the magnitude and breadth of CD8 T cell immunity following immunization with a nanoparticle neoantigen cancer vaccine. *The Journal of Immunology*. 2017;198(1_Supplement):73.20-73.20.
40. Benne N. Vaccination and targeted therapy using liposomes : opportunities for treatment of atherosclerosis and cancer. The Netherlands: Leiden University; 2020.
41. Salomon R, Dahan R. Next Generation CD40 Agonistic Antibodies for Cancer Immunotherapy. *Front Immunol*. 2022;13:940674.
42. McKinstry KK, Strutt TM, Kuang Y, Brown DM, Sell S, Dutton RW, Swain SL. Memory CD4+ T cells protect against influenza through multiple synergizing mechanisms. *J Clin Invest*. 2012;122(8):2847-56.
43. Belz GT, Wodarz D, Diaz G, Nowak MA, Doherty PC. Compromised influenza virus-specific CD8(+)-T-cell memory in CD4(+)-T-cell-deficient mice. *J Virol*. 2002;76(23):12388-93.

SUPPLEMENTARY DATA

Supplementary Table 1. Details of SARS-CoV2-derived peptides loaded into cationic liposomes and used for in vivo screening. Binding affinity to HLA-A*11:01 predicted using NETMHCpan4.0

Peptide name	Amino acid sequence	Predicted binding affinity to HLA-A*11:01 (nM)	Protein	Protein accession number and position
COVN361	KTFPPTEPK	7.7	Nucleoprotein	P0DTC9 [361-369]
COVS1020	ASANLAATK	12.3	Spike	P0DTC2 [1020-1028]
COVN134	ATEGALNTPK	27.5	Nucleoprotein	P0DTC9 [134-143]
COVS757	GSFCTQLNR	44.4	Spike	P0DTC2 [757-765]
COVN310	SASAFFGMSR	30.9	Nucleoprotein	P0DTC9 [310-319]



Chapter 8

General summary and future perspectives

GENERAL SUMMARY

The immune system is a set of organs, cells and molecules that defend the organism against pathogens or substances recognized as foreign. It can be broadly divided in two arms, the innate and the adaptive immunity. The innate immunity is the first line of defence against an infection, it is rapidly mounted, but it is not antigen-specific and it cannot generate immunological memory. The adaptive immunity, on the other hand, needs more time to develop since it requires the clonal expansion of antigen-specific immune cells but it can generate immunological memory that will rapidly mount a secondary immune response upon reinfection with the same pathogen. Antigen-presenting cells (APCs) are the connection between innate and adaptive immunity, since they can capture antigens, process them, and present them in their cell surface to cells from the adaptive immune system such as T cells, initiating the adaptive immune response¹. An over or under activation of the immune system is the root of many diseases. In autoimmune diseases, the natural tolerance towards self-antigens is broken, leading for example to the destruction of β cells in type 1 diabetes (T1D) or the myelin sheath of neurons in multiple sclerosis (MS)^{2,3}. Not only in autoimmune diseases, but also in other highly prevalent diseases, such as atherosclerosis, the main underlying cause of cardiovascular diseases, the inflammatory response triggered against self-antigens seems to be involved in the aetiology of the disease⁴. In other cases, the immune system can fail to mount a sufficient immune response against a pathogen leading to widespread infection that can cause the host's death. In this thesis, we show that liposomes, a versatile type of nanoparticle, can be applied to restore immune tolerance in autoimmune diseases and to activate antigen-specific protective immune responses against infections.

Nanoparticles can be used as delivery systems for both small molecules and macromolecules such as proteins, peptides or oligonucleotides. The majority of this thesis focuses on the use of liposomes, nanometric vesicles formed by a phospholipid bilayer enclosing an aqueous core. Liposomes are highly versatile delivery systems since they can transport both hydrophobic and hydrophilic cargo loaded in the phospholipid bilayer or in the aqueous core, respectively. Furthermore, fine-tuning their physicochemical properties such as size, shape, rigidity or surface charge (ζ -potential) allows the control of the liposome's biodistribution and biological effect⁵. Among the different applications for liposomes, antigen delivery is especially interesting. Liposomes can protect antigens from proteolytic degradation, and they can direct the antigen delivery to specialized cells such as APCs⁶. Furthermore, the co-delivery of antigens and molecules with adjuvant capacity allows the modulation of immune responses. Liposomes can transport cargo to APCs, such as dendritic cells (DCs), by taking advantage of the intrinsic high endocytic capacity of these

cells⁷. The type of antigen presentation by DCs determines the type of adaptive immune response. For example, the presentation of antigens in the context of a high expression of co-stimulatory molecules such as CD86, CD80 or CD40 and pro-inflammatory cytokines will skew the immune response towards a pro-inflammatory response mediated by Th1 or Th17 lymphocytes, necessary to fight viral and bacterial infections⁸. On the other hand, the presentation of antigens by DCs in the context of low levels of co-stimulatory molecules and high levels of anti-inflammatory cytokines will induce a tolerogenic responses mostly mediated by T regulatory cells (Tregs)⁹. The use of nanoparticles for the co-delivery of antigens and molecules that modulate the expression of co-stimulatory signals is therefore a promising strategy to apply in conventional prophylactic vaccines and tolerogenic vaccines to restore immune homeostasis in autoimmune diseases.

Although lipid nanoparticles have been widely and successfully used in the SARS-CoV2 vaccines against the COVID-19 pandemic, there are still many unknowns that prevent nanoparticle-based therapies and vaccines to realise their full potential. In this thesis, we try to shed light to some of the gaps in knowledge in the field. On one hand, there is still limited knowledge on the precise contribution of the different physicochemical properties of nanoparticles to the elicited immune response. This is particularly challenging to study in the case of liposomes where altering the lipid composition will likely lead to changes in several physicochemical and biological properties of the nanoparticle such as ζ -potential, rigidity and protein corona. Furthermore, although there have been significant advances in the last few years in the mass production of liposomes and lipid nanoparticles, certain formulations are still challenging to produce in a high-throughput manner. For instance, liposomes containing phospholipids with high transition temperatures such as DSPG. The high rigidity and negative charge of DSPG-containing liposomes are key for the induction of Treg responses by tolerogenic vaccines as previously shown¹⁰. Finally, in the case of tolerogenic vaccines, a key challenge to overcome is the need to precisely characterize the antigens and epitopes driving autoimmunity. This is specially challenging in diseases that are not classical autoimmune diseases, such as atherosclerosis, where the immune response towards self-antigens is one of the factors contributing to the disease's progression, together with genetic and environmental factors^{4, 11, 12}.

In **Chapter 2**, we review tolerogenic strategies against prevalent autoimmune diseases such as multiple sclerosis (MS) and type 1 diabetes (T1D). We summarize the lessons that can be learned from the efforts to bring these therapeutic approaches to the clinic and the challenges to apply tolerogenic therapies to atherosclerosis, one of the most prevalent chronic diseases in the western world¹³. Atherosclerosis is an inflammatory disease of the arteries, characterized by the

infiltration and accumulation of low-density lipoproteins (LDL) in the subendothelial space of the arteries, forming atherosclerosis plaques. The accumulation of LDL particles also triggers the recruitment of immune cells to the incipient lesion, initiating an inflammatory response that leads to further growth of the plaque¹⁴. These plaques can restrict blood flow to certain parts of the body or rupture generating a thrombus, which leads to the most common clinical manifestation of atherosclerosis in the form of myocardial infarction or stroke. Several lines of evidence highlight the importance of autoimmunity in the development of atherosclerosis. On one hand, the presence of auto-reactive B and T cells and circulating antibodies against LDL demonstrates that the immune response in atherosclerosis is, at least in part, directed towards self-antigens^{15, 16}. Furthermore, there is a clear correlation between atherosclerosis and classical autoimmune diseases, such as rheumatoid arthritis (RA), with RA patients having a significantly higher risk of suffering a cardiovascular event^{4, 17}. Finally, the opportunity to target the immune component of atherosclerosis as a therapeutic strategy is evidenced by the significant residual cardiovascular risk of patients after intensive statin therapy, mostly associated with higher levels of inflammatory markers¹⁸. Clinical trials, such as the CANTOS or COLCOT trials, have shown that systemic immune suppression can significantly reduce the incidence of cardiovascular events, but at the expense of higher risk of fatal infections^{19, 20}. Therefore, the side effects of chronic immune suppression would hardly be acceptable for the prevention of cardiovascular events. The induction of antigen-specific immune tolerance, mediated by Tregs, would be a better approach and it has been studied in clinical trials against RA, T1D and MS. In these diseases, both cell-based and peptide-based strategies have been used in clinical trials and have proven to be generally safe and well-tolerated. The use of cell-based approaches involves the *ex vivo* differentiation of DCs into tolerogenic DCs and the coating to the cells with the target antigens. The costs associated with the manufacture of these tolerogenic DCs has often limited the number of patients enrolled in the trials and therefore the power of the safety and efficacy conclusions²¹. The peptide-based approaches have shown promising results in RA, T1D and MS²²⁻²⁴, however in some cases the efficacy was limited to subgroup of patients with specific HLA types, as seen in a phase II trial with MS patients²². The use of cocktails of peptides instead of single peptides has shown better results²⁵. The careful selection of the peptide dose is important since too high doses can lead to unwanted pro-inflammatory T cell activation, therefore these clinical trials often include a dose escalation period²⁵. Finally, the administration route also plays a key role for peptide-based tolerance induction, with mucosal and intradermal routes showing the best results^{24, 26}. In summary, antigen-specific

tolerogenic therapies have shown to be safe but their effectiveness depends on the careful choice of the target antigen(s), dose and administration route.

A key knowledge gap that differentiates autoimmune diseases like MS and T1D from atherosclerosis is that while autoimmune responses against myelin and β cells proteins are clearly characterized, the antigens driving pro-atherogenic immune responses are far less established. The study of antigen-specific immune responses in atherosclerosis is essential for the development of tolerogenic vaccines against the disease. In **chapter 3**, we aim to shed light on this using an immunopeptidomics approach. Previous studies have made use of *in silico* analysis of candidate proteins such as ApoB100 to scan the amino acid sequence of the protein and determine potential good binders to HLA molecules^{27, 28}. In this chapter, we use immunopeptidomics to isolate and identify peptides presented by HLA class II molecules directly from atherosclerosis plaques of patients undergoing endarterectomy surgery. We identified 20 epitopes derived from ApoB100, the main protein in LDL particles. Using the expression of the T cell activation marker CD40L as a proxy, we show that a subset of 22% of atherosclerosis patients have detectable levels of CD4⁺ T cells that respond to these epitopes. Interestingly, the level of CD4⁺ T cell response in this subset of patients correlated positively with histologically determined plaque vulnerability. Future studies should investigate the use of these ApoB100-specific CD4⁺ T cell responses as biomarkers of atherosclerosis progression. Further characterization of this CD4⁺ T cell response showed that upon peptide stimulation, these cells produce IL-17 and IL-10, but also other cytokines such as IL-5, IL-9 or IL-6, suggesting that the ApoB100-specific T cell population does not present a unique phenotype. These findings are in line with previous studies showing that the ApoB100-specific T cell response in atherosclerosis evolves from a Treg mediated response towards a pathogenic Th1/Th17 phenotype in advanced stages of the disease²⁹. Restoring the immunological balance by inducing ApoB100-specific Tregs or preventing Th1/Th17 polarization using tolerogenic nanoparticles loaded with the epitopes identified here is a promising therapeutic strategy that should be explored further.

Besides the definition of the target antigens, the delivery system needs to be optimized for tolerance induction in human. Previous studies have shown that liposomes composed of DSPC:DSPG:Cholesterol are good candidates for this task and have shown promising results in animal models¹⁰. However, the first studies with this formulation in an *in vitro* human system did not recapitulate the tolerogenic properties seen in mice³⁰. In **chapter 4**, we show that the translation from pre-clinical models to patients might require the presence of a tolerogenic molecule such as 1 α ,25-dihydroxyvitaminD3 (vitaminD3). Liposomes loaded with vitaminD3 were able to induce a tolerogenic phenotype *in vitro* in human monocyte-derived DCs. This

tolerogenic phenotype was characterized by the expression of ILT3 and a lower expression of the co-stimulatory molecule CD83. Furthermore, these tolerogenic DCs were able to induce FoxP3⁺ CD25⁺ Tregs that also expressed high levels of CTLA-4 and TIGIT. The anionic DSPG liposomes loaded with vitaminD3 were also able to induce IL10-producing Tregs, an anti-inflammatory cytokine essential for the immunomodulatory function of Tregs. This is in line with mouse studies showing that anionic liposomes are better internalized by APCs and have better tolerogenic capacity than cationic liposomes³⁰. Most importantly, these tolerogenic DCs inhibited the polarization of T cells towards the pro-inflammatory subsets Th1 and Th17. In a further step towards the translation of these tolerogenic formulations to human, we studied the intradermal administration of vitaminD3-loaded liposomes in *ex vivo* human skin. We observed a selective migration of CD14⁺ dermal DCs, that have previously shown to be able to induce Tregs³¹. All in all, in this chapter we show that upon inclusion of vitaminD3, anionic liposomes can induce tolerogenic immune responses not only in animal models but also in human *in vitro* and *ex vivo* setups. The next steps in the clinical translation of peptide-based liposome vaccines will require the evaluation of antigen-specific T cell responses in *ex vivo* human models such as the intradermal skin injections shown in this chapter.

After showing in chapter 4 that DSPC:DSPG:Cholesterol liposomes incorporating vitaminD3 have potential applicability in humans, in **chapter 5** we aim to tackle the problem of the manufacturing of these formulations. Traditional lab-scale methods for the preparation of liposomes, such as the lipid film hydration method, have little upscale potential. In short, this method starts with the creation of a dry lipid film by evaporating the organic solvent in a rotary evaporator followed by hydration of the dry lipid film with an aqueous solvent that contains the antigen to be encapsulated³². The process often involves a freeze-drying step after the hydration of the lipid film to increase the loading efficiency of the antigen. The hydration step generates a suspension of large multilamellar vesicles that needs to be extruded through multiple filters at high pressure until the desired particle size is achieved. Furthermore, the extrusion process needs to occur at a temperature above the transition temperature of the phospholipids, which in the case of DSPC:DSPG:Cholesterol liposomes is 55°C. This process is labour intensive, involves multiple steps and it has high energy requirements, making very difficult the production of large batches of formulations necessary for the clinical development of these nanoparticles. The production of liposomes using microfluidics is a one-step process that does not require solvent evaporation or extrusion. There are commercially available systems such as the NanoAssemblr® platform from Precision Nanosystems, but this equipment can be expensive, microfluidics cartridges are not reusable, and the temperature control is not optimal. Therefore, in chapter 5 we propose the use of a reusable and off-the-

shelf glass herringbone micromixer for the preparation of DSPC:DSPG:Cholesterol liposomes. The formation of liposomes in this system is dominated by the controlled mix of an organic solvent containing phospholipids and an aqueous solvent containing the antigen to load³³. The micromixer can be fully submerged in a temperature-controlled water bath, ensuring the desired temperature in the mixing channel. Using this system, we show that the average particle size of the liposomes can be fine-tuned by changing the flow rate ratio (FRR) between organic and aqueous solvents and that peptides with a wide range of charge and hydrophobicity can be encapsulated. Furthermore, we show that the encapsulation efficiency of the tolerogenic adjuvant vitaminD3 in DSPC:DSPG:Cholesterol liposomes was substantially increased in the formulations prepared with microfluidics compared to the conventional lipid film hydration method. The biologically active form of vitaminD3 is costly therefore the increase in encapsulation efficiency presents a significant advantage. The manufacture of DSPC:DSPG:Cholesterol liposomes using microfluidics facilitates the production of these formulations under Good Manufacturing Practice (GMP) conditions³⁴, a pre-requirement for moving these tolerogenic nanoparticles closer to the clinic. Future development of the technology should focus on the use of scalable and in-line methods for the down-stream processing of formulations, for example using tangential flow filtration to separate the liposomes from the non-encapsulated peptides and adjuvants.

Besides the inclusion of tolerogenic molecules, such as vitaminD3, previous research has shown that nanoparticle rigidity is a key physicochemical parameter that determines the tolerogenic capacity of liposomes. For instance, highly rigid liposomes composed of DSPC:DSPG:Cholesterol have shown to have better capacity to induce Tregs compared to liposomes with a more fluid membrane like DOPC:DOPG³⁵. The level of unsaturation of the phospholipids' acyl chains and the presence of cholesterol in the bilayer are the main determinants of liposome rigidity³⁶. However, the lipid composition of the bilayer can also affect other properties of the nanoparticle such as the protein corona, the set of proteins that interact with the liposome surface in a biological fluid³⁷. In **chapter 6**, we use a hybrid nanoparticle consisting of a PLGA particle covered with a DOPC:DOPG lipid bilayer (DOPG/PLGA hybrids) in order to obtain a highly rigid nanoparticle but with fluid lipid bilayer. We show that while these particles can deliver the antigen to APCs and induce Treg responses *in vitro*, they fail to replicate the same effect *in vivo*. The DOPG/PLGA hybrid nanoparticles were not able to induce antigen-specific T cell proliferation *in vivo* while the DSPC:DSPG:Cholesterol liposomes induced significant T cell expansion. Furthermore, although previous studies have shown the capacity of rigid anionic liposomes to arrest the development of atherosclerosis in mice¹⁰, these hybrid particles did not have any effect on atherosclerosis progression

or plaque composition, nor did they induce antigen-specific T cell responses in this context. We hypothesized that the *in vivo* behaviour of these lipid nanoparticles may be more influenced by the protein corona than by the particle rigidity. The changes in average particle size, polydispersity index (Pdl) and surface charge (ζ -potential) of the formulations after incubation with mouse serum or foetal bovine serum confirm the formation of a protein corona when in a biological medium. Furthermore, the coating of the nanoparticles with proteins that have been previously reported to play a role in nanoparticle uptake, such as ApoE³⁸, ApoB100³⁹ or C1q¹⁰, revealed that ApoB100 might drive cell uptake in formulations with a DOPC:DOPG lipid bilayer, regardless of their rigidity, while the complement protein C1q is the main mediator of uptake for DSPC:DSPG:Cholesterol liposomes as previously reported¹⁰. The presence of cholesterol in the lipid bilayer is another important difference between the formulations studied here, therefore follow up studies should address the role of cholesterol in the formation and composition of the protein corona and how it influences the tolerogenic properties of lipid nanoparticles. This chapter highlights the complexity of assigning specific physicochemical properties of nanoparticles to a certain biological effect, since changes in the phospholipid composition affects nanoparticle rigidity but also determines the composition of the protein corona. Future studies should follow a comprehensive approach to determine the effect of small changes in phospholipid composition in both physicochemical properties of the nanoparticle, the protein corona composition and their biological effect. The large number of parameters to consider and the interaction between them might require the use of more sophisticated statistical methods, such as Design of Experiments (DoE), that allow the study of multiple parameters and their interactions in a time-efficient manner⁴⁰.

In **chapter 7** of this thesis, we focus on the other main application of liposome-based vaccines, the induction of protective immune responses against viruses. In the field of vaccines against respiratory viruses such as coronavirus and influenza, there is a need for subunit vaccines that can induce cellular immune responses locally in the lungs. Cationic liposomes have been studied before for their immune activating properties⁴¹ and these delivery systems present advantages for intranasal vaccination since the electrostatic interaction with the negatively charged surface mucosa improves the absorption of the formulation^{42, 43}. In this chapter, we present a subunit vaccine formulation based on cationic liposomes loaded with the adjuvant cyclic dimeric guanosine monophosphate (c-di-GMP) and different influenza and SARS-CoV2-derived antigens. A rapid prime and boost immunization regime with this formulation induces potent and long-lasting CD8⁺ T cell responses in mice. Compared to intravenous administration, the intranasal prime with this vaccine formulation induced more balanced systemic and lung-specific immune responses,

and more importantly this administration route allowed the induction of lung memory CD8⁺ T cell responses. Finally, we show that the vaccination with cationic liposomes loaded with c-di-GMP and the influenza epitope PA224 leads to a reduction of lung viral titers after challenge with PR8 H1N1 influenza virus compared to unvaccinated mice and that the intranasal prime immunization is essential for this protective effect of the vaccine. The induction of a protective immune response using an accelerated prime-boost regime can be key for the effective and fast immunization of the population in response to rapidly spreading respiratory viral infections such as SARS-CoV2 and influenza.

FUTURE PERSPECTIVES

In this thesis, we aim to move forward the field of immune-modulatory nanoparticles, both from the delivery system perspective and the identification of target antigens. Nowadays, the most advanced therapies used in the clinic to target excessive inflammation and autoimmunity are biologics, mainly monoclonal antibodies, such as Adalimumab, an anti-TNF α antibody, or interferons such as IFN- β ⁴⁴. Other tolerance-inducing therapies that did not reach the clinic yet but that are being tested in clinical trials are cell-based therapies. These therapies consist of the *ex vivo* modification of DCs or T cells to transform them into tolDCs or Tregs and subsequently transfer them back to the patient. A promising type of T cell therapy to treat autoimmunity are CAR-Tregs, engineered Tregs expressing a chimeric antigen receptor (CAR) to target specific antigens⁴⁵. Monoclonal antibodies and other immune suppressors currently used in clinical practice are not antigen-specific and induce general immune suppression leaving patients more prone to infections¹⁹. On the other hand, cell-based therapies such as tolDCs or CAR-Tregs are or can be antigen-specific, however the complex manufacture and their often-unstable tolerogenic phenotype are major limitations⁴⁶. Therefore, the + *in vivo* generation of tolDCs and Tregs, such as the approach proposed in this thesis, can be considered as the next major step forward in the field of antigen-specific immune modulation.

Several recommendations can be derived from this thesis as the field advances towards the clinical application of these therapeutic strategies. On one hand, the design of clinical trials to test efficacy of tolerogenic therapies against atherosclerosis represents a significant challenge due to the large and heterogeneous target population. Furthermore, the slow and progressive development of the disease makes necessary the follow up of patients in clinical trials over several years or even decades. Therefore, the initial clinical trials to put to test tolerogenic therapeutic strategies against atherosclerosis should target the subpopulation of patients that can potentially benefit the most from these therapies. In this context,

immunopeptidomics can be applied to identify common antigenic targets in cohorts of patients such as those with more vulnerable plaque characteristics or with high residual inflammatory risk.

Future clinical trials of tolerogenic nanoparticles might also benefit from research into less invasive and potentially more tolerogenic administration routes, such as intranasal and intradermal administration. The promising results from the intradermal administration of anionic liposomes in *ex vivo* human skin shown in chapter 4 of this thesis prompts further research into other administration routes, such as intranasal administration. Intranasal antigen delivery using anionic liposomes could harness the natural capacity of the airways mucosa to induce tolerogenic responses⁴⁷.

Although this thesis and previous research have shown the potential of anionic liposome to induce tolerance, the field would benefit from further optimisation of tolerogenic formulations. We observed that liposome formulations that have previously shown to have intrinsic tolerogenic capacity in mouse models, need to include a tolerogenic adjuvant such as vitaminD3 to induce tolerogenic responses in human *in vitro* and *ex vivo* models. This should be considered for the future optimisation of key parameters such as size, ζ -potential, rigidity and/or protein corona and these experiments should be carried out using human *in vitro* or *ex vivo* models as far as possible.

Apart from the liposomal formulations proposed in this thesis for the induction of immune tolerance, other type of nanoparticles have significant tolerogenic potential. One of these formulations are mRNA lipid nanoparticles (LNPs), which have demonstrated their efficacy as prophylactic vaccines during the SARS-CoV2 pandemic. Tolerogenic mRNA-LNP vaccines are being actively investigated by several industrial and academic research groups. These formulations present advantages over liposomes such as a higher and less variable loading efficiency of antigens due to the more consistent physicochemical properties of mRNA compared to peptides. Furthermore, these formulations can be used to deliver mRNA encoding for large proteins such as ApoB100, which might overcome the challenge of identifying minimal epitopes and tailoring the target antigens to the specific HLA types. This approach however also has limitations that must be overcome in the near future, such as the instability of mRNA compared to peptides/proteins. Furthermore, it is not yet clear if LNPs with anionic surface charge also have tolerogenic properties similar to the liposome counterpart and if including tolerogenic molecules like vitaminD3 will affect the loading of mRNA into the nanoparticle. As these gaps in knowledge are being actively investigated, tolerogenic mRNA-LNPs are becoming promising new tools for antigen-specific immune modulation.

CONCLUSIONS

In conclusion, this thesis shows the versatility of liposomes to induce both tolerogenic immune responses in the context of inflammatory or autoimmune diseases and protective immune responses against infections. We address some of the challenges in liposome-based therapies and seek to bridge critical knowledge gaps in the field. The identification of target antigens in the context of atherosclerosis, optimization of the delivery system and the development of scalable manufacturing methods are some of the issues covered in the chapters of this thesis. The research presented here reveals the applicability of immuno-peptidomics to study the precise antigens and epitopes driving immune responses in atherosclerosis but could also be useful in the context of classical autoimmune diseases. Furthermore, we lay the foundation for the clinical translation of tolerogenic anionic liposomes by performing human *in vitro* and *ex vivo* studies with these formulations. Finally, we also explore the use of cationic liposomes as prophylactic vaccines against viral infections and show their potential to generate protective T cell responses against influenza rapidly and efficiently. Overall, this thesis highlights the potential of liposome-based immunotherapies against autoimmune diseases and in the field of prophylactic vaccines and prompts further research to advance in the clinical translation of these formulations.

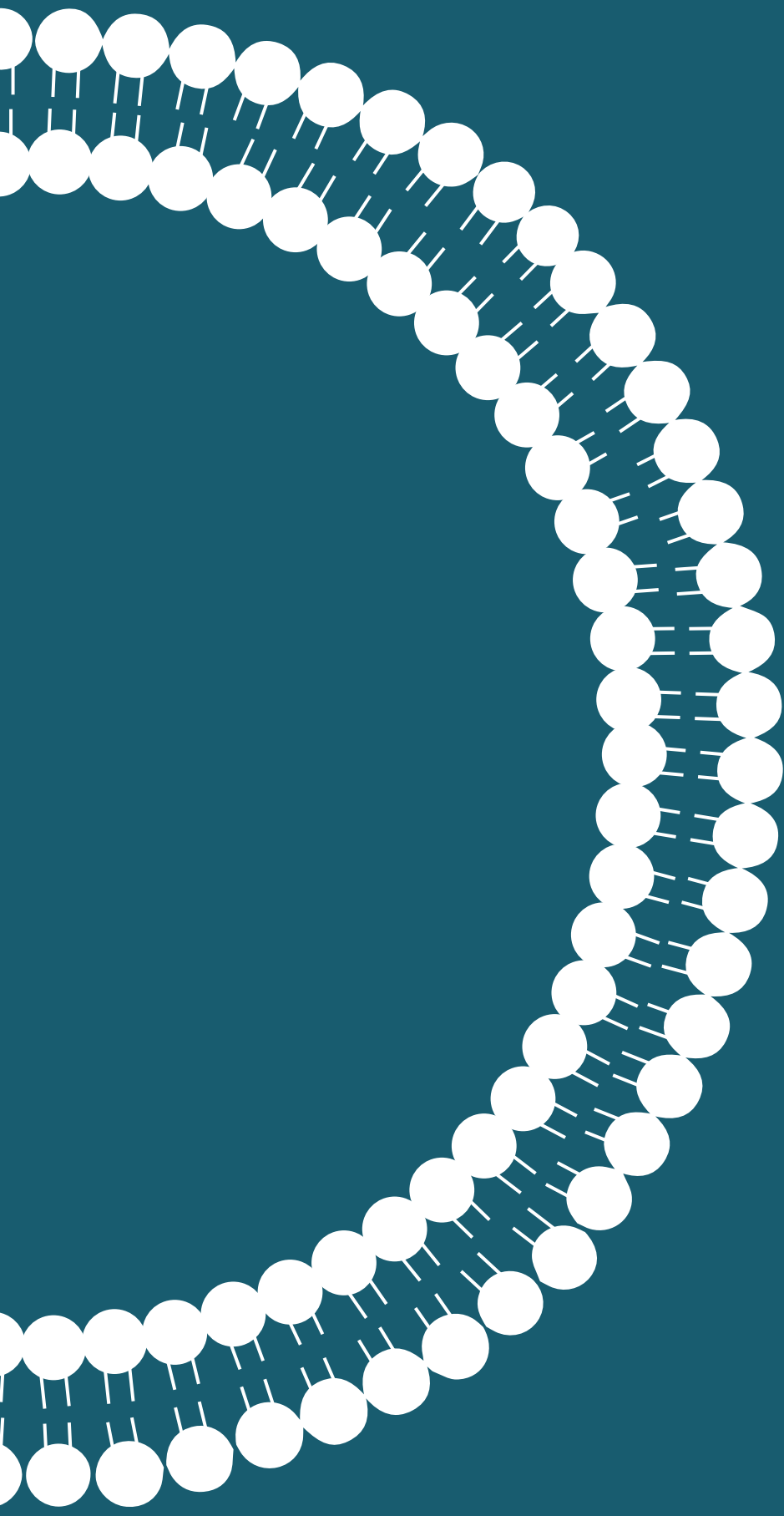
REFERENCES

1. Janeway Jr CA, Travers P, Walport M, Shlomchik MJ. Immunobiology 5 : the immune system in health and disease. New York: Garland Pub; 2001.
2. Zajec A, Trebusak Podkrajsek K, Tesovnik T, Sket R, Cugalj Kern B, Jenko Bizjan B, et al. Pathogenesis of Type 1 Diabetes: Established Facts and New Insights. *Genes (Basel)*. 2022;13(4).
3. Dendrou CA, Fugger L, Friese MA. Immunopathology of multiple sclerosis. *Nat Rev Immunol*. 2015;15(9):545-58.
4. Sanjadi M, Rezvanie Sichanie Z, Totonchi H, Karami J, Rezaei R, Aslani S. Atherosclerosis and autoimmunity: a growing relationship. *Int J Rheum Dis*. 2018;21(5):908-21.
5. Benne N, van Duijn J, Kuiper J, Jiskoot W, Slutter B. Orchestrating immune responses: How size, shape and rigidity affect the immunogenicity of particulate vaccines. *J Control Release*. 2016;234:124-34.
6. Schwendener RA. Liposomes as vaccine delivery systems: a review of the recent advances. *Ther Adv Vaccines*. 2014;2(6):159-82.
7. Platt CD, Ma JK, Chalouni C, Ebersold M, Bou-Reslan H, Carano RA, et al. Mature dendritic cells use endocytic receptors to capture and present antigens. *Proc Natl Acad Sci U S A*. 2010;107(9):4287-92.
8. Chen L, Flies DB. Molecular mechanisms of T cell co-stimulation and co-inhibition. *Nat Rev Immunol*. 2013;13(4):227-42.
9. Wakkach A, Fournier N, Brun V, Breittmayer JP, Cottrez F, Groux H. Characterization of dendritic cells that induce tolerance and T regulatory 1 cell differentiation in vivo. *Immunity*. 2003;18(5):605-17.
10. Benne N, van Duijn J, Lozano Vigario F, Lebox RJT, van Veelen P, Kuiper J, et al. Anionic 1,2-distearoyl-sn-glycero-3-phosphoglycerol (DSPG) liposomes induce antigen-specific regulatory T cells and prevent atherosclerosis in mice. *J Control Release*. 2018;291:135-46.
11. Nikpay M, Goel A, Won HH, Hall LM, Willenborg C, Kanoni S, et al. A comprehensive 1,000 Genomes-based genome-wide association meta-analysis of coronary artery disease. *Nat Genet*. 2015;47(10):1121-30.
12. Lechner K, von Schacky C, McKenzie AL, Worm N, Nixdorff U, Lechner B, et al. Lifestyle factors and high-risk atherosclerosis: Pathways and mechanisms beyond traditional risk factors. *Eur J Prev Cardiol*. 2020;27(4):394-406.
13. Dai H, Much AA, Maor E, Asher E, Younis A, Xu Y, et al. Global, regional, and national burden of ischaemic heart disease and its attributable risk factors, 1990-2017: results from the Global Burden of Disease Study 2017. *Eur Heart J Qual Care Clin Outcomes*. 2022;8(1):50-60.
14. Libby P. The changing landscape of atherosclerosis. *Nature*. 2021;592(7855):524-33.
15. Stemme S, Faber B, Holm J, Wiklund O, Witztum JL, Hansson GK. T lymphocytes from human atherosclerotic plaques recognize oxidized low density lipoprotein. *Proc Natl Acad Sci U S A*. 1995;92(9):3893-7.
16. Gounopoulos P, Merki E, Hansen LF, Choi SH, Tsimikas S. Antibodies to oxidized low density lipoprotein: epidemiological studies and potential clinical applications in cardiovascular disease. *Minerva Cardioangiol*. 2007;55(6):821-37.

17. England BR, Thiele GM, Anderson DR, Mikuls TR. Increased cardiovascular risk in rheumatoid arthritis: mechanisms and implications. *BMJ*. 2018;361:k1036.
18. Murphy SA, Cannon CP, Wiviott SD, McCabe CH, Braunwald E. Reduction in recurrent cardiovascular events with intensive lipid-lowering statin therapy compared with moderate lipid-lowering statin therapy after acute coronary syndromes: from the PROVE IT–TIMI 22 (Pravastatin or Atorvastatin Evaluation and Infection Therapy–Thrombolysis in Myocardial Infarction 22) trial. *Journal of the American College of Cardiology*. 2009;54(25):2358-62.
19. Ridker PM, Everett BM, Thuren T, MacFadyen JG, Chang WH, Ballantyne C, et al. Antiinflammatory Therapy with Canakinumab for Atherosclerotic Disease. *N Engl J Med*. 2017;377(12):1119-31.
20. Tardif JC, Kouz S, Waters DD, Bertrand OF, Diaz R, Maggioni AP, et al. Efficacy and Safety of Low-Dose Colchicine after Myocardial Infarction. *N Engl J Med*. 2019;381(26):2497-505.
21. Benham H, Nel HJ, Law SC, Mehdi AM, Street S, Ramnoruth N, et al. Citrullinated peptide dendritic cell immunotherapy in HLA risk genotype-positive rheumatoid arthritis patients. *Sci Transl Med*. 2015;7(290):290ra87.
22. Warren KG, Catz I, Ferenczi LZ, Krantz MJ. Intravenous synthetic peptide MBP8298 delayed disease progression in an HLA Class II-defined cohort of patients with progressive multiple sclerosis: results of a 24-month double-blind placebo-controlled clinical trial and 5 years of follow-up treatment. *Eur J Neurol*. 2006;13(8):887-95.
23. Alhadj Ali M, Liu YF, Arif S, Tatovic D, Shariff H, Gibson VB, et al. Metabolic and immune effects of immunotherapy with proinsulin peptide in human new-onset type 1 diabetes. *Sci Transl Med*. 2017;9(402).
24. Koffeman EC, Genovese M, Amox D, Keogh E, Santana E, Matteson EL, et al. Epitope-specific immunotherapy of rheumatoid arthritis: clinical responsiveness occurs with immune deviation and relies on the expression of a cluster of molecules associated with T cell tolerance in a double-blind, placebo-controlled, pilot phase II trial. *Arthritis Rheum*. 2009;60(11):3207-16.
25. Chataway J, Martin K, Barrell K, Sharrack B, Stolt P, Wraith DC, Group A-MS. Effects of ATX-MS-1467 immunotherapy over 16 weeks in relapsing multiple sclerosis. *Neurology*. 2018;90(11):e955-e62.
26. Jurynczyk M, Walczak A, Jurewicz A, Jesionek-Kupnicka D, Szczepanik M, Selmaj K. Immune regulation of multiple sclerosis by transdermally applied myelin peptides. *Ann Neurol*. 2010;68(5):593-601.
27. Tse K, Gonen A, Sidney J, Ouyang H, Witztum JL, Sette A, et al. Atheroprotective Vaccination with MHC-II Restricted Peptides from ApoB-100. *Front Immunol*. 2013;4:493.
28. Roy P, Sidney J, Lindestam Arlehamn CS, Phillips E, Mallal S, Armstrong Suthahar SS, et al. Immunodominant MHC-II (Major Histocompatibility Complex II) Restricted Epitopes in Human Apolipoprotein B. *Circ Res*. 2022;131(3):258-76.
29. Wolf D, Gerhardt T, Winkels H, Michel NA, Pramod AB, Ghosheh Y, et al. Pathogenic Autoimmunity in Atherosclerosis Evolves From Initially Protective Apolipoprotein B(100)-Reactive CD4(+) T-Regulatory Cells. *Circulation*. 2020;142(13):1279-93.
30. Nagy NA, Castenmiller C, Vigario FL, Sparrius R, van Capel TMM, de Haas AM, et al. Uptake Kinetics Of Liposomal Formulations of Differing Charge Influences Development of in Vivo Dendritic Cell Immunotherapy. *J Pharm Sci*. 2022;111(4):1081-91.

31. Bakdash G, Schneider LP, van Capel TM, Kapsenberg ML, Teunissen MB, de Jong EC. Intradermal application of vitamin D3 increases migration of CD14⁺ dermal dendritic cells and promotes the development of Foxp3⁺ regulatory T cells. *Hum Vaccin Immunother*. 2013;9(2):250-8.
32. Varypataki EM, van der Maaden K, Bouwstra J, Ossendorp F, Jiskoot W. Cationic liposomes loaded with a synthetic long peptide and poly(I:C): a defined adjuvanted vaccine for induction of antigen-specific T cell cytotoxicity. *AAPS J*. 2015;17(1):216-26.
33. Maeki M, Fujishima Y, Sato Y, Yasui T, Kaji N, Ishida A, et al. Understanding the formation mechanism of lipid nanoparticles in microfluidic devices with chaotic micromixers. *PLoS One*. 2017;12(11):e0187962.
34. Webb C, Forbes N, Roces CB, Anderluzzi G, Lou G, Abraham S, et al. Using microfluidics for scalable manufacturing of nanomedicines from bench to GMP: A case study using protein-loaded liposomes. *Int J Pharm*. 2020;582:119266.
35. Benne N, Lebourg RJT, Glandrup M, van Duijn J, Lozano Vigario F, Neustrup MA, et al. Atomic force microscopy measurements of anionic liposomes reveal the effect of liposomal rigidity on antigen-specific regulatory T cell responses. *J Control Release*. 2020;318:246-55.
36. Martinez-Seara H, Rog T, Pasenkiewicz-Gierula M, Vattulainen I, Karttunen M, Reigada R. Interplay of unsaturated phospholipids and cholesterol in membranes: effect of the double-bond position. *Biophys J*. 2008;95(7):3295-305.
37. Foteini P, Pippa N, Naziris N, Demetzos C. Physicochemical study of the protein-liposome interactions: influence of liposome composition and concentration on protein binding. *J Liposome Res*. 2019;29(4):313-21.
38. Neves AR, Queiroz JF, Lima SAC, Reis S. Apo E-Functionalization of Solid Lipid Nanoparticles Enhances Brain Drug Delivery: Uptake Mechanism and Transport Pathways. *Bioconjug Chem*. 2017;28(4):995-1004.
39. Ngo W, Wu JLY, Lin ZP, Zhang Y, Bussin B, Granda Farias A, et al. Identifying cell receptors for the nanoparticle protein corona using genome screens. *Nat Chem Biol*. 2022;18(9):1023-31.
40. Rampado R, Peer D. Design of experiments in the optimization of nanoparticle-based drug delivery systems. *J Control Release*. 2023;358:398-419.
41. Varypataki EM, Benne N, Bouwstra J, Jiskoot W, Ossendorp F. Efficient Eradication of Established Tumors in Mice with Cationic Liposome-Based Synthetic Long-Peptide Vaccines. *Cancer Immunol Res*. 2017;5(3):222-33.
42. Law SL, Huang KJ, Chou VH, Cherng JY. Enhancement of nasal absorption of calcitonin loaded in liposomes. *J Liposome Res*. 2001;11(2-3):165-74.
43. Heurtault B, Frisch B, Pons F. Liposomes as delivery systems for nasal vaccination: strategies and outcomes. *Expert Opin Drug Deliv*. 2010;7(7):829-44.
44. Strzelec M, Detka J, Mieszczak P, Sobocińska KM, Majka M. Immunomodulation—a general review of the current state-of-the-art and new therapeutic strategies for targeting the immune system. *Frontiers in Immunology*. 2023;14.
45. Cier RJC, Valentini N, Lamarche C. Unlocking the potential of Tregs: innovations in CAR technology. *Frontiers in Molecular Biosciences*. 2023;10.

46. Abhishek K, Nidhi M, Chandran S, Shevkoplyas SS, Mohan C. Manufacturing regulatory T cells for adoptive cell therapy in immune diseases: A critical appraisal. *Clinical Immunology*. 2023;251:109328.
47. Bedford GJ, Heinlein M, Garnham LA, Nguyen OHT, Loudovaris T, Ge C, et al. Unresponsiveness to inhaled antigen is governed by conventional dendritic cells and overridden during infection by monocytes. *Science Immunology*. 2020;5(52):eabb5439.



Appendices

Nederlandse Samenvattig

Curriculum Vitae

List of Publications

NEDERLANDSE SAMENVATTIG

Het immuunsysteem is een verzameling organen, cellen en moleculen die het organisme verdedigen tegen ziekteverwekkers of stoffen die als vreemd worden herkend. Het kan grofweg worden ingedeeld in twee armen, de aangeboren en de adaptieve immuniteit. De aangeboren immuniteit is de eerste verdedigingslinie tegen een infectie, wordt snel opgebouwd, maar is niet antigeen-specifiek en kan geen immunologisch geheugen genereren. De adaptieve immuniteit daarentegen is wel antigeen-specifiek, maar heeft meer tijd nodig om zich te ontwikkelen. Dit type immuunrespons kan een immunologisch geheugen genereren dat zich sneller zal ontwikkelen bij herinfectie met dezelfde ziekteverwekker. Antigeen-presenterende cellen (APCs) vormen de verbinding tussen aangeboren en adaptieve immuniteit. Deze cellen kunnen antigenen vangen, verwerken en op hun oppervlak presenteren aan andere cellen van het adaptieve immuunsysteem, zoals T-cellen, waardoor de adaptieve immuunrespons op gang komt. Een over- of onderactivatie van het immuunsysteem ligt aan de basis van veel ziekten. Bij auto-immuunziekten wordt de natuurlijke tolerantie ten opzichte van zelfantigenen doorbroken, wat bijvoorbeeld leidt tot de vernietiging van β -cellen bij type 1-diabetes (T1D) of de myelineschede van neuronen bij multiple sclerose (MS). Bij andere veel voorkomende ziekten, zoals atherosclerose de belangrijkste oorzaak van hart- en vaatziekten, is er ook een ontstekingsreactie tegen zelfantigenen betrokken bij de etiologie van de ziekte. In andere gevallen kan het immuunsysteem falen in het genereren van een afdoende immuunrespons tegen een ziekteverwekker, wat leidt tot een wijdverspreide infectie die fataal kan zijn. In dit proefschrift laten we zien dat liposomen, een soort nanodeeltjes, kunnen worden toegepast om de immuuntolerantie bij auto-immuunziekten te herstellen en beschermende immuunreacties tegen infecties te activeren.

Nanodeeltjes kunnen worden gebruikt als afgiftesysteem voor zowel kleine moleculen als macromoleculen zoals eiwitten, peptiden of oligonucleotiden. Dit proefschrift richt zich op het gebruik van liposomen, nanometrische blaasjes gevormd door een fosfolipidenbilaag die een waterige kern omsluit. Liposomen zijn zeer veelzijdige afgiftesystemen die zowel hydrofobe als hydrofiële ladingen kunnen vervoeren, respectievelijk geladen in de fosfolipidenbilaag of in de waterige kern. Bovendien kan het biologische effect van liposomen worden gecontroleerd door hun fysisch-chemische eigenschappen, zoals grootte, vorm, stijfheid of oppervlaktelading, nauwkeurig af te stellen. Van de verschillende toepassingen van liposomen is vooral de toediening van antigenen interessant. Liposomen kunnen antigenen beschermen tegen afbraak en ze kunnen de antigeenafgifte richten op gespecialiseerde cellen zoals APCs. Liposomen kunnen lading transporteren naar APCs, zoals dendritische cellen (DCs), door gebruik te maken

van de intrinsieke hoge opname capaciteit van deze cellen. De manier waarop DCs het antigeen presenteren zal het type adaptieve immuunrespons bepalen. Bijvoorbeeld, de presentatie van antigenen in de context van een hoge expressie van co-stimulatoire moleculen zoals CD86, CD80 of CD40 en pro-inflammatoire cytokines zal de immuunrespons doen overhellen naar een pro-inflammatoire respons gemedieerd door Th1 of Th17 lymfocyten, noodzakelijk om virale en bacteriële infecties te bestrijden. Aan de andere kant zal de presentatie van antigenen door DCs in de context van lage niveaus van co-stimulatoire moleculen en hoge niveaus van ontstekingsremmende cytokinen een tolerogene respons induceren die voornamelijk gemedieerd wordt door T-regulerende cellen (Tregs). Het gebruik van nanodeeltjes voor de co-bezorging van antigenen en moleculen die de expressie van co-stimulatoire eiwitten moduleren is daarom niet alleen een veelbelovende strategie om toe te passen in conventionele profylactische vaccins, maar ook bij tolerogene vaccins om de immuunhomeostase bij auto-immuunziekten te herstellen.

Hoewel lipide nanodeeltjes op grote schaal en met succes zijn gebruikt in de SARS-CoV2 vaccins tegen de COVID-19 pandemie, zijn er nog veel onbekendheden die verhinderen dat op nanodeeltjes gebaseerde therapieën en vaccins hun volledige potentieel realiseren. In dit proefschrift proberen we licht te werpen op enkele hiaten in de kennis op dit gebied.

In **hoofdstuk 2** bespreken we tolerogene strategieën tegen veel voorkomende auto-immuunziekten zoals multiple sclerose (MS) en type 1 diabetes (T1D). We vatten de lessen samen die kunnen worden geleerd uit de inspanningen om deze therapeutische benaderingen naar de kliniek te brengen en de uitdagingen om tolerogene therapieën toe te passen op atherosclerose, een van de meest voorkomende chronische ziekten in de westerse wereld. Atherosclerose is een ontstekingsziekte van de slagaders, gekenmerkt door infiltratie en ophoping van lipoproteïnen met een lage dichtheid (LDL) in de subendotheliale ruimte van de slagaders, waardoor atheroscleroseplaques worden gevormd. De ophoping van LDL-deeltjes veroorzaakt een ontstekingsreactie die leidt tot verdere groei van de plaque. Deze plaques kunnen de bloedstroom naar bepaalde delen van het lichaam beperken of scheuren waardoor een bloedprop ontstaat, wat leidt tot de meest voorkomende klinische manifestatie van atherosclerose in de vorm van een myocardinfarct of beroerte. Klinische studies hebben aangetoond dat systemische immuunsuppressie de incidentie van cardiovasculaire voorvallen aanzienlijk kan verminderen door de ontstekingsreactie te verminderen, maar ten koste van een hoger risico op dodelijke infecties. Deze neveneffecten zijn nauwelijks aanvaardbaar voor de preventie van hart- en vaatziekten. De inductie van antigeen-specifieke immuuntolerantie zou een betere aanpak zijn en dit is reeds onderzocht in klinische

studies tegen andere auto-immuunziekten. Deze therapeutische strategieën zijn veilig gebleken en werden goed verdragen in klinische studies, maar hun doeltreffendheid hangt af van de zorgvuldige keuze van de doelantigenen, de dosis en de toedieningsweg.

De studie van antigeen-specifieke immuunreacties in atherosclerose is essentieel voor de ontwikkeling van tolerogene vaccins tegen de ziekte, omdat de antigenen die pro-atherogene immuunreacties veroorzaken niet goed gekarakteriseerd zijn. In **hoofdstuk 3** gebruiken we immuno-peptidomics om peptiden, gepresenteerd door HLA-klasse II moleculen, rechtstreeks uit atherosclerotische plaques van patiënten die een endarterectomie ondergaan, te isoleren en te identificeren. We identificeerden 20 epitopen afkomstig van ApoB100, het belangrijkste eiwit in LDL-deeltjes, en toonden aan dat 22% van de atherosclerosepatiënten detecteerbare niveaus van CD4⁺ T-cellen heeft die reageren op deze epitopen. Interessant genoeg correleert het niveau van de CD4⁺ T cel respons in deze subset van patiënten positief met de kwetsbaarheid van de plaque. Verdere karakterisering van deze cellen toonde aan dat ze IL-17 en IL-10 produceren, maar ook andere cytokinen zoals IL-5, IL-9 of IL-6, wat suggereert dat de ApoB100-specifieke T-celpopulatie geen uniek fenotype heeft. Het herstellen van de immunologische balans door het induceren van ApoB100-specifieke Tregs of het voorkomen van Th1/Th17-polarisatie met behulp van tolerogene nanodeeltjes geladen met de hier geïdentificeerde epitopen zou derhalve een veelbelovende therapeutische strategie tegen hart- en vaatziekten kunnen zijn.

Naast de definitie van de doelantigenen moet het toedieningssysteem worden geoptimaliseerd voor tolerantie-inductie bij de mens. In **hoofdstuk 4** hebben we aangetoond dat voor de vertaling van preklinische modellen naar patiënten de aanwezigheid van een tolerogene molecule zoals 1 α ,25-dihydroxyvitamineD3 (vitamineD3) nodig kan zijn. Liposomen geladen met vitamine D3 waren in staat om *in vitro* een tolerogeen fenotype te induceren in humane monocyt-afgeleide DCs en deze tolerogene DCs waren in staat om FoxP3⁺ CD25⁺ Tregs te induceren die ook IL-10 produceerden, een belangrijke ontstekingsremmende cytokine. Bovendien remden deze tolerogene DCs de polarisatie van T cellen naar de pro-inflammatoire subsets Th1 en Th17. Tot slot laten we ook zien dat intradermale toediening van liposomen geladen met vitamine D3 in *ex vivo* humane huid de selectieve migratie induceerde van CD14⁺ dermale DCs, waarvan eerder is aangetoond dat ze Tregs kunnen induceren. De volgende stappen in de klinische vertaling van peptide-gebaseerde liposoomvaccins vereisen de evaluatie van antigeen-specifieke T celresponsen in *ex vivo* humane modellen zoals de intradermale huidinjecties die in dit hoofdstuk zijn getoond.

Nadat we hebben aangetoond dat DSPC:DSPG:Cholesterol liposomen met vitamine D3 potentieel toepasbaar zijn bij mensen, willen we in **hoofdstuk 5** het probleem van de productie van deze formuleringen aanpakken. Traditionele laboratoriummethoden voor de bereiding van liposomen hebben weinig opschalingspotentieel. De laboratoriumschaalmethode om liposomen te bereiden is arbeidsintensief, bestaat uit meerdere stappen en vereist veel energie, waardoor de productie van grote batches formuleringen erg moeilijk is. De productie van liposomen met microfluidica is daarentegen een continu proces in één stap. In hoofdstuk 5 stellen we het gebruik voor van een herbruikbare glazen visgraat micromixer voor de bereiding van DSPC:DSPG:Cholesterol liposomen. Met behulp van dit systeem laten we zien dat de gemiddelde deeltjesgrootte van de liposomen nauwkeurig kan worden afgesteld door de stromingscondities te veranderen en dat peptiden met een breed scala aan lading en hydrofobiciteit kunnen worden ingekapseld. Verder laten we zien dat de inkapselingsefficiëntie van het tolerogene adjuvans vitamine D3 in DSPC:DSPG:Cholesterol liposomen aanzienlijk verhoogd was in de formuleringen bereid met microfluidics vergeleken met de conventionele methode. De biologisch actieve vorm van vitamine D3 is duur, daarom is de toename in efficiëntie van de inkapseling een belangrijk voordeel. De productie van DSPC:DSPG:Cholesterol liposomen met microfluidics vergemakkelijkt de productie van deze formuleringen onder Good Manufacturing Practice (GMP) omstandigheden, een eerste vereiste om deze tolerogene nanodeeltjes dichter bij de kliniek te brengen.

Naast de opname van tolerogene moleculen, zoals vitamine D3, heeft eerder onderzoek aangetoond dat de stijfheid van de nanodeeltjes een belangrijke fysisch-chemische parameter is die de tolerogene capaciteit van liposomen bepaalt. De lipidensamenstelling en de aanwezigheid van cholesterol in de bilaag bepaalt de stijfheid van het nanodeeltje, maar kan ook andere eigenschappen beïnvloeden, zoals de eiwitcorona, de verzameling eiwitten die in een biologische vloeistof interacteren met het liposoomoppervlak. In **hoofdstuk 6** gebruiken we een hybride nanodeeltje dat bestaat uit een PLGA-deeltje bedekt met een DOPC:DOPG-lipidenbilaag (DOPG/PLGA hybriden) om een zeer stijf nanodeeltje te verkrijgen, maar met een vloeibare lipidenlaag. We laten zien dat deze deeltjes weliswaar het antigeen kunnen afleveren aan APCs en Treg-responsen kunnen opwekken *in vitro*, maar dat ze er niet in slagen hetzelfde effect te bereiken *in vivo*. Hoewel eerdere studies hebben aangetoond dat stijve anionische liposomen de ontwikkeling van atherosclerose in muizen kunnen stoppen, hadden deze hybride deeltjes geen effect op de progressie van atherosclerose of de samenstelling van de plaque. We stelden de hypothese dat het *in vivo* gedrag van deze lipide nanodeeltjes meer beïnvloed wordt door de proteïne corona dan door de stijfheid van de deeltjes. De studie van de rol van verschillende eiwitten in de opname van nanodeeltjes onthulde dat ApoB100 de celopname zou

kunnen stimuleren in formuleringen met een DOPC:DOPG lipidenbilaag, ongeacht hun stijfheid, terwijl het complementeiwit C1q de belangrijkste mediator van opname is voor DSPC:DSPG:Cholesterol liposomen, zoals eerder gemeld. Dit hoofdstuk laat de complexiteit zien van het toewijzen van specifieke fysisch-chemische eigenschappen van nanodeeltjes aan een bepaald biologisch effect. Toekomstige studies moeten een allesomvattende aanpak volgen om het effect van kleine veranderingen in de fosfolipidensamenstelling op zowel de fysisch-chemische eigenschappen van het nanodeeltje, de proteïne corona samenstelling en hun biologische effect te bepalen.

In **hoofdstuk 7** van dit proefschrift richten we ons op de andere belangrijkste toepassing van vaccins op basis van liposomen, de inductie van beschermende immuunresponsen tegen virussen. Op het gebied van vaccins tegen respiratoire virussen zoals coronavirus en influenza is er behoefte aan subunitvaccins die cellulaire immuunresponsen lokaal in de longen kunnen induceren. Kationische liposomen zijn eerder bestudeerd voor hun immuunactiverende eigenschappen en deze afgiftesystemen bieden voordelen voor intranasale vaccinatie omdat de elektrostatistische interactie met het negatief geladen slijmvliesoppervlak de absorptie van de formulering verbetert. In dit hoofdstuk presenteren we een subunitvaccinformulering op basis van kationische liposomen geladen met het adjuvans cyclisch dimeer guanosinemonofosfaat (c-di-GMP) en verschillende van influenza en SARS-CoV2 afgeleide antigenen. Een snel start- en boost-immunisatieregime met deze formulering induceert krachtige en langdurige CD8⁺ T-celresponsen in muizen. Vergeleken met intraveneuze toediening, induceerde een eerste intranasale toediening met deze vaccinformulering meer gebalanceerde systemische en longspecifieke immuunresponsen, en wat nog belangrijker is, deze toedieningsroute maakte de inductie van geheugen CD8⁺ T celresponsen in de longen mogelijk. Tot slot laten we zien dat vaccinatie met deze liposomen leidt tot een vermindering van de virale belasting van de longen na een uitdaging met influenzavirus. De inductie van een beschermende immuunrespons met behulp van een versneld 'prime-boost'-regime kan essentieel zijn voor een effectieve en snelle immunisatie van de bevolking als reactie op zich snel verspreidende virale infecties van de luchtwegen, zoals SARS-CoV2 en influenza.

Concluderend toont dit proefschrift de veelzijdigheid van liposomen om zowel tolerogene immuunreacties te induceren in de context van ontstekings- of auto-immuunziekten als beschermende immuunreacties tegen infecties. We behandelen enkele van de uitdagingen in liposoomtherapieën en proberen kritieke hiaten in de kennis op dit gebied te overbruggen. In het algemeen benadrukt dit proefschrift het potentieel van op liposomen gebaseerde immuuntherapieën tegen auto-immuunziekten en op het gebied van profylactische vaccins, en zet aan tot verder onderzoek om de klinische vertaling van deze formuleringen te bevorderen.

CURRICULUM VITAE

Fernando Lozano Vigario was born in Guareña (Spain) on September 11th, 1992. He received his primary education at Nuestra Señora de los Dolores school and his secondary education at I.E.S. Eugenio Frutos High School. In 2010, he enrolled in the bachelor of Biochemistry at University of Seville (Spain). He graduated in 2016 with double specialization in Molecular Biochemistry and Biotechnology. During this time in Seville, he performed his bachelor research project at the department of Microbiology under the supervision of Dr. F.J. López Baena.

In September 2016, he moved to Leiden (The Netherlands) and enrolled in the master of Bio-Pharmaceutical Sciences at Leiden University. He performed his master research project entitled “Liposomes containing 1,2-Distearoyl-sn-glycero-3-phosphoglycerol (DSPG) as potential treatment to control inflammation in atherosclerosis” in the Division of BioTherapeutics in the Leiden Academic Centre for Drug Research (LACDR) under the supervision of Naomi Benne. As part of the master in Bio-Pharmaceutical Sciences, he also performed a research internship at Janssen Vaccines and Prevention B.V. focusing on the development of liposomal adjuvant formulations containing QS-21 and/or 3D-(6-acyl) PHAD in microfluidics system, under the supervision of Dr. Edina Couteau. Fernando obtained his master’s degree *cum laude* in October 2018. From December 2018 until December 2023, he performed his doctoral research in the Division BioTherapeutics under the supervision of Dr. Bram Slütter, prof. dr. Joke Bouwstra and prof. dr. Alexander Kros. The results from this research are presented in this book.

In March 2024, Fernando joined Neogene Therapeutics (Amsterdam, The Netherlands) as Senior Research Associate where he works on the development of T cell therapies against cancer.

LIST OF PUBLICATIONS

Benne N, van Duijn J, **Lozano Vigario F**, Leboux RJT, van Veelen P, Kuiper J, Jiskoot W, Slütter B. Anionic 1,2-distearoyl-sn-glycero-3-phosphoglycerol (DSPG) liposomes induce antigen-specific regulatory T cells and prevent atherosclerosis in mice. *J Control Release*. 2018; 291:135-146.

Benne N, Leboux RJT, Glandrup M, van Duijn J, **Lozano Vigario F**, Neustrup MA, Romeijn S, Galli F, Kuiper J, Jiskoot W, Slütter B. Atomic force microscopy measurements of anionic liposomes reveal the effect of liposomal rigidity on antigen-specific regulatory T cell responses. *J Control Release*. 2020; 318:246-255.

Lozano Vigario F, Kuiper J, Slütter B. Tolerogenic vaccines for the treatment of cardiovascular diseases. *EBioMedicine*. 2020; 57:102827.

Keij FM, Koch BEV, **Lozano Vigario F**, Simons SHP, van Hasselt JGC, Taal HR, Knibbe CAJ, Spaink HP, Reiss IKM, Krekels EHJ. Zebrafish larvae as experimental model to expedite the search for new biomarkers and treatments for neonatal sepsis. *J Clin Transl Sci*. 2021; 5(1):e140.

Nagy NA, Castenmiller C, **Lozano Vigario F**, Sparrius R, van Capel TMM, de Haas AM, van Kooyk Y, van Ree R, Tas SW, Geijtenbeek TBH, Jiskoot W, Slütter B, de Jong EC. Uptake Kinetics of Liposomal Formulations of Differing Charge Influences Development of in Vivo Dendritic Cell Immunotherapy. *J Pharm Sci*. 2022; 111(4):1081-1091.

Lozano Vigario F, Nagy NA, The MH, Sparrius R, Bouwstra JA, Kros A, Jiskoot W, de Jong EC, Slütter B. The Use of a Staggered Herringbone Micromixer for the Preparation of Rigid Liposomal Formulations Allows Efficient Encapsulation of Antigen and Adjuvant. *J Pharm Sci*. 2022; 111(4):1050-1057

Nagy NA, **Lozano Vigario F**, Sparrius R, van Capel TMM, van Ree R, Tas SW, de Vries IJM, Geijtenbeek TBH, Slütter B, de Jong EC; DC4Balance consortium. Liposomes loaded with vitamin D3 induce regulatory circuits in human dendritic cells. *Front Immunol*. 2023; 14:1137538.

de Jong MJM, Schaftenaar FH, Depuydt MAC, **Lozano Vigario F**, Janssen GMC, Peeters JAHM, Goncalves L, Wezel A, Smeets HJ, Kuiper J, Bot I, van Veelen P, Slütter B. Virus-Associated CD8+ T-Cells Are Not Activated Through Antigen-Mediated Interaction Inside Atherosclerotic Lesions. *Arterioscler Thromb Vasc Biol*. 2024; 44.

Nagy NA, Hafkamp FMJ, Sparrius R, Bas R, **Lozano Vigario F**, van Capel TMM, van Ree R, Geijtenbeek TBH, Slütter B, Tas SW, de Jong EC. Retinoic acid-loaded liposomes induce human mucosal CD103+ dendritic cells that inhibit Th17 cells and drive regulatory T-cell development in vitro. *Eur J Immunol*. 2024; 2:e2350839.